Roope Eskola

VALUE CREATION IN THE MANUFACTURING INDUSTRY BASED ON THE SIMULATION

ACTA UNIVERSITATIS LAPPEENRANTAENSIS 1061

Roope Eskola

VALUE CREATION IN THE MANUFACTURING INDUSTRY BASED ON THE SIMULATION

Dissertation for the degree of Doctor of Science (Technology) to be presented with due permission for public examination and criticism in the Auditorium A122 at Lappeenranta-Lahti University of Technology LUT, Lahti, Finland on the 9th of December, 2022, at 1 p.m.

Acta Universitatis
Lappeenrantaensis 1061

Supervisors Professor Aki Mikkola, D.Sc.
LUT School of Energy Systems
Lappeenranta-Lahti University of Technology LUT
Finland

Professor Olli Kuivalainen, D.Sc.
LUT School of Business and Management
Lappeenranta-Lahti University of Technology LUT
Finland

Associate professor Lea Hannola, D.Sc.
LUT School of Engineering Science
Lappeenranta-Lahti University of Technology LUT
Finland

Reviewers Professor Juho Könnö, D.Sc.
Department of Materials and Mechanical Engineering
Oulu University
Finland

Professor Minna Lanz, D.Sc.
Department of Mechanical Engineering
Tampere University
Finland

Opponents Professor Juho Könnö, D.Sc.
Department of Materials and Mechanical Engineering
Oulu University
Finland

Professor Petr Noskievič, D.Sc
Faculty of Mechanical Engineering
Technical University of Ostrava
Czech Republic

ISBN 978-952-335-902-4
ISBN 978-952-335-903-1 (PDF)
ISSN 1456-4491 (Print)
ISSN 2814-5518 (Online)

Lappeenranta-Lahti University of Technology LUT
LUT University Press 2022

Abstract

Roope Eskola
Value creation in manufacturing industry based on the simulation
Lappeenranta 2022
67 pages
Acta Universitatis Lappeenrantaensis 1061
Diss. Lappeenranta–Lahti University of Technology LUT
ISBN 978-952-335-902-4, ISBN 978-952-335-903-1 (PDF)
ISSN 1456-4491 (Print), ISSN 2814-5518 (Online)

Digitalization and globalization challenge companies to remain competitive to survive. Digitalization is disrupting traditional business models and reshaping organizational structures but also offering new opportunities to improve products. For example, various different simulation approaches are widely utilized in modern manufacturing. Using industry case examples, this dissertation examines how simulation is currently being used.

The objective of the dissertation is to provide manufacturing industry insight into how simulation can be implemented from both technological and management perspectives. The included research publications cover technically oriented articles with industrial use cases for physics-based simulation and management-oriented articles that study value creation and digital business ecosystems.

The included articles make several contributions regarding the development of simulation modeling as well as providing information as to how value is created via simulation in manufacturing. Therefore, the information provided is useful to promote and assist further research in the field.

Keywords: Simulation, Value Creation, Digital Business Ecosystem, Manufacturing, Industry

Acknowledgements

This research was carried out between 2018 and 2022 by the Laboratory of Machine Design at LUT University in cooperation with the Raute Corporation. In that time, I had the pleasure of working with skillful and inspirational experts from both Raute and LUT.

I would like to express my gratitude to my main supervisor Professor Aki Mikkola for his support along the way. I also want to thank Professor Olli Kuivalainen and Associate Professor Lea Hannola for their guidance. I am also grateful for Associate Professor Marko Matikainen for his help with LaTeX.

I thank the reviewers Professor Juho Könnö and Professor Minna Lanz for their valuable comments, which clearly helped to improve the dissertation. In addition, I thank all the co-authors. I am especially grateful to Sami Suuronen, Jussi Ojalainen, Heikki Korpilahti, Dmitry Gradov, and Babak Bozorgmehri. These are amazing persons and hardworking skillful professionals. I would also like to thank Scott Semken, who's proofreading made my text more authentically English.

Raute Corporation deserves my gratitude as an excellent employer, but especially I want to thank my supervisor Mr. Mika Hyysti for his support in all matters during my dissertation process. I also thank Mevea Ltd., a provider of advanced simulation software, for encouraging support that motivated me to finalize this dissertation.

I thank my parents, sisters, and brothers with their families for being in my life. I also thank my grandparents Arvo and Helmi Eskola for the example they set by believing in a simple life and honest and hard work. Finally, I express my gratitude to my family for their support. Especially, I am grateful to my lovely wife for her sweetness and endless love.

Roope Eskola
December 2022
Lahti, Finland

To my family

Contents

List of publications

Publication I

Eskola, R., Korpilahti, H., Bozorgmehri, B., Matikainen K. M., and Mikkola, A. "Real-time multi-body co-simulation model of veneer peeling lathe." *International Journal of Computer-integrated Manufacturing*, 1-23, 2022

Publication II

Gradov, D., Yusuf, O., Ojalainen, J., Suuronen, J., Eskola, R., Roininen, L., and Koiranen, T. "Modelling of a continuous veneer drying unit of industrial scale and model-based ANOVA of the energy efficiency." *Energy*, 244, Part A, 122673, 2022

Publication III

Mohammadi, M., Eskola, R., and Mikkola, A. "Constructing a Virtual Environment for Multibody Simulation Software Using Photogrammetry." *Applied Sciences*, 10, 4079, 2020

Publication IV

Cheikh-el-Chabab, M., Kuivalainen, O., Andersson, U. R., Eskola, R., and Mikkola, A. "Using Real-time Simulation in Company Value Chains and Business Models for Value Creation." *In: Ukko J., Saunila M., Heikkinen J., Semken R.S., Mikkola A. (eds.) Real-time Simulation for Sustainable Production - Enhancing User Experience and Creating Business Value*, 177-195, 2021

Publication V

Suuronen, S., Ukko, J., Eskola, R., Semken, S., and Rantanen, H. "Systematic literature review for digital business ecosystems in the manufacturing industry: prerequisites, challenges, and benefits.", *CIRP Journal of Manufacturing Science and Technology*, 37, 414-426, 2022

Author's contribution

Publication I

The author was designated first author and as such the contributor with primary responsibility. The author planned research and supported research with expert knowledge from the industrial side. Co-author Heikki Korpilahti was mainly responsible for the co-simulation procedure, and Babak Bozorgmehri was responsible for the FEM simulations. Computing reference results and writing the first manuscript was the responsibility of the author. In addition to these tasks, the author helped produce the included figures.

Publication II

The author was designated fourth co-author and was responsible for planning the simulation research into the continuous veneer dryer. The author supported and guided overall research with expert knowledge from the industrial side. This was conducted together with co-author Jussi Ojalainen. In addition to these tasks, the author was involved with the writing of the first manuscript. The author also helped in the production of the included figures.

Publication III

The author was designated second co-author and was responsible for methods used to verify results. The author guided overall research with expert knowledge from the industrial side. In addition to these tasks, the author was involved with the writing of the first manuscript.

Publication IV

The author was designated fourth co-author and was responsible for writing the first manuscript and providing the expert view from the industrial side.

Publication V

The author was designated second co-author and was responsible for focusing the message of the paper and providing the expert view from the industrial side. In addition to these tasks, the author contributed to the writing and proofreading of the paper.

Alphabetical symbols

A_v	Contact area of veneer
$A_1 ... A_6$	Empirical constants
$\mathbf{b}_j$	Joint type of which connects to neighboring body j
c	Concentration of water vapour
d_i	Contact interpenetration of ith time step
$\mathbf{d}_j$	Joint type of which connects to neighboring body j
$\mathbf{D}_j$	Matrix of body j
$\mathbf{e}_j$	Vector of body j
$\bar{\mathbf{F}}_{j,\mathrm{con}}, \bar{\mathbf{F}}_{j+1,\mathrm{con}}$	Vectors of contact force
$\bar{\mathbf{F}}_{\mathrm{ext}}$	Vector of external force
$\bar{\mathbf{F}}_{\mathrm{int}}$	Vector of internal force
$\dot{\mathbf{g}}_j$	Velocity of the center of the mass of body j with respect to the global coordinate system
$\ddot{\mathbf{g}}_j$	Acceleration of the center of the mass of body j with respect to the global coordinate system
$\mathbf{I}$	Identity matrix
k_g	Convective mass transfer coefficient
$\mathbf{M}$	Mass matrix of the system
M^{H_2O}	Molar mass of water
n	Degrees of freedom
O_a, O_b	Cylinder cap end points
p	Pressure
$\mathbf{q}$	Generalised global coordinates
$\dot{\mathbf{q}}$	Generalized velocity with respect to the global coordinate system
$\ddot{\mathbf{q}}$	Generalized acceleration with respect to the global coordinate system
$\mathbf{Q}$	Force vector of the system
$\mathbf{Q}_j$	Force vector of body j
$\mathbf{R}$	Orthogonal complement of the jacobian matrix
r_{cyl}	Radius of cylinder
$\dot{\mathbf{s}}_j$	Velocity of the intermediate coordinate system of body j
$\ddot{\mathbf{s}}_j$	Acceleration of the intermediate coordinate system of body j
T	Air temperature
t	Time
$\mathbf{u}$	Vector between two ends of a roller
$\mathbf{v}$	Vector carrying the cylinder cable O_a to point p

$\mathbf{Z}_b$	Velocity-level body coordinates of body b
z_j	Relative coordinates of body j

Greek symbols

α, Ω, μ	Penalty factors
$\boldsymbol{\lambda}$	Vector of lagrangian multipliers which represent the reaction force components
ω_j	Angular velocity vector of body j
$\dot{\omega}_j$	Angular acceleration vector of body j
δ	Differentiation increment
γ_+, γ_-	Flow correction factors
θ_1, θ_2	Angles of body 1 and 2, corresponding
$\mathbf{\Phi}_{,\mathbf{q}}^T$	Jacobian of the constraint equations $\mathbf{\Phi}(\mathbf{q}(t))$ with respect to the generalized coordinates

Abbreviations

3D	Three-dimensional
BE	Business Ecosystem
CFD	Computational Fluid Dynamics
DBE	Digital Business Ecosystem
DE	Digital Ecosystem
DP	Digital Platform
DT	Digital Twin
ERP	Enterprise Resource Planning
HW	Hardware
IP	Internet Protocol
I/O	Input/Output
MBD	Model Based Definition
LVL	Laminated Veneer Lumber
PID	Proportional-Integral-Derivative
PLC	Programmable Logic Controller
SM	Smart Manufacturing
SW	Software
TCP	Transmission Control Protocol
UAV	Unmanned Aerial Vehicle
VR	Virtual Reality

Chapter 1

Introduction

In today's rapidly changing global markets, industries are becoming not only interconnected, but also interdependent. To survive, digitalization and globalization are increasing the pressure on companies to remain competitive. Merely adapting technology is not enough. Companies must also understand business trends and the complexity of modern technology.

Simultaneously, digitalization is disrupting traditional business models and reshaping organizational structures [142]. To better understand digitalization as a phenomenon, scholars have increasingly begun to examine digital ecosystems [17, 108, 101], digital business ecosystems [110] and digital platforms [15, 31].

In addition, the business ecosystem is no longer seems to be sufficient to ensure success in manufacturing. Survival depends on successful integration with the digital ecosystem. Combining business and digital ecosystems results in new collaborative organizational networks that are referred to as Digital Business Ecosystems (DBEs) [116, 110]. Figure 1.1 illustrates.

In the manufacturing literature, the DBE has studied in many contexts. For example, numerous studies have looked at upgrading traditional manufacturing to Smart Manufacturing (SM) [72, 77, 134, 111]. The goal of SM is to have fully integrated, collaborative manufacturing systems that meet changing demands and conditions in real time in the factory, in the supply network, and satisfying customer needs in the marketplace [72, 92]. Industry 4.0 is usually referred to as Smart Manufacturing.

Industry 4.0 refers to the emergence and diffusion of a range of new digital industrial technologies, e.g., in relation to automation and data exchange in manufacturing technologies [118, 55]. Moreover, studies about Digital Twins (DT)

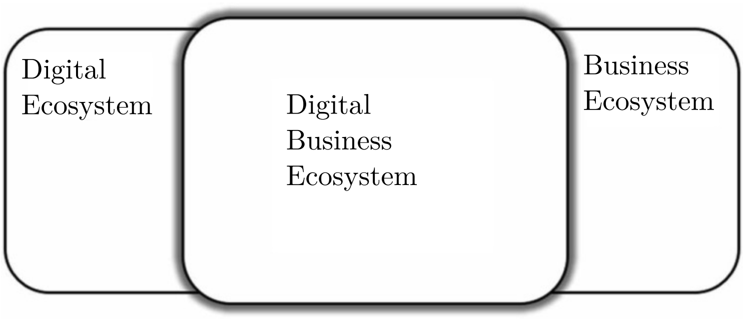

Figure 1.1. Digital ecosystem, business ecosystem, and digital business ecosystem alignment [119].

and how they are used in manufacturing have been of interest [78, 122, 123, 60, 133, 103]. A DT is a digital representation of a real-world system or entity.

DTs related to manufacturing lines and based on simulation are studied in this dissertation. State of the art DTs are real-time simulation models based on multibody dynamics that can manage a large number of interconnected rigid and flexible bodies [11]. These multibody-based approaches can be combined with actuator models to enable the description of multi-physical systems [105]. Multibody-based approaches and real-time simulation seems to be a well-studied research field; however, the research literature seems to suffer from a shortcoming of practical industrial case examples. To alleviate this shortcoming, this dissertation provides industrial case example of real-time simulation model based on multibody dynamics.

One presented industrial case is about a veneer peeling lathe. The developed real-time model of the lathe can be used in various different product processes such as in product development, the service businesses, and marketing. Figure 1.2 shows the veneer peeling lathe simulation 3D model in the Unity environment.

A second industrial case example of simulation introduced in this dissertation is a process simulation study of a continuous veneer dryer. Optimization of the drying process is a topic of interest from both economic and environmental standpoints. Drying is the most energy intensive process in a plywood mill, and the quality of veneer sheets, which should be within the optimal range for gluing of plywood panels, depends on moisture content.

The possible next step from these examples is taking simulator-driven design methodologies to a new level by developing and utilizing real-time simulator-driven processes. This will provide visibility and accessibility to multiple stakeholders in every part of the product life cycle and therefore enhance the potential of new business models to drive increased competitiveness. However, this new field of

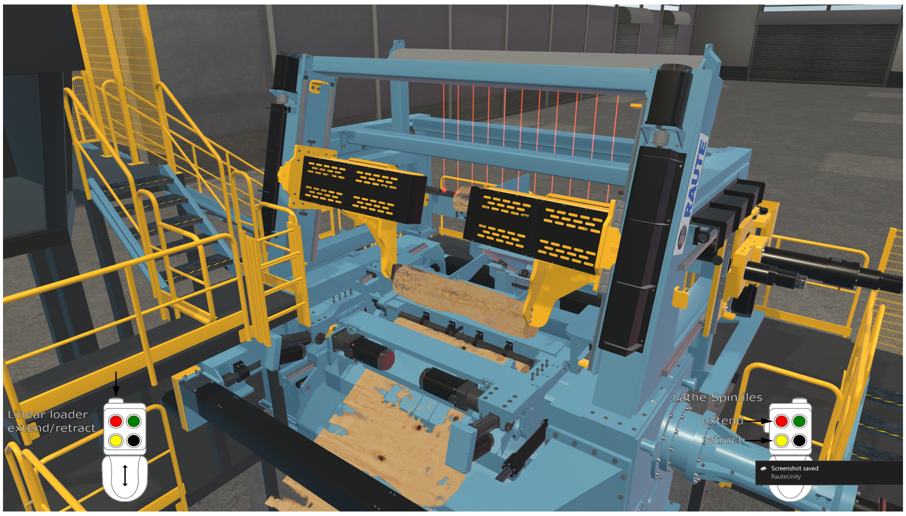

Figure 1.2. Veneer peeling lathe 3d model visualization in Unity virtual environment.

technology is not fully mature and is currently only being applied in limited cases, so there are many benefits yet to be discovered and proven.

1.1 Research problem

The original goal of this dissertation was to illustrate how simulation is typically utilized in manufacturing. Therefore, this dissertation was planned to describe the development of simulation models for true industrial-level case examples. Additionally, the dissertation was intended to explore value creation related to simulation and learn how digitalization could affect business models in manufacturing. Therefore, the overall research problem of this study was as follows.

Research problem: *How is simulation best developed and utilized in manufacturing?*

In this study, the research problem and most of the studies rely on real-life needs from the manufacturing industry.

1.2 Research questions

The aim this dissertation was to present and share with the research community what kind of simulations are utilized in real life by a manufacturing company. Therefore, Research Question 1 was formatted as such.

RQ1: *How is physics-based simulation best used to benefit the development of veneer production machinery?*

The veneer peeling lathe is the core of veneer production, and that is why it was first chosen as the subject of this research. Thus, Publication I describes the development process of a real-time physics-based simulator for a veneer peeling lathe. As protecting the environment is becoming increasingly important, the savings in energy usage in plywood mills is also becoming more important. And veneer drying is the most energy intensive process in plywood production. Therefore, Publication II focused on the development of process simulation for continuous veneer dryer.

In relation to the lathe simulator developed in Publication I, it was important to address the real life need for a realistic VR environment for the simulator. Thus, Research Question 2 was formatted.

RQ2: *How can authentic VR environments for physics-based real-time simulators be produced?*

Publication III presents a solution that satisfies that need. In addition to the development of simulation focused research, this dissertation aimed to study value creation related to simulation. Accordingly, Research Question 3 was formatted as follows.

RQ3: *How might real-time physics-based simulation change business models in manufacturing?*

Publication IV studied company value chains and business models in relation to value creation with real-time simulation. The next step was to research how real-time simulation and other digitalization processes will affect manufacturing business strategies. Publication V was a literature review that provides new insights in relation to digital business ecosystems in manufacturing industry.

1.3 Scientific contribution of this dissertation

This dissertation presents the five main contributions shown in Figure 1.3. The publications can be divided roughly into two different groups: technical contributions and business perspectives.

Publication I: The publication offers a novel scientific contribution with its presentation of a co-simulation-based solution procedure for the veneer peeling

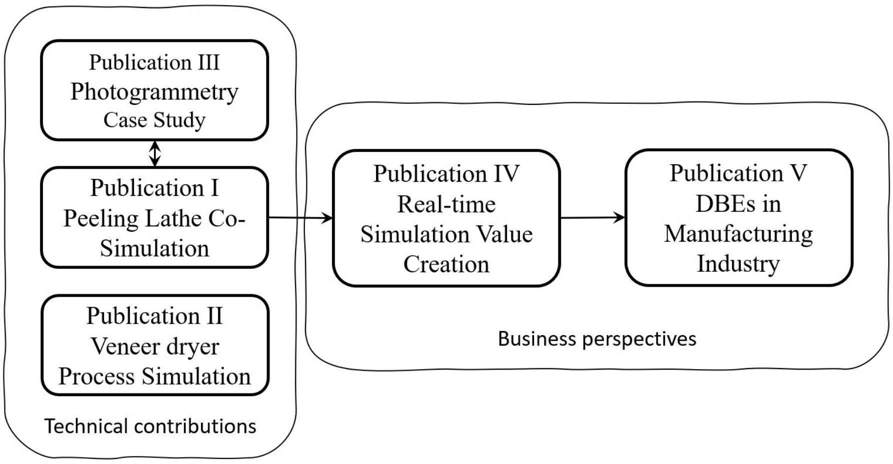

Figure 1.3. Role of each publication in this dissertation.

process using an approximated multibody approach in conjunction with the Atkins cutting force description. The accuracy and robustness of a simple description of the Atkins orthogonal force model was studied against a finite element model of the veneer peeling process. The simulation procedure for the proposed veneer peeling process was verified by comparing the output quantities and cutting force, respectively, against experimental measurements from an actual peeling lathe and a finite element model solution.

Publication II: As a second scientific contribution, this publication provides a second industrial case example that introduces the modeling principles for the veneer dryer. The implementation of the convective dryer model in the MATLAB Simulink environment and the methodology of the statistical analysis are described, and results from the model simulations and sensitivity analysis are presented.

Publication III: A third scientific contribution is the description of a method to generate a working environment for real-time multibody-based simulation models. The environment is based on an existing real-world location selected as the case study, the campus area of Lappeenranta-Lahti University of Technology LUT in Finland.

Publication IV: This publication contributes to the dissertation by describing how incorporating real-time simulation in different value chain processes can affect business models and benefit various stakeholders. The primary objective is to explain how real-time simulation tools can increasingly represent real-world functionality in today's businesses and emerging industries. This innovation has increased global competition to raise product quality and lower production costs and has ensured real-time access to relevant product and production data for the involved parties. Therefore, companies are lowering the barriers to participation in their product development and support processes and giving multiple parties better access to data by exchanging it through autonomous systems embedded throughout the value chain. To cope with these technological changes, industries have had to evolve and face the changing market. In this new environment, it is necessary to think more about creating value based on real-time simulation.

Publication V: This dissertation, via Publication V, contributes and provides new insights to the under researched topic of digital business ecosystems in manufacturing by revealing prerequisites, challenges, and benefits and proposing research topics for further studies. The study should be of benefit to directors and managers working in the manufacturing industry. Manufacturers can start considering how the impending digitalization of their industry might affect their businesses and their business models. The study should enhance understanding of the digital business ecosystem and how it will affect the entire manufacturing industry.

Chapter 2

Studies on business perspectives

This chapter presents the main findings from two different research articles addressing digitalization and business ecosystems. Section 2.1 provides information about real-time simulation models and value creation with the real-time simulation models. The following three sections present the main findings from a literature review article about DBEs for manufacturing. The literature review findings are tagged according to the three research questions addressing prerequisites, challenges, and the benefits for manufacturing DBEs.

2.1 Real-time simulation models and value creation

A complete real-time simulation model integrates the appropriate elements; including the models of environment, mechanics, control system, and user input; and predicts their interaction to simulate the dynamics of an entire system [84]. The user's main role is to provide input signals via the control console to direct the control system. The control system is where most of the input/output data is processed and synchronized with other subsystems. Actuators produce the forces needed to drive the mechanical subsystem. For example, hydraulic actuators output the required forces to the mechanical system, which responds by moving within its motion constraints. Multibody system dynamics is the basis of the mechanical subsystem modeling, and it includes the description, e.g., of the bodies, joints, contacts, and tires. In a multibody approach, the set of position coordinates can be defined using generalized global or relative coordinates [30]. A selected set of coordinates is also used to define the velocities and accelerations of the system bodies.

To express the equations of motion, the dynamic equilibrium of the system must be defined. This equilibrium can be determined using an approach such as the principle of virtual work. A multibody system is a constrained system, so the constraints must be considered when defining the equations of motion. There are several ways to express them including coordinate partitioning, the penalty method, the augmented Lagrangian method [13], the collision response model [69], and the lumped LuGre friction model [65]. Furthermore, the hydraulic system model that describes the actuators is often based on lumped fluid theory, where the hydraulic circuit is divided into discrete volumes with the assumption that the pressure is distributed equally [135].

Simulation tools such as these have helped decrease cost and improve simulation capabilities, making it possible to model and predict real-world behaviors. As a result, the capabilities of real-time simulation and its ability to solve real-world problems have improved. In addition to the reduction in modeling cost, the new techniques have been made more available and accessible to a larger number of users for multiple applications [14]. The importance of properly understanding the needs and wants of customers during the product design process, and therefore involving customers in the actual process through a virtual prototyping experience with real-time simulation tools, has driven the need for improved real-time simulation. In real-time simulation, the time required to perform computational functions and accurately compute equations must be synchronized and must be faster than the simulation time-step for the simulation to acceptably represent its physical counterpart with equivalent performance [14]. For each time-step, the simulator takes the following actions [14]:

1. Reading inputs and generating outputs,
2. Solving model equations,
3. Exchanging results with other simulation crossing, and
4. Waiting for the start of the next step.

As implied in the previous steps, all output data can be exchanged and shared. This capability enables a new form of communication between stakeholders, which could include current or potential customers, other dealers involved in the sales action such as sub-retailers and wholesalers, partners and investors, or any other party that makes use of the simulator-gathered real-time data.

Traditionally, product and service development decisions are made, for the most part, by the few experts tasked with directly addressing development issues and questions [87]. A certain approach could even be paternalistic, for example, see [10]. In this approach, customer needs and wants are often solicited via verbal or written interviews. For a completely new product, this approach is problematic, because describing a concept-level product to customers is difficult, and it is equally difficult for customers to fully understand a new product's potential advantages or disadvantages.

Furthermore, if the product is the result of radical innovation, customers may not even be able to articulate what their specific needs might be [87]. This problem can be alleviated by developing real-time simulation-driven processes, see example in Figure 2.1, which can be accomplished, in practice, by developing a toolset that gives multiple stakeholders access to machine research and development, production planning, and customer services via virtual worksites that can provide fully configurable, real-time, virtual prototyping. To this end, it is critical to employ server-based virtual environments.

With a server-based virtual environment, any number of stakeholders can simultaneously work with the virtual machine. The environment also makes it possible to set up and modify included models. All in all, these processes can function as tools for open innovation and crowd-sourcing [43].

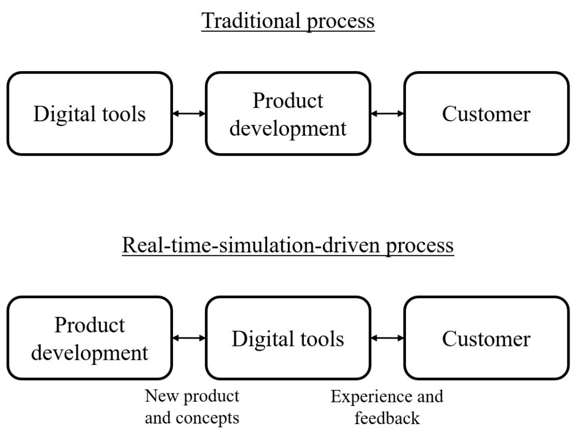

Figure 2.1. Role of digital tools in product development process.

2.2 Main prerequisites for DBE in manufacturing

The Business Ecosystem (BE) is obviously a necessary layer in a DBE [116]. In addition, the Digital Ecosystem (DE) is a second layer needed [116]. The DE layer provides the digital technical capabilities that enable the development of a digital business ecosystem in manufacturing. The presence of a digital ecosystem and business ecosystem in manufacturing alone does not enable member cooperation in a DBE. There must also be a Digital Platform (DP).

A DP is the technological infrastructure that enables the efficient development, configuration, and delivery of advanced services [42, 106, 142]. Regarding the role of the DP in a DBE, [46] argued that not all digital platforms can become industry wide. A digital platform must gain acceptance from the DBE members in manufacturing. To earn this acceptance, the DP must (1) perform a function that is essential to the broader technological system and (2) solve a business problem for a significant percentage of firms and users in the manufacturing industry [46]. Openness of the platform, trust, and security are the main reasons for restricting members to use the platform [124].

The digital platform of a DBE must have strong leadership in manufacturing. The keystone company's role is to ensure that each member of the DBE remains in good health [24]. The digital platform owner must offer value to encourage members to join the digital platform in manufacturing. A DP usually relies on the technological leadership of the one or two firms that provide the platform [126]. To ensure that a DBE does not fail at the onset, it should make it as easy as possible for potential members to participate [27]. Finally, trust is one of the most important prerequisites to building a successful DBE. Even if a system has high-level technological features, lack of trustworthiness may be the highest barrier to its success [139] in manufacturing. Table 2.1 itemizes the prerequisites and gives a definition for each.

2.3 Main challenges for DBE in manufacturing

Digital platforms play a key role in a digital business ecosystem for manufacturing. Launching a digital platform for the consumer industry faces a typical chicken-and-egg hurdle [99]. In manufacturing, leaders and competitors in a DBE have to navigate a complex landscape where both competition and collaboration occur. This is a new landscape for traditional manufacturing, and it brings new challenges and threats. There are multiple ways to structure digital platforms. DP success or failure depends in the long run on its capability to implement a feasible layered modular architecture for other members [93]. [41] recognized that DP leaders must commit to equitably sharing profits with the other DP members. Squeezing from complementary members negatively affects DP growth. DP leaders should encourage external content providers to stimulate growth and contribute to the platform's success [45, 53, 141].

A robust DBE comprises many manufacturing companies and members. Unlike standalone corporations, digital business ecosystems are not hierarchically controlled [62]. A winner-take-all situation is more likely in a DBE, when networks are positive and strong, multihoming to other networks is expensive, and there are no differentiation opportunities in manufacturing [35]. The challenge is how to maximize external innovation with the greatest amount of multi-sided benefits and trust. However, the data that drives manufacturing processes and the enterprise are sensitive, which causes a series of data problems such as data fusion, data

Table 2.1. Prerequisites for a digital business ecosystem in manufacturing [119].

Prerequisites for DBE	Definition	References
1. Business ecosystem	BE is one layer in a DBE	[88, 89, 116, 62]
2. Digital ecosystem	DE is one layer in a DBE	[17]
3. Digital platform(s)	DPs enable DBE members to enhance DBE performance, innovate, collaborate, deliver services and give vision to manufacturing asset through DT	[85, 46, 42, 143, 106, 142, 78]
4. Digital platform acceptance from the DBE members	Without acceptance by the members, DPs are useless.	[46],
5. Members interacting through DPs	Members active role needed in DPs to gain benefits of DBE.	[2, 102, 127, 109, 124]
6. DP requires strong leadership	Strong leadership increases the chance to succeed and adapt to changes.	[61, 140, 24, 125, 51]
7. DP must offer value for the members.	Increasing members value in DP will also boost its adoption.	[137]
8. Easy access to DP membership	A lower entry-point for members minimizes expansion risks at all levels and layers.	[27]
9. Trust	Trust can be the highest barrier to success of DBE.	[139, 124]

synchronization, data calculation, data security, etc. [124]. Table 2.2 itemizes the challenges and gives a definition for each.

2.4 Main benefits for DBE in manufacturing

In DBEs, a digital platform enables companies to innovatively discover different kinds of new business opportunities, where charging fees can be earned by both sides via transactions or advertising [34]. The value created by networks is substantially greater than what an individual company can produce on its own [2]. Physical machines become more valuable, when applications and services for them are available, which can trigger positive feedback cycles [7]. The digital platform and digital servitization are not only changing the way manufacturers innovate products and services, they are also transforming how members create, deliver, and capture customer value.

Combining more data and more DBE-platform members results in a greater

Table 2.2. Challenges for DBE in manufacturing [119].

Challenges for DBE	Definition	References
1. Launching DP for a successful DBE	The typical chicken-and-egg problem, SM challenges, information integration, costs, required effort to create DT	[40, 131, 132]
2. DBE is a new environment	DBE is a new and complex landscape with both competition and collaboration.	[61, 115, 1]
3. DP (system) structure	There are multiple ways to structure a DP.	[143, 51, 93, 54, 23, 103]
4. Commitment to share profits	Leader should not squeeze profits from their developers.	[132]
5. DP Leadership	There should be a balance of control of and freedom for DP members.	[141, 53, 45]
6. DBE size comes with its own challenges	A DBE comprises many companies and members (compared to individual company structure).	[62, 25, 97, 113, 73, 67]
7. Winner-take-all situation	The DP owner plays a monopoly role in its industry.	[145]
8. Building trust	Member trust in data, systems, and sharing the benefits with high expectations	[139, 124, 103, 82, 5, 71, 104]

potential for boosting innovation, competition, and productivity over a wide range of fields [21, 4]. The data availability also improves decision-making processes [112, 78], new product development [120], and customer relationships [21, 29, 81]. As manufacturing becomes more digital and openness allows stakeholders to better manage and capture data, more innovative ideas will come from outside the company [36, 47] providing incremental and radical service innovation opportunities [66, 90]. Digital platform members tend to share a common belief in the aims of the platform, and member performance is tied to overall performance of the business ecosystem [61]. A healthy DBE can be a barrier to entry for rival technologies [48], and it can entice new members to join.

Continuous progress results in a need for new technologies and innovations, which consequently results in the need for new kinds of resources [93] in manufacturing. A single company does not possess all the resources and knowledge needed to explore and continuously exploit changing markets. International new ventures are disrupting existing ecosystems, radically changing existing business models, and reshaping industry structures [39, 100]. Digital platform environments are an opportunity for new ventures, but a threat to established DBE members.

In DBEs, digital platforms minimize the costs of searching for both seeking services and service providers [51]. Companies are increasingly shifting from being vertical silos towards becoming modular clusters. Why? Modularity provides more opportunity to offer customers a product with specific options. In addition to giving the customer a product that better meets his or her needs, in the long run, the modularity lowers cost overall by restructuring for the entire manufacturing industry. Table 2.3 itemizes the benefits and gives a definition for each.

Table 2.3. Benefits of DBE and definitions in manufacturing [119].

Benefits for DBE	Definition	References
1. New business opportunities	A DBE provides new business opportunities for its members.	[94, 34, 83, 68, 98]
2. Value co-creation	Value is co-created with member co-operation, and processes can improve through data-driven evidence-based practices.	[7, 89, 2, 3, 22, 117, 31, 78, 76, 28, 23, 121, 114, 79]
3. Innovation increase	A company's innovation capability is strengthened by exposure to other innovation types.	[52, 138, 29, 64, 56, 74, 58, 81, 20, 21, 26, 75, 47, 59, 112, 4, 120, 36, 90]
4. Gain competitive advantage	A healthy DBE improves all members and builds a barrier against rivals. It can offer new dimensions to competitive advantage.	[48, 61, 3, 129, 49, 78, 123, 107]
5. Resources and knowledge increase	A DBE can fill key resource gaps.	[61, 96, 93]
6. New venture potential	The new venture potential arising from a DBE is usually underestimated.	[57, 39, 100, 16, 93]
7. Cost and risk management	DBE decreases overall costs and risks, when there are members innovating and offering solutions.	[34, 70, 80, 51]
8. Provides modularity to fulfill customer needs	Modularity offers a greater opportunity fulfill customer needs.	[12]

Chapter 3

Technical tools and industrial case examples

This chapter presents a set of technical tools used to explore two example cases of industrial simulation via multibody dynamic real-time simulation: a veneer peeling lathe and the continuous veneer dryer process. Section 3.1 describes the mathematics behind an efficient multibody dynamics approach. The Section 3.2 presents the technical tools and multibody approach used in the peeling lathe simulation case, and Section 3.3 describes the main methods used for the veneer dryer process simulation case. Moreover, Section 3.4 briefly describes a photogrammetry method that can be used to develop virtual environments for real-time simulators.

3.1 Multibody system dynamics

A numerically efficient multibody simulation model for a dynamic system that consists of a relatively large number of bodies can be obtained using a semi-recursive approach [30]. This section briefly highlights the semi-recursive approach used for the peeling lathe co-simulation study.

Semi-recursive method

In recursive kinematics, the position, velocity, and acceleration of the interconnected bodies are described in terms of a set of relative coordinates with a chain or a tree-like system configuration. This set of coordinates is selected so they only describe kinematically admissible displacements. Accordingly, in the description of an open-loop system, constraint equations are avoided, and the equations of motion comprise the same number of generalized coordinates as the number of degrees of freedom n [6].

When a recursive approach is applied to a closed loop system, it must be converted into an open loop system. An open loop system is then returned back to a closed loop system by imposing constraint conditions. Finally, these constraint conditions can be integrated into the equations of motion using the method of Lagrange multipliers, the penalty approach, the augmented Lagrangian method, or a method based on coordinate partitioning.

One often-used global multibody approach is the augmented Lagrangian method. When using this method, the equations of motion of a constrained system can be written in terms of a set of generalized global coordinates q in the following form:

$$\mathbf{M}\ddot{\mathbf{q}} + \mathbf{\Phi}^{T}_{,\mathbf{q}}\alpha\left(\ddot{\mathbf{\Phi}} + 2\Omega\mu\dot{\mathbf{\Phi}} + \Omega^2\mathbf{\Phi}\right) + \mathbf{\Phi}^{T}_{,\mathbf{q}}\boldsymbol{\lambda} = \mathbf{Q}(\mathbf{q},\dot{\mathbf{q}}), \tag{3.1}$$

where $\dot{\mathbf{q}}$ and $\ddot{\mathbf{q}}$ are the generalized velocity and acceleration with respect to the global coordinate system, respectively, $\mathbf{M}$ is mass matrix of the system, $\mathbf{\Phi}^{T}_{,\mathbf{q}}$ is the Jacobian of the constraint equations $\mathbf{\Phi}(\mathbf{q}(t))$ with respect to the generalized coordinates $\mathbf{q}$, $\mathbf{Q}$ is a force vector that accounts for the externally applied forces and the quadratic velocity vector, α, Ω μ are the penalty factors, $\boldsymbol{\lambda}$ is a vector of Lagrangian multipliers which represent the reaction force components. The constraints equations can be differentiated with respect to time as follows:

$$\dot{\mathbf{\Phi}} = \mathbf{\Phi}_{,\mathbf{q}}\dot{\mathbf{q}} + \mathbf{\Phi}_{,t} \quad \text{and} \quad \ddot{\mathbf{\Phi}} = \mathbf{\Phi}_{,\mathbf{q}}\ddot{\mathbf{q}} + \mathbf{\Phi}_{,\mathbf{q}t}\dot{\mathbf{q}} + \mathbf{\Phi}_{,tt}. \tag{3.2}$$

In this form of the augmented Lagrangian method, all the penalty terms related to fictitious potential, dissipation, and kinetic energies are included in the method. The classical augmented Lagrangian method has shown that error in the constraint equations is minimized by iterating Lagrange's multipliers. When this approach is used to express the equations of motion, the generalized coordinates within each time step can be iterated by updating Lagrange's multipliers in the following form:

$$\left(\mathbf{M} + \mathbf{\Phi}^{T}_{,\mathbf{q}}\alpha\mathbf{\Phi}_{,\mathbf{q}}\right)\ddot{\mathbf{q}}_{i+1} = \mathbf{Q} - \mathbf{\Phi}^{T}\alpha\left(\mathbf{\Phi}_{,\mathbf{q}t}\dot{\mathbf{q}}_i + \mathbf{\Phi}_{,tt} + 2\Omega\mu\mathbf{\Phi}_{,t} + \Omega^2\mathbf{\Phi}\right) - \mathbf{\Phi}^{T}_{,\mathbf{q}}\boldsymbol{\lambda} \tag{3.3a}$$

$$\boldsymbol{\lambda}_{i+1} = \boldsymbol{\lambda}_i + \alpha\left(\ddot{\mathbf{\Phi}} + 2\Omega\mu\dot{\mathbf{\Phi}} + \Omega^2\mathbf{\Phi}\right), \tag{3.3b}$$

where $\boldsymbol{\lambda}_{i=1} = 0$ for the first iteration indicates that the penalty terms only remain active to compensate for the constraint violations during the first iteration. For more details see [30].

The equations of motion represented in Equation (3.1) can be rewritten in terms of a set of relative coordinates. To this end, the following velocity and acceleration vectors associated with the intermediate coordinate system of body j are defined such that they initially coincide with the origin of the global coordinate system:

$$\mathbf{Z}_j = \begin{bmatrix} \dot{\mathbf{s}}_j \\ \boldsymbol{\omega}_j \end{bmatrix} \tag{3.4}$$

and

$$\dot{\mathbf{Z}}_j = \begin{bmatrix} \ddot{\mathbf{s}}_j \\ \dot{\boldsymbol{\omega}}_j, \end{bmatrix} \tag{3.5}$$

where $\dot{\mathbf{s}}_j$ is the velocity and $\ddot{\mathbf{s}}_j$ is the acceleration of the intermediate coordinate system of body j [44]. In Equations (3.4) and (3.5), $\boldsymbol{\omega}_j$ is an angular velocity vector and, correspondingly, $\dot{\boldsymbol{\omega}}_j$ is the angular acceleration vector with respect to the global coordinates system. To be able to express the equations of motion by employing the relative coordinates, it is important to find the relations between the velocity and acceleration in the generalized coordinates used in Equation (3.1) and those introduced in Equations (3.4) and (3.5). This can be accomplished as follows:

$$\dot{\mathbf{q}}_j = \begin{bmatrix} \dot{\mathbf{g}}_j \\ \boldsymbol{\omega}_j \end{bmatrix} = \begin{bmatrix} \mathbf{I}^{3\times3} & \tilde{\mathbf{g}}_j \\ \mathbf{0}^{3\times3} & \mathbf{I}^{3\times3} \end{bmatrix} \begin{bmatrix} \dot{\mathbf{s}}_j \\ \boldsymbol{\omega}_j \end{bmatrix} = \mathbf{D}_j \mathbf{Z}_j, \tag{3.6}$$

$$\ddot{\mathbf{q}}_j = \begin{bmatrix} \ddot{\mathbf{g}}_j \\ \dot{\boldsymbol{\omega}}_j \end{bmatrix} = \begin{bmatrix} \mathbf{I}^{3\times3} & \tilde{\mathbf{g}}_j \\ \mathbf{0}^{3\times3} & \mathbf{I}^{3\times3} \end{bmatrix} \begin{bmatrix} \ddot{\mathbf{s}}_j \\ \dot{\boldsymbol{\omega}}_j \end{bmatrix} + \begin{bmatrix} \tilde{\boldsymbol{\omega}}_j^2 \mathbf{g}_j \\ \mathbf{0}^{3\times1} \end{bmatrix} = \mathbf{D}_j \dot{\mathbf{Z}}_j + \mathbf{e}_j \tag{3.7}$$

where $\dot{\mathbf{g}}_j$ and $\ddot{\mathbf{g}}_j$ are the velocity and the acceleration, respectively, of the center of the mass of body j with respect to the global coordinate system, $\mathbf{I}$ is the identity matrix, $\tilde{\mathbf{g}}_j$ and $\tilde{\boldsymbol{\omega}}_j$ are the skew-symmetric matrices corresponding to vectors $\mathbf{g}_j$ and $\boldsymbol{\omega}_j$. Using Equations (3.6) and (3.7), matrix $\mathbf{D}_j$ and vector $\mathbf{e}_j$ can be defined for each body of the system. Using matrix $\mathbf{D}_j$ and vector $\mathbf{e}_j$, mass matrix $\mathbf{M}_j$ and the force vector $\mathbf{Q}_j$ of body j can be re-expressed as

$$\bar{\mathbf{M}}_j = \mathbf{D}_j^T \mathbf{M}_j \mathbf{D}_j, \tag{3.8}$$

$$\bar{\mathbf{Q}}_j = \mathbf{D}_j^T (\mathbf{M}_j \mathbf{e}_j - \mathbf{Q}_j). \tag{3.9}$$

The relative velocity and acceleration associated with body j can be written in the following form

$$\mathbf{Z}_j = \mathbf{Z}_{j-1} + \mathbf{b}_j \dot{z}_j \tag{3.10}$$

$$\dot{\mathbf{Z}}_j = \dot{\mathbf{Z}}_{j-1} + \mathbf{b}_j \ddot{z}_j + \mathbf{d}_j, \tag{3.11}$$

where z_j describes the relative coordinate(s) of body j (note that this is a scalar for a body that is connected to a neighboring body by a revolute joint or a translational joint) and $\mathbf{b}_j$ and $\mathbf{d}_j$ describe the type of joint.

Assuming matrix $\mathbf{R}$ to be an orthogonal complement of the Jacobian matrix $\boldsymbol{\Phi}_{\mathbf{q}}$ whose columns are the basis of the null-space of $\boldsymbol{\Phi}_{\mathbf{q}}$, the following relationships between the Cartesian velocities, accelerations and the relative ones can be established:

$$\mathbf{Z} = \mathbf{R}\dot{\mathbf{z}} \tag{3.12}$$

$$\dot{\mathbf{Z}} = \mathbf{R}\ddot{\mathbf{z}} + \dot{\mathbf{R}}\dot{\mathbf{z}}, \tag{3.13}$$

where $\mathbf{R}$ is the velocity transformation matrix that relates the relative coordinates and generalized coordinates in Equations (3.4) and (3.5). The variation of power of the system can be expressed with respect to Equations (3.6) and (3.7)

$$\left(\bar{\mathbf{M}}\dot{\mathbf{Z}} - \bar{\mathbf{Q}}\right) \cdot \delta\mathbf{Z} = 0. \tag{3.14}$$

Substituting Equation Equation (3.12) and Equation (3.13) into (3.14) and considering that velocity variation is independent, the final form of equations of motion can be written for an open loop system in the following form:

$$\mathbf{R}^T\bar{\mathbf{M}}\mathbf{R}\ddot{\mathbf{z}} = \mathbf{R}^T(\mathbf{Q} - \bar{\mathbf{M}}\dot{\mathbf{R}}\dot{\mathbf{z}}), \tag{3.15}$$

where

$$\bar{\mathbf{M}} = \mathrm{diag}(\bar{\mathbf{M}}_1, \cdots, \bar{\mathbf{M}}_j) \quad \text{and} \quad \bar{\mathbf{Q}} = [\bar{\mathbf{Q}}_1^T, \cdots, \bar{\mathbf{Q}}_j^T]^T.$$

In the semi-recursive approach, the equations of motion for a closed loop system can be derived by utilizing the cut-joint method and then accounting for the associated constraints using the augmented Lagrangian method as explained earlier and in [30, 44]. The augmented Lagrangian can be used in the same manner as in the global method in Equation (3.3a):

$$\left(\mathbf{M}^* + \boldsymbol{\Phi}_{,\mathbf{z}}^T\alpha\boldsymbol{\Phi}_{,\mathbf{z}}\right)\ddot{\mathbf{z}}_{i+1} = \mathbf{Q}^* - \boldsymbol{\Phi}^T\alpha\left(\boldsymbol{\Phi}_{,\mathbf{z}t}\dot{\mathbf{z}}_i + \boldsymbol{\Phi}_{,tt} + 2\Omega\mu\boldsymbol{\Phi}_{,t} + \Omega^2\boldsymbol{\Phi}\right) - \boldsymbol{\Phi}_{,\mathbf{z}}^T\boldsymbol{\lambda} \tag{3.16a}$$

$$\boldsymbol{\lambda}_{i+1} = \boldsymbol{\lambda}_i + \alpha\left(\ddot{\boldsymbol{\Phi}} + 2\Omega\mu\dot{\boldsymbol{\Phi}} + \Omega^2\boldsymbol{\Phi}\right), \tag{3.16b}$$

where $\mathbf{M}^* = \mathbf{R}^T\bar{\mathbf{M}}\mathbf{R}$, $\mathbf{Q}^* = \mathbf{R}^T(\bar{\mathbf{Q}} - \bar{\mathbf{M}}\dot{\mathbf{R}}\dot{\mathbf{z}})$ and $\boldsymbol{\lambda}_{i=1} = \mathbf{0}$ for the first iteration at the beginning of the simulation. The zero value for the initial guess indicates that at the first iteration, the constraint equations are enforced with respect to the pure penalty method, and with the rest of the iteration, the initial values for the Lagrange multipliers are amended to a set of optimum values. Iteration can begin using any other numerical values. That, however, might lead to an extended iteration process at the beginning of the simulation. The initial guess, $\boldsymbol{\lambda}_{i=1} = \mathbf{0}$, is only used once in the beginning of the simulation. The equation of motion can be integrated with respect to time using the explicit fourth-order Runge-Kutta method similarly to the global methods case.

The force vector contribution in the general form of equations of motion (3.16) can be more explicitly described in terms of components of $\bar{\mathbf{Q}}$ and analogous to Equations (3.9) and (3.15) as follows:

$$\bar{\mathbf{Q}} = \bar{\mathbf{F}}_{\text{ext}} + \bar{\mathbf{F}}_{\text{int}} + \bar{\mathbf{F}}_{\text{con}} \tag{3.17}$$

where:

$$\bar{\mathbf{F}}_{\text{con}} = \left[\cdots, \bar{\mathbf{F}}_{j,\text{con}}, \bar{\mathbf{F}}_{j+1,\text{con},\cdots}\right] \tag{3.18}$$

in which $\bar{\mathbf{F}}_{j,\text{con}}$ and $\bar{\mathbf{F}}_{j+1,\text{con}}$ are the vectors of contact forces (contact related action–reaction of the normal and frictional fields), i.e., between the wooden log and the cutting blade, $\bar{\mathbf{F}}_{\text{ext}}$ contains the components of the vector of external forces, i.e., the surface forces exerted by the support rollers, and $\bar{\mathbf{F}}_{\text{int}}$ is the vector of internal force, i.e., in the flexible wooden log.

3.2 Veneer peeling lathe example

The veneer peeling lathe is a machine that produces veneer to make plywood and Laminated Veneer Lumber (LVL). It can also be used as a covering surface for other panels or boards. The basic principle of the rotary peeling process has been established for decades. In the peeling process, the wood log is revolved using spindles or rollers as a cutting blade cuts inwards from the outer surface of the log.

The peeling process involves more than just cutting away the veneer, as shown in Figure 3.1. First, a linear feeder conveys logs from a log pile into a step feeder after which the logs are fed, one by one, into a centering device working in conjunction with an $X - Y$ block charger that rotates the log and measures its geometry with laser scanners. Then, the rotational center is optimized using an algorithm. In most cases, the main parameter for this optimization is maximized veneer recovery from the log.

Following the centering procedure, transfer arms move the centered log accurately to the lathe to be peeled. During peeling, the veneer cutting zone is supported by a pressure nose bar, which can either be a fixed bar or a roller, to ensure a continuous veneer mat (chip) [128]. Veneer qualities that can be affected by the nose-bar are surface smoothness, cracking, and thickness fluctuation. To achieve uniform thickness of the veneer along the length of the log during peeling, support rollers support it on its side opposite the blade. The produced veneer mat is then transferred down the line by a conveyor for further processing.

Figure 3.1. Veneer peeling lathe.

Co-simulation of Multibody model of veneer peeling lathe

The peeling lathe was implemented as a co-simulation model with lathe mechanics, actuators, and sensors modeled in Mevea software. A separate model was made for the peeling process written in Julia. Real PLC hardware that is used to control actual lathes was connected to the lathe MBD model via an I/O interface that uses a TCP/IP socket connection to transfer data between the PLC and lathe model. Similarly, a TCP/IP socket interface was used to transfer data between the lathe MBD and the peeling process models enabling the co-simulation of lathe mechanics and the forces arising from peeling a log. A schematic of the co-simulation and control model is seen in Figure 3.2.

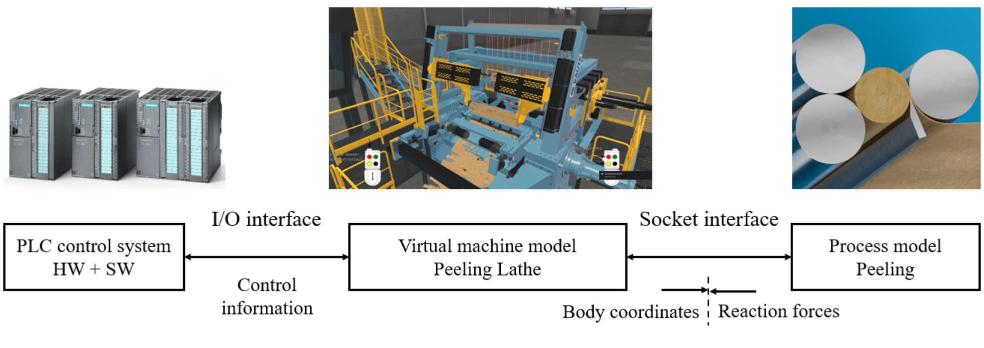

Figure 3.2. Co-simulation model structure and interface of the PLC control system [37].

The lathe was controlled by the PLC, which sends position and velocity-based targets to the PID controllers that drive the actuators responsible for moving the different lathe components. Feedback from the lathe to the PLC consists of lathe component positions and whether a move target was reached or not and feedback from the virtual sensors implemented in the MBD model, for example the laser scanners used by the pre-centering unit to scan the log shape.

To begin peeling, a log arrives at the main lathe spindles. Its location and orientation is sent to the process model along with the world locations of the support rollers, main spindles, and peeling knife. In the process model, log orientation is synchronized to the read location and then updated based on spindle rotation throughout the peeling step. The locations of the support rollers, peeling knife, and spindles are continuously updated from the MBD model. In addition to calculating the cutting force using Atkins' equations, the peeling process model handles collision detection and handling between the log and support rollers and peeling knife. The procedure mentioned above is briefly illustrated by Figure 3.3.

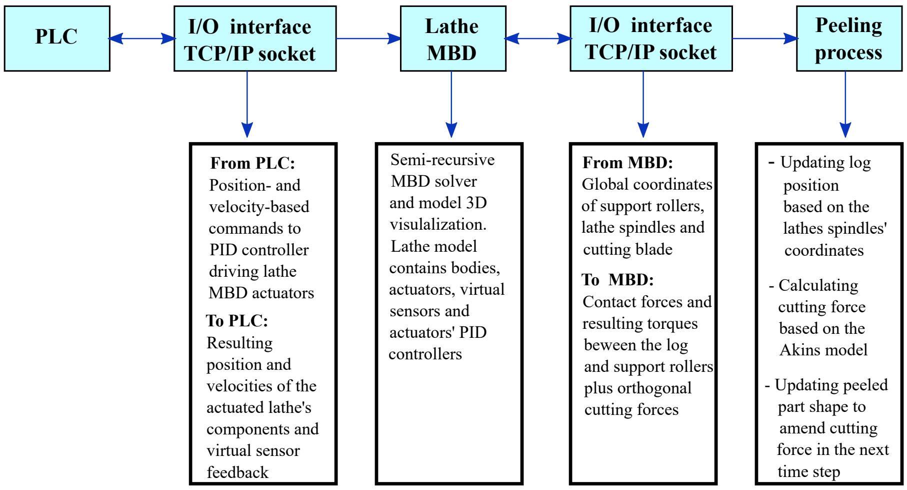

Figure 3.3. Flowchart of the steps of the proposed co-simulation procedure [37].

Contact description in peeling process model

In the simulation procedure, the contact detection task between the log and the peeling tool of the lathe is accomplished in the peeling process model using position and orientation information. Due to the irregular shape of the log, see Figure 3.4, the log comes into contact with the peeling tool at multiple locations. The contact constraints between the log and neighboring bodies are enforced using the penalty method as explained in [32]. Friction between contact pairs is in turn modeled using the LuGre dynamic friction model [95]. The time integration associated with LuGre friction is accomplished outside of the equations of motion.

In this study, the peeling forces were computed using fracture mechanics based off the cut by shear equations introduced in [8].

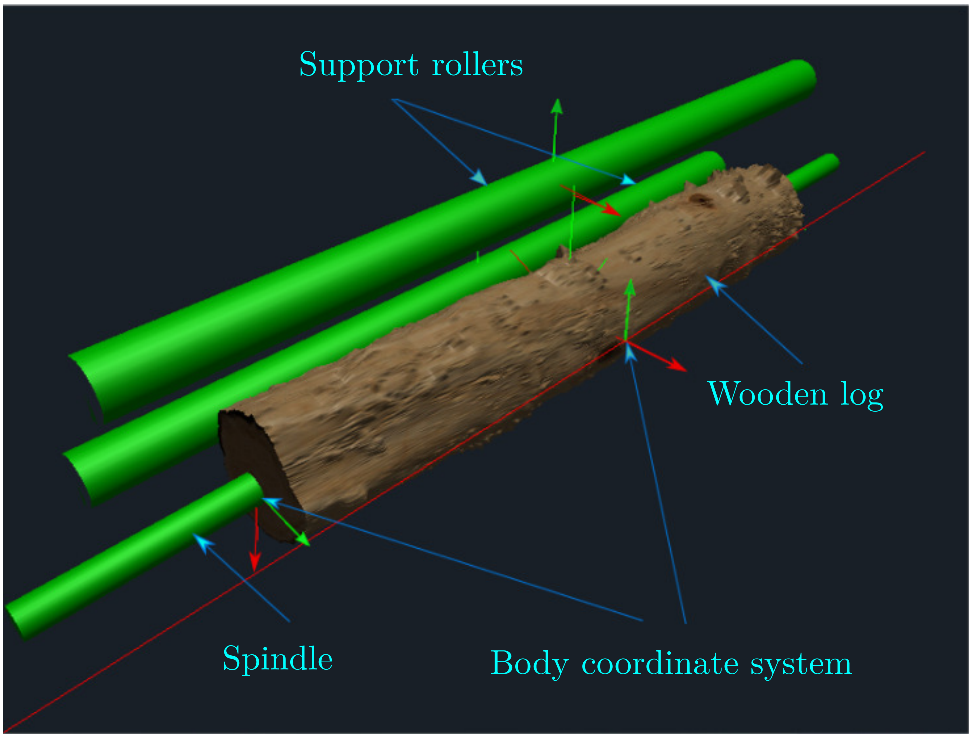

Figure 3.4. A schematic view of a raw log under peeling process [37].

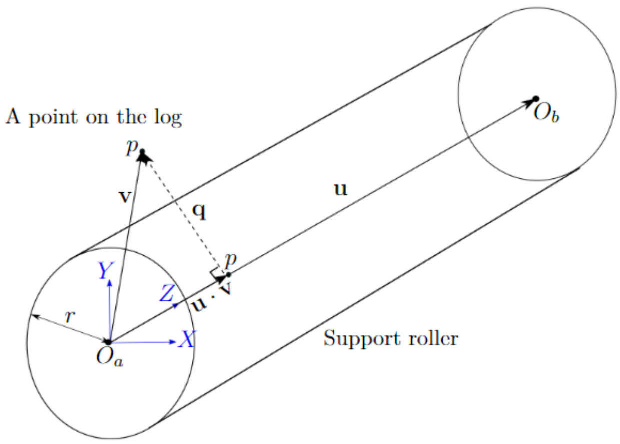

Figure 3.5. A simple representation of the contact detection task [37].

Algorithm 1 Contact detection algorithm to check if the contact points candidates are inside of the cylinder shown in Figure 3.5

1: **if** $0 < \text{d} < ||\mathbf{u}||^2$ **then** ▷ The contact point candidate is located between the cylinder caps
2: **if** $||\mathbf{q}||^2 < r_{cyl}^2$ **then** ▷ The contact point candidate is inside the cylinder
3: The gap function (penetration due to contact) is given by Equation (3.22).
4: **end if**
5: **end if**

Contact detection between the log, the support rollers, and the roller nose bar was accomplished using a point-in-cylinder procedure. In this study, the rollers and the nose bar were modeled as cylinders. A vector between two ends of a roller is denoted **u**, and correspondingly, a length of the roller can be obtained as $||\mathbf{u}||^2$. A contact event between a cylinder and arbitrary point p can be detected using Algorithm 1. First, a vector carrying the cylinder cap end O_a to point p denoted **v** was defined according to Figure 3.5. Determining if the point p lies between log end caps O_a and O_b can be checked using the following equation:

$$0 < d < ||\mathbf{u}||^2, \tag{3.19}$$

where

$$d = \mathbf{u} \cdot \mathbf{v}. \tag{3.20}$$

Correspondingly, point p lies within the cylinder radius if $||\mathbf{q}||^2 < r_{cyl}^2$ where

$$||\mathbf{q}||^2 = \mathbf{v} \cdot \mathbf{v} - \frac{d^2}{||\mathbf{u}||^2}. \tag{3.21}$$

The contact interpenetration d_i can be now calculated as follows:

$$d_i = \sqrt{r_{cyl}^2 - ||\mathbf{q}_i||^2}, \tag{3.22}$$

where subscript i denotes the current time step.

3.3 Veneer dryer example

Drying is a crucial step in veneer production aimed at producing optimal product moisture content veneers for further processes. In the veneer dryer, veneers are conveyed horizontally through connected chambers where hot air is blown transversely across them. The optimal drying process is dynamically maintained via the PID controllers, which manipulate opening rate of the damper lids, that are connected to the sensors monitoring the air properties in the chambers of the drying unit.

The typical veneer dryer, shown in Figure 3.6, consists of a drying section, comprising 16 drying cells, 2 smoke or sealant cells adjacent to the outer cells of the drying section, and 3 sequential cells of cooling section. Convective evaporation takes place in the drying cells, where radiator-heated air is blown continuously across the veneer sheets. The outer drying cells of the drying section are connected to the sealants or smoke cells. Leaving the second smoke cell, the veneer plates pass through the cooling section for temperature conditioning before they can be handled. Steam or oil can be used as the working fluid in the radiators. A typical drying cell comprises a fan, a radiator, jet boxes, rollers, and an optional air inlet and outlet, as shown in Figure 3.7.

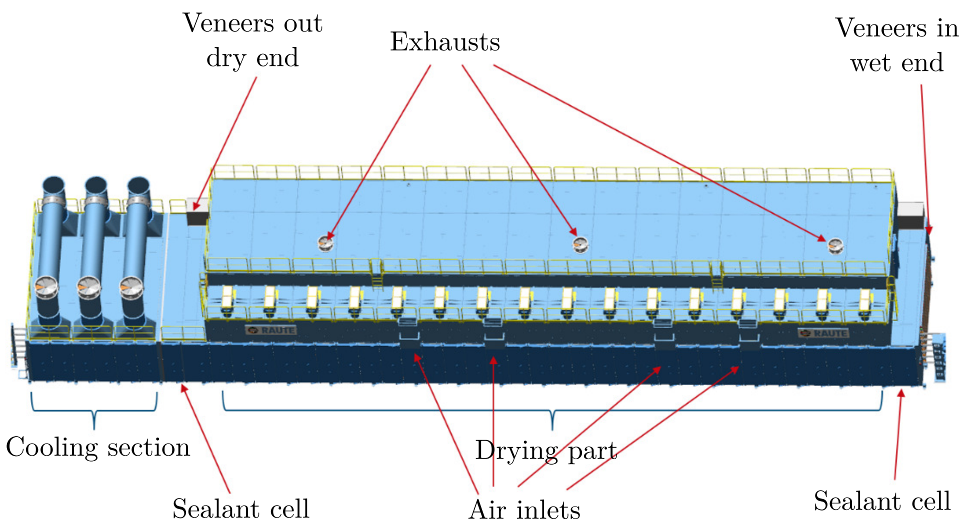

Figure 3.6. Illustration of the veneer dryer unit [50].

Principles and modelling concepts of convective drying

The thermodynamics of the convective drying process are derived from the ideal gas law. Dry air and water vapor coexist in a domain under ambient pressure as the sum of partial pressures:

$$p^{air} + p^{H_2O} = p^{atm}. \tag{3.23}$$

Water molecules can diffuse into the surrounding air from the veneer surface. The capacity of air to carry water vapor is limited by the atmospheric saturation pressure (atm).

$$p_{sat}^{H_2O} = \exp\left(\frac{A_1}{T} + A_2 + A_3 T + A_4 T^2 + A_5 T^3 + A_6 \ln T\right), \tag{3.24}$$

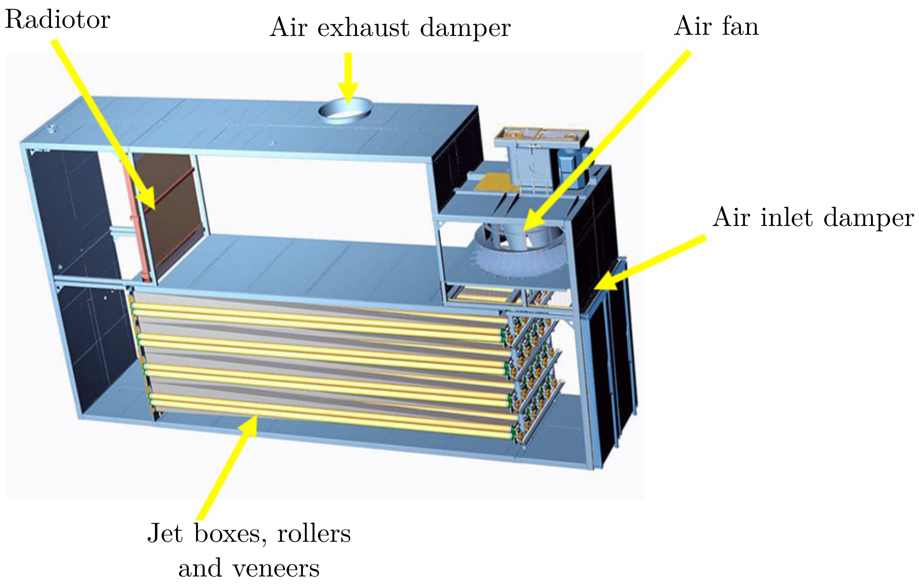

Figure 3.7. Illustration of the main features of a drying cell [50].

where T is the temperature of the air, and $A1...A6$ are the empirical constants. An increase in temperature leads to exponential growth of the saturation concentration of the water vapor. The molar flux of moisture from a surface to air can be expressed as follows:

$$M^{H_2O} = A_v k_g (p_{sat}^{H_2O} - p^{H_2O}), \tag{3.25}$$

where A_v is the contact area of veneer in m^2, k_g is the convective mass transfer coefficient in m/s [136]. Conversion of the molar flux into the mass flux results in the following expression

$$\dot{m}^{H_2O} = A_v M^{H_2O} k_g (c_{sat}^{H_2O} - c^{H_2O}), \tag{3.26}$$

where M^{H_2O} is the molar mass of water in $kg/kmol$, and c is the concentration of air water vapour in $kmol/m^3$.

The convective mass transfer coefficient describes the transport efficiency of the moisture from the surface to air, and it depends on the flow regime over the surface and water molecule diffusion. This can be correlated with Reynolds and Schmidt dimensionless numbers corresponding to convection viscosity and viscosity diffusion, respectively, of wood species. The convective mass transfer rate of moisture from a flat plate can be obtained from the experimental correlation:

$$k_g = ARe^{1/2}Sc^{1/3}, \tag{3.27}$$

where A is the empirical constant, 0.332 and 0.664 for laminar and turbulent regimes, respectively [136].

The geometry of the surface and the surrounding structures greatly affect the mass transfer coefficient. For simplified cases of flat or cylindrical surfaces in open space, the constants are sufficiently accurate. With complicated structures, however, such as the perforated jet boxes in the dryer in Figure 3.8, computational fluid dynamics (CFD) analysis can provide more accurate values [63].

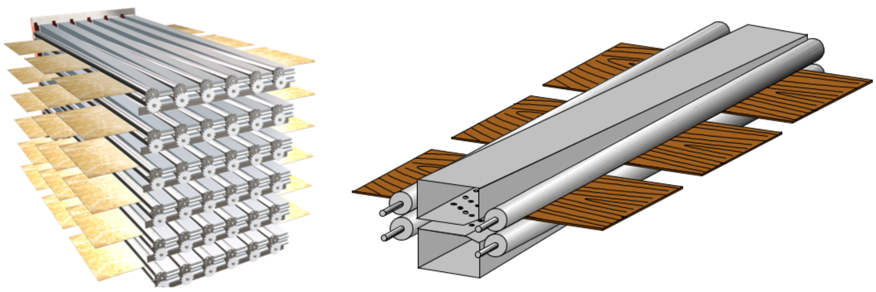

Figure 3.8. Illustration of the veneer conveying structures on the left and jet boxes on the right [50].

Higher air temperatures increase saturation concentration and, therefore, moisture capacity, which promotes higher drying rate. Diffusion of moisture through the veneer layers lowers the veneer surface drying rate. In practice, the diffusion time scale is small, because the veneer sheets are thin, and because the moisture migrates from the middle of the sheets in both directions towards the veneer surfaces. Temperature affects moisture diffusion in veneer fibers and can be described theoretically by Fick's Law of diffusion or empirically. Theoretical assumptions can introduce bias. When a moist veneer plate enters the first drying chamber moisture transport is increased due to convective heating during the induction period until a constant drying rate is reached. A constant drying rate is maintained until veneer humidity reaches a critical value and water diffusion becomes the limiting factor of the drying process, as illustrated in Figure 3.9. The reduction in drying rate continues until an equilibrium moisture content is reached, at which point, drying stops. The moisture-driven limitation of the constant drying rate can be measured experimentally under similar conditions. The measured isotherm of the falling rate is normalized for modeling purposes. The empirical approach is a consistent and a simpler alternative to a detailed CFD simulation of moisture transport through the material.

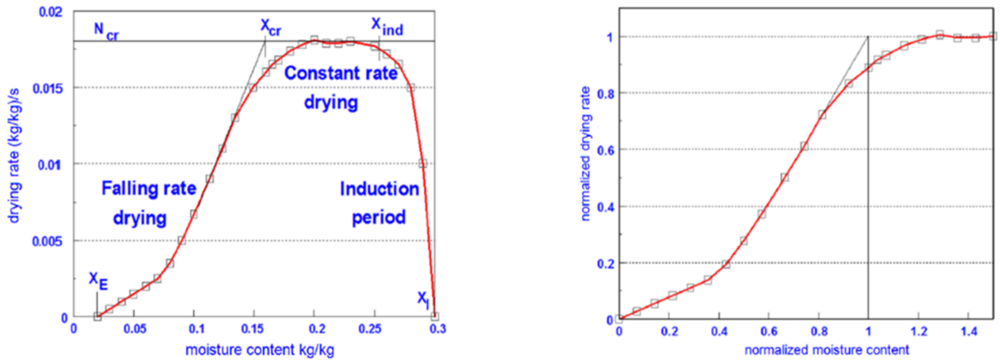

Figure 3.9. Normalisation of typical empirical drying rates as a function of moisture on the left and normalised quantities on the right [19].

Modelling continuous drying unit with MATLAB Simulink

The Simulink model was designed with the following assumptions and simplifications:

- The model excludes minor factors of influence
- the fan maintains a constant volumetric flow rate,
- the heating agent is at a constant temperature,
- the air stream is assumed to be perfectly mixed flow within sub-blocks,
- no temperature gradient profiles are considered in the veneer plates and metal parts,
- heat exchange with the outer atmosphere is not modeled,
- the effect of veneer temperature on moisture diffusion is omitted, and
- fan sub-blocks are isolated from each other.

The MATLAB Simulink modeling environment takes a block-based approach where the functional blocks are explicitly connected with the signal routes. The overall view of the model built in Simulink follows the construction of the real dryer as presented in Figure 3.10 The constituent elements are shown in Figure 3.11. The lines denote signals paths delivering values between the elements. The composition of all the drying cells is identical.

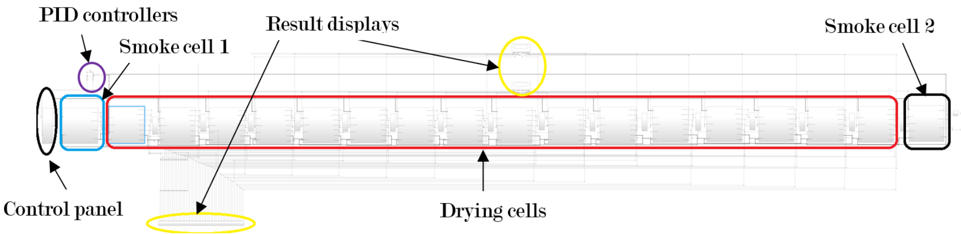

Figure 3.10. Architecture of the drying model in MATLAB Simulink [50].

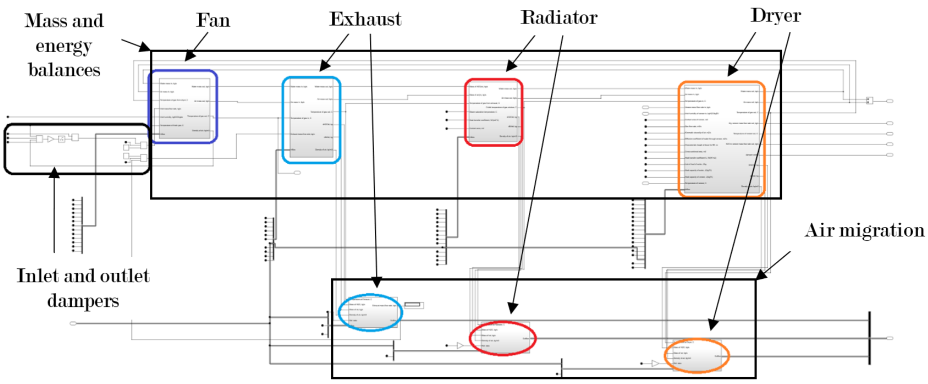

Figure 3.11. The drying cell in Simulink [50].

3.4 Photogrammetry approach

This section introduces a procedure to construct a three-dimensional environment using photogrammetry and graphical software. Photogrammetry uses contact-free sensors, which makes it possible to build three-dimensional models of expensive, fragile, toxic, or visible but inaccessible objects. It also makes it possible to document the changes of an object or area, such as a building construction.

Photogrammetry suffers from a number of shortcomings such as sensitivity to light conditions. The light source can be optimized for small objects, but in the case of outdoor objects and environments, optimization of lighting conditions remains a challenge.

A large number of images are needed to construct a three-dimensional model with high precision. In general, to build an initial three-dimensional model of a single object, a minimum of two planar images, with known offset, is necessary [130]. Unmanned Aerial Vehicles (UAVs) offer a functional and affordable method for taking thousands of images of a wide area (including tall structures such as buildings) [18, 33]. Assisted by UAVs, photogrammetry can be extended to cover areas in the scale of square kilometers. Figure 3.12 presents a procedure for using photogrammetry to construct a three-dimensional model of an area/object.

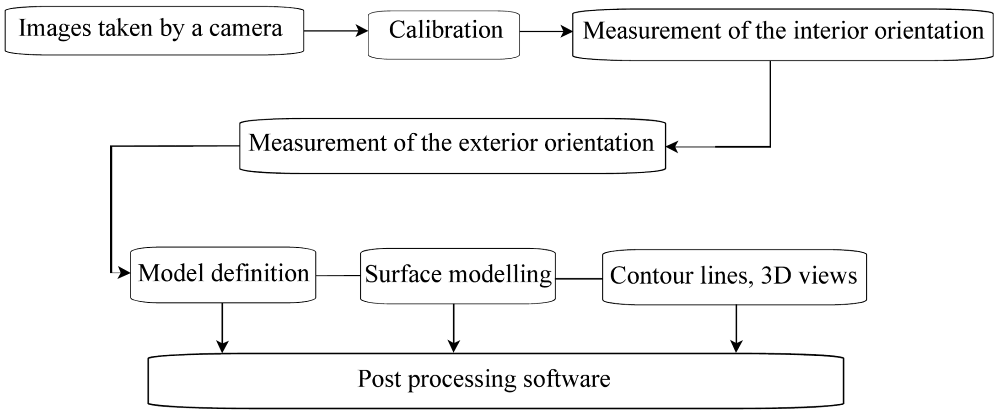

Figure 3.12. Overview of the photogrammetry procedure [86].

As Figure 3.12 illustrates, obtained images should be calibrated to calculate the distance between the camera and the object [9]. In the figure, exterior orientation means calculation of the exterior coordinates, which are the location of the projection center and the rotation angles of the object with respect to the considered global coordinate system. Surface modeling can be applied to the object to visualize textures. In the final step, postprocessing is done to build a three-dimensional model of the object.

To put it simply, photogrammetry makes it possible to build three-dimensional models out of planar images. To this end, postprocessing software compares two images taken of an object or area and recognizes identical points. See Figure 3.13. "Overlapping" between images helps to simplify the identical point recognition process and increases the quality of the object's textures. In addition, "shape matching" can be assisted to match corresponding points in two overlapping images.

The shape matching technique comes in different varieties. One common technique compares the shape of objects in two images without color consideration. This simplifies the process and reduces computational time. By considering corresponding points and the orientation of the cameras, the location of points in the three-dimensional environment can be estimated.

Even though the photogrammetry approach is extensively used to generate virtual realistic environments, it still faces some barriers and limitations. In most cases, the geometry and exact location of the object under investigation should be estimated. Transparent and dark colored objects, as well as tiny objects, pose challenges for photogrammetry [144, 91, 38]. Furthermore, there are some limitations when

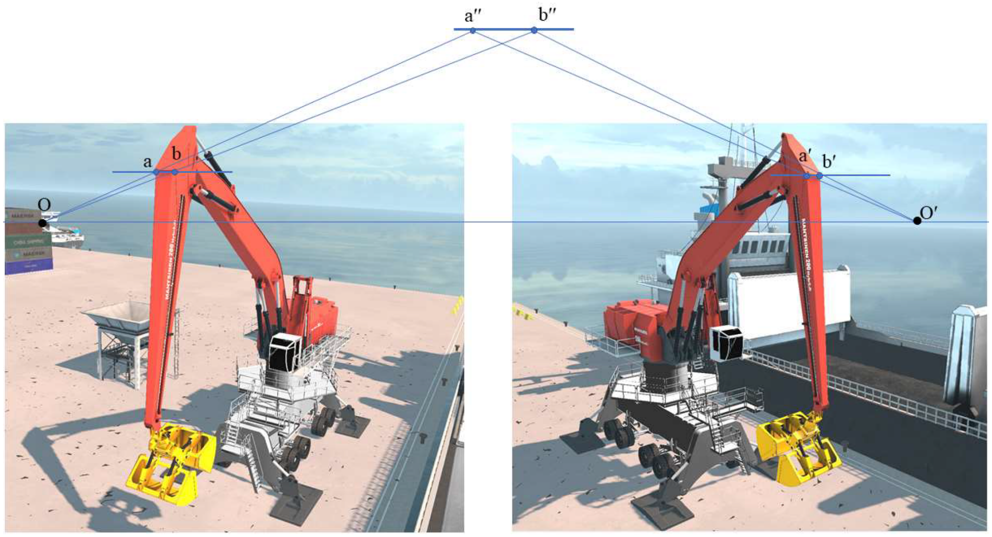

Figure 3.13. Estimation of three-dimensional specifications of a vehicle by comparing two planar images [86].

using photogrammetry and laser scanning procedures. Objects that are small, shiny, and transparent cannot be accurately captured in photogrammetry and laser scanning procedures. In addition, materials that absorb or diffuse the laser beams are barriers to accurately collecting point cloud data during the laser scanning procedure.

Chapter 4

Main numerical results of industrial case examples

This chapter presents the main simulation results for the industrial simulation example cases of a veneer peeling lathe and the process of a continuous veneer dryer. Section 4.1 presents the main results from the peeling lathe simulation case. Section 4.2 presents the main results from the veneer dryer process simulation case.

4.1 Veneer peeling lathe

Despite the existing limitations in the definition of the real-time model the introduced approach is able to predict the behavior of the lathe within a reasonable accuracy. To gain insight into the accuracy of the introduced real-time model and to investigate the possible discrepancies between the experimentally measured model and the simulated model in real-time, the following comparisons and discussions elaborate the findings.

Figure 4.1 shows both the measured and calculated cutting blade (knife) distances from the peeling center over the simulation duration. As can be seen from the figure, regardless of the starting point, both the simulated and the measured results are almost coincident until t=21 s. At 21 s, the calculated distance begins to rapidly increase. 1.5 to 2 s later, the measured distance also begins to increase at a similar rate. At the end of the simulation, the calculated knife distance is about 70 mm greater than the measured distance.

Figure 4.2 displays the output power measured against the values resulting from the simulation. As expected, the measurement recorded a considerable jump in power at about 1 s. This can be explained with reference to Figure 4.1 where the cutting knife in the measured model recorded a sudden, significant displacement. Figure 4.3 compares the measured input motor power of the actual machine with that predicted by the simulation model.

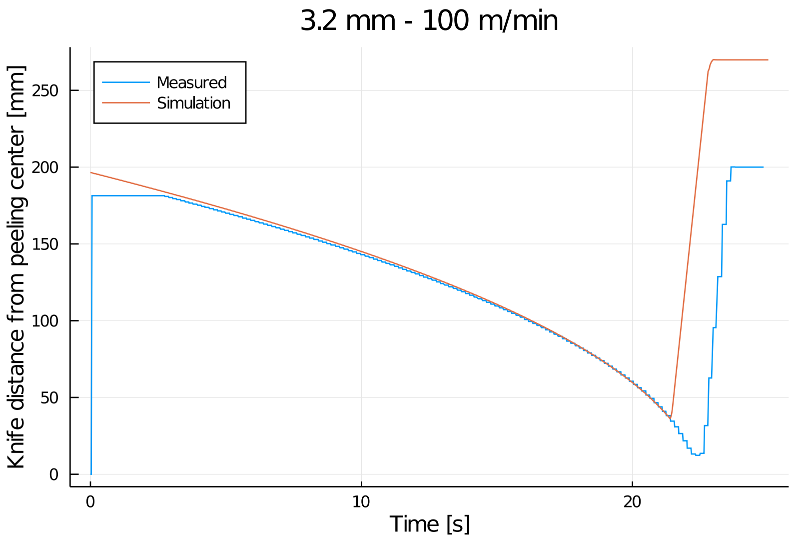

Figure 4.1. Comparison of the cutting knife distance from the peeling center over simulation and measurement operation time in the case of a dry run without a log [37].

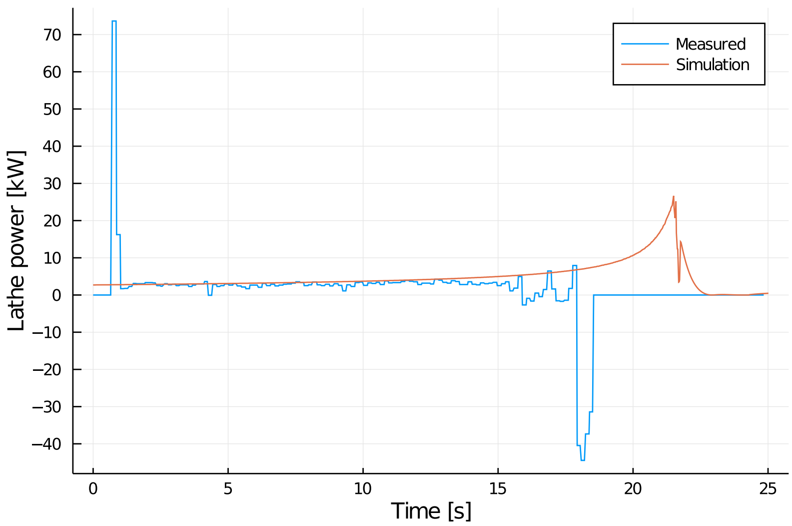

Figure 4.2. Comparison of the power measured during operation against that obtained within the simulation time in the case of a dry run without a log [37].

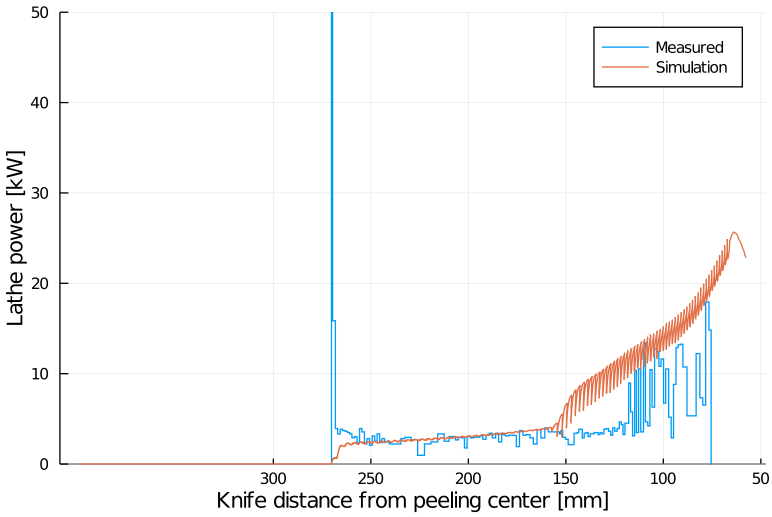

Figure 4.3. Comparison of the lathe motor power measured during operation against that obtained within time during log peeling process [37].

The differences seen between the simulated and measured data can be justified as follows:

1. Log diameter differs between the measured and simulated run. The simulated log had a maximum radius of around 150 mm, which can be seen in Figure 4.3 by the increase in required power. Measurement starts at around 120 mm radius.

2. The lathe power cut off earlier in the measurement when compared to the simulation. In a real lathe, the last part of the peeling is done with the spindles retracted and the log is rotated only by the backup rolls and round knife bar. In Figure 4.3, the moment the peeling enters the final stage and the spindles are retracted, the motor power drops to zero as the spindles' rotation is stopped. In the simulation, this last part is omitted and, instead, the log is always held in place and rotated via the spindles.

3. Noise in measurement data. One possible reason for the differences is that due to backup rolls and round knife bar increase the rotational torque, and occasionally, the spindles have to slow down to keep the tangential velocity at the set point.

4. The spike downwards in the measured lathe power at about 18 s in Figure 4.2 comes from the fact that a real lathe utilizes the electric motor for braking, making it function as a generator during the slowing down of the spindles' rotation.

4.2 Veneer dryer

This section presents the main results from the veneer dryer process simulation. First, the most simplified simulation, without air flowing freely between cells, was tested to limit the number of factors affecting the overall performance of the drying chambers. In addition, all the inlet and outlet dampers operated without PID controllers (fixed free parameters). The second simulation included air transport between the drying chambers while the dampers worked as in the previous simulation case. In the final case, the dryer worked in fully operative mode with active dampers. The simulation results achieved at different initial conditions are presented together for comparison purposes as presented in Table 4.1.

The dryer performance from startup to steady-state operation was simulated using three sets or cases of operational conditions. The simulation results obtained at different initial conditions are presented in Table 4.1. Drying rate curves for various simulation scenarios are presented in Figure 4.4.

The veneer enters a drying cell with zero gas-veneer contact area at the start, i.e., the moment the veneer sheets enter the drying chamber. This contact area grows as the veneer is transported through the cell. The dynamic movement of the transported veneer was modeled in the simulations, which resulted in inclined vertical lines for the drying curves. As soon as the veneer reaches maximum contact area, other limiting factors, such as the bearing capacity of the moist air and the humidity of the veneer, become dominant.

Table 4.1. Operating conditions of the veneer dryer unit simulated using the MATLAB model Cases [50].

Cases	Drying chamber connection	PID controller parameter, $k^{-(1/2)}$	Active inlet dampers	Active outlet dampers
1	No	2	All	All
2	Yes	2	All	All
3	Yes	$0.025 - 35$	4, 6, 10, 12	2, 8, 14

Fully isolated drying cells have high air humidity, which limits the drying rate in all the cells in Figure 4.6. Because air is able to flow freely between cells, fresh air flux increases the moisture saturation concentration and improves drying rate. Smart control of the inlet and outlet dampers preserves the balance more efficiently, resulting in higher drying rates.

Figure 4.5 presents the gas temperature at the fan sub-block. Pressure grows rapidly in an isolated cell as the temperature rises, pushing the outlet damper lid into the open position to let the air out. The outlet damper lid position affects

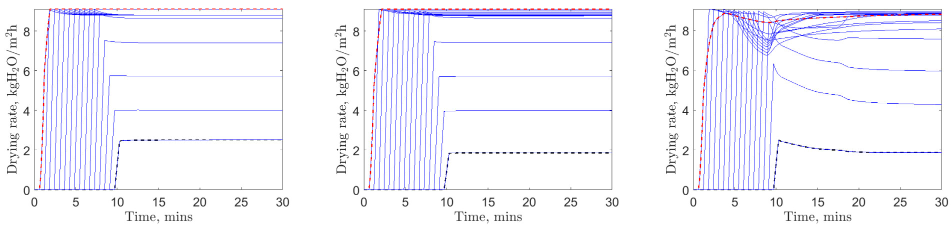

Figure 4.4. Simulation results for the drying rate in drying cells in three different simulation scenarios (cases 1-3) - The drying rate of the first drying cell chamber is plotted with red dashes, the last chamber with black dashes and the other chambers with blue lines [50].

air humidity, which in turn influences drying rate. Reduced density gas carries less energy, which results in the temperature drop of air into the cells in case 1. As the Figure 4.5 illustrates, the outer drying cells 1 and 16 have lower air temperatures due to the connections with the smoke cells. The energy balance between convective heat transfer from gas to veneer and evaporation of water explains the plateau in the temperature of the veneer seen in cells 6 - 12.

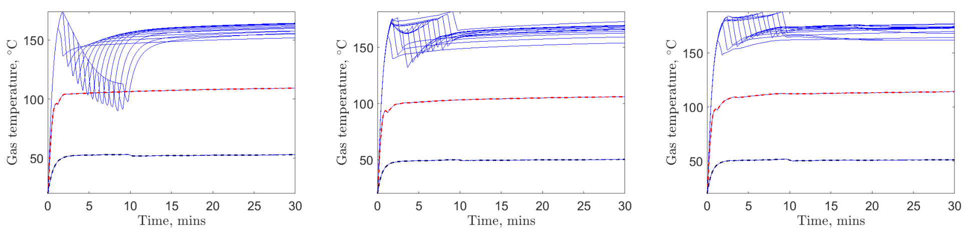

Figure 4.5. Simulation results for air temperature at the fan sub-block in the drying cells in three different simulation scenarios (cases 1-3) - The air temperature in the first drying cell chamber is plotted with red dashes, the last chamber with black dashes and the other chambers with blue lines [50].

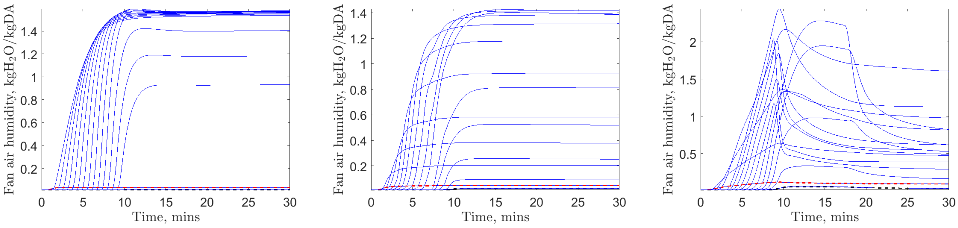

Figure 4.6. Simulation results for air humidity in the dryer sub-block in drying cells in three different simulation scenarios (cases 1-3) - The drying rate of the first drying cell chamber is plotted with red dashes, the last chamber with black dashes and the other chambers with blue lines [50].

Chapter 5

Conclusions

The original goal of this dissertation was to present how the simulation is utilized in manufacturing in real life. Accordingly, the research problem was formatted *"How is simulation best developed and utilized in manufacturing?"*. Overall, it seems that all publications presented are focused on the set research problem.

This dissertation has presented two valuable real-life case examples of how physics-based simulation can be utilized to address the needs of the manufacturing industry. In *Publication I*, an industrial case example study of a veneer peeling lathe was presented. The introduced simulator predicted the general behaviors of the actual peeling lathe with calculated parameter values that were similar if not identical to the measurement data taken from an actual peeling lathe. The presented results are sufficiently accurate to be used as a product development tool. Furthermore, the introduced simulator can be used to teach lathe operators how to operate the peeling lathe and how to more easily solve special cases.

Additionally, In *Publication II* the second industrial case example simulation study presented was about the veneer dryer process. The dynamic simulator for a continuous veneer dryer was built using the computational tools of MATLAB Simulink. The tested model gave adequate results that obeyed the physical principles of thermodynamics. The validated model seems to be useful for optimizing the process of convective drying for the veneer sheets. Therefore, it seems that Research Question 1: "How is physics-based simulation best used to benefit the development of veneer production machinery?" was answered.

Research Question 2 was set *"How can authentic VR environments for physics-based real-time simulators be produced?"* In answer, Publication III presents a procedure for generating a three-dimensional environment based on a photogrammetry approach. The study shows that by taking a photogrammetry-based approach, it is possible to generate environments that exist in the real world. Furthermore, the graphical software can be connected to the simulation software, which makes it possible to operate physics-based simulation models in their real environments.

In addition to the technical contributions, this dissertation was also aiming to study the business perspectives of real-time simulation and digitalization in relation to manufacturing. Research Question 3 was *"How might real-time physics-based simulation change business models in manufacturing?"*.

To answer RQ3, Publication IV studied company value chains and business models in relation to value creation with real-time simulation. Its findings verify that real-time simulation clearly offers advantages. Simulations can lead to higher success rates for new product launches as well as cost savings. However, a successful R&D operation and product development model based on real-time simulation requires manufacturers to upgrade their capabilities. For example, they must bring on new skills to manage various stakeholders. Required marketing capabilities may also relate to the product development processes, for instance, by which firms develop and manage product and service offerings and market information management. In addition, Publication V presented five future trends for DBEs in manufacturing as candidates for further research.

1. DBE environments are increasingly being pushed by technology leaders in the manufacturing industry,
2. Because there are several technology leaders in manufacturing reluctant to work with competitors, production factories will soon be presented with multiple digital twins,
3. To maximize the full potential of DBE and to avoid the service and digitalization paradox, the technology leader should open its business to other ecosystem members,
4. New ventures will positively impact the DBE in manufacturing,
5. A digital platform can establish two- and multisided markets and fuel the next round of innovations and value co-creation in manufacturing.

Answers have been provided to all the targeted research questions. The dissertation has shared state of art research from an industrial point of view while combining publications from the development of industrial scale simulators and publications with business perspectives.

REFERENCES

[1] Aarikka-Stenroos, L., and Jaakkola, E. Value co-creation in knowledge intensive business services: A dyadic perspective on the joint problem solving process. *Industrial Marketing Management 41*, 1 (2012), 15–26.

[2] Adner, R. Match your innovation strategy to your innovation ecosystem. *Harvard Business Review 84*, 4 (2006), 98–107;148.

[3] Adner, R., and Kapoor, R. Value creation in innovation ecosystems: How the structure of technological interdependence affects firm performance in new technology generations. *Strategic Management Journal 31*, 3 (2010), 306–333.

[4] Akter, S., and Fosso Wamba, S. Big data analytics in e-commerce: a systematic review and agenda for future research. *Electronic Markets 26*, 2 (2016), 173–194.

[5] Al-Rubaye, S., Kadhum, E., Ni, Q., and Anpalagan, A. Industrial internet of things driven by sdn platform for smart grid resiliency. *IEEE Internet of Things Journal 6*, 1 (2017), 267–277.

[6] Anderson, K. An order n formulation for the motion simulation of general multi-rigid-body constrained systems. *Computers & structures 43*, 3 (1992), 565–579.

[7] Arthur, W. B. Competing technologies, increasing returns, and lock-in by historical events. *Economic Journal 99*, 394 (1989), 116–131.

[8] Atkins, A. Modelling metal cutting using modern ductile fracture mechanics: quantitative explanations for some longstanding problems. *International journal of mechanical sciences 45*, 2 (2003), 373–396.

[9] Atkinson, K. *Close Range Photogrammetry and Machine Vision.* Whittles Publ., 1996.

[10] Baden-Fuller, C., and Haefliger, S. Business models and technological innovation. *Long Range Planning 46*, 6 (2013), 419–426.

[11] Baharudin, M., Rouvinen, A., Korkealaakso, P., and Mikkola, A. Real-time multibody application for tree harvester truck simulator. *Proceedings of the Institution of Mechanical Engineers, Part K: Journal of Multi-body Dynamics 228*, 2 (2014), 182–198.

[12] Baldwin, C. Y., and Woodard, C. J. The architecture of platforms: A unified view. *Platforms, Markets and Innovation 32* (2009), 19–44.

[13] Bayo, E., and Ledesma, R. Augmented Lagrangian and mass-orthogonal projection methods for constrained multibody dynamics. *Nonlinear Dynamics 9*, 1-2 (1996), 113–130.

[14] Bélanger, J., Venne, P., and Paquin, J.-N. The what, where and why of real-time simulation. *Planet Rt 1*, 1 (2010), 37–49.

[15] Boudreau, K. J. Let a thousand flowers bloom? an early look at large numbers of software app developers and patterns of innovation. *Organization Science 23*, 5 (2012), 1409–1427.

[16] Boudreau, K. J. Platform boundary choices & governance: Opening-up while still coordinating and orchestrating. In *Entrepreneurship, innovation, and platforms*, vol. 37. Emerald Publishing Limited, 2017, pp. 227–297.

[17] Briscoe, G. Digital ecosystems. *arXiv preprint arXiv:0909.3423* (2009).

[18] Burkart, A., Cogliati, S., Schickling, A., and Rascher, U. A novel UAV-based ultra-light weight spectrometer for field spectroscopy. *Sensors Journal, IEEE 14*, 1 (2014), 62–67.

[19] Burnaev, E., Panin, I., and Sudret, B. Efficient design of experiments for sensitivity analysis based on polynomial chaos expansions. *Annals of Mathematics and Artificial Intelligence 81*, 1 (2017), 1–21.

[20] Ceccagnoli, M., Forman, C., Huang, P., and Wu, D. Co-creation of value in a platform ecosystem: The case of enterprise software. *MIS Quarterly 36*, 1 (2012), 263–290.

[21] Chen, H., Chiang, R. H., and Storey, V. C. Business intelligence and analytics: From big data to big impact. *MIS quarterly* (2012), 1165–1188.

[22] Chen, Z., Dahlgaard-Park, S. M., and Yu, L. Service quality management and ecosystem theory. *Total Quality Management & Business Excellence 25*, 9-10 (2014), 1190–1205.

[23] Cheng, J., Zhang, H., Tao, F., and Juang, C.-F. Dt-ii:digital twin enhanced industrial internet reference framework towards smart manufacturing. *Robotics and Computer-Integrated Manufacturing 62* (2020).

[24] Clarysse, B., Wright, M., Bruneel, J., and Mahajan, A. Creating value in ecosystems: Crossing the chasm between knowledge and business ecosystems. *Research Policy 43*, 7 (2014), 1164–1176.

[25] Cooper, R. G., and Sommer, A. F. Agile–stage-gate for manufacturers: Changing the way new products are developed integrating agile project management methods into a stage-gate system offers both opportunities and challenges. *Research-Technology Management 61*, 2 (2018), 17–26.

[26] Cusumano, M., Yoffie, D., and Gawer, A. *The Future of Platforms.* MIT Sloan Management Review, 2020.

[27] Cusumano, M. A., and Gawer, A. The elements of platform leadership. *MIT Sloan management review 43*, 3 (2002), 51.

[28] Da Xu, L., He, W., and Li, S. Internet of things in industries: A survey. *IEEE Transactions on Industrial Informatics 10*, 4 (2014), 2233–2243.

[29] Davenport, T. H., et al. Competing on analytics. *Harvard business review 84*, 1 (2006), 98–107;134.

[30] De Jalon, J. G., and Bayo, E. *Kinematic and dynamic simulation of multibody systems: the real-time challenge.* Springer Science & Business Media, 2012.

[31] De Reuver, M., Sørensen, C., and Basole, R. C. The digital platform: a research agenda. *Journal of Information Technology 33*, 2 (2018), 124–135.

[32] Drumwright, E. A fast and stable penalty method for rigid body simulation. *IEEE Transactions on Visualization and Computer Graphics 14*, 1 (2008), 231–240.

[33] Eisenbeiss, H. *UAV Photogrammetry.* PhD thesis, ETH Zurich, 2009.

[34] Eisenmann, T., Parker, G., and Van Alstyne, M. W. Strategies for two-sided markets. *Harvard Business Review 84*, 10 (2006), 92–101;149.

[35] Eisenmann, T. R., Parker, G., and Van Alstyne, M. Opening platforms: How, when and why? *Platforms, Markets and Innovation 6* (2009), 131–162.

[36] Eloranta, V., and Turunen, T. Platforms in service-driven manufacturing: Leveraging complexity by connecting, sharing, and integrating. *Industrial Marketing Management 55* (2016), 178–186.

[37] Eskola, R., Korpilahti, H., Bozorgmehri, B., Matikainen, M. K., and Mikkola, A. Real-time multi-body co-simulation model of a veneer peeling lathe. *International Journal of Computer Integrated Manufacturing* (2022), 1–23.

[38] Esmaeili, H., Thwaites, H., and Woods, P. C. Workflows and challenges involved in creation of realistic immersive virtual museum, heritage, and tourism experiences: A comprehensive reference for 3D asset capturing. IEEE, pp. 465–472.

[39] Evans, D. S., and Schmalensee, R. *Matchmakers: The new economics of multisided platforms*. Harvard Business Review Press, 2016.

[40] Evans, P. C., and Basole, R. C. Revealing the api ecosystem and enterprise strategy via visual analytics. *Communications of the ACM 59*, 2 (2016), 26–28.

[41] Farrell, J., and Katz, M. L. Innovation, rent extraction, and integration in systems markets. *The Journal of Industrial Economics 48*, 4 (2000), 413–432.

[42] Franco, R., Ortiz Bas, , and Lario Esteban, F. Modeling extended manufacturing processes with service-oriented entities. *Service Business 3*, 1 (2009), 31–50.

[43] Füller, J., Schroll, R., and von Hippel, E. A. User generated brands and their contribution to the diffusion of user innovations. *Research Policy 42*, 6-7 (2012), 1197–1209.

[44] García Jalón, J. d., Álvarez, E., De Ribera, F., Rodríguez, I., and Funes, F. A fast and simple semi-recursive formulation for multi-rigid-body systems. In *Advances in Computational Multibody Systems*. Springer, 2005, pp. 1–23.

[45] Gawer, A. Towards a general theory of technological platforms. In *summer conference* (2010), pp. 16–18.

[46] Gawer, A., and Cusumano, M. How companies become platform leaders. *MIT Sloan Management Review 49*, 2 (2008), 28–35.

[47] Gawer, A., and Cusumano, M. A. Industry platforms and ecosystem innovation. *Journal of Product Innovation Management 31*, 3 (2014), 417–433.

[48] Gawer, A., Cusumano, M. A., et al. *Platform Leadership: How Intel, Microsoft, and Cisco Drive Industry Innovation*, vol. 5. Harvard Business School Press Boston, 2002.

[49] Ghazawneh, A., and Henfridsson, O. Governing third-party development through platform boundary resources.

[50] Gradov, D. V., Yusuf, Y. O., Ohjainen, J., Suuronen, J., Eskola, R., Roininen, L., and Koiranen, T. Modelling of a continuous veneer drying unit of industrial scale and model-based anova of the energy efficiency. *Energy 244* (2021).

[51] Greve, H., and Song, S. Amazon warrior: How a platform can restructure industry power and ecology. *Advances in Strategic Management 37* (2017), 299–335.

[52] Gupta, A. K., and Wilemon, D. L. Accelerating the development of technology-based new products. *California management review 32*, 2 (1990), 24–44.

[53] Hagiu, A. Two-sided platforms: Product variety and pricing structures. *Journal of Economics and Management Strategy 18*, 4 (2009), 1011–1043.

[54] Hakanen, E., and Rajala, R. Material intelligence as a driver for value creation in iot-enabled business ecosystems. *Journal of Business & Industrial Marketing* (2018).

[55] Hannibal, M., and Knight, G. Additive manufacturing and the global factory: Disruptive technologies and the location of international business. *International Business Review 27*, 6 (2018), 1116–1127.

[56] Heffner, M., and Sharif, N. Knowledge fusion for technological innovation in organizations. *Journal of Knowledge Management 12* (2008), 79–93.

[57] Henfridsson, O., and Bygstad, B. The generative mechanisms of digital infrastructure evolution. *MIS Quarterly 37* (2013), 907–931.

[58] Hienerth, C., and Lettl, C. Exploring how peer communities enable lead user innovations to become standard equipment in the industry: Community pull effects. *Journal of Product Innovation Management 28*, s1 (2011), 175–195.

[59] Hienerth, C., Lettl, C., and Keinz, P. Synergies among producer firms, lead users, and user communities: The case of the lego producer–user ecosystem. *Journal of Product Innovation Management 31*, 4 (2014), 848–866.

[60] Hu, L., Nguyen, N.-T., Tao, W., Leu, M. C., Liu, X. F., Shahriar, M. R., and Al Sunny, S. N. Modeling of cloud-based digital twins for smart manufacturing with mt connect. *Procedia Manufacturing 26* (2018), 1193–1203.

[61] Iansiti, M., and Levien, R. *The Keystone Advantage: What the New Dynamics of Business Ecosystems Mean for Strategy, Innovation, and Sustainability.* Harvard Business Press, 2004.

[62] Jacobides, M., Cennamo, C., and Gawer, A. Towards a theory of ecosystems. *Strategic Management Journal 39*, 8 (2018), 2255–2276.

[63] Jamaleddine, T. J., and Ray, M. B. Application of computational fluid dynamics for simulation of drying processes: A review. *Drying technology 28*, 2 (2010), 120–154.

[64] Jeppesen, L. B., and Frederiksen, L. Why do users contribute to firm-hosted user communities? the case of computer-controlled music instruments. *Organization science 17*, 1 (2006), 45–63.

[65] Johanastrom, K., and Canudas-De-Wit, C. Revisiting the lugre friction model. *IEEE Control Systems Magazine 28*, 6 (2008), 101–114.

[66] Johansson, A. E., Raddats, C., and Witell, L. The role of customer knowledge development for incremental and radical service innovation in servitized manufacturers. *Journal of Business Research 98* (2019), 328–338.

[67] Kohtamäki, M., Parida, V., Patel, P. C., and Gebauer, H. The relationship between digitalization and servitization: The role of servitization in capturing the financial potential of digitalization. *Technological Forecasting and Social Change 151* (2020), 119804.

[68] Kohtamäki, M., Partanen, J., Parida, V., and Wincent, J. Non-linear relationship between industrial service offering and sales growth: The moderating role of network capabilities. *Industrial Marketing Management 42*, 8 (2013), 1374–1385.

[69] Korkealaakso, P., Rouvinen, A., Moisio, S., and Peusaari, J. Development of a real-time simulation environment. *Multibody System Dynamics 17*, 2 (2007), 177–194.

[70] Kotha, S., and Basu, S. Amazon and ebay: Online retailers as market makers. *The market makers: How retailers are reshaping the global economy* (2011), 155–180.

[71] Kowalkowski, C., Gebauer, H., and Oliva, R. Service growth in product firms: Past, present, and future. *Industrial Marketing Management 60* (2017), 82–88.

[72] Kusiak, A. Smart manufacturing. *International Journal of Production Research 56*, 1-2 (2018), 508–517.

[73] Lager, T. A conceptual framework for platform-based design of non-assembled products. *Technovation 68* (2017), 20–34.

[74] Law, C. C., and Ngai, E. W. An empirical study of the effects of knowledge sharing and learning behaviors on firm performance. *Expert Systems Applications 34*, 4 (2008), 2342–2349.

[75] Lee, S. M., Olson, D. L., and Trimi, S. Co-innovation: convergenomics, collaboration, and co-creation for organizational values. *Management decision 50* (2012), 817–831.

[76] Lin, S.-W., Miller, B., Durand, J., Joshi, R., Didier, P., Chigani, A., Torenbeek, R., Duggal, D., Martin, R., Bleakley, G., et al. Industrial internet reference architecture technical report. *Industrial Internet Consortium (IIC), Tech. Rep* (2015).

[77] Liu, Q., Leng, J., Yan, D., Zhang, D., Wei, L., Yu, A., Zhao, R., Zhang, H., and Chen, X. Digital twin-based designing of the configuration, motion, control, and optimization model of a flow-type smart manufacturing system. *Journal of Manufacturing Systems 58* (2021), 52–64.

[78] Lu, Y., Liu, C., Wang, K.-K., Huang, H., and Xu, X. Digital twin-driven smart manufacturing: Connotation, reference model, applications and research issues. *Robotics and Computer-Integrated Manufacturing 61* (2020), 101837.

[79] Lu, Y., and Xu, X. Cloud-based manufacturing equipment and big data analytics to enable on-demand manufacturing services. *Robotics and Computer-Integrated Manufacturing 57* (2019), 92–102.

[80] Lusch, R., and Nambisan, S. Service innovation: A service-dominant logic perspective. *MIS Quarterly: Management Information Systems 39*, 1 (2015), 155–175.

[81] McAfee, A., Brynjolfsson, E., Davenport, T. H., Patil, D., and Barton, D. Big data: the management revolution. *Harvard business review 90*, 10 (2012), 60–68, 68, 128.

[82] Menon, K., Kärkkäinen, H., and Gupta, J. P. Role of industrial internet platforms in the management of product lifecycle related information and knowledge. In *IFIP International Conference on Product Lifecycle Management* (2016), Springer, pp. 549–558.

[83] Menor, L. J., and Roth, A. V. New service development competence in retail banking: Construct development and measurement validation. *Journal of Operations Management 25*, 4 (2007), 825–846.

[84] Mevea. Product development, [online document], 2018.

[85] Meyer, M., and Mugge, P. Make platform innovation drive enterprise growth. *Research-Technology Management 44*, 1 (2001), 25–39.

[86] Mohammadi, M., Eskola, R., and Mikkola, A. Constructing a virtual environment for multibody simulation software using photogrammetry. *Applied Sciences 10*, 12 (2020), 4079.

[87] Mohr, J., Sengupta, S., and Slater, S. *Marketing of High-Technology Products and Innovations*, third ed. Prentice-Hall, 2001.

[88] Moore, J. Predators and prey: a new ecology of competition. *Harvard Business Review 71*, 3 (1993), 75–86.

[89] Moore, J. The death of competition: Leadership strategy in the age of business. *Ecosystems* (1996).

[90] Myhren, P., Witell, L., Gustafsson, A., and Gebauer, H. Incremental and radical open service innovation. *Journal of Services Marketing 32*, 2 (2017), 101–112.

[91] Nikolakopoulos, K. G., Soura, K., Koukouvelas, I. K., and Argyropoulos, N. G. UAV vs classical aerial photogrammetry for archaeological studies. *Journal of Archaeological Science: Reports 14* (2017), 758–773.

[92] NIST. Smart manufacturing operations planning and control program, [online document], 2021.

[93] Ojala, A., Evers, N., and Rialp, A. Extending the international new venture phenomenon to digital platform providers: A longitudinal case study. *Journal of World Business 53*, 5 (2018), 725–739.

[94] Oliva, R., and Kallenberg, R. Managing the transition from products to services. *International Journal of Service Industry Management 14* (2003), 160–172.

[95] Olsson, H. Control systems with friction.

[96] Oviatt, B. M., and McDougall, P. P. Defining international entrepreneurship and modeling the speed of internationalization. *Entrepreneurship Theory and Practice 29*, 5 (2005), 537–553.

[97] Parida, V., Sjödin, D., and Reim, W. Reviewing literature on digitalization, business model innovation, and sustainable industry: Past achievements and future promises. *Sustainability 11*, 2 (2019), 391.

[98] Parida, V., Sjödin, D. R., Wincent, J., and Kohtamäki, M. Mastering the transition to product-service provision: Insights into business models, learning activities, and capabilities. *Research-Technology Management 57*, 3 (2014), 44–52.

[99] Parker, G. G., and Van Alstyne, M. W. Two-sided network effects: A theory of information product design. *Management Science 51*, 10 (2005), 1494–1504.

[100] Parker, G. G., Van Alstyne, M. W., and Choudary, S. P. *Platform Revolution: How Networked Markets Are Transforming the Economy–and How to Make Them Work for You.* WW Norton & Company, 2016.

[101] Peláez, J. I., Cabrera, F. E., and Vargas, L. G. Estimating the importance of consumer purchasing criteria in digital ecosystems. *Knowledge-Based Systems 162* (2018), 252–264.

[102] Peltoniemi, M. Preliminary theoretical framework for the study of business ecosystems. *E:CO Emergence: Complexity and Organization 8*, 1 (2006), 10–19.

[103] Qi, Q., Tao, F., Zuo, Y., and Zhao, D. Digital twin service towards smart manufacturing. *Procedia Cirp 72* (2018), 237–242.

[104] Raddats, C., Kowalkowski, C., Benedettini, O., Burton, J., and Gebauer, H. Servitization: A contemporary thematic review of four major research streams. *Industrial Marketing Management 83* (2019), 207–223.

[105] Rahikainen, J., Mikkola, A., Sopanen, J., and Gerstmayr, J. Combined semi-recursive formulation and lumped fluid method for monolithic simulation of multibody and hydraulic dynamics. *Multibody System Dynamics 44*, 3 (2018), 293–311.

[106] Ransbotham, S., and Kane, G. Membership turnover and collaboration success in online communities: Explaining rises and falls from grace in wikipedia. *MIS Quarterly: Management Information Systems 35*, 3 (2011), 613–627.

[107] Rosen, R., Von Wichert, G., Lo, G., and Bettenhausen, K. D. About the importance of autonomy and digital twins for the future of manufacturing. *IFAC-PapersOnLine 48*, 3 (2015), 567–572.

[108] Selander, L., Henfridsson, O., and Svahn, F. Capability search and redeem across digital ecosystems. *Journal of Information Technology 28*, 3 (2013), 183–197.

[109] Senyo, P., Liu, K., and Effah, J. A framework for assessing the social impact of interdependencies in digital business ecosystems. *IFIP Advances in Information and Communication Technology 527* (2018), 125–135.

[110] Senyo, P. K., Liu, K., and Effah, J. Digital business ecosystem: Literature review and a framework for future research. *International Journal of Information Management 47* (2019), 52–64.

[111] Shahbazi, Z., and Byun, Y.-C. Integration of blockchain, iot and machine learning for multistage quality control and enhancing security in smart manufacturing. *Sensors 21*, 4 (2021), 1–21.

[112] Sharma, R., Mithas, S., and Kankanhalli, A. Transforming decision-making processes: a research agenda for understanding the impact of business analytics on organisations. *European Journal of Information Systems 23*, 4 (2014), 433–441.

[113] Sjödin, D., Parida, V., Kohtamäki, M., and Wincent, J. An agile co-creation process for digital servitization: A micro-service innovation approach. *Journal of Business Research 112* (2020), 478–491.

[114] Söderberg, R., Wärmefjord, K., Carlson, J. S., and Lindkvist, L. Toward a digital twin for real-time geometry assurance in individualized production. *CIRP annals 66*, 1 (2017), 137–140.

[115] Srinivasan, A., and Venkatraman, N. Entrepreneurship in digital platforms: A network-centric view. *Strategic Entrepreneurship Journal 12*, 1 (2018), 54–71.

[116] Stanley, J., and Briscoe, G. The abc of digital business ecosystems. *Communications Law 15*, 1 (2010), 12–25.

[117] Storbacka, K., Brodie, R. J., Böhmann, T., Maglio, P. P., and Nenonen, S. Actor engagement as a microfoundation for value co-creation. *Journal of Business Research 69*, 8 (2016), 3008–3017.

[118] Strange, R., and Zucchella, A. Industry 4.0, global value chains and international business. *Multinational Business Review 25*, 3 (2017), 174–184.

[119] Suuronen, S., Ukko, J., Eskola, R., Semken, R., and Rantanen, H. A systematic literature review for digital business ecosystems in the manufacturing industry: Prerequisites, challenges, and benefits. *CIRP Journal of Manufacturing Science and Technology 37* (2022), 414–426.

[120] Tan, K. H., and Zhan, Y. Improving new product development using big data: A case study of an electronics company. *R&D Management 47*, 4 (2017), 570–582.

[121] Tao, F., Cheng, J., Qi, Q., Zhang, M., Zhang, H., and Sui, F. Digital twin-driven product design, manufacturing and service with big data. *International Journal of Advanced Manufacturing Technology 94*, 9-12 (2018), 3563–3576.

[122] Tao, F., Qi, Q., Wang, L., and Nee, A. Digital twins and cyber–physical systems toward smart manufacturing and industry 4.0: Correlation and comparison. *Engineering 5*, 4 (2019), 653–661.

[123] Tao, F., and Zhang, M. Digital twin shop-floor: A new shop-floor paradigm towards smart manufacturing. *IEEE Access 5* (2017), 20418–20427.

[124] Tao, F., Zhang, Y., Cheng, Y., Ren, J., Wang, D., Qi, Q., and Li, P. Digital twin and blockchain enhanced smart manufacturing service collaboration and management. *Journal of Manufacturing Systems* (2020).

[125] Teece, D. Business ecosystems. entry in, 2014.

[126] Teece, D. Dynamic capabilities and (digital) platform lifecycles. *Advances in Strategic Management 37* (2017), 211–225.

[127] Teece, D. J. Explicating dynamic capabilities: The nature and microfoundations of (sustainable) enterprise performance. *Strategic Management Journal 28*, 13 (2007), 1319–1350.

[128] Thibaut, B., Denaud, L., Collet, R., Marchal, R., Beauchêne, J., Mothe, F., Méausoone, P.-J., Martin, P., Larricq, P., and Eyma, F. Wood machining with a focus on french research in the last 50 years. *Annals of Forest Science 73*, 1 (2015), 163–184.

[129] Tiwana, A., and Konsynski, B. Complementarities between organizational it architecture and governance structure. *Information Systems Research 21*, 2 (2010), 288–304.

[130] Uggla, G. 3D city models-a comparative study of methods and datasets, 2015.

[131] Uysal, M., and Mergen, A. Smart manufacturing in intelligent digital mesh: Integration of enterprise architecture and software product line engineering. *Journal of Industrial Information Integration 22* (2021).

[132] Wang, J., Xu, C., Zhang, J., Bao, J., and Zhong, R. A collaborative architecture of the industrial internet platform for manufacturing systems. *Robotics and Computer-Integrated Manufacturing 61* (2020).

[133] Wang, J., Ye, L., Gao, R. X., Li, C., and Zhang, L. Digital twin for rotating machinery fault diagnosis in smart manufacturing. *International Journal of Production Research 57*, 12 (2019), 3920–3934.

[134] Wang, P., and Luo, M. A digital twin-based big data virtual and real fusion learning reference framework supported by industrial internet towards smart manufacturing. *Journal of Manufacturing Systems 58* (2021), 16–32.

[135] Watton, J. *Fluid Power Systems: Modeling, Simulation, Analog and Microcomputer Control*. Prentice-Hall, Inc., 1989.

[136] Welty, J. R., Wicks, C. E., and Wilson, R. E. *Fundamentals of momentum, heat, and mass transfer*. John Wiley & Sons, 1969.

[137] Wernerfelt, B. Tacit collusion in differentiated cournot games. *Economics Letters 29*, 4 (1989), 303–306.

[138] Wheelwright, S. C., and Clark, K. B. *Revolutionizing Product Development: Quantum Leaps in Speed, Efficiency and Quality*. Simon and Schuster, 1992.

[139] Wiedmann, K.-P., Hennigs, N., Varelmann, D., and Reeh, M.-O. Determinants of consumers' perceived trust in it-ecosystems. *Journal of Theoretical and Applied Electronic Commerce Research 5*, 2 (2010), 137–154.

[140] Williamson, P., and De Meyer, A. Ecosystem advantage: How to successfully harness the power of partners. *California Management Review 55*, 1 (2012), 24–46.

[141] Yoffie, D. B., and Kwak, M. With friends like these: The art of managing complementors. *Harvard business review 84*, 9 (2006), 88–98, 157.

[142] Yoo, Y., Boland Jr, R. J., Lyytinen, K., and Majchrzak, A. Organizing for innovation in the digitized world. *Organization Science 23*, 5 (2012), 1398–1408.

[143] Yoo, Y., Henfridsson, O., and Lyytinen, K. The new organizing logic of digital innovation: An agenda for information systems research. *Information Systems Research 21* (12 2010), 724–735.

[144] Yu, I., Mortensen, J., Khanna, P., Spanlang, B., and Slater, M. Visual realism enhances realistic response in an immersive virtual environment-part 2. *Computer Graphics and Applications, IEEE 32*, 6 (2012), 36–45.

[145] Zhu, F., and Iansiti, M. Entry into platform-based markets. *Strategic Management Journal 33*, 1 (2012), 88–106.

Publication I

Eskola, R., Korpilahti, H., Bozorgmehri, B., Matikainen, M., and Mikkola, A.
Real-time muti-body co-simulation model of veneer peeling lathe

Reprinted with permission from
International Journal of Computer Integrated Manufacturing
2022

INTERNATIONAL JOURNAL OF COMPUTER INTEGRATED MANUFACTURING
https://doi.org/10.1080/0951192X.2022.2128216

Taylor & Francis
Taylor & Francis Group

OPEN ACCESS Check for updates

Real-time multi-body co-simulation model of a veneer peeling lathe

Roope Eskola[a,b], Heikki Korpilahti[a], Babak Bozorgmehri[b,c,d], Marko K. Matikainen[b] and Aki Mikkola[b]

[a]Raute Corporation, Research and Development, Lahti, Finland; [b]Mechanical Engineering, School of Energy Systems, LUT University, Lappeenranta, Finland; [c]Department of Mechanical Engineering, KU Leuven, Belgium; [d]DMMS, Flanders Make, KU Leuven, Belgium

ABSTRACT

This paper introduces a real-time co-simulation model for the prediction of the dynamics behavior of a veneer peeling lathe machine. The real-time co-simulation model introduced is described in the framework of multi-body system dynamics. It makes use of a co-simulation procedure in which a semi-recursive multi-body approach is combined with a detailed contact description. In the employed closed-loop semi-recursive method, the constraint conditions are carried out in the system motion differential equations via the augmented Lagrangian method. A contact procedure is presented to describe the contact between the wooden log and the cutting blade and the support rollers. The results obtained by the co-simulation are compared against those experimentally measured through a peeling lathe machine in operation and an approximate finite element model of the peeling process. According to the numerical results, it is concluded that the real-time simulation model can predict dynamic performance of the complicated system of a veneer peeling lathe in real-time. Solvability of equations of motion makes the introduced model suitable to be utilized in a number of product process purposes such as marketing, training and product development projects.

ARTICLE HISTORY
Received 20 August 2021
Accepted 12 September 2022

KEYWORDS
Contact description; Co-simulation; Finite element model; Orthogonal cutting force; Veneer peeling lathe; Real-time multi-body system

1. Introduction

Modern multi-body simulation techniques have enabled the precise description of complex mechanical systems such as vehicles and rotating machines. In many applications, a solution of the relevant equations of motion can be synchronized into real-time. This capability has been available for more than three decades de Jalón and Bayo (1994). The capability of real-time simulation has been applied to a number of applications including user training Baharudin et al. (2014), maintenance applications Korkealaakso (2009), marketing and product development Jaiswal et al. (2019). These multi-body-based approaches can be combined with the models of actuators enabling the description of multi-physical systems Rahikainen et al. (2018).

Multi-body approaches can be categorized based on the generalized coordinates used in the description of kinematics. In the global approaches, the set of coordinates that define absolute translations and rotations of each body of the system are employed. It is worth noting that in the global methods the set of generalized coordinates are not affected by constraints as they are accounted for by a separate vector of constraints. This facilitates the implementation of the global methods, but mitigates the computational efficiency compared to the topological approaches. As an alternative for the global approach, a system topology can be utilized in the description of kinematics. In these topological methods, relative coordinates between the bodies are used. For the open- and closed-loop systems, the use of relative coordinates leads to a computationally powerful procedure of semi-recursive formulation. To take advantage of both methods, Cuadrado et al. (2004) introduced a hybrid formulation composed of the penalty method as an efficient global approach and the semi-recursive formulation. They examined the proposed method in the simulation of a car and made a comparison against the predecessor formulations from the global and topological categories.

Wood is regarded as a highly anisotropic material with a considerable moisture content. This indicates that in addition to the ductile behavior under compression, wood is prone to experience two-fracture modes simultaneously when undergoing normal and

CONTACT B Bozorgmehri babak.bozorgmehri@kuleuven.be

shear deformations. Therefore, establishing a sufficiently accurate relationship between the damage of the wood material model and its effective elastic properties is a critical and complicated task. Moreover, description of a fracture model for the prediction of the peeling process requires experimental measurement of a number of stress-based failure criteria, also known as damage initiation functions Matzenmiller, Lubliner, and Taylor (1995); Orlowski et al. (2013). In the simulation of an orthogonal cutting process in woodworking application, wood should be modeled as an anisotropic elastic-plastic material in which separation of two surfaces releases an amount of energy that is known as the material's fracture toughness. It should be recalled that in the orthogonal cutting, the cutting blade is perpendicular to the direction of motion and the depth of cut corresponds to the feed (i.e. uncut chip thickness) Merchant (1945). This is in contrast to the oblique cutting process in which the cutting blade is at an oblique angle to the direction of motion. It should not be confused with the tangential cutting force that implies on the tangential component of the cutting force applied from the cutting blade. Nairn (2015) modeled the orthogonal cutting with a particular emphasis on material behavior Sulsky, Chen, and Schreyer (1994). In the developed approach, the cutting patch (pre-defined crack) was characterized based on the cohesive zone model Needleman (1987). Subsequently, in Nairn (2016), it was demonstrated that the cutting force in steady-state regime remains constant and can be characterized as a function of a variety of variables. Atkins (2003) showed that the shear plane angle and, consequently, the cutting force depends on the material, the cutting blade rake angle and the depth of cut. This cutting force was later used by Atkins (2005) to determine the fracture toughness and shear yield strength in a wide range of materials including wood and polymers.

In this paper, the tangential cutting force is described according to the Atkins model Atkins (2003) and is incorporated into the system equations of motion in the framework of rigid multi-body dynamics. The use of the rigid multi-body and the closed-loop semi-recursive formulation, in particular, as the underlying formulation for the description of the dynamics of the peeling process has computational merits. This mainly stems from considerably fewer number of degrees-of-freedom to be solved with the employed multi-body system approach. This is particularly the case when comparing the semi-recursive multi-body approach against other multi-body formulations or the finite element methods. The other important motivation to bias the presented approach against the finite element model of the peeling lathe system is the computational effort required to model the contact between the wood and the cutting blade under the plastic deformation and material removal. In the case of the finite element approach, some possible sources of instabilities such as non-physical vibration, non-converged solution or the large number of the demanded Newton's iterations, and extremely small time step that arise from the long-run contact-related elastic-plastic deformation may take place. These limitations would affect the capability of the simulated model in real-time which is the main objective of the presented real-time to provide an efficient and robust tool for the purpose of marketing and product development.

In the three-dimensional finite element model of the peeling process, the variation of the orthogonal cutting force exerted from the cutting blade's edge in terms of the varying rake angles and peeling velocities were investigated while the fracture model is based on the traction-separation behaviour using a cohesive zone element Needleman (1987). Speaking of orthogonal cutting process, the effect of the cutting speed intervals on the stress residuals in a cutting tool is studied by Aydın (2017) using a two-dimensional finite element model. Furthermore, they introduced a finite element-based approach with a displacement-based failure criterion in Aydın and Köklü (2020) and with a Arbitrary Eulerian Lagrangian (ALE) scheme in Aydın and Köklü (2017) to predict the cutting force in the high-speed milling of metal alloys. On the contrary to Aydın and Köklü (2017); Aydın (2017); Aydın and Köklü (2020), the finite element model presented in this work is using a predefined crack based on a cohesive zone model to simulate peeling process and the calculation of the orthogonal cutting force.

The simulator introduced in this paper consists of a multi-body system dynamics model of a peeling lathe, a process model, PLC control systems and an authentic operator's work bench with controls. The multi-body system dynamics model was described using a semi-recursive approach in which the kinematics of the system is described using relative joint coordinates. In this study, cut-joints that are needed to handle a closed-loop system were accounted for using an augmented approach. In the operation of a peeling lathe, the contact between the wood and the blade is critical. To address this, the paper also introduces a novel contact modeling approach tailored to analyze the lathe operation. The contact model introduced is implemented in the Julia programming language coupled with multi-body simulation using a co-simulation on the Mevea platform Moisio et al. (2013). The contact detection algorithm made use of measured geometries from the real logs. The contact model used was based on the penalty forces and friction associated with the contacts was described according to a LuGre friction model. As will be shown in this paper, the real-time model of a lathe can be used in a number of different product processes such as in product development, service business and marketing.

The novelties of the paper and contribution to knowledge of this work are succinctly listed as follows:

- Proposing a co-simulation-based solution procedure for a veneer peeling process using an approximated multibody approach in conjunction with the Atkins cutting force description. The co-simulation procedure is detailed in Section 3.1.
- Comparison of accuracy and robustness of a simple description of the Atkins orthogonal force model against a finite element model of the veneer peeling process. This is presented in Section 4.1.
- Verification of the proposed simulation procedure of the veneer peeling process by comparing the output quantities and particularly the cutting force, respectively, against an experimental measurement and a finite element model. Section 5 is allocated to discuss over verification of the co-simulation.

The remainder of this study is of the following organization: Section 2 briefly reviews the semi-recursive multi-body approach initially studied in de Jalón and Bayo (1994) and the contributing the equations of motion which will be used in the application of the veneer peeling lathe that is presented in detail in Section 3. In Section 3, the crucial terms contributing to the veneer lathe's equations of motion, i.e. the contact-related terms are explained in the framework of the Atkins model Atkins (2003). Section 4 details the co-simulation procedure of the veneer lathe machine with its environment implementation and a number of output parameters are plotted to verify the robustness of the simulated model by comparing against the real-world veneer lathe machine and a finite element description of the peeling process.

2. Multi-body system dynamics

A numerically efficient multi-body simulation model for a dynamic system that consists of a relatively large number of bodies can be obtained using a semi-recursive approach de Jalón and Bayo (1994); Avello et al. (1993); de Jalón et al. (2005). This Section briefly highlights the approach used.

2.1. Semi-recursive method

In recursive kinematics, the position, velocity and acceleration of the interconnected bodies are described in terms of a set of relative coordinates by utilizing a chain or a tree-like configuration of the system. This set of coordinates are selected such that they only describe kinematically admissible displacements. Accordingly, in the description of an open-loop system, the constraint equations are avoided and the equations of motion consist of the same number of generalized coordinates as the number of degrees-of-freedom n Anderson (1992).

When a recursive approach is applied to a closed-loop system, it must be converted into an open-loop system. An open loop system is then returned back to a closed-loop system by imposing constraint conditions. Finally, these constraint conditions can be implemented into the equations of motion by employing approaches such as the method of Lagrange multipliers, penalty method, augmented Lagrangian method or the method based on coordinates partitioning.

One often-used global multi-body approach is the augmented Lagrangian method. When using this method, the equations of motion of a constrained system can be written in terms of a set of generalized global coordinates $\mathbf{q}$ in the following form:

$$\mathbf{M}\ddot{\mathbf{q}} + \mathbf{\Phi}^T_{,\mathbf{q}}\alpha(\ddot{\mathbf{\Phi}} + 2\Omega\mu\dot{\mathbf{\Phi}} + \Omega^2\mathbf{\Phi}) + \mathbf{\Phi}^T_{,\mathbf{q}}\boldsymbol{\lambda} = \mathbf{Q}(\mathbf{q}, \dot{\mathbf{q}}), \tag{1}$$

where $\dot{\mathbf{q}}$ and $\ddot{\mathbf{q}}$ are the generalized velocity and acceleration with respect to the global coordinate system, respectively, $\mathbf{M}$ is mass matrix of the system, $\mathbf{\Phi}^T_{,\mathbf{q}}$ is the Jacobian of the constraint equations $\mathbf{\Phi}(\mathbf{q}(t))$ with respect to the generalized coordinates $\mathbf{q}$, $\mathbf{Q}$ is a force vector that accounts for the externally applied forces and the quadratic velocity vector, α, Ω and μ are the penalty factors, $\boldsymbol{\lambda}$ is a vector of Lagrangian multipliers, which represent the reaction force components. The constraint equations can be differentiated with respect to time as follows:

$$\dot{\mathbf{\Phi}} = \mathbf{\Phi}_{,\mathbf{q}}\dot{\mathbf{q}} + \mathbf{\Phi}_{,t} \quad \text{and} \quad \ddot{\mathbf{\Phi}} = \mathbf{\Phi}_{,\mathbf{q}}\ddot{\mathbf{q}} + \mathbf{\Phi}_{,\mathbf{q}t}\dot{\mathbf{q}} + \mathbf{\Phi}_{,tt}. \tag{2}$$

In this form of the augmented Lagrangian method, all the penalty terms related to fictitious potential, dissipation and kinetic energies are included in the method. As it is known from the classical augmented Lagrangian method, the error in the constraints equations is minimized by iterating Lagrange's multipliers. When this approach is used to express the equations of motion, the generalized coordinates within each time step can be iterated by updating Lagrange's multipliers in the following form:

$$\left(\mathbf{M} + \mathbf{\Phi}^T_{,\mathbf{q}}\alpha\mathbf{\Phi}_{,\mathbf{q}}\right)\ddot{\mathbf{q}}_{i+1} = \mathbf{Q} - \mathbf{\Phi}^T\alpha\left(\mathbf{\Phi}_{,\mathbf{q}t}\dot{\mathbf{q}}_i + \mathbf{\Phi}_{,tt} + 2\Omega\mu\mathbf{\Phi}_{,t} + \Omega^2\mathbf{\Phi}\right) - \mathbf{\Phi}^T_{,\mathbf{q}}\boldsymbol{\lambda} \tag{3a}$$

$$\boldsymbol{\lambda}_{i+1} = \boldsymbol{\lambda}_i + \alpha\left(\ddot{\mathbf{\Phi}} + 2\Omega\mu\dot{\mathbf{\Phi}} + \Omega^2\mathbf{\Phi}\right), \tag{3b}$$

where $\boldsymbol{\lambda}_{i=1} = 0$ for the first iteration indicates that the penalty terms only remain active to compensate for the constraint violations during the first iteration. For more details see de Jalón and Bayo (1994).

The equations of motion represented in Equation 1 can be rewritten in terms of a set of relative coordinates. To this end, the following velocity and acceleration vectors associated with the intermediate coordinate system of body j are defined such that they initially coincide with the origin of the global coordinate system:

$$\mathbf{Z}_j = \begin{bmatrix} \dot{\mathbf{s}}_j \\ \boldsymbol{\omega}_j \end{bmatrix} \tag{4}$$

and

$$\dot{\mathbf{Z}}_j = \begin{bmatrix} \ddot{\mathbf{s}}_j \\ \dot{\boldsymbol{\omega}}_j, \end{bmatrix} \tag{5}$$

$\dot{\mathbf{s}}_j$ is the velocity and $\ddot{\mathbf{s}}_j$ is the acceleration of the intermediate coordinate system of body j de Jalón et al. (2005). In Equations 4 and 5, $\boldsymbol{\omega}_j$ is an angular velocity vector and, correspondingly, $\dot{\boldsymbol{\omega}}_j$ is the angular acceleration vector with respect to the global coordinate system. To be able to express the equations of motion by employing the relative coordinates, it is important to find the relations between the velocity and acceleration in the generalized coordinates used in Equation 1 and those introduced in Equations 4 and 5. This can be accomplished as follows:

$$\dot{\mathbf{q}}_j = \begin{bmatrix} \dot{\mathbf{g}}_j \\ \boldsymbol{\omega}_j \end{bmatrix} = \begin{bmatrix} \mathbf{I}^{3\times3} & \tilde{\mathbf{g}}_j \\ \mathbf{0}^{3\times3} & \mathbf{I}^{3\times3} \end{bmatrix} \begin{bmatrix} \dot{\mathbf{s}}_j \\ \boldsymbol{\omega}_j \end{bmatrix} = \mathbf{D}_j\mathbf{Z}_j, \tag{6}$$

and

$$\ddot{\mathbf{q}}_j = \begin{bmatrix} \ddot{\mathbf{g}}_j \\ \dot{\boldsymbol{\omega}}_j \end{bmatrix} = \begin{bmatrix} \mathbf{I}^{3\times3} & \tilde{\mathbf{g}}_j \\ \mathbf{0}^{3\times3} & \mathbf{I}^{3\times3} \end{bmatrix} \begin{bmatrix} \ddot{\mathbf{s}}_j \\ \dot{\boldsymbol{\omega}}_j \end{bmatrix} + \begin{bmatrix} \tilde{\boldsymbol{\omega}}_j^2\mathbf{g}_j \\ \mathbf{0}^{3\times1} \end{bmatrix} = \mathbf{D}_j\dot{\mathbf{Z}}_j + \mathbf{e}_j \tag{7}$$

where $\dot{\mathbf{g}}_j$ and $\ddot{\mathbf{g}}_j$ are the velocity and the acceleration, respectively, of the center of the mass of body j with respect to the global coordinate system, $\mathbf{I}$ is the identity matrix, $\tilde{\mathbf{g}}_j$ and $\tilde{\boldsymbol{\omega}}_j$ are the skew-symmetric matrices corresponding to vectors $\mathbf{g}_j$ and $\boldsymbol{\omega}_j$. Using Equations 6 and 7, matrix $\mathbf{D}_j$ and vector $\mathbf{e}_j$ can be defined for each body of the system. Using matrix $\mathbf{D}_j$ and vector $\mathbf{e}_j$, mass matrix $\mathbf{M}_j$ and the force vector $\mathbf{Q}_j$ of body j can be re-expressed as

$$\bar{\mathbf{M}}_j = \mathbf{D}_j^T\mathbf{M}_j\mathbf{D}_j, \tag{8}$$

and

$$\bar{\mathbf{Q}}_j = \mathbf{D}_j^T(\mathbf{M}_j\mathbf{e}_j - \mathbf{Q}_j). \tag{9}$$

The relative velocity and acceleration associated with body j can respectively be written in the following forms

$$\dot{\mathbf{Z}}_j = \dot{\mathbf{Z}}_{j-1} + \mathbf{b}_j\dot{z}_j \tag{10}$$

$$\ddot{\mathbf{Z}}_j = \ddot{\mathbf{Z}}_{j-1} + \mathbf{b}_j\ddot{z}_j + \mathbf{d}_j, \tag{11}$$

where $\dot{z}_j$ and $\ddot{z}_j$ respectively describe the relative velocity and acceleration of body j (note that this is a scalar for a body that is connected to a neighboring body by a revolute joint or a translational joint) and $\mathbf{b}_j$ and $\mathbf{d}_j$ describe the type of joint.

Assuming matrix $\mathbf{R}$ to be an orthogonal complement of the Jacobian matrix $\mathbf{\Phi_q}$ whose columns are the basis of the null-space of $\mathbf{\Phi_q}$, the following relationships between the Cartesian velocities, accelerations and the relative ones can be established:

$$\dot{\mathbf{Z}} = \mathbf{R}\dot{\mathbf{z}} \tag{12}$$

$$\ddot{\mathbf{Z}} = \mathbf{R}\ddot{\mathbf{z}} + \dot{\mathbf{R}}\dot{\mathbf{z}}, \tag{13}$$

where $\mathbf{R}$ is the velocity transformation matrix that relates the relative coordinates and generalized coordinates in Equations 4 and 5. The variation of power of the system can be expressed with respect to Equations 6 and 7.

$$(\bar{\mathbf{M}}\dot{\mathbf{Z}} - \bar{\mathbf{Q}}) \cdot \delta\mathbf{Z} = 0. \tag{14}$$

Substituting Equation 12 and Equation 13 into Equation 14 and taking into account that the relative variation of velocities are independent, the final form of the equations of motion can be written for an open-loop system in the form:

$$\mathbf{R}^T\bar{\mathbf{M}}\mathbf{R}\ddot{\mathbf{z}} = \mathbf{R}^T(\bar{\mathbf{Q}} - \bar{\mathbf{M}}\dot{\mathbf{R}}\dot{\mathbf{z}}), \tag{15}$$

where

$$\bar{\mathbf{M}} = \mathrm{diag}(\bar{\mathbf{M}}_1, \cdots, \bar{\mathbf{M}}_j) \quad \text{and} \quad \bar{\mathbf{Q}} = [\bar{\mathbf{Q}}_1^T, \cdots, \bar{\mathbf{Q}}_j^T]^T.$$

In the semi-recursive approach, the equations of motion for a closed-loop system can be derived by utilizing the cut-joint method and then account for the associated constraints using the augmented Lagrangian method as explained earlier and in de Jalón and Bayo (1994); de Jalón et al. (2005). The augmented Lagrangian can be used in the same manner as in the global method in Equation 3a :

$$\left(\mathbf{M}^* + \mathbf{\Phi}_{,\mathbf{z}}^T\alpha\mathbf{\Phi}_{,\mathbf{z}}\right)\ddot{\mathbf{z}}_{i+1} = \mathbf{Q}^* - \mathbf{\Phi}^T\alpha(\mathbf{\Phi}_{,\mathbf{z}t}\dot{\mathbf{z}}_i + \mathbf{\Phi}_{,tt} + 2\Omega\mu\mathbf{\Phi}_{,t} + \Omega^2\mathbf{\Phi}) - \mathbf{\Phi}_{,\mathbf{z}}^T\boldsymbol{\lambda} \tag{16a}$$

$$\boldsymbol{\lambda}_{i+1} = \boldsymbol{\lambda}_i + \alpha\left(\ddot{\mathbf{\Phi}} + 2\Omega\mu\dot{\mathbf{\Phi}} + \Omega^2\mathbf{\Phi}\right), \tag{16b}$$

where $\mathbf{M}^* = \mathbf{R}^T\bar{\mathbf{M}}\mathbf{R}$, $\mathbf{Q}^* = \mathbf{R}^T(\bar{\mathbf{Q}} - \bar{\mathbf{M}}\dot{\mathbf{R}}\dot{\mathbf{z}})$ and $\boldsymbol{\lambda}_{i=1} = \mathbf{0}$ for the first iteration at the beginning of the simulation. It is worth recalling that the zero value for the initial guess indicates that at the first iteration, the constraint equations are enforced with respect to the pure penalty method, and with the rest of the iteration, the initial values for the Lagrange multipliers are amended to a set of optimum values. Iterations can get started by any other numerical values. That, however, might lead to an extended iteration process at the beginning of the simulation. It is also important to note the initial guess $\boldsymbol{\lambda}_{i=1} = \mathbf{0}$ is only used once in the beginning of the simulation. The equations of motion can be integrated with respect to time using the explicit fourth-order Runge-Kutta method similar to the case in the global methods.

The force vector contribution in the general form of equations of motion 16 can be more explicitly described in terms of components of and analogous to Equations 9 and 15 as follows:

$$\bar{\mathbf{Q}} = \bar{\mathbf{F}}_{\text{ext}} + \bar{\mathbf{F}}_{\text{int}} + \bar{\mathbf{F}}_{\text{con}} \tag{17}$$

where:

$$\bar{\mathbf{F}}_{\text{con}} = [\cdots, \bar{\mathbf{F}}_{j,\text{con}}, \bar{\mathbf{F}}_{j+1,\text{con},\cdots}] \tag{18}$$

in which $\bar{\mathbf{F}}_{j,\text{con}}$ and $\bar{\mathbf{F}}_{j+1,\text{con}}$ are the vector of contact forces (contact-related actionreaction of the normal and frictional fields) i.e. between the wooden log and the cutting blade and are anticipated to explain in detail in Section 3.4, $\bar{\mathbf{F}}_{\text{ext}}$ contains the components of the vector of external forces, i.e. the surface forces exerted by the roller supports (nose-bar), and $\bar{\mathbf{F}}_{\text{int}}$ is the vector of internal force i.-e. in the flexible wooden log.

It should be emphasized that the rigid multibody description of the veneer peeling lathe including all the related components (spindle, wooden log, support rollers and the connecting joints) are modeled and simulated in real-time using the Mevea software environment. To investigate the model-reality mismatch by virtue of the simplification made to approximate the real-word veneer lathe with a system of multi-rigid-body, a finite element model of the rotary peeling process is introduced in Section 3 and is further studied in Section 4. In this way, robustness and reliability of the introduced approach to simulate the peeling process is investigated by comparison against the finite element model of the rotary peeling process, and also by comparing against the measurements by the available real-world veneer lathe. For this reason, a new set of parameters for description of the robustness and reliability of the introduced approach (e.g. uncertainty or disturbance effects) are avoided introducing with the presented system equations of motion **16.**

3. Veneer peeling lathe

In this study, a veneer peeling lathe based on the multi-body system dynamics presented in Section 2 and the cutting force description presented in Section 3.4 is introduced. As the title implies, a veneer peeling lathe is a machine that produces veneer to make plywood and laminated veneer lumber (LVL) or to be used as a covering surface for other panels or boards. In the peeling process, the wood log is revolved by using spindles or rollers allowing the veneer to be cut from the outer surface of the log by means of a cutting blade.

The veneer qualities can be affected by the nose-bar are surface smoothness, cracking and thickness fluctuation. In addition, to achieve a uniform thickness veneer to the log lengthwise, the log is supported on the opposite side of the blade during peeling by support rollers. The produced veneer mat is then transferred down the line by a conveyor on to further processes which are not included in this study.

Although the principle of peeling remains unchanged, the modern peeling lathes differ from the old ones. Modern lathes are larger in size and produce more capacity with better veneer quality and with less operators compared to the older machines. This has been accomplished through the use of automation and novel sensor technology. In addition to this, modern lathes are processing smaller size plantation logs more and more instead of the larger rain forests trees to cope with the change in climate and regulations. Moreover, the latest modern lathes are also equipped with electrical actuators that are more energy efficient than older ones which are ran by hydraulic actuators. Annual uptimes are also increased to maximize annual production capacity, and machines are wired and equipped with sensors for predictive maintenance purposes.

Research articles about veneer peeling are mainly focused on process studies about veneer quality or veneer recovery for some specific wood species with some specific sets of process parameters such as correlation between force exerted from the cutting tool and the depth of cut Thibaut and Beauchêne (2004). A significant collection of works are reviewed by Thibaut, Denaud, and Collet (2016). The veneer peeling lathe itself is studied in Xiong and Guo (2016) where the peeling knife movement is modeled and simulated. The study is focused on rotating angle, i.e. pitch angle, of the peeling knife and introduces a mathematical simulation model to describe it.

3.1. Co-simulation of multi-body model of veneer peeling lathe

In this section, a real-time model of a modern peeling lathe is described. The lathe consists of different components, such as linear and step feeders, an XY-precentering unit, transfer arms and the main lathe responsible for peeling a log. The linear and step feeders are in front of the lathe and deliver a wooden log to the precentering unit, where the log shape is scanned using laser sensors. After scanning, the precentering unit calculates the optimal position for the log in the lathe to maximize veneer production, precentering spindles then move to adjust the log position before transfer arms move the log from precentering unit to the lathe main spindles and peeling begins.

The peeling lathe is implemented as a co-simulation model where the lathe mechanics, actuators and sensors are modelled in Mevea software, and a separate model was made for the peeling process written in Julia. Real PLC hardware that is used to control physical lathes is connected to the lathe MBD model via an I/O interface which uses TCP/IP socket connection to transfer data between the PLC and lathe model. Similarly, a TCP/IP socket interface is used to transfer data between the lathe MBD and the peeling process models enabling the co-simulation of lathe mechanics and the forces arising from peeling a log. A schematic of the co-simulation and control model is seen in Figure 1 and topology of the lathe mechanics can be seen in Figure 2. The lathe MBD model consists of 26 bodies and 130 constraints.

The lathe is controlled by the PLC, which sends position and velocity-based targets to PID controllers that drive the actuators responsible for moving different lathe components. Feedback from the lathe to the PLC consists of lathe components' positions and whether a move target was reached or not, as well as feedback from the virtual sensors implemented in the MBD model, for example the laser scanners used by the precentering unit to scan the log shape. At the beginning of peeling, when a log arrives to the main lathe spindles, its location and orientation is sent to the process model along with world locations of the support rollers, main spindles and peeling knife. In the process model, the log orientation is synchronized to the read location and after that it is updated based on the spindles' rotation until the end of the peeling. Locations of the support rollers, peeling knife and spindles are continuously updated from the MBD model. In addition to calculating

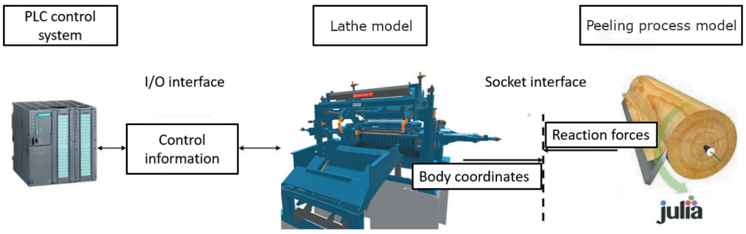

Figure 1. Co-Simulation model structure and interface of the PLC control system.

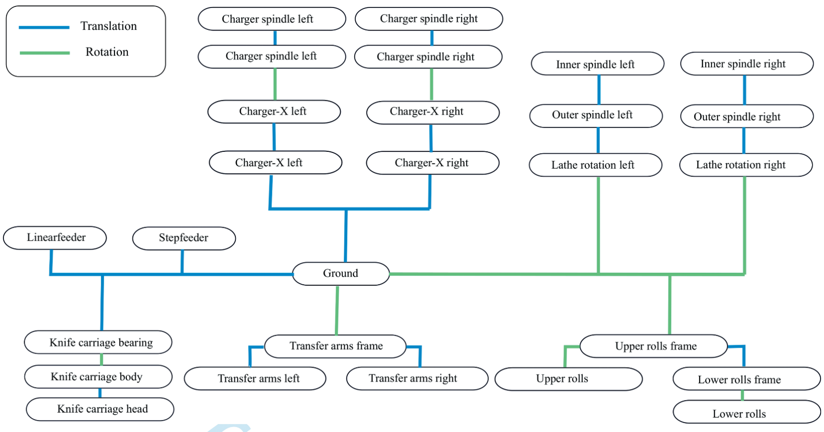

Figure 2. Topology of the lathe model. The blue lines indicate translational joints between the bodies and, correspondingly, the rotational joints are shown by green lines.

the cutting force using Atkins' equations, the peeling process model handles collision detection and handling between the log and support rollers and peeling knife. The procedure mentioned above is briefly illustrated by Figure 3. The flowchart in Figure 3 aims to correlate the hardware schematically representing the co-simulation procedure of the peeling process in Figure 1 with the required steps and conditions explained in this subsection. It should be remarked that the co-simulation procedure (illustrated by Figures 1 and 3 is simply a solution to the problem of that Mevea software Mevea (2005–2020) was not able to handle both the peeling process and MBD model of the lathe.

3.2. Contact description in peeling process model

In the simulation procedure, the contact detection task between the log and the peeling tool of the lathe is accomplished in the peeling process model using position and orientation information. Due to the irregular shape of the log, see Figure 4, the log comes into contact with the peeling tool at multiple locations. The contact constraints between the log and the neighboring bodies are enforced using the penalty method as explained in Drumwright (2008). Friction between contact pairs is in turn modeled using the LuGre dynamic friction model Olsson (1996). It is noteworthy to point out that the time integration associated with LuGre friction is accomplished outside of the equations of motion. In this study, the peeling forces are computed using fracture mechanics-based off-cut by shear equations introduced in Atkins (2003). Details of the peeling force computing will be explained at a later Section. Figure 4 shows a schematic view of a log under peeling process.

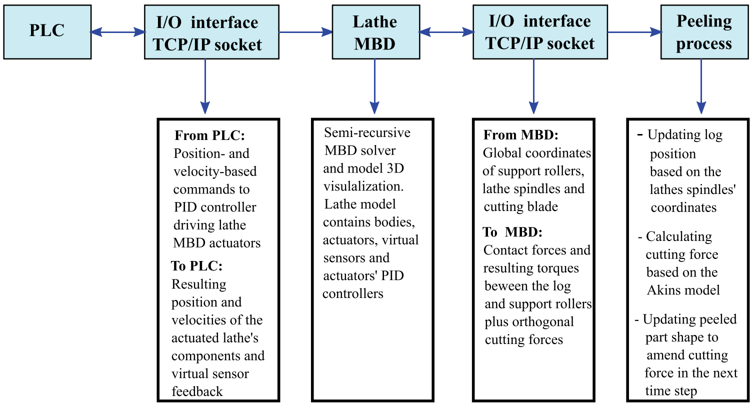

Figure 3. Flowchart of the steps of the proposed co-simulation procedure.

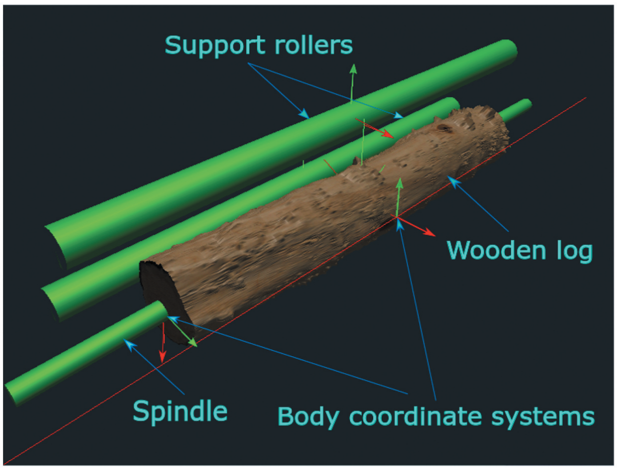

Figure 4. A schematic view of a raw log under peeling process.

The log's geometry for the purpose of real-time simulation is generated from the $X-Y$ charger scanner during peeling process in the production lines. The $X-Y$ charger is a centering device that determines the optimal peeling center for logs in order to maximize veneer recovery/yield. The geometry data used in this study include natural asymmetric shapes such as logs with anisotropic cross-sections or devoid of straightness in the longitudinal direction. In the process model, the geometry of a log is defined as the points cloud. The points, in turn, are arranged into a set of 360 collocated points (one measurement point per degree of a full circle circumference) which determine the log's circumference profile. The sequence of profiles in the log longitudinal direction characterizes the overall shape of log to be processed. In practice, the number of profiles can vary from a few up to full resolution of the scanner data. The accuracy of the log's geometry affects the number of calculations that have to be accomplished in the process model. Accordingly, to ensure the real-time computation, the geometry description must be balanced with respect to the available CPU power. In the simulation model used, a hundred profiles (describing cross-sections along the longitudinal direction) are used to describe the log geometry. Due to the noise produced when processing with the raw data scanner, data preprocessing filters were implemented into the process model to sanitize and to smooth out the geometry representation. Note that the noisy geometry data does not affect the determination of the optimal peeling center search, but makes the contact search task and peeling force calculation cumbersome.

3.3. Contact detection in peeling process model

Contact detection between the log, the support rollers and the round knife-bar is accomplished using point-in-cylinder procedure. In this study, the rollers and the knife-bar are modeled as cylinders. A vector between two ends of a roller is denoted **u** and correspondingly, a length of the roller can be obtained as $\|\mathbf{u}\|^2$. A contact event between a cylinder and arbitrary point p can be detected using Algorithm 1 . First, a vector carrying the cylinder cap end O_a to point p denoted **v** is defined according to Figure 5. Next, it can be checked if the point p lies between end caps O_a and O_b of the log using the following equation:

$$0 < d < \|\mathbf{u}\|^2, \tag{19}$$

where

$$d = \mathbf{u} \cdot \mathbf{v}. \tag{20}$$

Correspondingly, point p lies within the cylinder radius if $\|\mathbf{q}\|^2 < r_{cyl}^2$ where

$$\|\mathbf{q}\|^2 = \mathbf{v} \cdot \mathbf{v} - \frac{d^2}{\|\mathbf{u}\|^2}. \tag{21}$$

The contact interpenetration d_i can be now calculated as follows:

$$d_i = \sqrt{r_{cyl}^2 - \|\mathbf{q}_i\|^2}, \tag{22}$$

where subscript i denotes the current time step.

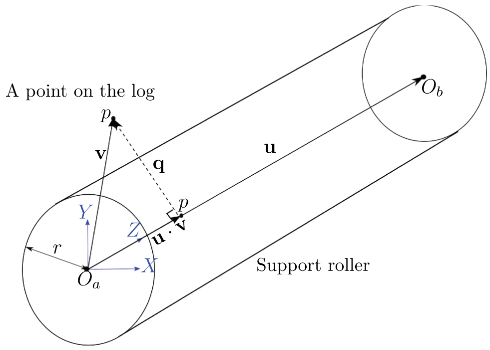

Figure 5. A simple representation of the contact detection task.

The peeling process is crucial in plywood and LVL production because the veneer quality determines a large part of the quality and properties of the plywood or LVL end products. It has been experimentally observed that the peeling process takes place at the border between off-cut formation by a shear plane and that by bending. This mechanism can be verified by lathe inspections in which there is an evident that the cracks are propagating from the surface almost perpendicularly from the cutting direction into the veneer. If the cracks propagate through the whole thickness of the veneer, it would break into fragments. A nose-bar is used to compress the wood just before the tool edge to keep the peeling process mainly by shear cutting, and thus, inhibiting the formation of checking and cutting by bending Atkins (2009a); Thibaut and Beauchêne (2004). As the veneer is the end product from the peeling process and its quality plays a major role in the quality of the plywood and LVL product, it is important that the cutting is kept in the shear mode as much as possible.

3.4. Cutting force description in peeling process model

In this study, the cutting mode is restricted to an off-cut formation by shear. The cutting model is based on

Algorithm 1. Contact detection algorithm to check if the contact points candidates are inside of the cylinder shown in Figure 5

```
if 0 < d < ||u||^2 then   ▷ The contact point candidate is located between the cylinder caps
    if ||q||^2 < r_cyl^2 then   ▷ The contact point candidate is inside the cylinder
        The gap function (penetration due to contact) is given by Equation (22).
    end if
end if
```

the single shear plane model introduced by Ernst and Merchant (1941), enhanced by including the work of formation of free surfaces as shown by Atkins (2003). Although the shear plane cutting model originated from metal cutting theory, the addition of material dependent parameters affecting the shear plane angle has allowed it to be generalized to other materials with differing properties. As an example, Wyeth has employed the Atkins' model to Nylon 66 Wyeth (2007) and dry Douglas Wyeth, Goli, and Atkins (2009). Orlowski et al. (2013) have used the approach to predict the cutting forces for sawing of Pinus Sylvestris with sash gang saw, circular and band sawing machines. In Figure 6, force equilibrium circle, parameters and speed diagram of Ernst-Merchant model are presented.

As shown in Figure 6, the resultant force F_R is decomposed into components F_C and F_v that are, respectively, tangential and normal (radial) to the tool motion path. In Figure 6, F_C is also known as the orthogonal cutting force component and F_{SP} is the cutting force within which the shear and ploughing mechanisms are included Junz Wang and Zheng (2002). Unlike Ernst-Merchant theory Ernst and Merchant (1941); Stephenson and Agapiou (2016) in which the force-balance equations were used, Atkins describes the cutting work-balance equation in steady state as follows:

$$\begin{aligned} F_C v &= \tau_y \gamma h_0 w v \\ &+ [F_C \sec(\beta_{fr} - \alpha_r)\sin(\beta_{fr})] v \frac{\sin(\phi)}{\cos(\phi - \alpha_r)} \\ &+ R w v, \end{aligned} \quad (23)$$

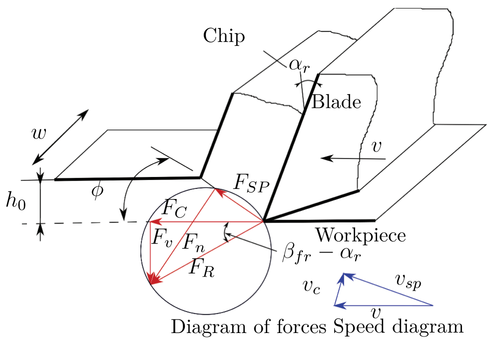

Figure 6. Cutting process forces based on Ernst-Merchant model.

where v is the cutting velocity, τ_y is shear yield strength, γ is the shear strain parallel to the shear plane, h_0 is the depth of cut, w is the cut width, β_{fr} is the friction angle, α_r is the tool rake angle, ϕ is the shear plane angle and R is fracture toughness of the material which is per definition the specific work done when a new surface is formed. As it is evidenced by the work-balance Equation 23, on contrary to the Ernst & Merchant theory, the friction between at the cutting tool (blade) and the peeling surface taken into account. The three terms in the right hand side of Equation 23 describe in order: the work done by plastic deformation parallel to the shear plane, work of friction between the chip and the tool rake face and the work needed for the formation of new surfaces Atkins (2003). The shear strain parallel to the shear plane appeared in Equation 23 can be expressed as

$$\gamma_\varepsilon = \frac{\cos(\alpha_r)}{\cos(\phi - \alpha_r)\sin(\phi)}. \quad (24)$$

After substitution the shear strain (24) into Equation 23 , the resulting force-balance equation is of the following form:

$$F_C = w\tau_y h_0 \frac{\cos(\beta_{fr}-\alpha_r)}{\sin(\phi)\cos(\phi+\beta_{fr}-\alpha_r)} \left[1 + \frac{R\cos(\alpha_r-\phi)\sin(\phi)}{\tau_y h_0 \cos(\alpha_r)}\right]. \quad (25)$$

Equation 25 describes Ernst & Merchant's force-balance equation in the case where the effect of fracture toughness is removed by setting R to be equal to zero Boothroyd (1988). According to Ernst and Merchant (1941), the shear plane angle ϕ changes during cutting such that the work provided by $F_C v$ is minimized. The shear plane angle can be found by differentiating Equation 25 with respect to ϕ and then solving for ϕ. The closed form solution for shear plane angle was introduced by Williams Wyeth, Goli, and Atkins (2009) and is

$$\cot(\phi) = \tan(\beta_{fr} - \alpha_r) \pm \sqrt{1 + \tan^2(\beta_{fr} - \alpha_r) + Z\tan(\beta_{fr} - \alpha_r)}, \quad (26)$$

where $Z = \frac{R}{\tau_y h_0}$ is a parameter which ties the shear plane angle to material-dependent properties and to the depth of cut Atkins (2009a). After the shear plane angle is solved, the force F_C parallel to the tool path can be solved by rewriting Equation 23 to get

$$F_C = \frac{w\tau_y \gamma h_0}{Q} + \frac{Rw}{Q}, \quad (27)$$

where Q is given by

$$Q = 1 - \frac{\sin(\phi)\sin(\beta_{fr})}{cos(\beta_{fr} - \alpha_r)\cos(\phi - \alpha_r)}. \quad (28)$$

The shear force applying along the shear plane is given as follows:

$$F_S = F_c \cos\phi - F_v \sin\phi, \quad (29)$$

where

$$F_v = F_C \tan(\beta_{fr} - \alpha_r) \quad (30)$$

is the normal component of the force applied to the tool path. Thibault & Beauchene did an experimental analysis of wood mechanical properties during green wood peeling and found that the friction angle β_{fr} is not highly dependent on cutting force values nor temperature of the wood, but cutting speed has a significant effect on it. There is, in fact, a linear relationship between friction angle and cutting speed in semi-logarithmic scale with a cutting speed range of 1 . . . 1000 mm/s. The friction angle roughly is the half of the cutting speed increases from 1 mm/s to 1000 mm/s. This has such a large effect on the cutting process that it cannot be neglected from the model Thibaut and Beauchêne (2004). Accordingly, the change in friction angle can be approximated as

$$\beta_{fr} = 28\,log\,(v) - 4.667, \quad (31)$$

where the cutting velocity v is expressed in mm/s. It is noteworthy mentioning that the tangential cutting force $F_c \equiv \overline{F}_{con} = \text{average}(\overline{\mathbf{F}}_{con})$ as introduced in Section 2.

3.5. Finite element model of peeling process

To provide a deeper insight into the tangential cutting force F_c that is discussed in detail in the following section, a comparison is presented here between the tangential cutting force given on the basis of the Atkins model Atkins (2003) and one computed according to a finite element implementation of the peeling process in the veneer lathe machine. The cutting force description based on the Atkins model is to be compared against the quasi-static and dynamics analyses of the peeling process in a veneer lathe. In the finite element approach using commercial finite element software ABAQUS, the crack propagation during the peeling process is described based on the damage model using cohesive zone elements within a pre-defined crack path. The material description of the wood is based on the Saint Venant – Kirchhoff material model in the framework of the three-dimensional orthotropic elasticity.

4. Numerical results

This section is allocated to elaborate the peeling process model using the finite element method briefly explained in Section 3.5 and the co-simulation procedure of the veneer peeling lathe in operation. First, the implemented finite element model of the peeling process is investigated in terms of the parameters sensitivity including the varying rakes angles and peeling velocities. Second, the co-simulation environment and the details of the simulation aspects are presented. Third, the co-simulation results are presented, including the practical engineering output quantities and also the theoretical contact-related quantities.

4.1. Finite element implementation of the peeling process: cutting (contact-related) force study

Table 1 provides the material properties of the soft wood specie, Spruce Sitka (can be found in Green, Winandy, and Kretschmann (1999)) and also the wood fracture characteristics chosen for the finite element analyses. The fracture characteristics are adopted from Reiterer, Sinn, and Stanzl-Tschegg (2002) and are used to specify the cohesive zone element parameters in the finite element analyses.

The blade can either be assumed to be a discretized rigid body or be modeled as a deformable body made of steel. The finite element representation of the peeling process is illustrated by Figure 7. The cohesive element under large adhesive deformation is specified in the figure. The finite element simulation in Figure 7 is based on the quasi-static analysis when rake angle is assumed to be $\alpha_r = 67.5^{\circ}$ which is the value of the rake angle in the case of the models based on the co-simulation, finite element and the experimental measurement, respectively, presented in Sections 4.3, 5.1 and 5.2 . Figure 8 shows the cutting force as a function of the six ascending values for the rake angle when performing a quasi-static analysis based on the finite element model and Equation 25 . It can be seen from Figure 8 that the cutting forces are affected by the

Table 1. Parameters of the soft wood Spruce Sitka and the fracture characteristics.

Parameters	Value
Density ρ [kg/m^3]	550
Young's modulus in longitudinal direction E_L [MPa]	10080
Young's modulus in radial direction E_R [MPa]	1377
Young's modulus E_T in tangential direction [MPa]	814
Poisson ratio in *LR* plane ν_{LR}	0.399
Poisson ratio in *LT* plane ν_{LT}	0.618
Poisson ratio in *RT* plane ν_{RT}	1.090
Poisson ratio in *RL* plane ν_{RL}	0.056
Poisson ratio in *TL* plane ν_{TL}	0.038
Poisson ratio in *TR* plane ν_{TR}	0.664
Mode I stress factor (shear strength for peeling) [Mp]	9.559
Mode I fracture critical energy density G^f_{TL} [J/mm^2]	0.000840
log length [mm]	1500
log radius [mm]	150

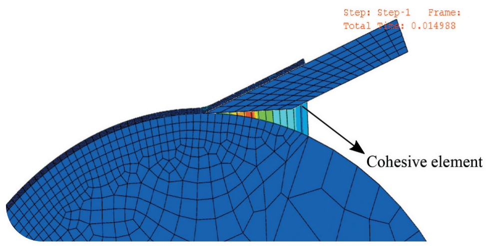

Figure 7. Illustration of peeling process in the quasi-static analysis. The depth of cut is 3 mm and rake angle is 67.5°. The cohesive element adhesion-like deformation is specified.

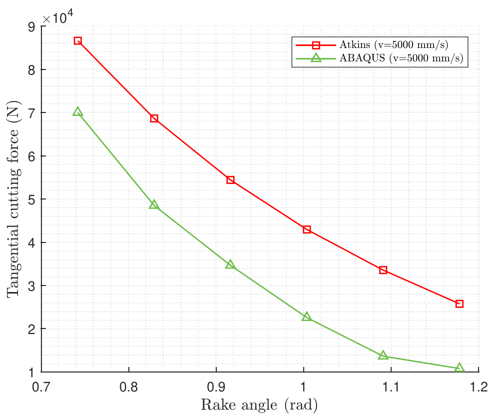

Figure 8. Comparison of the tangential cutting forces. The results are obtained using the Atkins model and the finite element model that represents the peeling process. The finite element model is solved using the quasi-static analysis when an equivalent rotation to the peeling speed of 5000 mm/s is prescribed. The depth of peeling cut is assumed to be 3 mm.

rake angle in both cases of the finite element and the Atkins models, resembling each other's trend. It is

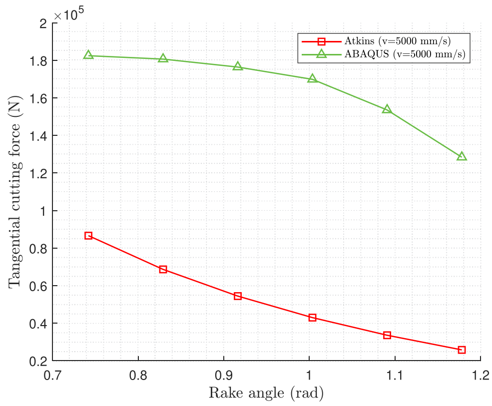

Figure 9. Comparison of the tangential cutting forces between the Atkins model and that obtained by the finite element representation of peeling process using dynamics analysis when the peeling speed is 5000 mm/s. The depth of peeling is assumed to be 3 mm.

worth mentioning that the results of the quasi-static simulation are based on the relatively thin depth of cut, i.e. 3 mm and the prescribed rotation of 0.375 rad is equivalent to the cutting velocity when the simulation time is 0.015 s.

Figure 9 plots the cutting forces as a function of the rake angle in the case of a dynamic analysis. Again, the results are based on the finite element model in ABAQUS and Atkins model (Equation 25). Figure 9 shows two significant discrepancies between the value of cutting forces corresponding to each rake angle and between the directions of the concavity of the curves for the finite element and Atkins solutions. The difference between the quasi-static and dynamic analyses can be explained by recalling the fact that the Atkins model describes the cutting force based on the geometrical parameters and material properties such as shear strength. The effects of the inertia, the material law used in modeling the wood, and the fracture/damage model are not considered in Atkins model while; however, they do contribute to the finite element solution of the cutting force. Accordingly, the non-linearities in the contact dynamics stemming from the large elastic-plastic deformation during the peeling come into the picture, which are absent in the Atkins model and are also hidden in the quasi-static analysis in ABAQUS. This quasi-static attribution of the Atkins model will further be illustrated by a set of results for cutting force versus rake angle. Therein, the depth of peeling cut is assumed to be 10 mm, the quantity which plays a crucial role in both the dynamics of the finite element and the Atkins force models. Figure 10 plots the cutting force values corresponding to the six rake angle. Analogous to Figure 9, the quasi-static analysis was performed with the finite element model, but the depth of cut was increased to 10 mm to investigate its effect on the results agreement. As expected, the Atkins model conforms to the finite element solution more amenable and for the higher values of the rake angle the two solutions are almost coincident. Predictably, Figure 11 indicates a stronger agreement in terms of values of the reaction (cutting) force imposed by the rigid blade between the two approaches: the finite element and Atkins. On the contrary, the direction of the concavity of the two curves are oppositely disposed to each other, that was the case for the other dynamic analysis shown in Figure 9 in which the concavity direction suddenly changed at rake angle of 0.8 rad. Finally, Figure 12 shows a difference between the curves' direction representing the cutting force against the rake angles that is now more significant than that under the lower cutting speed of 5000 mm/s. This latter finding and all the above discussions over the two finite element and Atkins solutions, concretely support the statement over the quasi-static attribution of the Atkins model.

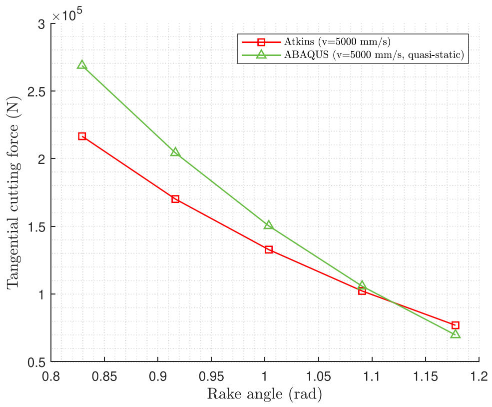

Figure 10. Comparison of the tangential cutting forces. The results are obtained using the Atkins model and the finite element model that represents the peeling process. The finite element model is solved using the quasi-static analysis when an equivalent rotation to peeling speed of 5000 mm/s is prescribed. The depth of peeling cut is assumed to be 10 mm.

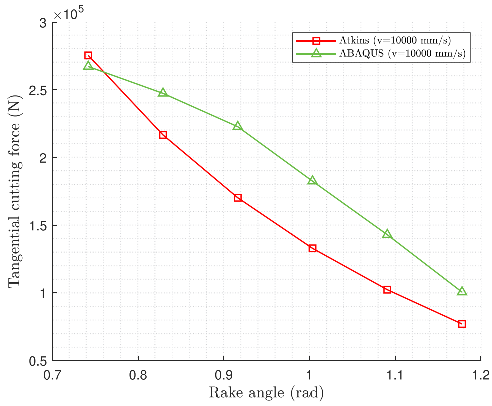

Figure 11. Comparison of the tangential cutting forces between the Atkins model and that obtained by the finite element representation of peeling process in a veneer lathe using dynamics analysis when the peeling speed is 5000 mm/s. The depth of peeling is assumed to be 10 mm.

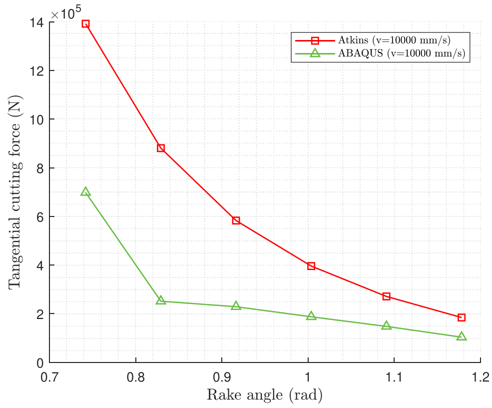

Figure 12. Comparison of the tangential cutting forces between the Atkins model and that obtained by the finite element representation of peeling process using dynamics analysis when the peeling speed is 10,000 mm/s. The depth of peeling is assumed to be 10 mm.

On the other hand, the finite element approach is highly sensitive to the increasing peeling velocity. This can be interpreted from Figures 11 and 12 where the cutting forces follow two different behaviors with respect to the rake angles. Moreover, in the case of the peeling depth of 3 mm, the solution in the finite element was not converged when the peeling speed was set to be 10,000 mm/s that is abstained from presenting here. As a summary, with respect to the computational cost of the finite element approach, the Atkins model was found to have some merits over the finite element approach integrated with the multi-body system approach.

4.2. Co-simulation environment: implementation aspects and imposition of contact-related constraint

In this study, the fourth-order Runge-Kutta time integration scheme with time step of 1 ms was used to compute dynamic performance of the lathe operation. As explained before, the PLC automation was connected to a simulation model to ensure that its control resembles a real lathe control. The co-simulation procedure used allows the saving and plotting of several data sources, a few of which are introduced in this chapter. The simulation was run on a Windows 10 environment. The contact model was implemented using Julia v1.5 and the lathe multi-body model was simulated in a C++ environment. Communication between Julia and the lathe model was accomplished via a TCP/IP socket connection. Visualization of the lathe model can be done using Mevea visualization component Mevea (2005–2020), or via a link to Unity (game engine) Unity (2005–2020) scene built for the simulation model.

Process model visualization was implemented in OpenGL/Julia and runs with the process model and can be toggled on or off. Due to the fact that Julia is a garbage collected (GC) language, the dynamic memory allocation is avoided in the simulation of the loops in the process model. By skipping the memory allocation during the loops simulation, Julia performs sufficiently fast to be used as the main programming language for the model. So, it justifies employing Julia rather than some low-level languages such as C++. The developed simulator was operated mostly in automatic mode, however, user interface was also developed. The simulator is controlled from the lathe operator's work bench with authentic controls such as joysticks and a touch screen, shown in Figure 13.

The time step during the simulation of the lathe is limited due to hydraulics model Oshtorjani, Mikkola, and Jalali (2019), and it was set to be 0.001 s. A considerable effort was placed on the implementation of the contact model to take advantage of the modern

Figure 13. Simulator has an authentic operator chair with controls and touch screen user interface.

CPU's pipe-lined nature. The CPU cache locality was kept in mind when selecting the suitable data structures and algorithms. In addition, the contact search and handling were written using Single Instruction Multiple Data (SIMD) to make use of data level parallelism. Auto vectorization by the compiler was relied on the less emerged calculation loops. This also requires to check the resulted assembly code to make sure that the vectorization has been used. After the contact events between a log and the bodies have been detected, the contact constraints are imposed using the penalty method according to Drumwright (2008) as follows:

$$F_{penalty} = k_p d_i - k_v \dot{s}_n + k_i I_{term}, \tag{32}$$

where k_p is the contact stiffness, k_v is the damping coefficient, $\dot{s}_n$ is the relative velocity of the bodies along the contact normal direction, k_i is the integration coefficient, and I_{term} is a term associated with the integration. The integration term used in Equation 32 is calculated according to Atkins (2009b) in the following form:

$$I_{term} = \sum_{i=-101}^{-1} \lambda^{t-t_i-1} \max d(y, t_i), \tag{33}$$

where t is the current time step, t_i is previous time step, $d(y, t_i)$ is the penetration depth of point y at time step t_i and λ is a factor which reduces the contribution of the previous penetrations. A setting of $0.8 < \lambda < 0.9$ is recommended Drumwright (2008). For every time step, only the maximum penetration depth between the body and the log is tracked as shown in the Equation 33. Note that the tracking is limited to the most recent hundred steps to optimize computational effort related to the force calculation during continuous contact. During normal operation, the backup rolls and the knife-bar are not intended to have sudden contact with the log, but instead provide constant contact pressure to prevent log deformation away from the peeling knife.

In this study, friction associated with the contacts is described using the LuGre friction model. It is a continuation of the Dahl friction model and is able to describe important friction phenomena such as hysteresis and stick-slip condition Olsson (1996). The friction between bodies is modeled based on the average elastic deformation of bristles, which simulates the micro-scale imperfections on the contact surfaces. The bristles function as springs and the friction force is thus related to the bristles' stiffness. When the force moving the bodies increases over the bristles' capacity to deform, they start to slide and the bodies begin to move relative to each other. The average bristle deflection z_b is modeled with the following differential equation

$$\dot{z}_b = \dot{s}_t - \sigma_0 \frac{\dot{s}_t}{g} z_b, \tag{34}$$

where $\dot{s}_t$ is the relative tangential velocity of the contact points, σ_0 is the bristle stiffness, $g(\dot{s}_t)$ is a velocity dependent friction function that affects the average bristle deflection. A common description of the friction function that captures Coulomb and Stribeck effects is of the following form:

$$g = F_C + (F_S - F_C) e^{\sqrt{-\frac{\dot{s}_t}{s_s}}}, \tag{35}$$

where e is Napier's constant and s_s is the Stribeck velocity Åström and de Wit (2008). Friction force in the contact can be calculated as

$$F_f = \sigma_0 z_b + \sigma_1 \dot{z}_b + \sigma_2 \dot{s}_t, \tag{36}$$

where σ_0 is the bristle stiffness, σ_1 is the bristle damping coefficient and σ_2 is the viscous friction coefficient Olsson (1996); Åström and de Wit (2008).

Table 2. Parameters of the soft wood Scots pine and the fracture characteristics used with the numerical simulations in Section 4.

Parameters	Value
Density ρ [kg/m^3]	550
Young's modulus in longitudinal direction E_L [MPa]	10080
Young's modulus in radial direction E_R [MPa]	1377
Young's modulus in tangential E_T direction [MPa]	814
Poisson ratio in LR plane ν_{LR}	0.399
Poisson ratio in LT plane ν_{LT}	0.618
Poisson ratio in RT plane ν_{RT}	1.090
Poisson ratio in RL plane ν_{RL}	0.056
Poisson ratio in TL plane ν_{TL}	0.038
Poisson ratio in TR plane ν_{TR}	0.664
Mode I stress factor (shear strength for peeling) [Mp]	9.559
Mode I fracture critical energy density G^f_{TL} [J/mm^2]	0.00084
log length [mm]	1500
log radius [mm]	150

4.3. Co-Simulation results: practical engineering and the theoretical contact-related quantities

The log specimen is Scots Pine (pinus sylvestris) with the length of 1500 mm, radius of 150 mm. The peeling speed is 100 m/min and the depth of peeling cut is set to be 3.2 mm. The detailed material properties and fracture characteristics of the wood specie used in the simulations and experiments of this example are collected in Table 2. In the co-simulation of peeling process, the wood material parameters used, namely, the fracture toughness R and shear yield strength τ_y, were taken from Orlowski et al. (2013), where the parameters were experimentally measured for Scots Pine. In Figure 14, the torque and power of the lower support roller motor are depicted. As can be seen from the figure, the support roller's motor torque is affected by the friction between the roller and the log.

In normal operation, the support rollers contribute work into rotating the log. This is to minimize the risk of spin-out occurring where the log end caps fail to transmit torque and break, causing the spindles to function as drills and penetrate into the log. The spin-out could take place if all the needed torque comes solely from spindles.

Figure 15 shows the contact forces associated with the lower support roller. These results are obtained from contact description of the process model. The contact forces are expressed in the global reference frame due to the lengthwise axis of support rollers being parallel with the global Z-axis.

Figure 16 shows the torque obtained from the friction model. The torque applies between the lower support roller and the log. In Figure 17, the torque and power curves of the main motor

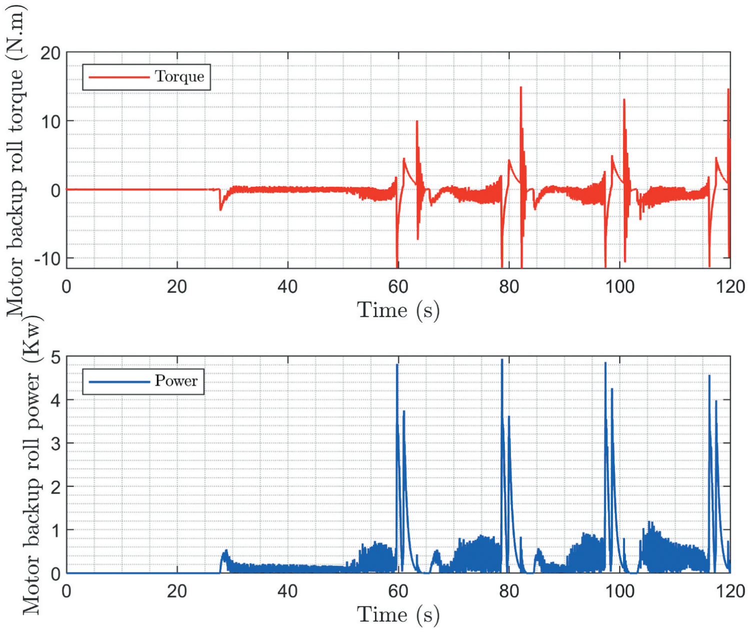

Figure 14. Torque and power of the lower support roller motor with the co-simulated model.

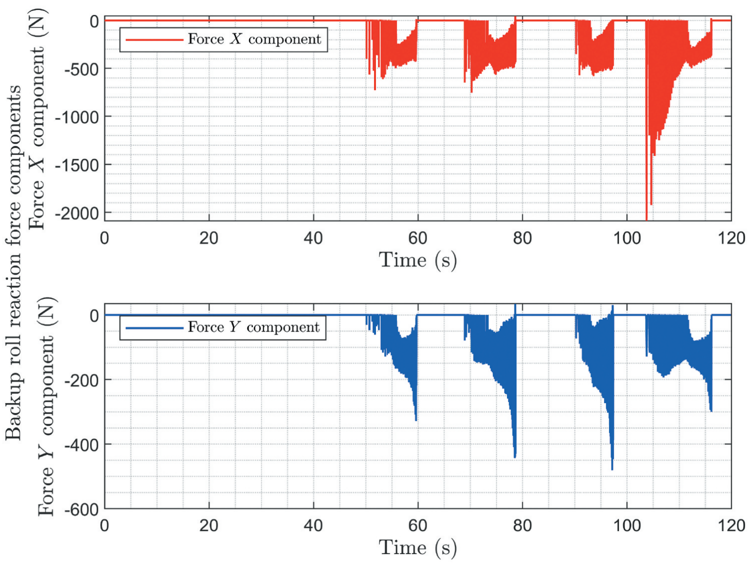

Figure 15. Lower support roller forces with the co-simulated model.

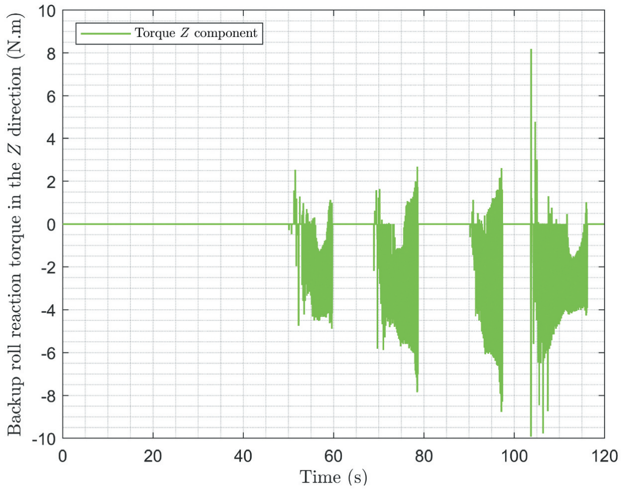

Figure 16. Lower support roller torques with the co-simulated model.

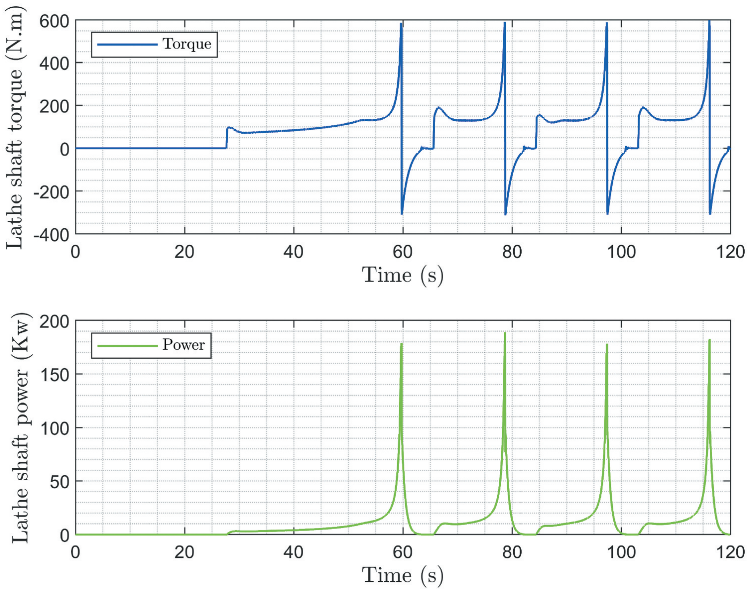

Figure 17. Torque and power of the lathe spindle motor with the co-simulated model.

responsible for lathe spindles' rotation are shown. There are four peeling cycles visible, roughly corresponding to time ranges 30–60 s, 65–80 s, 85–100 s and 105–120 s. The first cycle is longer due to knife carriage being farther away from the spin center compared to the other cycles. At the start of a peeling cycle, there is a jump in motor torque after which the torque lowers a bit when the

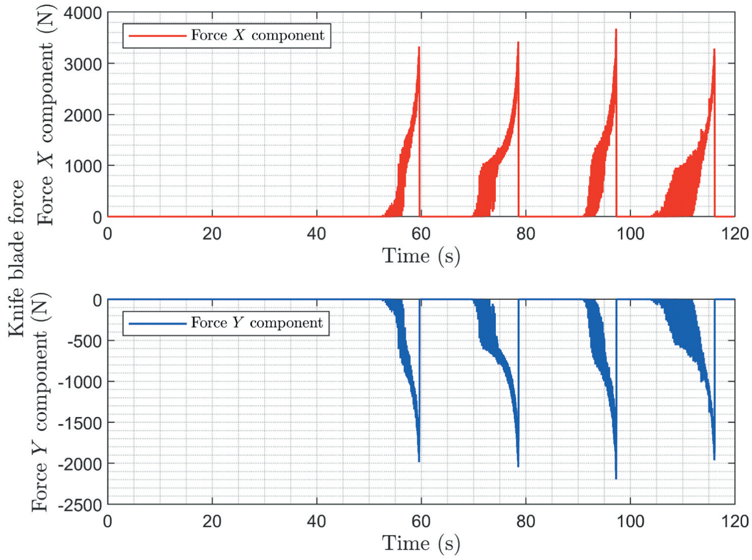

Figure 18. Blade forces with the co-simulated model. The force components in the *z* direction are basically zero.

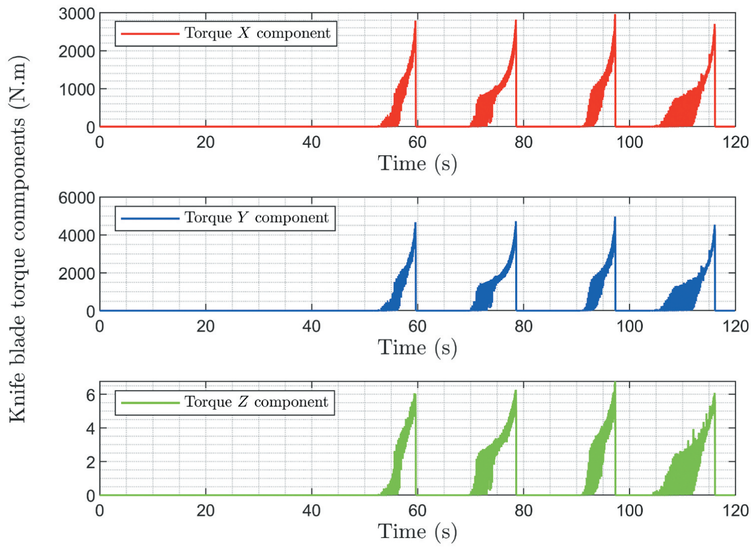

Figure 19. Blade torques with the co-simulated model.

target angular velocity is reached. The motor torque increases through the peeling cycle because the tangential velocity is kept constant during peeling. Angular velocity of the spindles is linked to the radius of the log and in order for the tangential velocity to stay constant, angular velocity must be increased as the log radius gets smaller. Therefore during peeling, the motor is constantly accelerating the rotation of lathe spindles.

Figures 18 and 19 respectively show the cutting forces and resulting torques expressed in global reference frame that affect the knife carriage body. Cutting forces and torques arising from peeling are calculated in the process model, transformed and then distributed to relevant bodies, such as lathe spindles and knife carriage and then sent to the multi-body model during synchronization step.

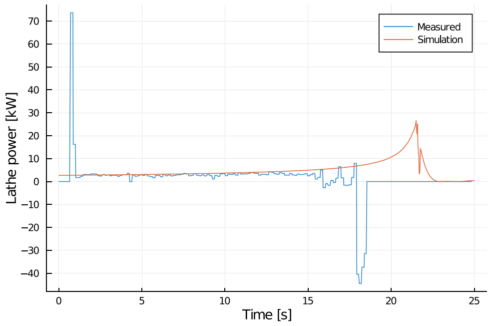

Figure 21. Comparison of the power measured during operation against that obtained within the simulation time in the case of a dry run without a log.

5. Verification and discussion

Despite the existing limitations briefly mentioned in Section 1 in the definition of the real-time model, the introduced approach is able to predict the behavior of the lathe within a reasonable accuracy. To get an insight into the accuracy of the introduced real-time model and to investigate the possible discrepancies between the experimentally measured model and the simulated model in real-time, the following comparisons and discussions elaborate the findings.

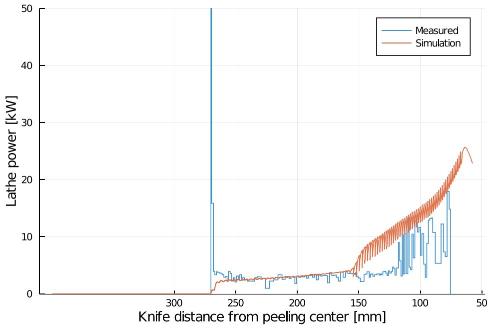

Figure 22. Comparison of the lathe motor power measured during operation against that obtained within time during log peeling process.

5.1. Experimental measurement

Figure 20 shows the cutting blade (knife) distance from the peeling center over the simulation time in the case of the measured and simulated models. As can be seen from the figure, regardless of the starting point, both the simulated and the measured results are almost coincident until $t = 21$ s), and afterwards

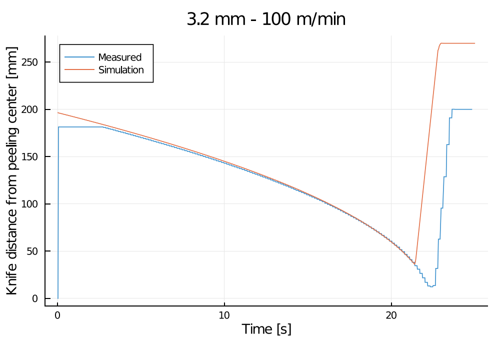

Figure 20. Comparison of the cutting knife distance from the peeling center over simulation and measurement operation time in the case of a dry run without a log.

they follow a similar pattern while with the simulation, the knife distance starts to increase earlier (within 1.5–2 s) than in the measurement. Figure 21 displays the output power measured against the values resulting from the simulation. As expected, after 1 s, the measurement recorded a considerable jump in the power values. This can be explained with reference to Figure 20, where the cutting knife in the measured model recorded a sudden, significant displacement. Figure 22 compares the input power of the motor of a real machine and the simulation model. The difference between simulated and measured data can be justified as follows:

- Log diameter differs between the measured and simulated run. The simulated log had a maximum radius of around 150 mm, which can be seen in Figure 22 by the increase in the required power. Measurement starts at around 120 mm radius.

- The lathe power cut-off earlier in the measurement when compared to the simulation. In a real lathe, the last part of the peeling is done with the spindles retracted and the log is rotated only by the backup rolls and round knife bar. In Figure 22, the moment of the peeling enters the final stage and the spindles are retracted, the motor power drops to zero as the spindles' rotation is stopped. In the simulation, this last part is omitted and, instead, the log is always held in place and rotated via the spindles.
- Noise in measurement data. One possible reason for the differences is that due to backup rolls and round knife bar increase the rotational torque, and occasionally, the spindles have to slow down to keep the tangential velocity at the set point. The backup and/or round knife-bar's tangential speeds are sometimes set to be slightly higher than the spindles' to ensure that they contribute to the rotational work. It is worth mentioning that the settings are based on the operator's experience.
- The spike downwards in the measured lathe power at about 18 s in **Figure 21** comes from the fact that a real lathe utilizes the electric motor for braking, making it function as a generator during the slowing down of the spindles' rotation.

5.2. Finite element model

In the finite element model in ABAQUS, the wood material constants of Scots Pine in the orthotropic elasticity are calculated with respect to the material properties in Table 2. In the table, the material properties for Scots Pine specimen are adopted from Aira, Arriaga, and Íñiguez González (2014). The fracture characteristics are given in Orlowski et al. (2013) that are used to define the cohesive zone element in the quasi-static analysis in ABAQUS. The nonlinear quasi-static analysis was preferred over the nonlinear transient dynamic on the basis of the rationale given in Section 3.5. The finite element model consists of a rotating wooden log, the revolute joints and the discretized blade. A rotation of 0.1666 rad equivalent

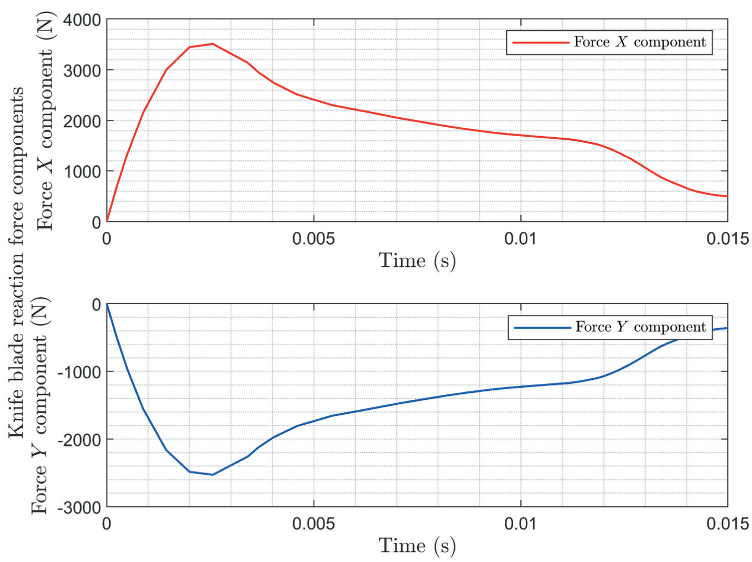

Figure 23. Blade reaction force components obtained by the finite element model of peeling process in ABAQUS. The results are based on the quasi-static analysis when an equivalent rotation to peeling speed of 100 m/min is applied within time span of 0.015 s.

Table 3. Comparison between the solutions of maxima of the tangential and vertical cutting forces obtained by the proposed co-simulation procedure and the finite element model in ABAQUS.

Solution	Tangential cutting force [N]	Vertical cutting force [N]
Co-simulation	3427.1	− 2045.2
Finite element	3508.9	− 2527.4

to the peeling speed of 100 m/min is imposed through the revolute joints within time span of 0.015 s. The solution procedure is based on the discussion presented in Section 3.5. The thickness of the cohesive element is set to be 0.001 mm. As mentioned earlier in this section, the contact-related quantities and more specifically contact force components (blade cutting force components) during peeling process are sought after. By virtue of the high computational cost of the simulation of the peeling process within significant amount of time that is the case with the co-simulation solution, the full finite element simulation is avoided.

Figure 23 shows the tangential and vertical components of the cutting force imposed from the knife blade within the simulation under the prescribed rotation. Considering the short-run simulation, the finite element solutions for the cutting force components are good in accordance comparing with Figure 18. To more concisely and precisely compare the extrema of the cutting force solutions obtained by the finite element and co-simulated models, the extrema of the cutting force components are collected in Table 3. It should be mentioned that in the case of the co-simulation, the extrema of the cutting force components are computed by taking an average of the extrema of four rounds of peeling. The cutting forces imposed from the blade are evaluated by taking the average of nodal forces along the knife blade's cutting edge. As evidenced by Table 3, the maxima of tangential forces given by the two solution approaches are in good agreement. However, the minima of the vertical components differ, but still they are acceptable in accordance considering the multiple different contributing variables in the two solution procedures, such as the existing of the roller supports in the co-simulation. Moreover, the tangential cutting force is of higher importance in peeling process and should be studied with a particular attention.

6. Conclusions

In this study, a real-time simulator for a veneer peeling lathe was introduced to represent a physics-based model of the peeling lathe machine through which the following outcome were observed. The multibody system dynamics model was combined with a contact description procedure according to Atkins model of the orthogonal cutting force Atkins (2003) using a co-simulation procedure.

- With the introduced simulator, features are identifiable even though the quantity of measurements may not be identical to the data taken from a real peeling lathe. This was shown by comparing the relative distance between the cutting blade and the log under peeling within simulation time and the relative distance measured during the peeling process in a real lathe machine.
- The power generated by the lathe motor during simulation was compared against that measured using an operating lathe motor with and without loaded log.
- Moreover, the accuracy of the cutting force components are investigated by introducing a finite element model of the peeling process. The solutions for the cutting force components given by the finite element approach, particularly the tangential component, were in a good agreement with those acquired using the co-simulation of the peeling process.
- The presented results are accurate enough to be used as a tool in product development. Furthermore, the developed simulator can also be used for operator training purposes because, even though peeling is an automatic process. There is still a need for operator actions in some special and rare cases. Using the introduced simulator, operators can learn how to operate with a real peeling lathe and learn how to solve special cases easily.
- Finally, the following improvements would increase the accuracy of the simulation in future developments:
- One of them could be the enhancement of the power transmission components with a more detailed evaluation of the friction parameters to achieve more accurate results. A straightforward

way to accomplish this would be running the prototype through a few work cycles with different speeds without a log and measuring the consumed currents, and then adjust the parameters contributing to the friction model to match the measurements. Another future improvement would be the development of the simulator to be able to describe the spindle-less peeling.

- Moreover, the process model of the veneer cutting could be developed further with some peeling tests to include the material properties of a number of wood species.
- The long-term development goal would be to make a process model capable of predicting the produced veneer quality. Thereto, the findings of the presented finite element solution, e.g., in terms of different veneer thicknesses and peeling velocities inspire great motivation towards such a development.

Acknowledgment

This study was partially funded by the Business Finland and ITEA3 project “MOSIM”.

Disclosure statement

No potential conflict of interest was reported by the author(s).

Funding

The work was supported by the Business Finland .

ORCID

Babak Bozorgmehri http://orcid.org/0000-0003-2400-6768

References

Aira, J. R., F. Arriaga, and G. Íñiguez González. 2014. “Determination of the Elastic Constants of Scots Pine (Pinus Sylvestris L.) Wood by Means of Compression Tests.” *Biosystems Engineering* 126: 12–22.

Anderson, K. S. 1992. “An Order N Formulation for the Motion Simulation of General Multi-Rigid-Body Constrained Systems.” *Computers & Structures* 43 (3): 565–579.

Åström, K. J., and C. C. de Wit. 2008. “Revisiting the LuGre Friction Model.” *IEEE Control Systems Magazine* 28: 101–114.

Atkins, A. G. 2003. “Modelling Metal Cutting Using Modern Ductile Fracture Mechanics: Quantitative Explanations for Some Longstanding Problems.” *International Journal of Mechanical Sciences* 45: 373–396.

Atkins, A. G. 2005. “Toughness and Cutting: A New Way of Simultaneously Determining Ductile Fracture Toughness and Strength.” *Engineering Fracture Mechanics* 72 (6): 849–860.

Atkins, A. G. 2009a. *The Science and Engineering of Cutting*. 1st ed. Oxford, United Kingdom: Elsevier.

Atkins, A. G. 2009b. “Toughness and Processes of Material Removal.” *Wear* 267: 1764–1771.

Avello, A., J. M. Jimenez, E. Bayo, and J. Garca de Jalón. 1993. “A Simple and Highly Parallelizable Method for Real-Time Dynamic Simulation Based on Velocity Transformation.” *Computer Methods in Applied Mechanics and Engineering* 107 (3): 313–339.

Aydın, M. 2017. “Prediction of Cutting Speed Interval of Diamond-Coated Tools with Residual Stress.” *Materials and Manufacturing Processes* 32 (2): 145–150.

Aydın, M., and U. Köklü. 2017. “Identification and Modeling of Cutting Forces in Ball-End Milling Based on Two Different Finite Element Models with Arbitrary Lagrangian Eulerian Technique.” *International Journal of Advanced Manufacturing Technology* 92 (1): 1465–1480.

Aydın, M., and U. Köklü. 2020. “Analysis of Flat-End Milling Forces Considering Chip Formation Process in High-Speed Cutting of Ti6al4v Titanium Alloy.” *Simulation Modelling Practice and Theory* 100: 102039.

Baharudin, M. E., A. Rouvinen, P. Korkealaakso, and A. Mikkola. 2014. “Real-Time Multibody Application for Tree Harvester Truck Simulator.” *Proceedings of the Institution of Mechanical Engineers, Part K: Journal of Multibody Dynamics* 228 (2): 182–198.

Boothroyd, G. 1988. *Fundamentals of Metal Machining and Machine Tools*. Vol. 28. Boca Raton, USA: CRC Press.

Cuadrado, J., D. Dopico, M. Gonzalez, and M. A. Naya. 2004. “A Combined Penalty and Recursive Real-Time Formulation for Multibody Dynamics.” *Journal of Mechanical Design* 126 (4): 602–608.

de Jalón, J. G., E. Álvarez, F. de Ribera, I. Rodríguez, and F. Funes. 2005. ”A Fast and Simple Semi-Recursive Formulation for Multi-Rigid-Body Systems.” In *Advances in Computational Multibody Systems*. edited by, J. A. Ambrósio. Computational Methods in Applied Sciences 1–23. Dordrecht: Springer.

de Jalón, J. G., and E. Bayo. 1994. *Kinematic and Dynamic Simulation of Multibody Systems: The Real-Time Challenge*. New York, United States of America: Springer-Verlag.

Drumwright, E. 2008. “A Fast and Stable Penalty Method for Rigid Body Simulation.” *IEEE Transactions on Visualization and Computer Graphics* 14: 231–240.

Ernst, H., and M. E. Merchant. 1941. “Chip Formation, Friction and High Quality Machined Surfaces.” *Surface Treatment of Metals American Society for Metals* 29: 299–378.

Green, D. W., J. E. Winandy, and D. E. Kretschmann. 1999. *Wood Handbook: Wood as an Engineering Material Chapter 4*. Wisconsin: Forest Products Laboratory USDA Forest Service Madison.

Jaiswal, S., P. Korkealaakso, R. Åman, J. Sopanen, and A. Mikkola. 2019. "Deformable Terrain Model for the Real-Time Multibody Simulation of a Tractor with a Hydraulically Driven Front-Loader." *IEEE Access* 7: 172694–172708.

Junz Wang, J.-J., and C. M. Zheng. 2002. "An Analytical Force Model with Shearing and Ploughing Mechanisms for End Milling." *International Journal of Machine Tools & Manufacture* 42 (7): 761–771.

Korkealaakso, P. 2009. "Real-Time Simulation of Mobile and Industrial Machines Using the Multibody Simulation Approach." PhD diss., Lappeenranta University of Technology.

Matzenmiller, A., J. Lubliner, and R. L. Taylor. 1995. "A Constitutive Model for Anisotropic Damage in Fiber-Composites." *Mechanics of Materials* 20 (2): 125–152.

Merchant, M. E. 1945. "Mechanics of the Metal Cutting Process. II. Plasticity Conditions in Orthogonal Cutting." *Journal of Applied Physics* 16 (6): 318–324.

Mevea. 2005–2020. "Mevea Simulation Software." https://mevea.com/solutions/software .

Moisio, S., B. León, P. Korkealaakso, and A. Morales. 2013. "Model of Tactile Sensors Using Soft Contacts and Its Application in Robot Grasping Simulation." *Robotics and Autonomous Systems* 6 (1): 1–12.

Nairn, J. A. 2015. "Numerical Simulation of Orthogonal Cutting Using the Material Point Method." *Engineering Fracture Mechanics* 149: 262–275.

Nairn, J. A. 2016. "Numerical Modelling of Orthogonal Cutting: Application to Woodworking with a Bench Plane." *Interface Focus* 6 (3): 20150110.

Needleman, A. 1987. "A Continuum Model for Void Nucleation by Inclusion Debonding." *Journal of Applied Mechanics* 54 (3): 525–531.

Olsson, H. 1996. "Control Systems with Friction." PhD diss., Lund Institute of Technology.

Orlowski, K. A., T. Ochrymiuk, A. G. Atkins, and D. Chuchala. 2013. "Application of Fracture Mechanics for Energetic Effects Predictions While Wood Sawing." *Wood Science and Technology* 47 (5): 949–963.

Oshtorjani, M. K., A. Mikkola, and P. Jalali. 2019. "Numerical Treatment of Singularity in Hydraulic Circuits Using Singular Perturbation Theory." *IEEE/ASME Transactions on Mechatronics* 24 (1): 144–153.

Rahikainen, J., A. Mikkola, J. Sopanen, and J. Gerstmayr. 2018. "Combined Semi-Recursive Formulation and Lumped Fluid Method for Monolithic Simulation of Multibody and Hydraulic Dynamics." *Multibody System Dynamics* 44 (3): 293–311.

Reiterer, A., G. Sinn, and S. E. Stanzl-Tschegg. 2002. "Fracture Characteristics of Different Wood Species Under Mode I Loading Perpendicular to the Grain." *Materials Science and Engineering: A* 332 (1): 29–36.

Stephenson, D. A., and J. S. Agapiou. 2016. *Metal Cutting Theory and Practice*. Boca Raton, USA: CRC press.

Sulsky, D., Z. Chen, and H. L. Schreyer. 1994. "A Particle Method for History-Dependent Materials." *Computer Methods in Applied Mechanics and Engineering* 118 (1–2): 179–196.

Thibaut, B., and J. Beauchêne. 2004. "Links Between Wood Machining Phenomena and Wood Mechanical Properties: The Case of 0°/90° Orthogonal Cutting of Green Wood." In *Proceedings of the 2nd International Symposium on Wood Machining*, Vienna, Austria, 149–160.

Thibaut, B., L. Denaud, and R. Collet. 2016. "Wood Machining with a Focus on French Research in the Last 50 Years." *Annals of Forest Science* 73 (1): 163–184.

Unity. 2005–2020. "Unity Technologies." https://unity.com/solutions.

Wyeth, D. J. 2007. "An Investigation into the Mechanics of Cutting Using Data from Orthogonally Cutting Nylon 66." *International Journal of Machine Tools & Manufacture* 48: 896–904.

Wyeth, D. J., G. Goli, and A. G. Atkins. 2009. "Fracture Toughness, Chip Types and the Mechanics of Cutting Wood. A Review." *Holzforschung* 63: 168–180.

Xiong, G.-M., and L.-J. Guo. 2016. "Modeling and Simulation of the Knife Movement for Veneer Lathe." In *International Conference on Artificial Intelligence: Techniques and Applications*, Shanghai, China.

Publication II

Gradov, D., Yusuf, O., Ojainen, J., Suuronen, J., Eskola, R., Roininen, L., and Koiranen, T.

Modelling of a continuous veneer drying unit of industrial scale and model-based ANOVA of the energy efficiency

Reprinted with permission from
Energy
244, Part A, 122673, 2022

Energy 244 (2022) 122673

Contents lists available at ScienceDirect

Energy

journal homepage: www.elsevier.com/locate/energy

Modelling of a continuous veneer drying unit of industrial scale and model-based ANOVA of the energy efficiency

Dmitry Vladimirovich Gradov [a, *], Yusuf Oluwatoki Yusuf [b], Jussi Ojalainen [c], Jarkko Suuronen [a], Roope Eskola [c], Lassi Roininen [a], Tuomas Koiranen [a]

[a] School of Engineering Science, Lappeenranta-Lahti University of Technology (LUT), P.O. Box 20, FI-53851, Lappeenranta, Finland
[b] Faculty of Information Technology and Communication Sciences, Tampere University, P.O. Box 1001, FI-33014, Tampere, Finland
[c] Research and Development Department, Raute Oyj, P.O. Box 69, FI-15551, Nastola, Finland

ARTICLE INFO

Article history:
Received 15 August 2021
Received in revised form
7 November 2021
Accepted 17 November 2021
Available online 19 November 2021

Keywords:
Continuous veneer dryer
Heat and mass transfer
Process and automation modelling
ANOVA
Energy analysis
Process optimisation

ABSTRACT

Drying, a crucial step in process engineering aimed at producing optimal product moisture content, has evolved over time from batch processing methods to continuous processing alternatives. Continuous drying methods offer uniform moisture content of the product at lower operational cost. In this study, a continuous veneer drying model was developed based on mass and energy balances. The simulated veneer dryer is a semiautomatic machine designed to maximise the drying process efficiency via control mechanisms such as the veneer transport rate, fan speed, opening angle of the inlet and outlet dampers, and radiator temperature. In the dryer, veneer plates are conveyed horizontally through the number of connected chambers where hot air is blown transversely. The optimal drying process is dynamically maintained via the Proportional—integral—derivative controllers, manipulating the rate of the damper lids opening, that are connected to the sensors monitoring the air properties in the chambers of the drying unit. The model-based sensitivity analysis ANOVA was carried out for energy optimisation purposes. The analysis outcomes indicated that radiator temperature, initial moisture content of veneer sheets and conveyor speed are the most influential parameters affecting the drying rate. Automatic control of damper lids provides optimal temperature and moisture content of drying environment at lower energy costs.

1. Introduction

Veneers are highly demanded construction materials due to their remarkable properties such as aesthetically pleasing appearance, light weight, strength, shape stability, soundproof and low heat conduction properties. The quality of veneer sheets is moisture dependent, which should be within the optimal range for gluing. Optimal moisture content varies depending on wood type, composition of glue, panel type and other factors. Demirkir et al. [1] state that the optimal moisture content of veneer sheets should be below 7%, whereas Ozsahin & Aydin [2]; who used a neural network on experimental data to predict the optimal veneer drying temperature for good bonding, claim that the moisture should be about 3%. In the case of over drying, unconditioned veneer plates tend to cause poor gluing due to insufficient absorption of glue aqueous component. However, high moisture content decreases the glue viscosity, which, in turn, can cause veneer sheet misalignment during hot pressing due to high shear stress [3,4]. Recently, Ozsahin & Aydin [2] used neural network on experimental data to predict the optimal veneer drying temperature for good bonding in the process of manufacturing plywood panels. According to Johnsson et al. [5]; improving energy efficiency in wood processing industry is recognised as one of the most crucial actions for mitigating the climate change. Convective drying in veneer manufacture is a critical stage from the energy consumption perspective as it is responsible for up to 70% of the total energy consumption of plywood production [6,7]. Moreover, plywood drying alone has been estimated to contribute more than 30% to the global warming potential of total plywood production in China, which is equivalent to 6.3 tons of emitted CO_2 per cubic meter of ready product [8]. Optimisation of the drying process is therefore a topic of considerable interest from both economic and environmental standpoints. Based on a feasibility evaluation of wood

* Corresponding author.
E-mail address: dmitry.gradov@lut.fi (D.V. Gradov).

https://doi.org/10.1016/j.energy.2021.122673
0360-5442/© 2022 Published by Elsevier Ltd.

dryers Lamrani et al. [9] recommended waste heat recuperation.

To be able to control a process, the process mechanisms have to be adequately described and measures identified for determination of the optimal conditions of the process. Mathematical models based on energy and mass balances are capable of describing drying processes including convective dryers, see, for example, [10–19]. In particular, Euh et al. [20] developed a real-time drying control that was capable to improve the drying efficiency of a pneumatic conveying dryer. The veneer drying process is based on the physical principles of moist air thermodynamics and moisture mass transfer. Thus, the limiting factors of convective evaporation are air humidity, temperature and mass transfer rate of moisture from the veneer surface to the bulk of the air, as shown in Fig. 1. Process intensification and apparatus performance optimisation consequently tend to focus on these areas.

In the published literature, there are examples of convective dryers modelled at different scales and using different approaches. Thant et al. [12] proposed a simplified model for drying time estimation in a veneer jet dryer where internal and external moisture transport is considered. The model results agree with the experimental data reasonably well, however, the simulated time is quite short, during which the moisture transport to the veneer surface is intensive and doesn't limit the overall drying rate. The effect of air humidity and convective mass transfer was not considered. A CFD simulation was used by Rouch [13] to estimate the airflow hydrodynamics and heat transfer in a wood plates drying. A package of the plates was considered as porous media and the drying rate was assumed constant. Regardless of missing validation, the modelling approach is robust and the results are adequate. In another work, Sandoval Torres et al. [16] proposed a one-dimensional model for moisture transport through European oak and evaporation rate from the wood surface in a vacuum chamber. Wood layer was considered as porous medium. Assuming homogeneous air conditions in the vacuum chamber, the moisture transport due to convection was disregarded. Semiempirical models of a rotary dryer and a textile dryer were developed in MATLAB Simulink by Baxi et al. [17]. Based on mass and energy balances, both models included the effect of air convection, material residence time and convective heat transfer. The model performance appeared adequate; however, a validation is missing. Di Marco et al. [18] made a mathematical model for an air impingement dryer to evaluate the energy performance. The model prediction was within 5% deviation from experimental data with the assumption of constant humidity and temperature profiles in the dried tissue. It should be noted that thus far detailed dynamic models, describing a complex performance of a continuous convective drying unit, including humidity control mechanisms, have not been presented.

Experimental work, modelling and simulation are the three main approaches used in process engineering to understand phenomena such as drying [21]. A multiparameter model of a complex process requires performance evaluation using varying input parameters to foresee different scenarios of the modelled process outcomes as illustrated in Fig. 2. A comparative study of uncertainty quantification methods published by Cox & Baybutt [22] shows that the research on uncertainty quantification in models of physical processes dates as far back as 1981 [21]. Sensitivity analysis methods applied in different areas have been discussed in many studies, for example, [23–30].

Saltelli et al. [26] discussed the principles and methods of sensitivity analysis with succinct definition of sensitivity analysis as the study of how variation in output of a model is explained by variation in the model inputs. The classical methods of sensitivity analysis and their corresponding problems cases have been discussed in the works of [26,29,31,32]. Sensitivity analysis methods varies from the historical approach of local sensitivity analysis where the effect of local input perturbations on the model output is studied; design of experiment theory; Monte Carlo techniques and global sensitivity analysis that don't restrict the domain of model inputs [26].

Sałat et al. [33] used a blackbox approach to optimise the fan speed in an industrial scale convective dryer. Bose et al. [25] examined an uncertainty analysis of laminar aeroheating predictions for Mars entries. A Monte Carlo sensitivity and uncertainty analyses were used by Ref. [25] to investigate the effect of some selected parameters under Mars entry conditions of the model. The results gave a quantitative explanation of the uncertainties in the modelling parameters. Specifically, the collision integral in high and low catalytic regimes responsible for transport properties of mixtures contributes largely to the uncertainty.

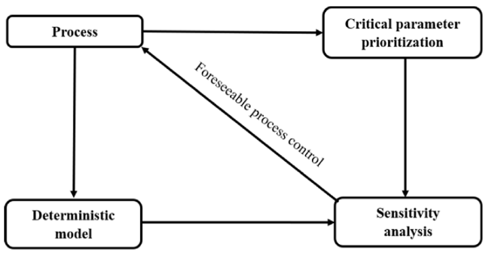

Fig. 2. Process performance predictability analysis of mechanistic model.

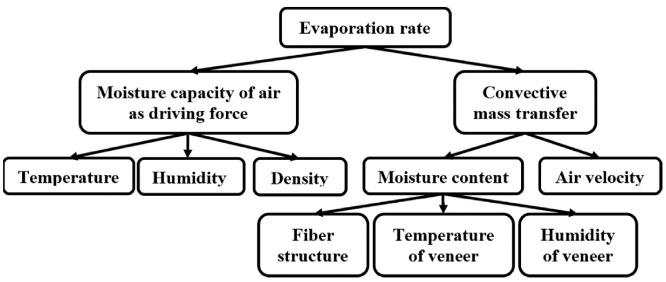

Fig. 1. Diagram of evaporation rate.

Woods & Lewis [32] reviewed methods from design of experiments developed from both physical experiments and those related to numerical models. The classes of factorial designs were used to investigate main effects and interactions in the model with the active input variables providing information for optimisation of the model output.

The aim of this work is to create a dynamic model describing the convective drying process of veneer in a continuous drying unit. The model comprises energy and mass balances of moving air and veneer passing through the dryer. The model is then used to analyse the variation of the crucial parameters within the expected range, defined based on the performance practice of the drying unit. This paper covers the principles of modelling for the convective drying in Section 2. Section 3 describes the implementation of the convective dryer model in the environment of MATLAB Simulink. The methodology of the statistical analysis is described in Section 4. The results from the model simulations and sensitivity analysis are presented in Section 5.

2. Principles and modelling concepts of convective drying

The thermodynamics of the convective drying process is derived from the ideal gas law. Dry air and water vapour coexist in a domain under ambient pressure which is the sum of their partial pressures:

$$p^{air} + p^{H20} = p^{atm} \tag{1}$$

Water molecules can diffuse from solid surface to air. Equilibrium moisture concentration in air is limited by the saturation pressure in the atmosphere:

$$p_{sat}^{H2O} = \exp\left(\frac{A}{T} + B + CT + DT^2 + GT^3 + ElnT\right), \tag{2}$$

where T is the temperature of the air, $A - E$ are the empirical constants [34]. An increase in temperature leads to exponential growth of the saturation concentration of the water vapour.

The molar flux of moisture from veneer plate to air can be expressed as follows:

$$\dot{M}^{H2O} = A_v k_g \left(p_{sat}^{H2O} - p^{H20}\right), \tag{3}$$

where A_v is the contact area of veneer, m^2; k_g is the convective mass transfer coefficient, m/s [35]. Molar flux conversion into mass flux results in the following expression:

$$\dot{m}^{H2O} = A_v M^{H2O} k_g \left(p_{sat}^{H2O} - p^{H20}\right), \tag{4}$$

where M^{H2O} is the molar mass of water, kg/kmol; c is the concentration of air water vapour, kmol/m^3. The convective mass transfer coefficient describes the transport efficiency of the moisture from the surface to the air bulk. It depends on airflow velocity at surface and water molecules diffusion. The convective mass transfer from a flat plate can be correlated with Reynolds ($\frac{\text{convection}}{\text{diffusion}}$) and Schmidt ($\frac{\text{viscosity}}{\text{diffusion}}$) dimension less numbers as follows:

$$k_g = ARe^{1/2}Sc^{1/3}, \tag{5}$$

where A is the empirical constant, 0.332 and 0.664 for laminar and turbulent regimes respectively [35].

The drying unit, shown in Fig. 3, consists of a drying section, comprising 16 drying cells, 2 smoke or sealant cells adjacent to the outer cells of the drying section, and 3 sequential cells of cooling section. The convective evaporation takes place in the drying cells, where blown air, heated by a radiator, streams continuously across the veneer sheets. The outer drying cells of the drying Section are connected to the sealants or smoke cells. Leaving the second smoke cell, the veneer plates pass through the cooling Section for temperature conditioning before they can be man handled. The hot fluid used in the radiators can be optionally steam or oil. A typical drying cell comprises a fan, a radiator, jet boxes, rollers, and optional air inlet and/or outlet, as shown in Fig. 4.

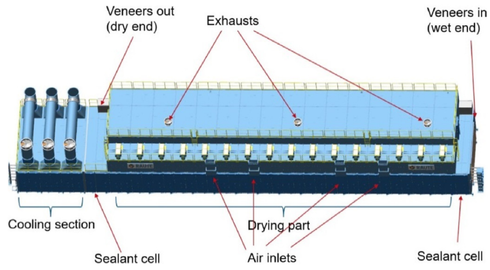

Fig. 3. Illustration of the veneer dryer unit.

The geometry of the surface and the surrounding structures affects the mass transfer coefficient greatly. For simplified cases of flat or cylindrical surfaces in open space, the constants are sufficiently accurate. With complicated structures, however, such as the perforated jet boxes in the dryer in Fig. 5, computational fluid dynamics (CFD) analysis can provide more accurate values [15].

Elevated temperature of the air increases the saturation concentration promoting higher drying rate. The diffusion of moisture through the veneer layers lowers the overall drying rate. In practice, the diffusion time scale is small as the veneer sheets are thin and the moisture migrates from the middle of the sheets in both directions towards surface. Temperature affects moisture diffusion through fibres which can be described by Fickian Law or empirically. When a moist veneer plate enters the first drying chamber the moisture transport is increased due to convective heating during the induction period until a constant drying rate is reached. A constant drying rate is maintained until veneer humidity reaches a critical value, whereupon the diffusion of the water becomes the limiting factor of the drying process, as illustrated in Fig. 6. The reduction in the drying rate continues until equilibrium moisture content is reached. The moisture driven limitation of the constant drying rate can be measured experimentally in similar conditions.

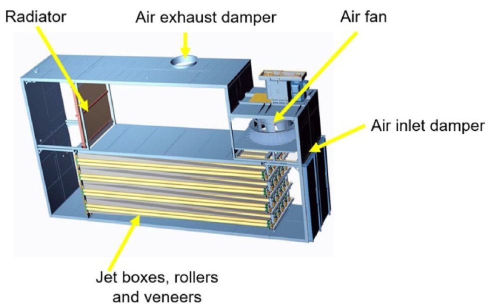

Fig. 4. Illustration of the main features in the drying cell.

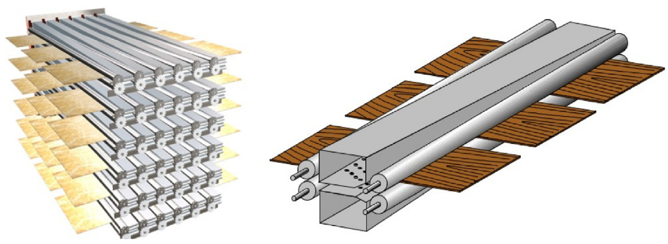

Fig. 5. Illustration of the rollers on the left and jet boxes on the right.

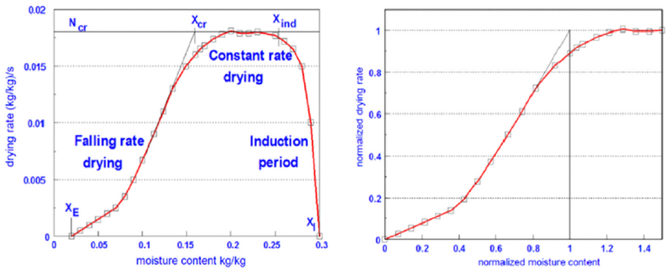

Fig. 6. Normalization of typical empirical drying rates as a function of moisture on the left and normalised quantities on the right [37].

The measured isotherm of the falling rate is normalised for modelling purposes. The empirical approach is a consistent and a simpler alternative to a detailed CFD model of the moisture transport through the material. Normalization procedure according to Equations (6) and (7) of the experimental data is shown in Fig. 6 [36].

$$\dot{m}_{evap}^{norm} = \frac{\dot{m}_{evap}^{i}}{\dot{m}_{evap}^{const}}. \tag{6}$$

$$X^{norm} = \frac{X_i - X_{eq}}{X_{cr} - X_{eq}}. \tag{7}$$

$$X = \frac{m^{H2O}}{m^{dry\ veneer}}, \tag{8}$$

where the where X is the moisture content of the dried veneer.

2.1. Design and functionalities of the drying cell

Drying cell is a functional unit in the veneer dryer; hence a single cell can be modelled and then combined in a battery of 16 units to make the model of the veneer drying part. The modelled drying cell was divided into four sub-blocks of different functionality following the design presented in Fig. 7 where air is assumed to be completely mixed.

The starting point for the model design was the fan, which blows air towards the radiator. The sub-block, colored in blue, includes the inlet damper for two reasons. The first reason is the compactness of the model. The driving force for incoming fresh air is the negative pressure created by the fan. As an input parameter to the function for the mass flow rate, it is convenient to locate the static pressure at the damper and the fan in the same sub-block. The second reason is to exclude the heat impact of fresh air on the veneer drying process. The exhaust sub-block occupies the space from the fan sub-block to the radiator and by default includes an outlet, which can be optionally deactivated. The radiator sub-block starts from the radiator and occupies the vertical path of the air until the veneer transport structure. The remaining space is marked as a dryer sub-block and includes the material and energy balances of the air and veneer.

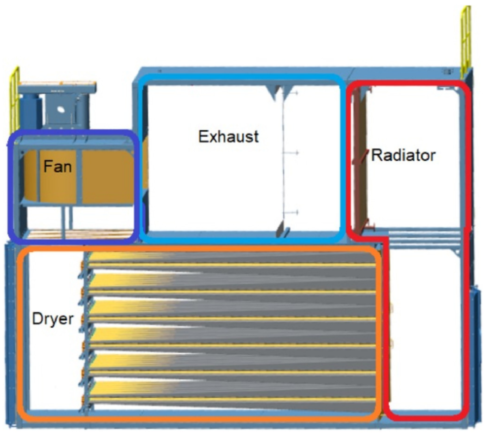

Fig. 7. Illustration of the drying cell with conditionally outlined sub-blocks.

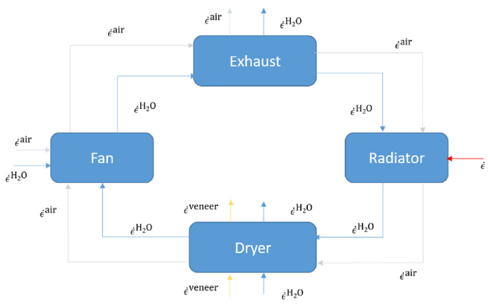

Fig. 8. Mass balance diagram of the drying cell.

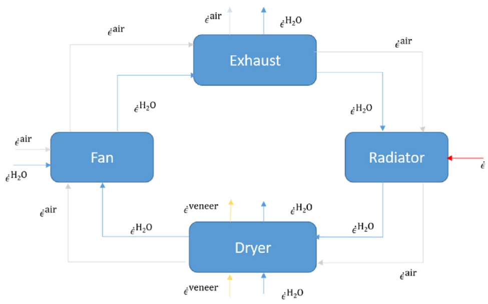

Fig. 9. Energy balance diagram of the drying cell.

The mass balance in a typical drying cell is presented schematically in Fig. 8, where the mass flow streams are shown. The material balance of air and water vapour has only one inlet and outlet that are in balance at the start but later can be changed dynamically by PID controllers. There is a source of water vapour evaporated from the veneer surface in the dryer sub-block. The released water reduces the veneer humidity via a sink term, which was added to the outlet mass flow rate in order to preserve the mass balance. Later, this artificial mechanism was removed until PID controllers and freely flowing air between cells were implemented.

Energy balance in a typical drying cell is presented in Fig. 9. Input fresh air reduces the energy and lowers the humidity. In the exhaust sub-block, the air loses energy through the air released to the outer environment. The radiator is the source of energy. The heat exchange and evaporation affect both the air and veneer energy streams. A detailed description of each sub-block is given in Section 3. The following features were implemented in the model: Mass and energy balances of air and veneer in the drying and smoke cells, a dynamic model of the radiator surface temperature, energy storage in the metal parts, the opening angle of the exhaust dampers is controlled by the PID controller, the opening angle of the inlet dampers is controlled by the PID controller, the recirculating gas moves between the cells based on static pressure, on/off switches for the inlet and outlet dampers, the properties of the air and veneer are adjustable, and the veneer transport speed and loading regime are adjustable.

3. Modelling continuous drying unit with MATLAB simulink

The Simulink model was designed with the following assumptions and simplifications: the model excludes minor factors of influence; the fan maintains a constant volumetric flow rate; the heating agent has constant temperature; the air stream is assumed as perfectly mixed flow within sub-blocks; no temperature gradient profiles are considered in the veneer plates and metal parts; no heat exchange with the outer atmosphere is modelled; the effect of veneer temperature on moisture diffusion is omitted; and fan sub-blocks are isolated from each other.

The modelling environment of MATLAB Simulink has block-based approach where the functional blocks that are explicitly connected with the signal routes. The overall view of the model built in Simulink follows the construction of the real dryer (see Fig. 10). The constituent elements are shown in Fig. 11.

The exhaust, radiator and dryer sub-blocks have additional modules, calculating the static pressure and the flow rates of air migration between adjacent cells. The airflow rates through the dampers are calculated separately using the signals from the PIDs, the air properties in the outer area, in the fan and exhaust sub-blocks. The mass and energy balances in fan sub-block are identical having two sources and one sink terms. The fresh air source term is the function of the negative static pressure created by the fan and the damper lid angle. The exhaust sub-block has a large adjacent area between drying cells. Pressure driven airflow between neighbouring cells was therefore implemented. It is described in Section 3.2. The outlet damper releases the moist air based on the static pressure. The balances are identical having two sink and one source term. The sink term is a lid and the angle of the position of the damper lid automatically driven by the PID controller. The radiator sub-block has a large adjacent area with a neighbouring drying cell. Airflow between neighbouring cells was therefore implemented. The energy balance has an extra source term of the radiator, which supplies energy via a convective heat transfer mechanism from the hot surface temperature of the radiator to the gas mixture. The mechanism of the heat exchange between the heating fluid (steam) and the radiator surface is implemented in the model. It is described in Section 3.3. The pressure drop of the gas passing through the radiator is significant. The geometric configuration of the radiator as well as the number of radiating plates affects the pressure drop.

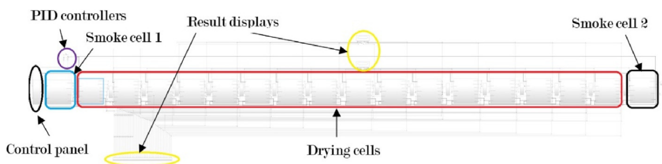

Fig. 10. Architecture of the drying model in MATLAB Simulink.

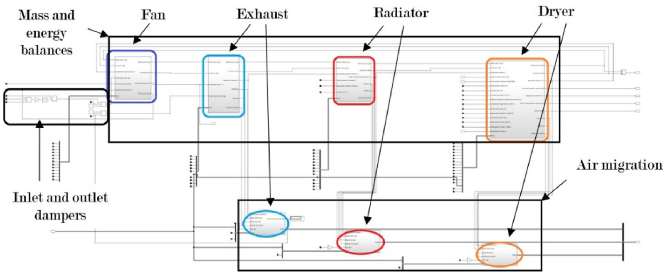

Fig. 11. Architecture of the drying cell in MATLAB Simulink.

The dryer sub-block has a large adjacent area between drying cells. Airflow through the adjacent area between neighbouring cells was therefore implemented. The static pressure of the hot gas passing through the jet box comprises less than 5% of the initial static pressure at fan, which was measured in an actual dryer on site.

The principle equations upon which the sub-blocks were built are listed below:

$$\dot{m}_{acc} = \dot{m}_{in} - \dot{m}_{out} \tag{9}$$

$$\rho^{mix} = \frac{m^{H2O} + m^{air}}{V} \tag{10}$$

$$f^{H2O} = \frac{m^{H2O}}{m^{H2O} + m^{air}} \tag{11}$$

$$\dot{m}^{mix}_{out} = \dot{q}_{fan}\rho^{mix}_{fan} \tag{12}$$

$$\dot{m}^{mix}_{damper} = A_{lid}\left(2\rho_{mix}P^{mix}_{st}\right)^{0.5} \tag{13}$$

$$P^{mix}_{st-ex} = P^{mix}_{st}\left(T_{ref}\right)\frac{\rho^{mix}(T)T}{\rho^{mix}\left(T_{ref}\right)} \tag{14}$$

$$P^{mix}_{st-rad} = C^{rad}_f P^{mix}_{st-ex} \tag{15}$$

$$P^{mix}_{st-dryer} = C^{dryer}_f P^{mix}_{st-ex} \tag{16}$$

$$\dot{m}^{H2O}_{veneer} = A_{veneer} f_{evap} k_g \left(c^{H2O}_{sat} - c^{H2O}\right) M^{H2O} \tag{17}$$

$$\dot{\varepsilon}_{acc} = \dot{\varepsilon}_{in} - \dot{\varepsilon}_{out} - f^{H2O}\dot{\varepsilon}_{heat} \tag{18}$$

$$\dot{\varepsilon} = \dot{m}h = \dot{m}c_p T \tag{19}$$

$$\dot{\varepsilon}_{evap} = \dot{m}^{H2O}_{veneer-air}\lambda_{H2O} \tag{20}$$

$$\dot{\varepsilon}_{rad} = U_{rad}A_{rad}\left(T_{rad} - T^{mix}_{in(exhaust)}\right) \tag{21}$$

$$\dot{\varepsilon}_{heat} = U_{veneer}A_{veneer}\left(T^{mix}_{in(exhaust)} - T^{veneer}_{in}\right) \tag{22}$$

$$T_{rad} = \frac{U_{rad}A_{rad}(T_{steam} - T_{rad})}{m_{rad}c^{metal}_p} \tag{23}$$

$$T^{mix}_{out} = \frac{\dot{\varepsilon}^{mix}_{acc}}{\dot{m}^{H2O}_{acc}c^{H2O}_p + \dot{m}^{air}_{acc}c^{air}_p} \tag{24}$$

The mass balance in the sub-blocks is described in Equation (9), where $\dot{m}_{acc}$ is the mass accumulated in a sub-block, and $\dot{m}_{in}$ and $\dot{m}_{out}$ are mass inflows and outflows respectively. The density of gas mixture in Equation (10) denoted as ρ^{mix} is the ratio of the gas masses (moisture mass m^{H2O} and air mass m^{air}) and the sub-block volume V. The vapour mass fraction in Equation (11) denoted as f^{H2O} is the ratio of the moisture mass to the mass of the gas mixture. The static pressures in the exhaust, radiator and dryer sub-blocks depend on the pressure loss in the corresponding sub-block (C^i_f) due to airflow channel construction as described in Equation (14)–16. The sink term of the mass flow rate $\dot{m}^{mix}$ is described in Equation (12), mass flow rate through dampers $m^{\cdot mix}$ is described in Equation (13), evaporation rate from veneer $\dot{m}^{H2O}$ is described in Equation (17), the energy rate $\dot{\varepsilon}$ is described in Equation (19), the energy transfer rate due to evaporation $\dot{\varepsilon}_{evap}$ is described in Equation (20), heat duty of radiator sub-block $\dot{\varepsilon}_{rad}$ is described in Equation (21), air-veneer heat transfer rate $\dot{\varepsilon}_{heat}$ is described in Equation (22), radiator temperature T_{rad} is described in Equation (23), temperature of leaving gas mixture T^{mix}_{out} is described in Equation (24). c_p is the specific heat capacity of a phase, U is the heat transfer coefficient, h is the enthalpy, λ is the latent heat. The phase components such as moisture (H_2O), dry air (air), and gas moist air (mix) are denoted as symbols superscripts, while the drying unit parts and flow directions are specified as symbol subscripts in the equations.

The experimental reference data was provided by Raute Oyj (Fig. 12).

The falling period of the normalised drying rate isotherm was fitted using the polynomial presented in Fig. 12. Similarly, the induction drying rate period can be modelled when the necessary data is provided as mentioned in Section 2; however, the temperature-induced moisture diffusion through the veneer thickness needs to be determined. In the current model, the moisture diffusion through the veneer thickness is not modelled explicitly but implicitly from the empirical drying rate isotherm.

To obtain the convective mass transfer coefficient, three

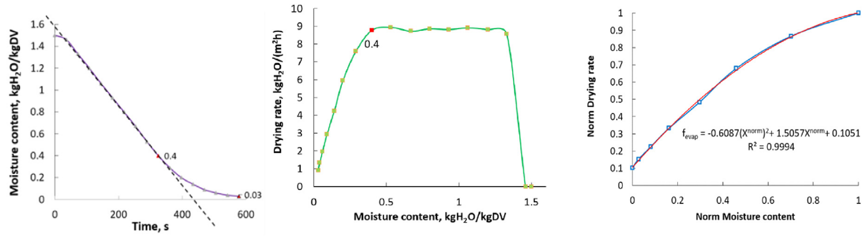

Fig. 12. Measured drying rate of veneer plate at 63 °C (left), derived drying isotherm (middle) and normalised drying isotherm (right). The blue line shows the curve while red line is polynomial trend line. (For interpretation of the references to color in this figure legend, the reader is referred to the Web version of this article.)

different methods were tested. Following the complexity growth of the methods, the first method was using a direct empirical value, which was taken as the most reliable number and set as a default. However, the flow rate at the fan affects the Schmidt and Reynolds numbers according to Equation (5), therefore, two other methods were implemented, namely: fully mechanistic formulations for the both dimensionless numbers and semi-empirical where an empirical value for the Reynolds number, provided by Raute Oyj, was used.

3.1. Airflow between adjacent sub-blocks of neighbouring cells

The mechanism of air transport from cell to cell is based on the static pressure at adjacent areas of parallel air flows where they interact. The pressure is linearly dependent upon the gas mixture density and temperature, as presented in Equation (14). Based on the pressure difference between adjacent sub-blocks of neighbouring cells, the mass flow rate can be found in a similar way to the mass flow rate through the damper in Equation (13). The sign of the pressure difference defines the direction of the flow. It must be noted that the corresponding density and temperature of the dominating airflow are to be used to preserve the mass and energy balances.

A different situation is found with smoke cells that don't have a fan but contact with a dryer sub-block in the outer drying cells. These cells are preheated with hot air coming from the radiator sub-block domain through a small "window". The reference static pressure approach in Equation (14) works fine to find the pressure difference between drying cells, but it is very inaccurate when a pressure value is used against the absolute pressure in the smoke cells, and it produces unrealistically high values of driving pressure. Therefore, in the outer drying cells, as well as the reference static pressure, the absolute pressure is also calculated, which is used to obtain the mass flow rate between the dryer sub-block and smoke cell. The other side of the smoke cell is connected to the outer atmosphere or the cooling section, which is assumed to have atmospheric conditions. The air mass flow rate is simulated based on the difference in absolute pressures. As the transported veneer is in contact with the air in the smoke cells, the heat exchange mechanism is implemented and evaporation is omitted.

3.2. Energy accumulation in metal parts

Metal parts such as fans, radiators, dryer walls, jet boxes, and rollers have significant mass that can accumulate and release energy. The corresponding energy balances including the heat transfer between the gas and metals were implemented in every sub-block. During heating up, the metal parts strip energy from the passing air which slows down the cooling process in the case of a sudden shutdown of the dryer.

3.3. Inlet and outlet dampers with PID controllers

PID controllers manage the position of the damper lids. The controllers use static pressure readings in the smoke cells as target parameters. Based on the conventional performance of the dryer, mild pressure (510 Pa) should be maintained to ensure fresh air is fed into the dryer from both ends. The free parameter of the PID controller, $k^{-0.5}$, controls the angle of the position of the damper lid that enhances or limits the airflow rate of Equation (25):

$$\dot{m}_{damper}^{mix} = A_{lid}\left(\frac{2\rho_{mix}P_{st}^{mix}}{k}\right)^{0.5} \tag{25}$$

The PID controllers are limited by a range of $k^{-0.5}$ to avoid the risk of the unrealistic values. In the current model, the free parameter is limited between 0.025 (almost closed) and 35 (fully open) according to the empirical data provided by the manufacturing company Raute Oyj.

4. Methodological framework for sensitivity analysis

Simulations in sensitivity analysis are conducted to account for the variation in the model output due to variation in the input [21]. The spread realised from using different initial values of the model are evaluated and analysed. This method can be represented as:

$$y = \mathscr{H}(x) \tag{26}$$

where $\mathscr{H}$ is a vessel function and in this case a deterministic Simulink model with input parameters of the model x constituting the feature space and an output vector $\boldsymbol{y}$ representing the final veneer humidity and power consumption throughout the drying process.

4.1. Factorial experimental design for continuous veneer unit model

A systematic approach to experimental design eliminates researcher's bias and reveals the interaction of the input signals and its effect onto the response variable [34]. Widely used experimental designs in both research and industrial setting are the full and fractional factorial designs [38–40]. The full factorial design requires L^k experiments, where L is the number of levels and k is the number of parameters in the experiment [40]. The use of a design matrix is to replace the ideal case of operational data as input to the model. The full factorial design gives a parsimonious modelling by constraining the parameters to all the discrete possible combinations of the levels across the factors [38]. The dimension of the feature space is a $p \times k$ matrix and the output from the model is a $n \times p$ matrix. This implies k parameters are to be varied for $p = L^k$ iterations and n is the model simulation time.

The parameters varied in the simulation were veneer initial, veneer humidity, radiator temperature, atmospheric pressure, conveyor belt speed, and volumetric flow rate of fan. The degree of variance for each parameter is subjective and it was chosen based on the practice of the drying unit operation in South Karelia region of Finland. The design matrix was converted from coded values to real values and used as model inputs, hence representing a 3^5 full factorial experiment.

4.2. Statistical framework for analysis of variance (ANOVA)

Statistical methods are used for explaining the relationship between the design response and the predictors [41,42]. ANOVA is used when predictors are fixed in advance or sampled together with the responses. The standard multiple linear regression model has the form:

$$y = X\beta + e \tag{27}$$

where y is the response vector, X is the design matrix, β is the coefficient vector and e is the error vector or residuals. The predicted value of the response is hence given by:

$$\hat{y} = X\hat{\beta} = X\left(X^T X\right)^{-1} X^T y = Hy \tag{28}$$

where H is the hat matrix and $\hat{\beta}$ is the least square estimate of (see Table 1) β.

Table 2 is populated with the statistics from the regression model and residuals.

The sum of squares in the ANOVA table is calculated as follows:

$$SS_{Reg} = \sum (y_i - \bar{y})^2 \tag{30}$$

$$SS_{Res} = \sum (y_i - \hat{y}_i)^2 = (y - X\hat{\beta})^T (y - X\hat{\beta}) = \hat{e}^T \hat{e} \tag{31}$$

$$SS_{Total} = \sum (y_i - \bar{y})^2 = (y - \bar{y})^T (y - \bar{y}) \tag{32}$$

For an experiment of k predictors and N observations, the regression model degrees of freedom (DF) is k, the residual degrees of freedom is $(N - k - 1)$, and the total degrees of freedom is $(N - 1)$. The mean square is the ratio of the sum of squares and their respective degrees of freedom.

Table 1
Variation of control parameters used in the sensitivity analysis.

Control parameter	Low	Medium	High
Initial veneer humidity (IVH) ($kgH_2O/kgDV$)	1.0	1.5	2.0
Radiator temperature (RT) (°C)	165	205	245
Atmospheric pressure (AP) (hPa)	973	1013	1053
Flow rate at fan (FR) (m^3/s)	15	25	35
Conveyor belt speed (CS) (m/s)	0.045	0.055	0.065

Table 2
ANOVA table statistics for regression model and residuals.

Source	Sum of Sq.	DF	Mean Sq.	F-statistic
Regression	*SSReg*	k	$SSReg/k$	$MSReg/MSRes$
Residual	*SSRes*	$N-k-1$	$SSRes/(N-k-1)$	
Total	*SSTotal*	$N-1$		

4.3. Multi-objective optimisation

Multi-objective optimisation techniques are useful in optimising problems with two or more often conflicting objective functions simultaneously. The application areas of multi-objective optimisation have triggered continuous research in meta-heuristic and multi-evolutionary optimisation techniques [43–45].

The goal attainment method described by Gembicki & Haimes [46] is widely used among the several techniques in multi-objective optimisation. The method involves a set of objective functions $F(x) = \{f_i(x)\}$, a set of corresponding goals to be reached for each objective function $F^*(x) = \{f_i^*(x)\}$, and weights $\omega = \{\omega_i\}$ that enable the under or over-achievement of the targets. The optimisation problem is hence constructed as:

to minimize γ,

subject to: $f_i(x) - \omega_i \gamma \le f_i^*(x)$,

$x \in X, \ \gamma \in \mathbb{R}$

where γ is the attainment factor and X is the parameter domain of interest.

The two model outputs, final veneer humidity and total power consumption are optimised with the goal attainment method.

The regression models from the ANOVA results are used as the objective function. Hence, the problem is reduced to a two-objective optimisation problem:

minimize γ,

subject to: $f_1(x) - \omega_1 \gamma \le f_1^*(x)$,

$f_2(x) - \omega_2 \gamma \le f_2^*(x)$.

$x \in X, \ \gamma \in \mathbb{R}$

The weights ω_i are chosen such that $\sum_{i=1}^{2} \omega_i = 1$.

5. Results and discussions

The performance of the simulator was evaluated in various work regimes, the results of which are presented in this section. First, the most simplified simulation without air flowing freely between cells was tested to limit the number of factors affecting the overall performance of the drying chambers. In addition, all the inlet and outlet dampers operated without PID controllers (fixed free parameter $k^{-0.5} = 2$ for outlet exhaust lids position that is based on the initial condition of the fresh air flow rate at inlet to maintain air mass balance). The second simulation included air transport between the drying chambers while the dampers worked as in the previous simulation case. In the last case, the dryer worked in fully operative mode with active dampers, as shown in Fig. 2. Inlet dampers 4, 6, 10, 12 and outlet dampers 2, 8, 14 were On while others were Off. The simulation results achieved at different initial conditions are presented together for comparison purposes as presented in Table 3.

The model was simulated for 1800 s with the time step of 0.01 s. The simulation took 4.5 min, of which compilation and initialisation took 2.5 min, approximately 0.7 ms per time step, using 8 CPUs i7-7000 and 32 Gb of operative memory. This information allows

Table 3
Operating conditions of the veneer dryer defined for simulation.

Cases	Drying chamber connection	PID controller parameter, $\boldsymbol{k}^{-0.5}$	Active inlet dampers	Active outlet dampers
1	No	2	All	All
2	Yes	2	All	All
3	Yes	0.025–35	4, 6, 10, 12	2, 8, 14

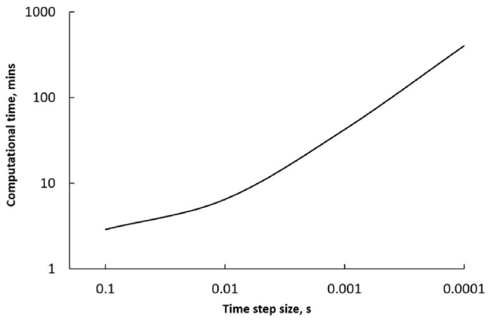

Fig. 13. Calculation time of 1 h simulation VS time step size at 8 CPUs i7-7000 and 32 Gb RAM.

planning the simulation time for the cases where other time step size is chosen, see, for example, Fig. 13. The maximum size of a single time step is limited by the residence time of air in the smallest sub-block, in this case 0.1 s. To obtain more accurate results, the time step size can be decreased to 0.001 s.

The dryer performance from the start to steady state operation was simulated using three sets or cases of operational conditions. The simulation results obtained at different initial conditions are presented in Table 3. Drying rate curves for various simulation scenarios are presented in Fig. 14. The veneer enters a drying cell with the gas-veneer contact area zero at the start, i.e. the moment the veneer sheets enter the drying chamber, and this contact area grows as the veneer is transported through the cell. The dynamic movement of the transported veneer was modelled in the simulations, which resulted in inclined vertical lines for the drying curves. As soon as the veneer reaches the maximum contact area, other limiting factors start dominating, such as the bearing capacity of the moist air and the humidity of the veneer.

Fully isolated drying cells have high air humidity, as seen in Fig. 17, which limits the drying rate in all the cells (see Fig. 14). The dynamic control of the dampers preserves the balance more efficiently. It can be used to minimize the heat duty of the radiators in the last five cells as the veneer approaches critical moisture content already in cell 12 of Figs. 14 and 18.

Fig. 15 presents the gas temperature at the fan sub-block. Pressure grows rapidly in an isolated cell as the temperature rises, pushing the outlet damper lid into the open position to let the air out. The outlet damper lid position affects the air humidity, which in turn influences the drying rate. The gas of reduced density carries less energy, which resulted in the temperature drop in case 1 of Fig. 15 when veneer enters the cells. The freely flowing air introduces more air into the cells. As can be seen in the figure, the outer drying cells 1 and 16 have lower air temperatures due to the connections with the smoke cells. The optimised work of the dampers keeps the air humidity below 0.6 $kgH_2O/kgDA$. The reduced drying rate caused the smaller final veneer temperature in case 1 of Fig. 16. The energy balance between convective heat transfer from gas to veneer and evaporation of water explains the plateau in the temperature of the veneer seen in cells 6–12.

The final moisture content of the veneer, shown in Fig. 18 is best controlled in the interconnected drying cells using the PID controllers. The dryer, operated according to the scenarios of Case 1 and 2, tends to overdry the veneer sheets that may lead to unwanted deformation and/or cracks. Hence, the operational conditions in Case 3, showed the best drying performance.

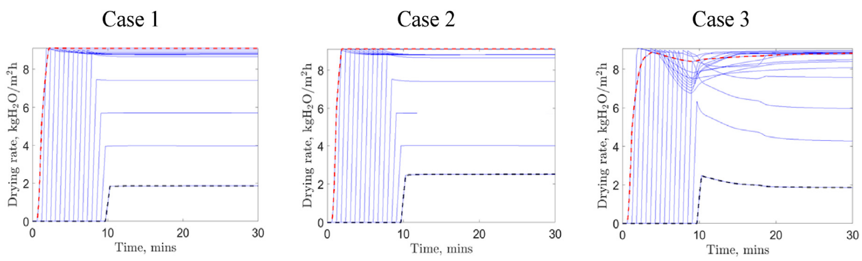

Fig. 14. Simulation results for the drying rate in drying cells at three different simulation scenarios (cases 1–3). The drying rate of the first drying cell chamber is plotted with red dashes, the last chamber with black dashes and other chambers with blue lines. (For interpretation of the references to color in this figure legend, the reader is referred to the Web version of this article.)

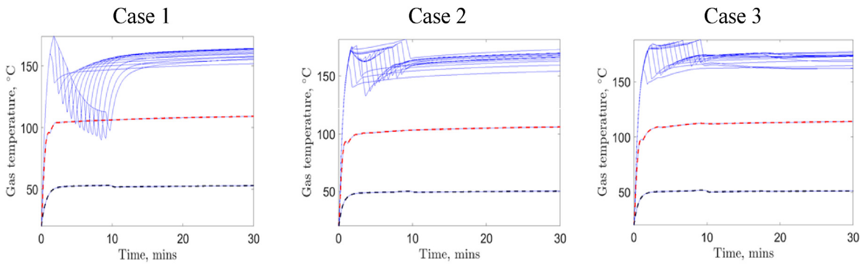

Fig. 15. Simulation results for air temperature at the fan sub-block in the drying cells in three different simulation scenarios (cases 1–3). The air temperature in the first drying cell chamber is plotted with red dashes, the last chamber with black dashes and other chambers with blue lines. (For interpretation of the references to color in this figure legend, the reader is referred to the Web version of this article.)

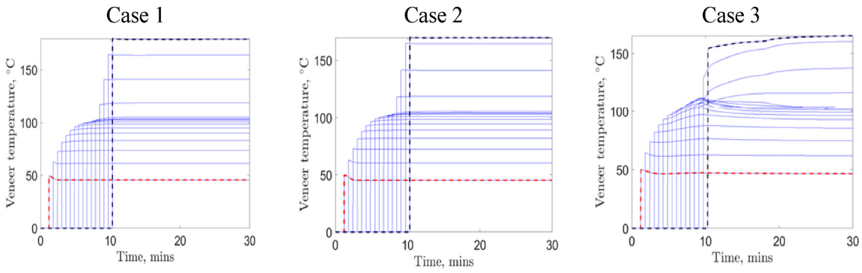

Fig. 16. Simulation results for the temperature of the veneer exiting the drying cells in three different simulation scenarios (cases 1–3). The veneer temperature in the first drying cell chamber is plotted with red dashes, the last chamber with black dashes and other chambers with blue lines. (For interpretation of the references to color in this figure legend, the reader is referred to the Web version of this article.)

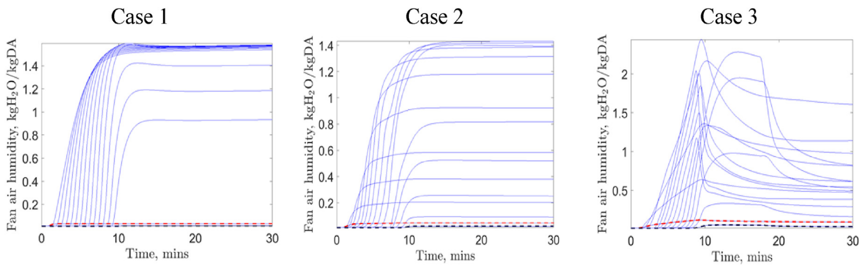

Fig. 17. Simulation results for air humidity in the fan sub-block in the drying cells in three different simulation scenarios (cases 1–3). The drying rate of the first drying cell chamber is plotted with red dashes, the last chamber with black dashes and other chambers with blue lines. (For interpretation of the references to color in this figure legend, the reader is referred to the Web version of this article.)

5.1. Sensitivity analysis results

The dryer model was used to simulate 30 min of drying performance. The control parameters were varied for the sensitivity analysis as described in Section 4.1. The simulated results of the final veneer humidity and the overall power consumption were stored for the ANOVA and optimisation of the parameters. The effect of the parameters was first examined graphically in Fig. 19. It is clear that radiator temperature is the major factor increasing the drying rate as shown in Fig. 19a. There is a slight relationship in term of the spread power consumption and initial veneer humidity in Fig. 19b.

The regression results for the final veneer humidity in Table 4 show the coefficients of the control parameters and their interactions. The initial veneer humidity and interaction between the humidity and the radiator temperature have t-value significantly different from zero hence contributing meaningfully to the output.

Fig. 21 presents the effect of radiator temperature and initial

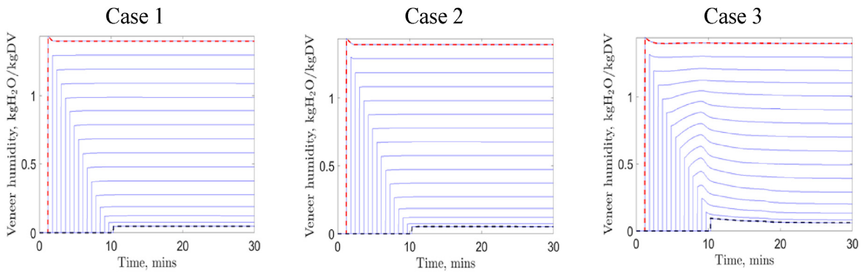

Fig. 18. Simulation results for the moisture content of the veneer exiting the drying cells in three different simulation scenarios (cases 1–3). The veneer moisture content in the first drying cell chamber is plotted with red dashes, the last chamber with black dashes and other chambers with blue lines. (For interpretation of the references to color in this figure legend, the reader is referred to the Web version of this article.)

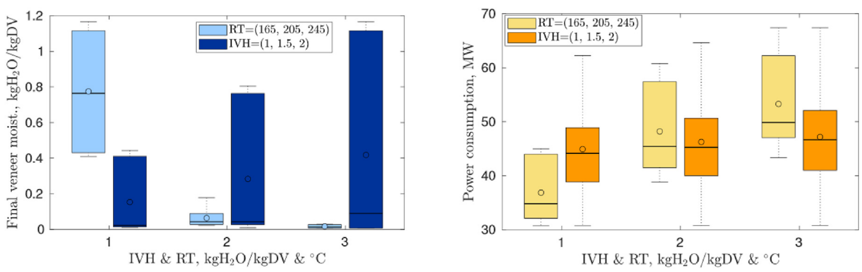

a) Simulated final veneer humidity at different initial veneer humidity and radiator temperature

b) Simulated power consumption at different initial veneer humidity and radiator temperature

Fig. 19. Design output of final veneer humidity and power consumption against radiator temperature and initial veneer humidity parameters.

veneer humidity values on the power consumption output. In an attempt to resolve the two conflicting objectives of minimising the final veneer humidity and power consumption, the goal attainment method of multi-objective optimisation is used. Hence, the objective functions are the regression models characterising the final veneer humidity output and power consumption output with regards to the design parameters. The goals values for both outputs are 0.05 $kgH_2O/kgDV$ and 30.7 MW respectively. The domain of the input parameters was restricted to the design in Table 1. A multi-objective optimisation problem was constructed as explained in Section 4.3, thus, the optimal parameter values and the corresponding function output are presented in Table 8 and Fig. 22.

The first set of the optimal values for both targets is 0.03 $kgH_2O/kgDV$ and 38.5 MW at initial veneer humidity of 1.5 $kgH_2O/kgDV$ and radiator temperature of 207.5 °C. The second set is 0.06 $kgH_2O/kgDV$ and 37.1 MW at initial veneer humidity of 1.5 $kgH_2O/kgDV$ and radiator temperature of 205 °C. At this point, an experienced decision marker is left to choose a desired solution from the available optimal values given.

6. Conclusions

Using the computational tools of MATLAB Simulink, a dynamic simulator for a continuous veneer dryer was built. The complicated mechanisms of heat and mass transfer inside the veneer dryer were described in a semi empirical model. The model describes the convective mass transfer of moisture from veneer plates continuously transported through the dryer sections where the heated air is blown by fans crosswise. In the model, a drying chamber is conditionally split into four sequentially connected sub-blocks, between which air can move. The system of damper lids operated by PID controllers is also modelled. The lids are opened more widely when the local air humidity rises. The moist air can move between the drying chambers towards the air outlet dampers driven by the static pressure.

The installed sensors ensure a slight underpressure atmosphere in the smoke cells through the action of the PID controllers linked to the outlet dampers. The underpressure maintains the fresh air inflow from the premises outside the dryer. The transported veneer

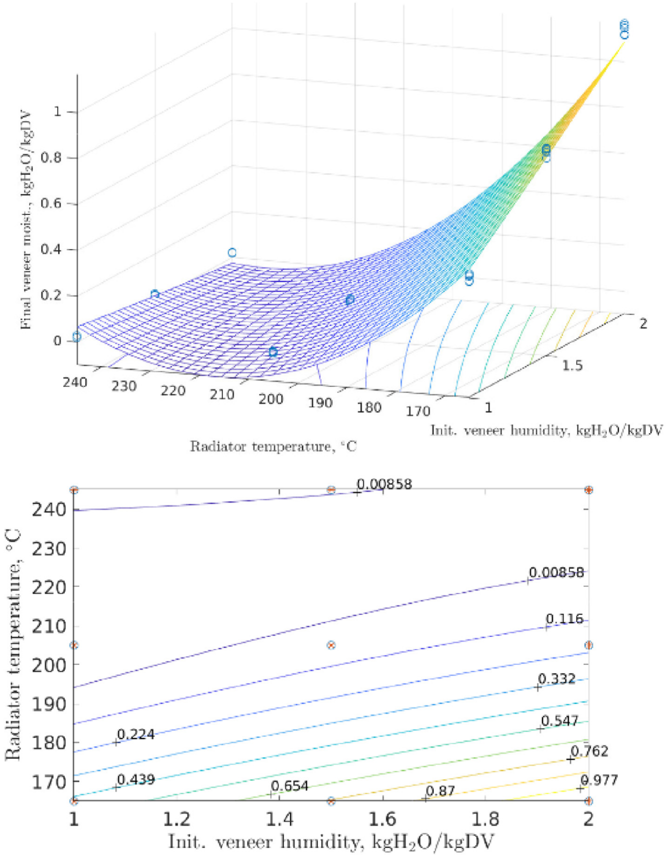

Fig. 20. Radiator temperature and initial veneer humidity parameters effect on final veneer humidity at conveyor speed 0.045 m/s, fan rate 35 m^3/s and atmospheric pressure 1013 hPa.

is heated while passing through the first seven cells until the maximum drying rate is reached. In the next five cells, the heat, removed during the active evaporation, is in balance with the heat transferred from hot air to the veneer. Then, the drying rate is gradually decreased and the veneer temperature rises to 150 °C in case 1 and to 180 °C in case 3. In the following cooling cells the temperature of the moving veneer drops to 30−40 °C, is a temperature suitable for manual handling. The mass and energy transport coefficients used in the convective drying model are empirical. The model performance is then compared and discussed. The simulation time is rather short from 10 to 20 min at reasonable time step size. The maximum time step size is limited by the air residence time in the fan sub-block.

The tested model shows adequate results obeying the physical principles of the thermodynamics. The validated model was used to optimise the process of convective drying for the veneer sheets. The veneer final moisture content at the end of the simulation was 0.04 $kgH_2O/kgDV$. The complicated mechanisms of heat and mass transfer inside the veneer dryer were simulated in three different scenarios stepwise increasing the model complexity. All three cases showed similar level of drying rate in the drying chambers. However, the simulated case 3, which is the closest to the practical running process, produced the driest veneer sheets and the least air humidity level in the drying chambers.

The selected operational parameters of the continuous veneer drying unit such as initial veneer humidity, radiator temperature, atmospheric pressure, fan speed, and conveyor belt speed were studied within the range of their practical variations via sensitivity analysis. The simulation outcomes using a balanced full factorial design indicated that the radiator temperature, the initial veneer

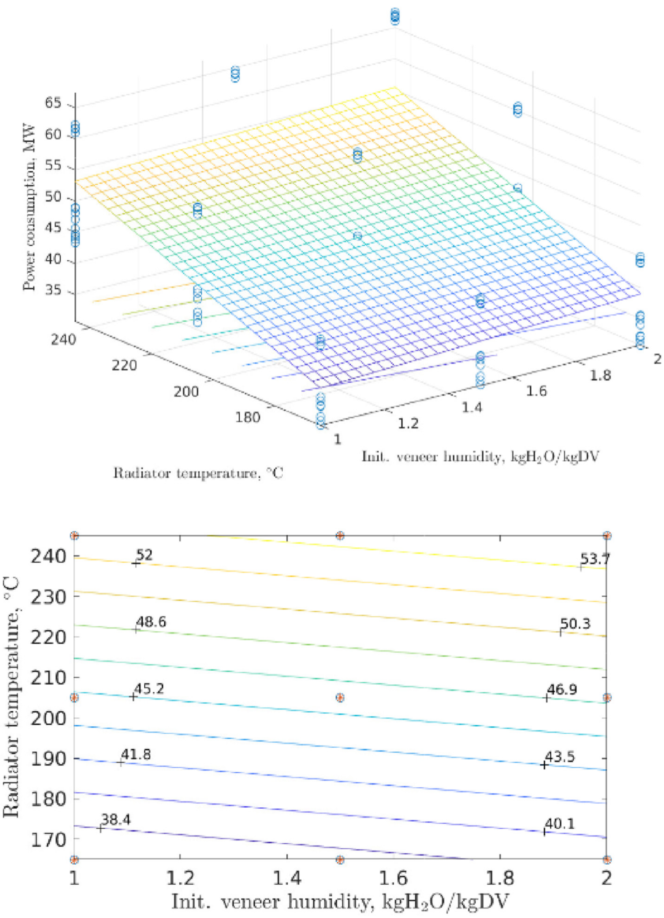

Fig. 21. Radiator temperature and initial veneer humidity parameters effect on power consumption output with conveyor speed at 0.045 m/s, fan rate at 35 m^3/s and atmospheric pressure at 1013 hPa.

humidity, and the fan rate were the most crucial parameters for the final veneer humidity output while all parameters except conveyor speed were significant for the power consumption output model. The regression model was used to characterise the relationship between the parameters and the model output. Subsequently, the ANOVA method was used to validate the regression model and a multi-objective optimisation to determine optimal set of parameters for the conflicting objective functions. The first model attains a high final veneer humidity with low radiator temperature and high initial veneer humidity, and a low final veneer humidity with high radiator temperature and low initial veneer humidity while the second model attains a high power consumption with high radiator temperature and high initial veneer humidity and a low power consumption with low radiator temperature and low initial veneer humidity. The multi-objective optimisation was instrumental in combining both objectives of minimising the final veneer humidity and power consumption. The analysis shows how a different combination of input parameters could affect final veneer humidity and power consumption, and the parameters with largest impact identified. The first optimal value for both final veneer humidity

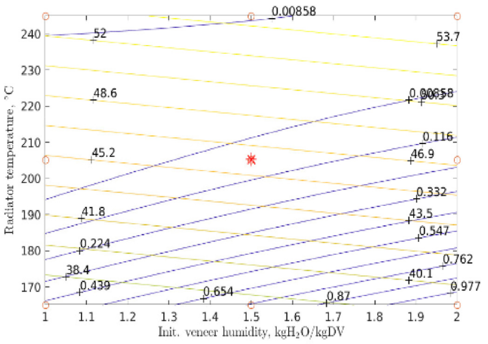

Fig. 22. Optimal values and response values for final veneer humidity and power consumption with conveyor speed at 0.045 m/s, fan rate at 35 m^3/s and atmospheric pressure at 1013 hPa.

Table 4
Regression estimates of parameter coefficients and test of significance for the final veneer humidity model.

Predictors	Coefficient	Standard Error	T-value	P-value
Intercept	0	6.432	0	1.000
IVH	1.970	0.326	6.052	0.000
FR	−0.009	0.016	−0.557	0.578
RT	−0.080	0.004	−18.48	0.000
CS	0	17.493	0	1.000
AP	$1.51 \cdot 10^{-4}$	$1.257 \cdot 10^{-4}$	1.2	0.231
IVH·ST	0.009	$2.6 \cdot 10^{-4}$	33.87	0.000
ST^2	$2.1 \cdot 10^{-4}$	$4.639 \cdot 10^{-6}$	45.08	0.000

The ANOVA results in Table 5 also show that the regression model significantly explains the variation. Fig. 20 presents the effect of radiator temperature and initial veneer humidity values on the final veneer humidity.

Table 5
ANOVA table statistics for regression model and residuals for final veneer moisture content.

Source	Sum of Sq.	DF	Mean Sq.	F-statistic	P-value
Regression	35.317	20	1.766	593.51	0.000
Residual	0.661	222	0.003		
Total	35.978	242			

A similar analysis was implemented for the power consumption from the regression model of the response surface graphs. The results for the power consumption, presented in Table 6 and Table 7, shows that the t-values of all parameters, except conveyor speed, are significant. The regression model doesn't consider the parameters interaction as the linear model is parsimonious enough to describe the model and the variations in the model.

Table 6
Regression estimates of parameter coefficients and test of significance for power consumption.

Predictors	Coefficient	Standard error	T-value	P-value
Intercept	1.746	6.818	0.256	0.798
IVH	2.266	0.455	4.982	0.000
FR	0.819	0.023	36.03	0.000
RT	0.205	0.006	36.09	0.000
CS	5.751	22.739	0.253	0.801
AP	0.0002	$6.475 \cdot 10^{-5}$	2.919	0.004

Table 7
ANOVA table statistics for regression model and residuals for power consumption.

Source	Sum of Sq.	DF	Mean Sq.	F-statistic	P-value
Regression	22,063	5	4412.6	526.77	0.000
Residual	1985.3	237	8.377		
Total	24,048	242			

Table 8
Optimal parameters values with corresponding target values of final veneer humidity and power consumption.

IVH	FR	RT	CS	AP	Veneer humidity	Power consumption
1.5	35	207.6	0.045	1013	0.03	38.5
1.5	35	205	0.045	973	0.06	37.1

and power consumption is 0.03 $kgH_2O/kgDV$ and 38.5 MW at initial veneer humidity of 1.5 $kgH_2O/kgDV$ and radiator temperature of 207.6 °C. The second optimal value for both final veneer humidity and power consumption is 0.07 $kgH_2O/kgDV$ and 37.1 MW at initial veneer humidity of 1.5 $kgH_2O/kgDV$ and radiator temperature of 205 °C. The results can be used as a guide for the real operational process in the case where a decision marker can select from varying optimal values.

Author contribution

Dmitry Gradov: Conceived and designed the analysis (Created the numerical model), Collected the data (Retrieved the data that were missing from the tech data package provided by the company), Contributed data or analysis tools (Performed some of the simulations), Performed the analysis (Validated the model, analyzed the results of ANOVA), Wrote the paper (The main part except ANOVA analysis part), Other contribution (Developed the work idea and structure, supervised ANOVA analysis). Yusuf Oluwatoki Yusuf: Performed the analysis (Performed ANOVA analysis), Wrote the paper (Described the ANOVA part). Jussi Ojalainen: Collected the data (Provided tech package for the work, consulted on the real dryer performance). Jarkko Suuronen: Conceived and designed the analysis: (Consulting on ANOVA analysis). Roope Eskola: Collected the data (Contributed to the tech package, provided by the company), Other contribution (Set the targets, performed supervision and the results assessment). Lassi Roininen: Conceived and designed the analysis Consulting on ANOVA analysis. Tuomas Koiranen: Conceived and designed the analysis (Consulted on mass and energy model basics, partake in trouble shooting of the model performance), Other contribution (Supervision, results assessment).

Declaration of competing interest

The authors declare that they have no known competing financial interests or personal relationships that could have appeared to influence the work reported in this paper.

Acknowledgement

The authors are grateful to Raute Oyj for the equipment provided, active supervision, and financial support.

Appendix

Operational conditions and constants	Values	Units
Air flow rate at the fan	25	m^3/s
Static pressure at 20 °C	0.005	Pa $m^3/(kg°C)$
Temperature of atmosphere	20	°C
Radiator temperature	205	°C
Humidity of air in atmosphere	80	%
Dryer production capacity	6	kg/s
Initial humidity of veneers	1.5	$kgH_2O/kgDV$
Speed of veeners transport	0.055	m/s
Atmospheric pressure	1013	hPa
Mass transfer	$3.26 \cdot 10^{-4}$	m/s
Density of dry veneer	430	kg/m^3
Heat capacity of water vapour	1900	J/(kg°C)
Heat capacity of veneer	1340	J/(kg°C) [47]
Heat capacity of dry air	1000	J/(kg°C)
Heat capacity of water	4200	J/(kg°C)
Heat capacity of stainless steel	500	J/(kg°C)
Molar mass of water	18	g/m
Latent heat of water	$2.26 \cdot 10^6$	J/kg
Convective mass transfer	$5.6 \cdot 10^{-4}$	m/s
Density of dry air	0.63	kg/m^3
Density of dry veneer	430	kg/m^3
Diffusivity of vapour through veneer	$2.7 \cdot 10^{-5}$	m^2/s
Kinematic viscosity of air	$1.48 \cdot 10^{-5}$	m^2/s
Diffusivity of vapour through veneer	$2.7 \cdot 10^{-5}$	m^2/s
Free parameter $k^{-0.5}$ in PID controllers	0.02535	

References

[1] Demirkir C, Özsahin S, Aydin I, Colakoglu G. Optimization of some panel manufacturing parameters for the best bonding strength of plywood. Int J Adhesion Adhes 2013;46:14–20. https://doi.org/10.1016/j.ijadhadh.2013.05.007.

[2] Ozsahin S, Aydin I. Prediction of the optimum veneer drying temperature for good bonding in plywood manufacturing by means of artificial neural network. Wood Sci Technol 2014;48:59–70. https://doi.org/10.1007/s00226-013-0583-2.

[3] Christiansen A. Effect of overdrying of yellow poplar veneer on physical properties and bonding. Holz als Rohund Werkstoff 1994;52:139–49. https://doi.org/10.1007/BF02615210.

[4] Northcott PL, Hancock WV, Colbech HGM. Water relations in phenolic (plywood) bonds. Forest Prod J 1962;12:478–86.

[5] Johnsson S, Andersson E, Thollander P, Karlsson M. Energy savings and greenhouse gas mitigation potential in the Swedish wood industry. Energy 2019;187:115919. https://doi.org/10.1016/j.energy.2019.115919.

[6] Baldwin RF. Veneer drying and preparation. In: Plywood and veneer-based products. San Francisco, California: Miller Freeman Books; 1995.

[7] Aydin I, Colakoglu G. Formaldehyde emission, surface roughness, and some properties of plywood as function of veneer drying temperature. Dry Technol 2005;23:1107–17. https://doi.org/10.1081/DRT-200059142.

[8] Jia L, Chu J, Ma L, Qi X, Kumar A. Life cycle assessment of plywood manufacturing process in China. Int J Environ Res Publ Health 2019;16:2037. https://doi.org/10.3390/ijerph16112037.

[9] Lamrani B, Kuznik F, Ajbar A, Boumaza M. Energy analysis and economic feasibility of wood dryers integrated with heat recovery unit and solar air heaters in cold and hot climates. Energy 2021;228:120598. https://doi.org/10.1016/j.energy.2021.120598.

[10] Gaillemard C. Modelling the moisture content of multiply paperboard in the paper machine drying section. Sweden: Ph.D. thesis KTH Royal Institute of Technology; 2006. https://www.diva-portal.org/smash/get/diva2:9961/FULLTEXT01.pdf.

[11] Smit G, Du Plessis J, du Plessis Sr J. Modelling of airflow through a stack in a timber-drying kiln. Appl Math Model 2007;31:270–82. https://doi.org/10.1016/j.apm.2005.11.003.

[12] Thant A, Yee S, Htike TT. Modeling drying time during veneer drying and comparison with experimental study. In: Proceedings of the international multiconference of engineers and computer scientists. IMECS; 2009 [Hong Kong], http://www.iaeng.org/publication/IMECS2009/IMECS2009_pp1911-1914.pdf.

[13] Rouch H. Fluid flow simulations using new cfd module – wood drying simulation. Proc COMSOL Conf Paris 2010:1–4. https://www.comsol.dk/paper/download/103597/rouch_paper.pdf.

[14] Laurijssen L, De Gram FG, Worrell E, Faaij A. Optimizing the energy efficiency of conventional multicylinder dryers in the paper industry. Energy 2010;35:3738–50. https://doi.org/10.1016/j.energy.2010.05.023.

[15] Jamaleddine TJ, Ray MB. Application of computational fluid dynamics for simulation of drying processes: a review. Dry Technol 2010;28:120–54. https://doi.org/10.1080/07373930903517458.

[16] Sandoval Torres S, Jomaa W, Puiggali JR, Avramidis S. Multiphysics modeling of vacuum drying of wood. Appl Math Model 2011;35:5006–16. https://doi.org/10.1016/j.apm.2011.04.011.

[17] Baxi H, Patel A, Barve J. Modelling and simulation of dryer system. In: 2015 international conference on industrial instrumentation and control (ICIC). IEEE; 2015. p. 1544–9.

[18] Di Marco P, Frigo S, Gabbrielli R, Pecchia S. Mathematical modelling and energy performance assessment of air impingement drying systems for the production of tissue paper. Energy 2016;114:201–13. https://doi.org/10.1016/j.energy.2016.08.011.

[19] Gluesenkamp KR, Boudreaux P, Patel VK, Goodman D, Shen B. An efficient correlation for heat and mass transfer effectiveness in tumbletype clothes dryer drums. Energy 2019;172:1225–42. https://doi.org/10.1016/j.energy.2019.01.146.

[20] Euh SE, Choi YS, Nam YS, Lee CG, Lee SY, Oh KC, et al. Development of a real-time drying control system for a pneumatic conveying dryer for sawdust in pellet production. Energy 2018;161:10–6. https://doi.org/10.1016/j.energy.2018.07.056.

[21] Zhang J, Yin J, Wang R. Basic framework and main methods of uncertainty quantification. Math Probl Eng 2020.

[22] Cox DC, Baybutt P. Methods for uncertainty analysis: a comparative survey. Risk Anal 1981;1:251–8. https://doi.org/10.1111/j.1539-6924.1981.tb01425.x.

[23] Kleijnen JP. Sensitivity analysis and optimization of system dynamics models: regression analysis and statistical design of experiments. Syst Dynam Rev 1995;11:275–88. https://doi.org/10.1002/sdr.4260110403.

[24] Kleijnen JP. An overview of the design and analysis of simulation experiments for sensitivity analysis. Eur J Oper Res 2005;164:287–300. https://doi.org/10.1016/j.ejor.2004.02.005.

[25] Bose D, Wright MJ, Palmer GE. Uncertainty analysis of laminar aeroheating predictions for mars entries. J Thermophys Heat Tran 2006;20:652–62. https://doi.org/10.2514/1.20993.

[26] Saltelli A, Ratto M, Andres T, Campolongo F, Cariboni J, Gatelli D, et al. Introduction to sensitivity analysis. Global sensitivity analysis. The primer. Wiley; 2008. p. 1–51. http://www.andreasaltelli.eu/file/repository/A_Saltelli_Marco_Ratto_Terry_Andres_Francesca_Campolongo_Jessica_Cariboni_Debora_Gatelli_Michaela_Saisana_Stefano_Tarantola_Global_Sensitivity_Analysis_The_Primer_Wiley_Interscience_2008_.pdf.

[27] Kalyanaraman J, Fan Y, Labreche Y, Lively RP, Kawajiri Y, Realff MJ. Bayesian estimation of parametric uncertainties, quantification and reduction using optimal design of experiments for CO_2 adsorption on amine sorbents. Comput Chem Eng 2015;81:376–88. https://doi.org/10.1016/j.compchemeng.2015.04.028.

[28] Bhattacharyya B. A critical appraisal of design of experiments for uncertainty quantification. Arch Comput Methods Eng 2018;25:727–51. https://doi.org/10.1007/s11831-017-9211-x.

[29] Cacuci DG. Sensitivity and Uncertainty Analysis. Theory. CRC Press; 2003. http://inis.jinr.ru/sl/tot_ra/0/0/3/Cacuci-Sensitiv.pdf.

[30] Lin G, Engel DW, Eslinger PW. Survey and Evaluate Uncertainty Quantification Methodologies. United States 2012. https://doi.org/10.2172/1035732.

[31] Borgonovo E, Plischke E. Sensitivity analysis: A review of recent advances. Eur J Oper Res 2016;248:869–87. https://doi.org/10.1016/j.ejor.2015.06.032.

[32] Woods D, Lewis S. Design of experiments for screening. Handbook of Uncertainty Quantification. Springer, Cham; 2017. https://doi.org/10.1007/978-3-319-11259-6_33-1.

[33] Sałat R, Awtoniuk M, Korpysz K. Black-box identification of a pilotscale dryer model: A Support Vector Regression and an Imperialist Competitive Algorithm approach. IFAC-PapersOnLine 2017;50:1559–64. https://doi.org/10.1016/j.ifacol.2017.08.309.

[34] ASHRAE. Handbook fundamentals. Atlanta: ASHRAE; 2005. https://shop.iccsafe.org/media/wysiwyg/material/8950P203-toc.pdf.

[35] Welty J, Rorrer GL, Foster DG. Fundamentals of Momentum, Heat, and Mass Transfer. 7th. John Wiley & Sons; 2019.. https://www.wiley.com/en-us/Fundamentals+of+Momentum%2C+Heat%2C+and+Mass+Transfer%2C+7th+Edition-p-9781119495413.

[36] Mujumdar AS. Impingement drying. Handbook of Industrial Drying. 4th. Taylor & Francis Group; 2014. p. 371–81.. https://doi.org/10.1201/b17208.

[37] Burnaev E, Panin I, Sudret B. Efficient design of experiments for sensitivity analysis based on polynomial chaos expansions. Ann Math Artif Intell 2017;81:187–207. https://doi.org/10.1007/s10472-017-9542-1.

[38] Antony J. Design of experiments for engineers and scientists. Elsevier; 2014. https://doi.org/10.1016/C2012-0-03558-2.

[39] Politis S, Colombo P, Colombo G, Rekkas D M. Design of experiments (DoE) in pharmaceutical development. Drug Dev Ind Pharm 2017;43:889–901. https://doi.org/10.1080/03639045.2017.1291672.

[40] Dante RC, Escamilla JL, Madrigal V, Theuss T, de Dios Caldero'n J, Solorza O, et al. Fractional factorial design of experiments for pem fuel cell performances improvement. Int J Hydrogen Energy 2003;28:343–8. https://doi.org/10.1016/S0360-3199(02)00069-1.

[41] Hoaglin DC, Welsch RE. The hat matrix in regression and ANOVA. Am

Statistician 1978;32:17–22. https://doi.org/10.2307/2683469.
[42] Faraway JJ. Practical regression and ANOVA with R. 2nd. CRC Press; 2014.. https://www.routledge.com/Linear-Models-with-R/Faraway/p/book/9781439887332.
[43] Ehrgott M. Multiobjective optimization. AI Mag 2008;29. https://doi.org/10.1609/aimag.v29i4.2198.
[44] Gaspar-Cunha A, Covas J. An Introduction to Multiobjective Optimization Techniques. Optimization in Polymer Processing. Nova Science Publishers; 2011.
[45] Coello CAC. Multi-objective Optimization. Springer, Cham; 2018. https://doi.org/10.1007/978-3-319-07153-4_17-1.
[46] Gembicki F, Haimes Y. Approach to performance and sensitivity multi-objective optimization: The goal attainment method. IEEE Trans Automat Control 1975;20:769–71. https://doi.org/10.1109/TAC.1975.1101105.
[47] Radmanovic' K, Dukic' I, Pervan S. Specific heat capacity of wood. Drv Ind: Znanstvenostru čni časopis za pitanja drvne tehnologije 2014;65:151.

Publication III

Mohammadi, M., Eskola, R., and Mikkola, A.

Constructing a Virtual Environment for Multibody Simulation Software Using Photogrammetry

Reprinted with permission from
Applied Sciences
10, 4079, 2020

applied sciences

MDPI

Article

Constructing a Virtual Environment for Multibody Simulation Software Using Photogrammetry

Manouchehr Mohammadi [1,*], Roope Eskola [1,2] and Aki Mikkola [1]

[1] Department of Mechanical Engineering, Lappeenranta-Lahti University of Technology, 53850 Lappeenranta, Finland; roope.eskola@raute.com (R.E.); aki.mikkola@lut.fi (A.M.)

[2] Raute Corporation, Research and Development, 15550 Lahti, Finland

* Correspondence: Manouchehr.Mohammadi@lut.fi; Tel.: +358-449395439

Received: 18 May 2020; Accepted: 10 June 2020; Published: 12 June 2020

Abstract: Real-time simulation models based on multibody system dynamics can replicate reality with high accuracy. As real-time models typically describe machines that interact with a complicated environment, it is important to have an accurate environment model in which the simulation model operates. Photogrammetry provides a set of tools that can be used to create a three-dimensional environment from planar images. A created environment and a multibody-based simulation model can be combined in a Unity environment. This paper introduces a procedure to generate an accurate spatial working environment based on an existing real environment. As a numerical example, a detailed environment model is created from a University campus area.

Keywords: laser scanning; photogrammetry; real-time simulation; three dimensional environment; unity software

1. Introduction

In general, real-time simulation models based on multibody system dynamics interact with the graphical environment to illustrate the feasibility of the model and its functionality. Figure 1 shows examples of real-time simulation models and their environments, in which the environments vary from simple, see Figure 1a, to highly detailed and complex, see Figure 1d.

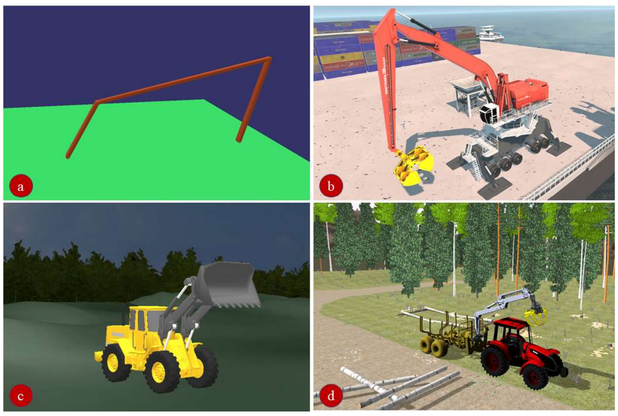

Figure 1. Simulation models with their working environments: (**a**) Four-bar mechanism. (**b**) Material handler. (**c**) Wheel loader. (**d**) Forestry vehicle.

A simulation model interacts with its environment via tires, tracks, or other bodies that it can come into contact with and moves the environmental objects; Figure 1c,d shows typical examples. Graphical software, such as Blender, and game engine software, such as Unity, Unreal Engine, and CryEngine, can be utilized to generate working environments [1–5]. Each software has its own advantages and disadvantages. In Unity, the C programming language is used, whereas Unreal Engine and CryEngine use the C++ language. Unity has the capability to compile games from different platforms [6], and offers preprogrammed three-dimensional models, cameras, and lights [7]. Unreal Engine is a license-free software.

Graphical software makes it possible to generate environments for use in electronic games, virtual reality applications [8], and simulations. Realistic environment is an important aspect of simulations used, for example, to train operators of industrial vehicles [9–11]. Such training can help operators perform more efficiently, prevent accidents, and increase safety [12–14]. Graphical software are also widely used in the development of high-quality three-dimensional environments for educational purposes [15–17].

Photogrammetry is an estimation of the geometric and semantic properties of objects based on image analysis [18]. In other words, it is an approach used to generate three-dimensional models from detailed images of an object/area [19]. Digital photogrammetry collects data about an environment by calculating the locations of objects based on a predefined coordinate system [20]. It has been applied in many different fields and studies, such as material testing [21], recognition of deformation of beam elements and structures in fire tests [22,23], measurement of vertical deflections in large constructions such as bridges [24], and measurement of the roughness of the soil surface for better understanding of erosion processes [25]. Researchers have also generated precise three-dimensional models of large assets such as museums and historical sites by employing photogrammetry and laser scanning approaches [26–29]. Many scholars have studied how to generate 3D models using point cloud data. Cielos et al. introduced a methodology for the creation of 3D models. The method employs a laser scanning concept with light detection. With the help of this method, point cloud data can be collected, even in harsh weather conditions, to construct the 3D models. In addition, the collected point data can be used directly in photogrammetric software [30]. Laser scanning is widely used in building construction applications to collect point cloud data and utilise them for creation of 3D outdoor and indoor models of buildings [31]. Laser scanning has also been used to extract accurate data from rock surfaces [32].

In recent years, photogrammetry concept has also been used for mobile phones to construct 3D models of indoor places and close-range distances [33,34]. Many studies have been conducted to increase the accuracy of the photogrammetry method in the applications of city planning and building recognition. Wang et al. has introduced a procedure-based online matching to increase the accuracy of the 3D models produced with the photogrammetry. The procedure has been applied in recognizing buildings in aerial images [35]. In addition, the photogrammetry method is currently being used for constructing historical and cultural buildings [36]. Scholars have utilized photogrammetry to create 3D models of historical sites, which were created using the graphical software (Unity) for the virtual reality aspect [37,38]. Topographic methods or linear variable differential transducers (LVDTs) are two examples of alternative approaches for creation of a three-dimensional model from an object or area. However, they have major disadvantages, such as requiring long processing time, intensive manual work, and limitations in points positioning in a structure [39].

Laser scanning is also an alternative approach to photogrammetry. A notable advantage of the laser scanning approach is that it allows the data of low-textured objects to be collected. This is a situation where the photogrammetry matching approach often fails. The laser scanning uses a Global Positioning System (GPS) and Internal Navigation System (INS) for sensor orientation [40], and derives three-dimensional coordinates using Time of Flight (TOF) [41]. The laser scanner transmits impulses towards an object and estimates the distance between the scanner and the object. In addition, the laser scanner sends a laser line to an object and records the laser line reflection to obtain the geometry of the object [42].

Laser scanning, mainly airborne laser scanning (ALS), and photogrammetry have some differences and similarities. For example, they both use GPS and digital sensors. On the other hand, ALS uses point sensors, whereas photogrammetry uses line sensors. ALS takes points out of an area and photogrammetry covers the whole area. The production time in ALS is typically longer than in photogrammetry [40]. Photogrammetry is an inexpensive, easy-to-set-up method. On the other hand, in photogrammetry, to capture images with an appropriate map, mainly in harsh weather conditions, an experienced operator is needed. For some laser scanners, an extra digital camera is needed to capture RGB colors of surfaces. The disadvantage of scanners that have their own digital camera, is their low geometric resolution [43]. Laser scanning has a higher measurement accuracy than photogrammetry, however laser scanning procedures mostly costs more than photogrammetry [44]. When the material of the model/object absorbs or diffuses the laser, the photogrammetry method mostly works properly [45]. A number of studies have been conducted to identify the material during 3D model constructions. One of the material recognition methods is to classify the images and laser scanning data based on the spectral categorization. In this method, the image will be classified and analyzed based on its wavelength. Furthermore, by image analyzing, the effect of the environmental phenomena on the buildings' surfaces can also be identified [46]. In some cases, laser scanning usage might be limited to short distances [47].

The laser scanning method also has some disadvantages. To collect accurate point cloud data via a laser scanner, the precision of the operator plays a crucial role. Furthermore, converting the collected point cloud data into a 3D model of buildings requires intensive work [48]. In addition, the laser scanner has to be relocated several times during the process; therefore, in the collected point cloud data, the buildings' deformation should be considered [49]. A number of scholars conducted studies on collecting point cloud data using various procedures. Wang et al. have accomplished a comprehensive study on different applications, such as photogrammetry, Lidar, as well as laser scanning, to collect 3D point clouds in the construction industry. Point cloud data can be used for different purposes and areas, such as civil engineering, construction industries, and tracing progress in building constructions [50].

The objective of this paper is to generate a working environment for real-time multibody based simulation models. The environment is created from an existing area in the real world. The campus area of Lappeenranta-Lahti University of Technology, LUT University, Finland is selected as the case study. In this study, Unity software was used to develop the campus environment.

2. Methodology

This section introduces a procedure to create a three-dimensional environment using photogrammetry and graphical software.

From a graphical point of view, a multibody simulation model consists of graphics of bodies and the working environment that the machine is interacting with. Multibody simulation software usually offers the possibility to create a simple environment. However, as will be shown in this paper, a multibody model can represented in a graphical software. The use of graphical software allows a detailed description of a working environment.

Photogrammetry Approach

Photogrammetry uses contact-free sensors, which makes it possible to create three-dimensional models of objects that are expensive, fragile, toxic, or visible but inaccessible. It also allows to document the changes of an object or area, such as a building construction.

Photogrammetry suffers from a number of shortcomings such as sensitivity to light conditions. The light source can be optimized for small objects but in the case of outdoor objects and environments, optimization of lighting conditions remains a challenge.

To create a three-dimensional model with high precision, a large number of images are needed. In general, to create an initial three-dimensional model of a single object, a minimum of two planar images with a known offset is necessary [7]. A functional and affordable method for taking thousands of images of a wide area (including tall structures such as buildings) is the use of Unmanned Aerial Vehicles (UAVs) [51,52]. Assisted by UAVs, photogrammetry can be extended to cover areas in the scale of square kilometers.

Figure 2 presents a procedure for using photogrammetry to create a three-dimensional model of an area/object.

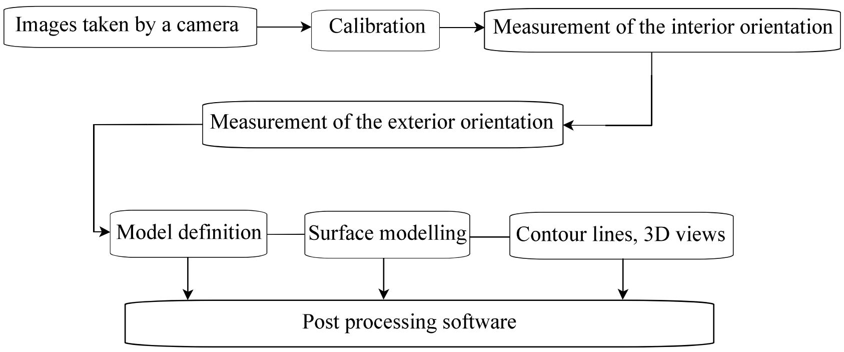

Figure 2. Overview of the photogrammetry procedure.

As Figure 2 illustrates, obtained images should be calibrated to calculate the distance between the camera and the object [53]. In the figure, exterior orientation means calculation of the exterior coordinates, which are the location of the projection center and the rotation angles of the object with respect to the considered global coordinate system. Surface modeling can be applied to the object to visualize the texture. In the final step, postprocessing is done to create a three-dimensional model of the object.

To put it simply, photogrammetry creates three-dimensional models out of planar images. To this end, postprocessing software compares two images taken of an object or area and recognizes identical points, see Figure 3. "Overlapping" between images helps to simplify the identical point recognition process and increases the quality of the object's texture. In addition, "shape matching" can be assisted to match corresponding points in two overlapping images. Shape matching technique has different varieties. One common technique compares the shape of objects in two images without color consideration. This simplifies the process and reduces computational time. By considering corresponding points and the orientation of the cameras, the location of points in the three-dimensional environment can be estimated.

Even though the photogrammetry approach is extensively used to generate virtual realistic environments, it still faces some barriers and limitations. In most cases, the geometry and exact location of the object under investigation should be estimated. Transparent and dark colored objects, as well as tiny objects, pose challenges for photogrammetry [27,54,55]. Furthermore, there are some limitations when using photogrammetry and laser scanning procedures. Objects that are small, shiny, and transparent cannot be accurately captured in photogrammetry and laser scanning procedures. In addition, materials that absorb or diffuse the laser beams, are barriers to accurately collecting point cloud data during the laser scanning procedure.

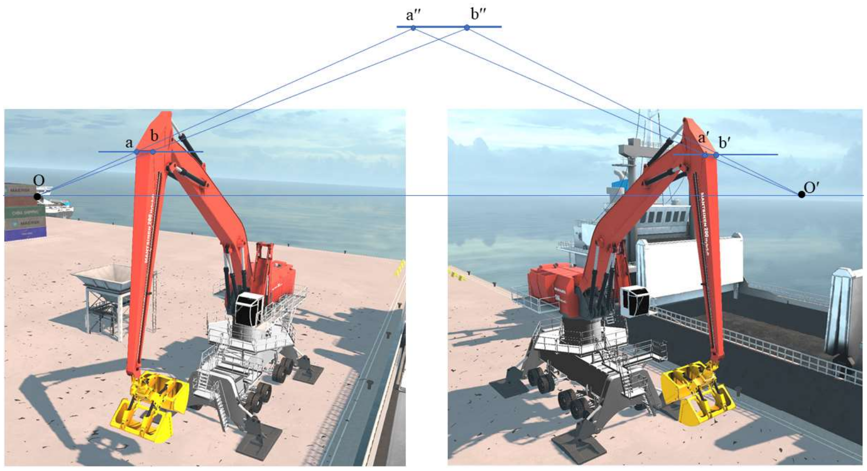

Figure 3. Estimation of three-dimensional specifications of a vehicle by comparing two planar images.

3. Example Case

In this study, a photogrammetry approach is used to create an environment model from the campus area of Lappeenranta-Lahti University of Technology (LUT University). The University is located in the south of Finland, Figure 4. The photogrammetry covered area in this study is approximately 40,000 square meters.

Figure 4. Lappeenranta-Lahti University campus area selected for the photogrammetry.

3.1. Equipment

In this study, to collect three-dimensional data for photogrammetry, a drone (as a UAV) and a laser scanner were used. The drone used is a phantom 4 RTK from DJI Technology INC., see Figure 5. The Phantom 4 RTK drone has a location system, communication , and propulsion systems, as well as a flight controller, and a battery. The maximum flight speed is 49.9 m per second and the drone weighs 1391 g. The battery life is sufficient for a 30 min flight. Horizontal accuracy for the Phantom 4 RTK is three centimeters and it stores three-dimensional observational data, which will be used with the postprocessing software. The three centimeter horizontal accuracy is the relative accuracy. As pointed out, there is a ground reference check point where the drone started to fly from. Note that, the reference spot was inside the campus area. The drone carries a 20 megapixel camera with a CMOS sensor. A three-axis gimbal is attached to the drone to provide stability for the camera and enable a high resolution and clear images. The drone is also equipped with obstacle sensors to prevent crashes during flight. The remote flight controller uses the GS RTK app to generate a flight plan. The controller has a built-in 5.5 inch (13.97 cm) screen which shows the flight map of the drone, see Figure 6.

Figure 5. Phantom 4 RTK drone and controller.

Figure 6. Flight maps of the chosen area for photogrammetry.

A laser scanner, Faro S70, was used to obtain a high-quality and accurate three-dimensional environment, see Figure 7. The laser scanner collects points in the order of millions (points cloud) to converge planar images to a three-dimensional model.The laser scanner also captures the textures of surfaces of buildings and other objects. It can be used both indoor and outdoor and it is suitable for distances between 0.6 m to 70 m. It can recognize the point locations with an accuracy of ±1 mm and can provide one million points per second.

Figure 7. FARO S70 laser scanner.

For the post processing step, the FARO S70 laser scanner uses FARO SCENE software or the Autodesk Reality Capture software, (ReCap software).

3.2. Procedure for Three Dimensional Environment

Figure 8 shows the process steps for a photogrammetry approach using a drone and a laser scanner to generate a three-dimensional environment for the use of real-time simulation.

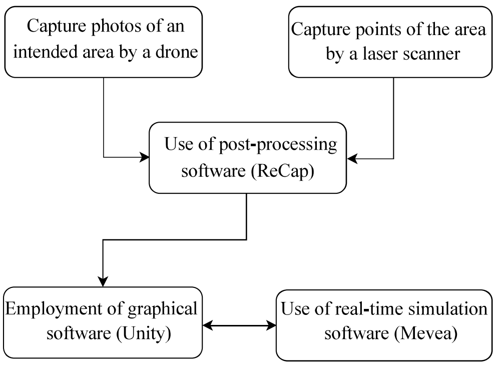

Figure 8. Process steps to generate an environment for real-time simulation software using a photogrammetry approach and Unity software.

As Figure 8 illustrates, the photogrammetry starts with the drone taking thousands of images. The drone flies at a specific height and takes images with a specified overlap between each two continuous images. Simultaneously, a laser scanner scans the environment and generates a point cloud of structures, the ground, trees and other objects. The images and point cloud are exported to a postprocessing software to generate an initial three-dimensional environment. ReCap software was utilized as the postprocessing software in this study. The generated initial environment is exported to a graphical software to create a detailed environment that can be employed in a real-time multibody simulation. In the procedures used, the drone captures the images and the laser scanner collects the point clouds. The laser scanner software has an altimeter, an inclinometer, a compass, and a color recognition feature.

Prior to starting photogrammetry and the laser scanning processes, a ground reference point for the laser scanner and the drone are defined. Based on the ground reference point, the postprocessing software identifies the corresponding points on surfaces in both methods. Prior to the operation, the laser scanner locations were predefined during its operation. This pre-definition helps with point matching and line matching between images and point cloud data.

The point cloud data collected by the laser scanner are exported to the photogrammetry software, ReCap, where the alignment between points is accomplished. Afterwards, the images are exported to the software, where the alignment between images will be done. At the final stage, the alignment between the point cloud data and images is accomplished based on the check points. As mentioned previously, the laser scanning process is performed to demonstrate the precise textures of the walls. At this stage, the multibody simulation software models can interact with the generated environment in the graphical software platform. Accordingly, there is no need to export the generated environment from the graphical software to the real-time simulation software. Instead, a model and its environment can be illustrated in the graphical software platform and controlled by the simulation software. Figure 9 shows an example of a model and an environment in the graphical software that can be controlled by the real-time simulation software. The graphics of the forklift model in Figure 9 were created in Blender software and the environment generated by Unity software.

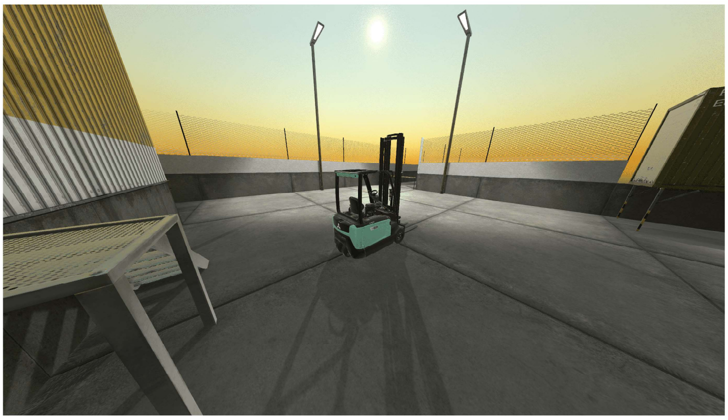

Figure 9. A fork lift model in its environment as an example of a combination between a real-time simulation software and Unity software.

Figure 6 shows the flight map of the drone for the targeted area. The drone started flying from a specified spot and, after arriving at a specific height, it flew horizontally with a horizontal velocity of ~20 km per hour while taking images. During its flight, the drone took approximately 1900 images with 80 percent overlap between continuous images. The percentage of the overlap can be defined by the controller before the flight. The maximum height that the drone flew was 50 m. Although in some photogrammetry procedures drones capture both nadiral and oblique images, in this case study, the drone captured nadiral images. The constructed 3D environment model is based on the nadiral images and point cloud, which is collected by the laser scanner.

To collect the point cloud data, the operators relocated the laser scanner to certain predefined locations. The whole process took nearly three hours. The obtained images and the point cloud data were transferred to the Recap software to build the three-dimensional environment. The ReCap software created a three-dimensional model, made some markers as Geo-references, and took measurements pertaining to the height. Finally, the Unity software prepared the environment for use in the simulation software

4. Discussion

As already stated, nearly 1900 images were taken of the campus area. In this section, a number of views of the campus area have been chosen for comparison to illustrate similarities and differences between the environment in the real world and the corresponding environment in Unity software, see Figures 10–13.

(**a**)

(**b**)

Figure 10. Comparison between the LUT University campus area in the real world and in Unity software using photogrammetry: (**a**) Real world and (**b**) Unity environment.

Figures 10a and 11a depict the campus area of the LUT University in the real world, and Figures 10b and 11b illustrate the area as it is created using photogrammetry. As the figures show, the created environment reflects the real world environment appropriately. Cloudy weather facilitated proper matching of the points collected by the laser scanner with the corresponding points in the images. As Figures 10b and 11b demonstrate, the physical dimensions of the buildings, their locations, as well as the distances between the structures have been correctly generated. The paths and streets are created without notable failures. Figures 12a,b and 13a,b show the main entrance of the University in the real world and in the graphical software, respectively. Comparing the point of views, the distances between points are measured in both the real world and the graphical software. Table 1 shows the values for the point distances. As the table shows, the 3D graphical environment constructed by photogrammetry procedure reflects the real world environment appropriately.

(**a**)

(**b**)

Figure 11. A comparison between the LUT campus buildings in real world and in the graphical software using the photogrammetry approach: (**a**) Real world and (**b**) Unity environment.

Figures 12a and 13a show the main entrance area of the LUT University main building. Figures 12b and 13b are the corresponding scenes generated using the photogrammetry approach. As the figures show, the postprocessing phase in the photogrammetry is accomplished with acceptable accuracy. Nearly all points (generated by the laser scanner) match properly with the corresponding points in the images taken by the drone. The buildings are created appropriately and there is no major distortion in the structures. Comparisons of the dimensions, colors, and textures in Figure 12a,b show that Figures 12b and 13a provide a highly accurate reflection of the real world. As pointed out, to construct the 3D environment model out of the planar images, photogrammetry has been used.

In this study, a laser scanner has been utilised to increase the visibility and accuracy of the building surfaces, such as walls and windows. In addition, the environment will be used in the application of physics based real-time simulation models. Therefore, both methods have been utilised to keep the environment as realistic as possible.

(**a**) (**b**)

Figure 12. LUT University main entrance in the real world and in the graphical software using the photogrammetry-based approach: (**a**) Real world and (**b**) Unity environment.

(**a**)

(**b**)

Figure 13. Comparison between the textures in the real world and created in the graphical software using the photogrammetry-based approach: (**a**) Real world and (**b**) Unity environment.

Table 1. The distance values shown in Figures 12a,b and 13a,b.

Name	D1 (m)	D2 (m)	D3 (m)	D4 (m)
Real world environment	5.6	4.3	6.45	19.6
Graphical software environment	5.6	4.3	6.45	19.6

As mentioned earlier, the graphical software can be connected to the simulation software to run simulation models. The environment of the LUT University campus area can be used for real-time simulation models. Figure 14 shows a real-time simulation model of an excavator which has been imported to the university campus environment.

Figure 14. Excavator model in the LUT campus area.

The model is of a real excavator with 22 tons of operating weight. The excavator-simulated model consists of nine bodies. Its hydraulic circuit system is modeled using Lumped Fluid Theory [56]. The definitions of the bodies and their constraints, as well as interactions between them are accomplished in real-time simulation software that employs the semi-cursive multibody method [57]. In addition, these equations of motions can be solved using the Runge–Kutta time integration [58]. The excavator graphical model was created using the Blender software. The graphics for the excavator consist of the graphics to illustrate the model and the collision graphics. The collision graphics define the contacts between the bodies as well as with the ground. By collecting data that the real-time simulation models provide, designers can analyze dynamic behavior and consequently improve the performance of the models. In this study, a 3D environment based on the real world has been constructed such that it interacts with real-time simulation models. In practice, the model interacts with the environment, for example, an excavator driver can drive and excavate soil and have the experience of both working with a real excavator, and working in an environment based on the real world. Furthermore, data collected for real-time simulation models is more reliable than operating in an imaginary environment. From an educational point of view, the use of digital twin models in an environment based on the real-world assists operators in learning more quickly and more precisely. In addition, with the help of the virtual reality concept, the education process can be made more functional and closer to the real-world.

5. Conclusions

In this paper, a procedure for generating a three-dimensional environment based on a photogrammetry approach is introduced. To create the environment, a drone and a laser scanner were used to take images and collect the point cloud data, respectively. Using a photogrammetry-based approach, it is possible to generate environments that exist in the real world. Furthermore, the graphical software can be connected to the simulation software, which makes it possible to operate physics-based simulation models in their real environments.

The procedure introduced was applied to create an environmental model of the campus area of the LUT University in Finland. A multibody simulation model of an excavator was exported to the campus area. The real-time simulation model is run in a *dynamic environment*, which means the generated three-dimensional environments can be updated based on renovations in the corresponding real environment.

Author Contributions: A.M. worked with the concept and editing the manuscript. M.M. worked on the literature review, writing the manuscript, and performed the experiments and results. R.E. contributed to the writing and methods used. All authors have read and agreed to the published version of the manuscript.

Funding: This research is in part funded by the Academy of Finland Grant No. 316106.

Conflicts of Interest: The authors declare no conflicts of interest.

References

1. Yang, C.W.; Lee, T.H.; Huang, C.L.; Hsu, K.S. Unity 3D Production and Environmental Perception Vehicle Simulation Platform. In Proceedings of the IEEE 2016 International Conference on Advanced Materials for Science and Engineering (ICAMSE), Tainan, Taiwan, 12–13 November 2016; pp. 452–455.
2. Vajak, D.; Livada, Č. Combining Photogrammetry, 3D Modeling and Real Time Information Gathering for Highly Immersive VR Experience. In Proceedings of the IEEE 2017 Zooming Innovation in Consumer Electronics International Conference (ZINC), Novi Sad, Serbia, 31 May–1 June 2017; pp. 82–85.
3. Fritsch, D.; Klein, M. 3D Preservation of Buildings–Reconstructing the Past. *Multimed. Tools. Appl.* **2018**, *77*, 9153–9170. [CrossRef]
4. Mach, V.; Valouch, J.; Adámek, M.; Ševčík, J. Virtual Reality–Level of Immersion Within the Crime Investigation. In *MATEC Web of Conferences*; EDP Sciences: Zlín, Czech Republic, 2019; Volume 292, p. 01031.
5. Chiu, Y.P.; Shiau, Y.C.; Song, S.J. A Study on Simulating Landslides Using Unity Software. In *Applied Mechanics and Materials*; Trans Tech Publications Ltd.: Baech, Switzerland, 2015; Volume 764, pp. 806–811.
6. Isar, C. A Glance into Virtual Reality Development Using Unity. *Inf. Econom.* **2018**, *22*. [CrossRef]
7. Uggla, G. 3D City Models-A Comparative Study of Methods and Datasets. Master's Thesis, School of Architecture and the Built Environment Royal Institute of Technology (KTH) Stockholm, Sweden, 2015.
8. Oqua, O.I.; Chen, J.; Annamalai, A.; Yang, C. 3D Printed Data Glove Design for VR Based Hand Gesture Recognition. In Proceedings of the IEEE 2018 11th International Workshop on Human Friendly Robotics (HFR), Shenzhen, China, 13–14 November 2018; pp. 66–71.
9. Brady, D.; Lee, A.; Pearce, A.; Shintaku, N.; Guerlain, S. Intelligent Cities: Translating Architectural Models Into a Virtual Gaming Environment for Event Simulation. In Proceedings of the IEEE 2015 Systems and Information Engineering Design Symposium, Charlottesville, VA, USA, 24 April 2015; pp. 369–373.
10. Silva, J.F.; Almeida, J.E.; Rossetti, R.J.; Coelho, A.L. A Serious Game for EVAcuation Training. In Proceedings of the 2013 IEEE 2nd International Conference on Serious Games and Applications for Health (SeGAH), Vilamoura, Portugal, 2–3 May 2013; pp. 1–6.
11. Chittaro, L.; Ranon, R. Serious Games for Training Occupants of a Building in Personal Fire Safety Skills. In Proceedings of the IEEE 2009 Conference in Games and Virtual Worlds for Serious Applications, Coventry, UK, 23–24 March 2009; pp. 76–83.
12. Bhide, S.; Riad, R.; Rabelo, L.; Pastrana, J.; Katsarsky, A.; Ford, C. Development of Virtual Reality Environment for Safety Training. In Proceedings of the IIE Annual Conference, Orlando, FL, USA, 19–23 May 2015; Institute of Industrial and Systems Engineers-Publisher (IISE): Norcross, GA, USA, 2015; p. 2302.
13. Sacks, R.; Perlman, A.; Barak, R. Construction Safety Training Using Immersive Virtual Reality. *Constr. Manag. Econ.* **2013**, *31*, 1005–1017. [CrossRef]
14. Friend, M.A.; Kohn, J.P. *Fundamentals of Occupational Safety and Health*; Rowman & Littlefield: Lanham, MD, USA, 2018.
15. Birt, J.; Stromberga, Z.; Cowling, M.; Moro, C. Mobile Mixed Reality for Experiential Learning and Simulation in Medical and Health Sciences Education. *Information* **2018**, *9*, 31. [CrossRef]
16. Wang, Y.; Yang, L.; Zhao, L.; Deng, Y. Design of Simulation Training System for Remote Sensing Large Data Processing of Natural Disasters. *J. Coast. Res.* **2018**, *83*, 328–334. [CrossRef]
17. Chou, Y.T.; Lee, B.W.; Shih, H.Y. Study on Educational Virtual Reality Implementation Using Knowledge-Based Engineering. In Proceedings of the 2018 IEEE International Conference on Advanced Manufacturing (ICAM), Yunlin, Taiwan, 16–18 November 2018; pp. 433–436.
18. ISPRM. International Society of Photogrammetry and Remote Sensing. 2019. Available online: https://www.isprs.org (accessed on 10 January 2020).

19. Mikhail, E.M.; Bethel, J.S.; McGlone, J.C. Introduction to Modern Photogrammetry. *NewYork* **2001**, *19*.
20. Linder, W. *Digital Photogrammetry*; Springer: Berlin, Germany, 2009.
21. Whiteman, T.; Lichti, D.; Chandler, I. Measurement of Deflections in Concrete Beams by Close-Range Digital Photogrammetry. In Proceedings of the Symposium on Geospatial Theory, Processing and Applications, Ottawa, ON, Canada, 9–12 July 2002; pp. 9–12.
22. Fraser, C. Automated Off-Line Digital Close-Range Photogrammetry: Capabilities & Application. In Proceedings of the 3rd International Image Sensing Seminar on New Developments in Digital Photogrammetry, Gifu, Japan, 24–27 September 2001.
23. Fraser, C.S.; Riedel, B. Monitoring the Thermal Deformation of Steel Beams via Vision Metrology. *ISPRS J. Photogramm. Remote. Sens.* **2000**, *55*, 268–276. [CrossRef]
24. Jáuregui, D.V.; White, K.R.; Woodward, C.B.; Leitch, K.R. Noncontact Photogrammetric Measurement of Vertical Bridge Deflection. *J. Bridge. Eng.* **2003**, *8*, 212–222. [CrossRef]
25. Rieke-Zapp, D.; Wegmann, H.; Santel, F.; Nearing, M. Digital Photogrammetry for Measuring Soil Surface Roughness. In Proceedings of the American Society of Photogrammetry & Remote Sensing 2001 Conference–Gateway to the New Millennium', St Louis, MO, USA, 23–27 April 2001; American Society of Photogrammetry & Remote Sensing: Bethesda, MD, USA, 2001.
26. Remondino, F.; Rizzi, A. Reality-Based 3D Documentation of Natural and Cultural Heritage Sites—Techniques, Problems, and Examples. *Appl. Geomater.* **2010**, *2*, 85–100. [CrossRef]
27. Esmaeili, H.; Thwaites, H.; Woods, P.C. Workflows and Challenges Involved in Creation of Realistic Immersive Virtual Museum, Heritage, and Tourism Experiences: A Comprehensive Reference for 3D Asset Capturing. In Proceedings of the IEEE 2017 13th International Conference on Signal-Image Technology & Internet-Based Systems (SITIS), Jaipur, India, 4–7 December 2017; pp. 465–472.
28. Smith, M.J.; Hamruni, A.M.; Jamieson, A. 3-D Urban Modelling Using Airborne Oblique and Vertical Imagery. In Proceedings of the ISPRS Hannover Workshop, Hannover, Germany, 2–5 June 2009.
29. Hashim, K.A.; Ahmad, A.; Samad, A.M.; NizamTahar, K.; Udin, W.S. Integration of Low Altitude Aerial & Terrestrial Photogrammetry Data in 3D Heritage Building Modeling. In Proceedings of the 2012 IEEE Control and System Graduate Research Colloquium, Selangor, Malaysia, 16–17 July 2012; pp. 225–230.
30. Rodríguez-Cielos, R.; Galán-García, J.L.; Padilla-Domínguez, Y.; Rodríguez-Cielos, P.; Bello-Patricio, A.B.; López-Medina, J.A. LiDARgrammetry: A New Method for Generating Synthetic Stereoscopic Products from Digital Elevation Models. *Appl. Sci.* **2017**, *7*, 906. [CrossRef]
31. Macher, H.; Landes, T.; Grussenmeyer, P. From point clouds to building information models: 3D semi-automatic reconstruction of indoors of existing buildings. *Appl. Sci.* **2017**, *7*, 1030. [CrossRef]
32. Yi, X.; Zhang, R.; Li, H.; Chen, Y. An MFF-SLIC Hybrid Superpixel Segmentation Method with Multi-Source RS Data for Rock Surface Extraction. *Appl. Sci.* **2019**, *9*, 906. [CrossRef]
33. Masiero, A.; Fissore, F.; Guarnieri, A.; Pirotti, F.; Visintini, D.; Vettore, A. Performance evaluation of two indoor mapping systems: Low-cost UWB-aided photogrammetry and backpack laser scanning. *Appl. Sci.* **2018**, *8*, 416. [CrossRef]
34. Dabove, P.; Grasso, N.; Piras, M. Smartphone-Based Photogrammetry for the 3D Modeling of a Geomorphological Structure. *Appl. Sci.* **2019**, *9*, 3884. [CrossRef]
35. Wang, Q.; Zhao, H.; Zhang, Z.; Cui, X.; Ullah, S.; Sun, S.; Liu, F. Line matching based on viewpoint-invariance for stereo wide-baseline aerial images. *Appl. Sci.* **2018**, *8*, 938. [CrossRef]
36. Manajitprasert, S.; Tripathi, N.K.; Arunplod, S. Three-Dimensional (3D) Modeling of Cultural Heritage Site Using UAV Imagery: A Case Study of the Pagodas in Wat Maha That, Thailand. *Appl. Sci.* **2019**, *9*, 3640. [CrossRef]
37. Soto-Martin, O.; Fuentes-Porto, A.; Martin-Gutierrez, J. A Digital Reconstruction of a Historical Building and Virtual Reintegration of Mural Paintings to Create an Interactive and Immersive Experience in Virtual Reality. *Appl. Sci.* **2020**, *10*, 597. [CrossRef]
38. Obradović, M.; Vasiljević, I.; Đurić, I.; Kićanović, J.; Stojaković, V.; Obradović, R. Virtual Reality Models Based on Photogrammetric Surveys—A Case Study of the Iconostasis of the Serbian Orthodox Cathedral Church of Saint Nicholas in Sremski Karlovci (Serbia). *Appl. Sci.* **2020**, *10*, 2743. [CrossRef]
39. Valença, J.; Julio, E.; Araújo, H. Applications of Photogrammetry to Structural Assessment. *Exp. Tech.* **2012**, *36*, 71–81. [CrossRef]

40. Baltsavias, E.P. A Comparison Between Photogrammetry and Laser Scanning. *ISPRS J. Photogramm. Remote. Sens.* **1999**, *54*, 83–94. [CrossRef]
41. Vosselman, G.; Maas, H.G. *Airborne and Terrestrial Laser Scanning*; CRC Press: Boca Raton, FL, USA, 2010.
42. Barsanti, S.G.; Remondino, F.; Visintini, D. Photogrammetry and Laser Scanning for Archaeological Site 3D Modeling–Some Critical Issues. In Proceedings of the 2nd Workshop on 'The New Technologies for Aquileia', Aquileia, Italy, 25 June 2012.
43. Lerma, J.L.; Navarro, S.; Cabrelles, M.; Villaverde, V. Terrestrial laser scanning and close range photogrammetry for 3D archaeological documentation: The Upper Palaeolithic Cave of Parpalló as a case study. *J. Archaeol. Sci.* **2010**, *37*, 499–507. [CrossRef]
44. Moon, D.; Chung, S.; Kwon, S.; Seo, J.; Shin, J. Comparison and utilization of point cloud generated from photogrammetry and laser scanning: 3D world model for smart heavy equipment planning. *Autom. Constr.* **2019**, *98*, 322–331. [CrossRef]
45. Xu, Z.; Wu, L.; Shen, Y.; Li, F.; Wang, Q.; Wang, R. Tridimensional reconstruction applied to cultural heritage with the use of camera-equipped UAV and terrestrial laser scanner. *Remote Sens.* **2014**, *6*, 10413–10434. [CrossRef]
46. Meroño, J.E.; Perea, A.J.; Aguilera, M.J.; Laguna, A.M. Recognition of materials and damage on historical buildings using digital image classification. *S. Afr. J. Sci.* **2015**, *111*, 1–9. [CrossRef]
47. Nouwakpo, S.K.; Weltz, M.A.; McGwire, K. Assessing the performance of structure-from-motion photogrammetry and terrestrial LiDAR for reconstructing soil surface microtopography of naturally vegetated plots. *Earth Surf. Process. Landf.* **2016**, *41*, 308–322. [CrossRef]
48. Lu, Q.; Lee, S. Image-based technologies for constructing as-is building information models for existing buildings. *J. Comput. Civ. Eng.* **2017**, *31*, 04017005. [CrossRef]
49. Pătrăucean, V.; Armeni, I.; Nahangi, M.; Yeung, J.; Brilakis, I.; Haas, C. State of research in automatic as-built modeling. *Adv. Eng. Inform.* **2015**, *29*, 162–171. [CrossRef]
50. Wang, Q.; Kim, M.K. Applications of 3D point cloud data in the construction industry: A fifteen-year review from 2004 to 2018. *Adv. Eng. Inform.* **2019**, *39*, 306–319. [CrossRef]
51. Burkart, A.; Cogliati, S.; Schickling, A.; Rascher, U. A Novel UAV-Based Ultra-Light Weight Spectrometer for Field Spectroscopy. *IEEE Sens. J.* **2013**, *14*, 62–67. [CrossRef]
52. Eisenbeiß, H. UAV Photogrammetry. Ph.D. Thesis, ETH Zurich, Zurich, Switzerland, 2009.
53. Atkinson, K.B. *Close Range Photogrammetry and Machine Vision*; Whittles Publishing: Dunbeath, UK, 1996.
54. Yu, I.; Mortensen, J.; Khanna, P.; Spanlang, B.; Slater, M. Visual Realism Enhances Realistic Response in an Immersive Virtual Environment-Part 2. *IEEE Comput. Graph. Appl.* **2012**, *32*, 36–45. [CrossRef]
55. Nikolakopoulos, K.G.; Soura, K.; Koukouvelas, I.K.; Argyropoulos, N.G. UAV vs Classical Aerial Photogrammetry for Archaeological Studies. *J. Archaeol. Sci. Rep.* **2017**, *14*, 758–773. [CrossRef]
56. Watton, J. *Modeling, Simulation, Analog and Microcomputer Control*; Prentice-Hall, Inc.: Upper Saddle River, NJ, USA,1989.
57. Slaats, P.M. *Recursive Formulations in Multibody Dynamics*; Technische Universiteit Eindhoven: Eindhoven, The Netherlands, 1991.
58. Yang, X.; Shen, Y. Runge–Kutta Method for Solving Uncertain Differential Equations. *J. Unce. Anal. Appl.* **2015**, *3*, 1–12. [CrossRef]

Publication IV

Cheikh-el-Chabab, M., Kuivalainen, O., Andersson, U. R., Eskola, R., and Mikkola, A

Using Real-time Simulation in Company Value Chains and Business Models for Value Creation. In: Ukko J., Saunila M., Heikkinen J., Semken R.S., Mikkola A. (eds.) Real-time Simulation for Sustainable Production - Enhancing User Experience and Creating Business Value

Reprinted with permission from
Routledge
177-195, 2021

14 Using real-time simulation in company value chains and business models for value creation

Maya Kristina Cheikh-el-Chabab, Olli Kuivalainen, Ulf R. Andersson, Roope Eskola and Aki Mikkola

14.1 Introduction

In today's rapidly changing global markets, industries are becoming not only interconnected, but also interdependent. Digitalization and globalization are increasing the pressure on companies to remain competitive to survive. Merely adapting technology is not enough. Companies must also understand business trends and the complexity of modern technology. Digitalization, in particular, has resulted in rapid development and a new complexity in electronics that is challenging upper and middle management to gain a better understanding of the new and emerging needs of their businesses. They must adapt by innovating and updating their business models to ensure their companies can fully benefit from the new technologies and offer their customers better value. Only a small percentage of companies believe existing business models will be sufficient to keep them profitable and economically viable as their industries continue digitalizing course and speed (Bughin *et al.*, 2018).

Revolutionary changes in business come about whenever growth of global innovation and competitiveness gives rise to advanced technologies that offer substantial benefit to industry. The introduction of water- and steam-powered mechanical manufacturing at the end of the 18th century (i.e., the "first wave" or industrial revolution), the division of labor in the beginning of the 20th century (i.e., the "second wave"), and the appearance of programmable logic controllers for production-process automation in the 1970s (i.e., the "third wave") were the main influencers of such revolutions (Brettel *et al.*, 2014). The latest transformations have introduced the business world to a whole new possibility of interactions between humans and machines in a cyber-physical world through a large network bringing upon a "fourth wave".

Industry 4.0 refers to the emergence and diffusion of a range of new digital industrial technologies, e.g., in relation to automation and data exchange in manufacturing technologies (Strange and Zucchella, 2017; Hannibal and Knight, 2018). In addition to technological innovations, companies have also had to undergo a huge shift in their organizational structure to cope with the new market complexity. Scholars have also recognized a shift from mass production to customized production, moving toward the co-creation of products with customers and that transformation's potential effects on value propositions and business models. This chapter examines real-time simulation as a result of the fourth wave of industrial revolution that has been triggered by the internet.

Real-time simulation is an important result of this latest revolution. It is a technology that is evolving rapidly and finding its way into specific industrial applications, because real-time simulation and its accurate physics-based representations resolve real-time problems by producing meaningful and timely information about product behaviors (Mevea, 2018a; Jaiswal *et al.*, 2019). Real-time simulation can accurately predict – in real time – the dynamic behaviors of complex mechanical systems, such as mobile machines (Khamim *et al.*, 2018). Real-time simulation techniques are being applied to develop advanced operator training simulators (Mevea, 2018a). Furthermore, several manufacturing companies use real-time simulation to improve their production processes, and real-time simulations can serve as a vehicle to demonstrate to potential customers the technical features of a product. Consequently, new applications in product development and beyond are emerging that account for the needs and wants of both customers and operators throughout the whole value chain process, a critically important benefit.

The possible next step is taking simulator-driven design methodologies to a new level by developing real-time simulator-driven processes. This development will provide visibility and accessibility to multiple stakeholders in every part of the product lifecycle and therefore enhance the potential of new business models to drive increased competitiveness. However, this new field of technology is not fully mature and is currently only being applied in limited cases, so there are many benefits yet to be discovered and proven.

This chapter describes how incorporating real-time simulation in different value chain processes can affect business models and benefit various stakeholders. The primary objective is to explain how real-time simulation tools can increasingly represent real-world functionality in today's businesses and emerging industries. This innovation has increased global competition to raise product quality and lower production costs and has ensured real-time access to relevant product and production data for the involved parties. Therefore, companies are weakening the barriers to participation in their product development and support processes and giving multiple parties better access to data by exchanging it through autonomous systems embedded throughout the entire value chain (Brettel *et al.*, 2014). To cope with these technological changes, industries have had to evolve and face the changing market. In this new environment, they are having to think more about creating value based on real-time simulation.

14.2 The effect of digitalization on the market

Impacting how companies do business, digitalization has launched a number of new trends. To better understand these trends, a better understanding of digitalization is needed. Some managers view digitalization as an upgrade of what their IT functions do for the company. Others are interested in digital marketing and sales. Bughin *et al.* (2018) defined digitalization as "the nearly instant, free, and flawless ability to connect people, devices, and physical objects anywhere". I-SCOOP (2019) referred to digitalization in business as enabling, improving and/or transforming business operations, business functions, business models and processes, and activities by leveraging digital technologies and making broader use of digitized data by turning it into actionable knowledge with a specific benefit in mind. This definition takes into consideration the importance of data gathered from different digitalization means. Other definitions have included the environmental aspect of digitalization and the adoption of digital technologies across all possible societal and human activities. However, in this chapter, the focus is on the definitions proposed by Bughin *et al.* (2018) and I-SCOOP (2019).

In 2018, CIMdata published an eBook entitled *Digital Twins: Changing the Way We Engineer Validate, Market, and Operate our Products*. The book introduced four different trends in business launched by digitalization (CIMdata, 2018).

The first is increased complexity, whether in product or ecosystem.[1] Product complexity does not only come from an increased number of assemblies, but also from current customer expectations when using electronics, software, and embedded systems, all of which are taken for granted. In addition to an increasing need to interconnect technologies, ordering and manufacturing are being challenged to meet sustainability conditions. As for ecosystem complexity, this phenomenon is shown in digitalization covering the entire product lifecycle process. Environmental responsibility is on one side and social responsibility is on the other as companies manufacture products that are increasingly interconnected to meet society's needs.

The second trend is giving the customer more choice. Today's customer demands flexibility and is given a wide range of choices, if not a fully customized product or service. Since companies are gaining access to much better means, materials, and solutions; customers expect reliable products of superior quality that have been well tested before product launch. Customers are also participating more in the feedback process and codeveloping products by providing improvement ideas. And, more companies are expected to provide customers more involvement opportunities.

The third trend is digitalization competitiveness, where companies not only focus on bringing improved and well-tested products to market, but they also focus on doing it quickly, responding rapidly to market changes to stay competitive in their field. CIMdata explained that virtual capabilities must be applied at all stages of the engineering process, from inception through product development to manufacturing to service. This requires data and process management, visualization, collaboration, and predictive capabilities. Achieving digitalization does not mean that a company has everything in digital form, but rather that it is capable of capturing and analyzing data and then using it for decision making.

The fourth trend is sustainable innovation, which is realized through the virtual environment. Virtuality impacts company competitiveness and profitability, resulting in transformation of the value proposition and the business model. CIMdata noted some of the virtual engineering practices in businesses. These include system modeling and simulation (SMS), BigData, digital twins, IoT (Internet of Things), IIoT (Industrial Internet of Things), and more. The increased use of advanced technologies has accelerated these trends, and industry must work constantly to keep pace.

These trends are driving the need for further research on each of these technologies to improve their implementation and better understand their impact. Real-time simulation is already being used by some companies, but not all its benefits have been fully employed throughout the whole value chain. Indeed, real-time simulation is mostly found as part of product development and not used in other value-creating activities. This chapter therefore focuses on real-time simulation and its potential benefits.

14.3 Real-time simulation models and How they Create Value for Customers

A complete real-time simulation model integrates the appropriate elements; including the models of environment, mechanics, control system, and user input; and predicts their interaction to simulate the dynamics of an entire system (Mevea, 2018b). The user's main role is to provide input signals via the control console to direct the control system. The control system is where most of the input/output data is processed and synchronized with other subsystems. Actuators produce the forces needed to drive the mechanical subsystem.

For example, hydraulic actuators output the required forces to the mechanical system, which responds by moving within its motion constraints. Multibody system dynamics is the basis of the mechanical subsystem modeling, and it includes the description, e.g., of the bodies, joints, contacts, and tires. In a multibody approach, the set of position coordinates can be defined using generalized global or relative coordinates (Jalon and Eduardo, 2012). A selected set of coordinates is also used to define the velocities and accelerations of the system bodies.

To express the equations of motion, the dynamic equilibrium of the system must be defined. This equilibrium can be determined using an approach such as the principle of Virtual Work. A multibody system is a constrained system, so the constraints must be considered when defining the equations of motion. There are several ways to express them including coordinate partitioning, the penalty method, the augmented Lagrangian method (Bayo and Ledesma, 1996), the collision response model (Korkealaakso *et al.*, 2007), and the lumped LuGre friction model (Astrom and Canudas-De-Wit, 2008). Furthermore, the hydraulic system model that describes the actuators is often based on lumped fluid theory, where the hydraulic circuit is divided into discrete volumes with the assumption that the pressure is distributed equally (Watton, 1989).

Simulation tools such as these have helped decrease cost and improve simulation capabilities making it possible to model and predict real-world behaviors. As a result, the capabilities of real-time simulation and its ability to solve real-world problems have improved. In addition to the reduction in modeling cost, the new techniques have been made more available and accessible to a larger number of users for multiple applications (Bélanger et al., 2010). The importance of properly understanding the needs and wants of customers during the product design process, and therefore involving customers in the actual process through a virtual prototyping experience with real-time simulation tools, has driven the need for improved real-time simulation.

In real-time simulation, the time required to perform computational functions and accurately compute equations must be synchronized and must be faster than the simulation time-step for the simulation to acceptably represent its physical counterpart with equivalent performance (*cf.*, Bélanger et al., 2010). For each time-step, the simulator takes the following actions (Bélanger et al., 2010):

1. Reading inputs and generating outputs,
2. Solving model equations,
3. Exchanging results with other simulation crossing, and
4. Waiting for the start of the next step.

As implied in the previous steps, all output data can be exchanged and shared. This capability enables a new form of communication between stakeholders, which could include current or potential customers, other dealers involved in the sales action such as sub-retailers and wholesalers, partners and investors, or any other party that makes use of the simulator-gathered real-time data.

Traditionally, product and service development decisions are made, for the most part, by the few experts tasked with directly addressing development issues and questions (Mohr *et al.*, 2010. A certain approach could even be paternalistic. For example, see Baden-Fuller and Haefliger, 2013). In this approach, customer needs and wants are often solicited via verbal or written interviews. For a completely new product, this approach is problematic, because describing a concept-level product to customers is difficult, and it is equally difficult for customers to fully understand a new product's potential advantages or disadvantages. Furthermore, if the product is the result of radical innovation, customers may not even be able to articulate what their specific needs might be (Mohr *et al.*, 2010).

This problem can be alleviated by developing real-time simulation-driven processes, which can be accomplished, in practice, by developing a toolset that gives multiple stakeholders access to machine research and development, production planning, and customer services via virtual worksites that can provide fully configurable, real-time, virtual prototyping. To this end, it is critical to employ server-based virtual environments (Figure 14.1). With a server-based virtual environment, any number of stakeholders can simultaneously work with the virtual machine. The environment also makes it possible to set up and modify included models. All in all, these processes can function as tools for open innovation and crowdsourcing (Füller *et al.* 2013).

14.4 Business model canvas as a tool to analyze the value chain

As mentioned in the preceding paragraphs, it is challenging for upper and middle management to understand the new and emerging needs of their businesses and adjust to them by innovating and updating their business models. However, so the added value produced reaches customer, it is of great importance to innovate and update business models to ensure they can fully benefit from the new technologies introduced to industry.

Studying the benefits of real-time simulation helps companies to better capture its full potential value and use it more extensively. With this use comes the need to adjust the business model to provide customers and other players in the value chain technological value. This can be done by considering and applying real-time simulation to different actions along the value chain. However, to identify exactly where this technology best functions, the business model canvas must be clarified.

As Osterwalder and Pigneur (2010) described, "The business model describes the rationale of how an organization creates, delivers, and captures value". His idea also identified nine building blocks that comprise the business model canvas. These include the following.

- ***Value proposition*** represents what the company is offering and makes customers consider buying. It shows the bundle of services and products that create value.
- ***Channels*** are the way the company intends to reach its customers and deliver its products or services by different means of communication, distribution, and sales.
- ***Customer relationships*** comprise the connections that a company establishes with each of its customers. These relationships could be automated or personalized to build a customer base, retrieve customers, or increase sales.
- ***Customer segments*** are the various market segments for which the organization is creating value, that is, its' most important customers. The company can serve one or more customer segments.
- ***Revenue streams* are** how the company makes money. Here, managers must determine what exactly customers value and what they are willing to pay for it.

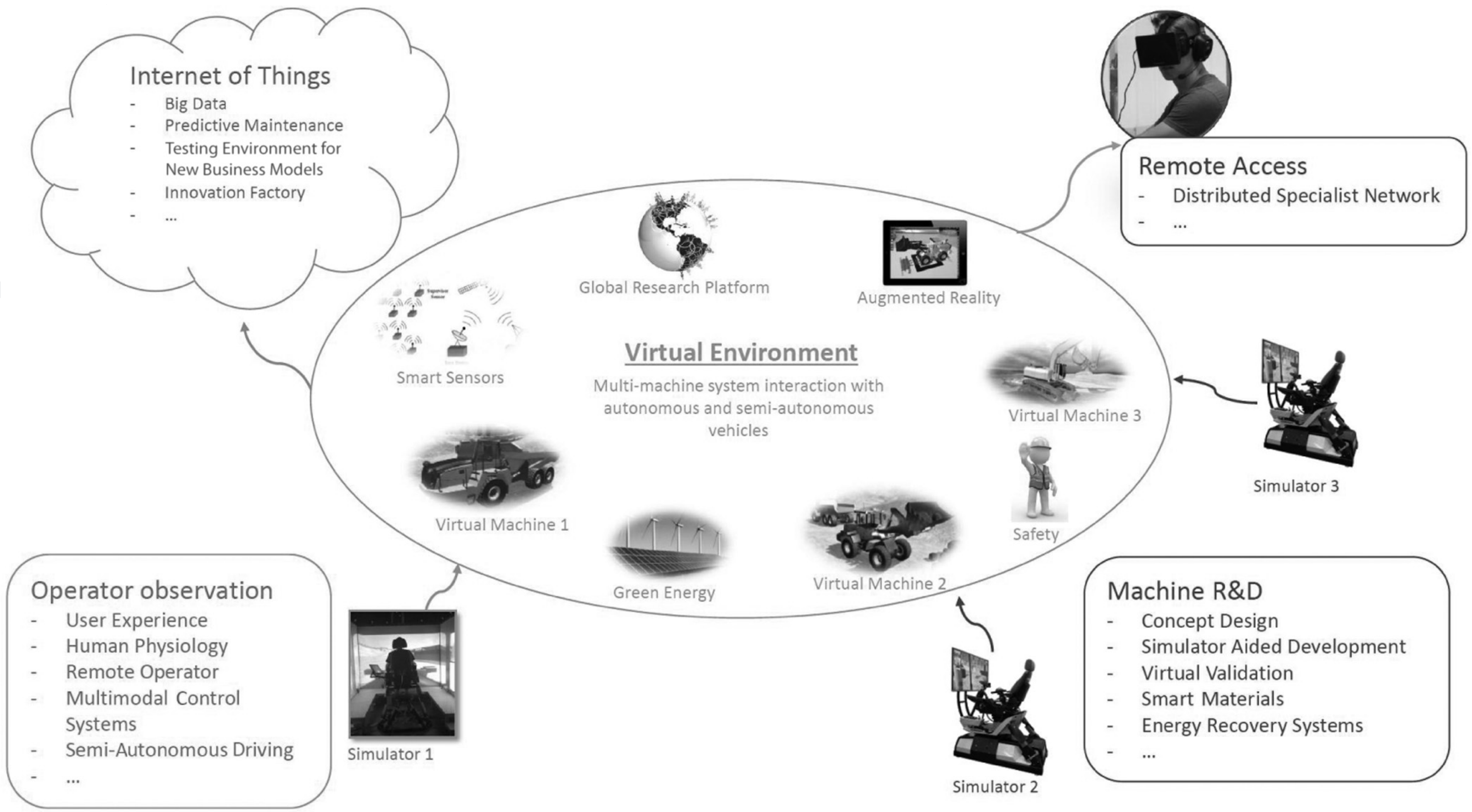

Figure 14.1 Virtual environment (Mevea, 2018a, 2018b, 2018c).

- ***Key resources*** are the most important assets held and owned by the company, rented from partners, or rented to other companies. These assets are important to offering value to customers, building relationships, and gaining revenue.
- ***Key activities*** serve as the most important activities for the company to deliver value, maintain customer relationships, and make revenue. They vary depending on the type of business model.
- ***Key partnerships*** constitute the partnership network of suppliers and partners. These partnerships take the shape of cooperation, joint ventures, alliances, and buyer–supplier relationships. The partnership network is especially important, because it results in and optimizes economies of scale, reducing the risk of uncertainty and granting the privilege of acquiring a particular resource or activity the company needs.
- ***Cost structure*** is understanding what the company must pay to create and deliver the value proposition. Cost structure has an effect over different blocks in the business model including value proposition, revenue streams, and long-term customer relationships.

This business model canvas has challenged previous assumptions that there is one coherent and understandable business model. It has made it easier for companies to follow these steps and compare themselves to other company models (Osterwalder and Euchner, 2019).

Innovating business models seems to be a method for companies to commercialize innovative ideas and technologies. However, business model innovation also complements process, product, and organizational innovation, which promotes more collaboration.

Chesbrough and Rosenbloom (2000) stressed the importance of having a proper business model that works with a company's new technology to create value and manage, not only technological uncertainties, but also economic and market uncertainties. They also explained that learning and searching for effective business models makes successfully adopting technology more likely. This search ensures that market needs are discovered and that customers receive best value. Zott *et al.* (2011) concluded that the business model plays an important role in unlocking the potential values of using technologies and converting them to potential outcomes. Companies can benefit from modifying their own business models to use real-time simulation. This way, they can remain competitive and offer value to their customers.

14.5 Applying real-time simulation to different alue chain activities

14.5.1 Applying real-time simulators in R&D and product development

Real-time simulation is being applied in many areas including traffic control, movies, gamification, and HVAC (heating, ventilation, and air-conditioning) systems (Pell *et al.*, 2016; Jaiswal *et al.*, 2018; Trcka and Hensen, 2010).

Companies are therefore becoming more aware of the advantages of using simulation to improve their businesses. More companies, such as Siemens and other German machine tool vendors, are developing simulation procedures that use data collected from machinery (Rubmann *et al.*, 2015). According to Rubmann, this has enabled operators to virtually test and optimize machine settings for new products before real-world introduction, thereby improving production quality and reducing setup times for the real machining processes by as much as 80%.

Product development is essential because it can influence an organization's competitive success, adaptation, and renewal (Brown and Eisenhardt, 1995). The vast amount of literature focusing on product development has described numerous reasons for successful new product introductions, as well as reasons for failure. A few of these reasons are addressed here. Ancona and Caldwell (1992) discovered that the most successful product development teams employed a wide-ranging external communication strategy, combining so-called ambassador and task coordination behaviors, that helped them secure resources, gain task-related information, and enhance product development performance. This type of communication connects product development to various stakeholders. There is an analogy between Ancona and Caldwell's (1992) ideas and the use of real-time simulation in product development.

Von Hippel (1982) showed that a real-time simulation process makes it easier for a company to make customers an important resource for their product development efforts. Djelassi and Decoopman (2013) reported that crowdsourcing can be helpful in mobilizing selected customers. Crowdsourcing can be defined as "the act of a company or institution taking a job traditionally performed by employees and outsourcing it to an undefined, generally large group of people in the form of an open call" (Howe, 2006a, 2006b). Crowdsourcing is a form of user-driven innovation and value co-creation through which companies can apply innovation (Hopkins, 2011). Real-time simulation can be used as a platform that fosters crowdsourcing-based outsourcing.

One example of using a "virtual machine" in product development might be its application in the development of new car models. Taking a simulator-driven approach would enable the recruitment of a large number of test drivers who could then test-drive several (virtual) prototypes or beta versions. This approach combines the classic idea of testing various product versions with customer-driven innovation. If this virtual machine approach is well executed, test users can experience virtual driving under assorted conditions and with different vehicle features over a substantially shortened schedule.

Receiving customer feedback effectively during the early phases of product development is an important benefit of a simulator-driven process, as it enables the involvement of a large group of potential users in the development process. To better involve potential users though, game-like elements can be added to the testing platform. Indeed, gamification can boost the commitment of test users and even encourage the participation of yet a larger number of participants (Hamari *et al.*, 2014).

The R&D real-time simulator approach offers benefits for both the product development cycle and the product itself. For example, it can result in better concept design and material savings for the final design, optimized based on data from a larger pool of potential users than would be available using classic marketing research methods.

This real-time simulation benefit type could be common in companies that have a complex and expensive production process (*cf.,* Bélanger *et al.*, 2010; Jaiswal *et al.*, 2019). Factories that are responsible for developing agricultural machinery, for instance, invest a lot of effort and resources during the model development process. A tool that can minimize risk and optimize test machine settings before building the actual machine would be welcome.

This is how real-time simulation can be utilized during the R&D process. It has proven to be an effective tool for machinery design, because the simulation model makes it possible to quickly understand how a machine's dynamic behaviors are affected by changing design variables. It can replace experimentation and consequently accelerate product development. Mevea (2018b) discussed that virtual prototyping in real-time simulation achieves significantly shorter lead times and decreases the cost of prototyping by reducing the need for numerous physical prototypes. It also tests the individual components of the product, how it performs in its environment, and how well it carries out the tasks it was designed for.

Operator experience is also critical when considering the dynamic performance of a machine. Real-time simulation gives a machine operator the opportunity to actively engage with a machine in operation, so the training simulator should feel and behave as realistically as possible. This is only possible if the real-time simulation model accurately accounts for the multiphysical behaviors of the mechanical components in response to actuations and correctly represents contact behaviors in accordance with control algorithm instructions.

14.5.2 Applying real-time simulators in training

Real-time simulation techniques are also being used to develop advanced operator training simulators. Compared to traditional training methodologies, simulation-based user training provides a number of advantages. Mevea (2018a) indicated that simulation could be used to generate training data, as well as to test solutions that can be used after training in various scenarios. For example, as operators are being trained, real-time simulation gives them experience in likely operating environments subject to a variety of adverse environmental conditions such as wind, rain, or fog. In every case, the simulator can let the operator experience how the machine "feels".

Accidents or injuries to personnel or property that might otherwise occur when an inexperienced operator learns on an actual machine can also be avoided. Moreover, the simulator can be used to take operators through various accident scenarios and instruct them on the most appropriate responses. This application is most beneficial for high-risk jobs. For example, the Finnair Flight

Academy uses real-life simulation to train its pilots and crew members, who are responsible for the safety of their passengers (Finnair Flying Academy, 2018). With this technology, they are able to simulate the physics, the flying process, the flying system, and the environment. Therefore, training the operators of hazardous systems with zero possibility of negative consequence is where real-time simulation is needed the most, because it provides actual experience with genuine real-time data to prevent accidents.

Further, traditional training processes require real machines that could otherwise be applied to productive service. Using real-time simulation in the training process frees up real machinery to carry out its intended purpose. Simulation-based user training makes it possible to carry out productive revenue-generating work while simultaneously saving costs and eliminating adverse environmental impact.

14.5.3 Applying real-time simulators to predict faults

In the extant literature, most real-time simulation-related articles focus on computational aspects or purposes, such as developing systems and software algorithms. Little attention is given to problem-solving aspects (De Souza *et al.*, 2014). Some researchers have even discussed the use of simulation to conduct real-time tests. De Souza *et al.* (2014) explained that these tests would help develop new embedded algorithms and control techniques for dynamic systems such as motors, industrial processes, automobiles, and aircrafts. On the other hand, real-time simulation can also be used subsequent to machine introduction to improve value-chain processes including design, production, and even aftersales services.

Trcka and Hensen (2010) mentioned that real-time simulation can also be applied to make production processes more flexible. They were able to prove that real-time simulation tools can be used during machine operation to predict and monitor performance and detect and identify abnormalities in system behavior.

In their studies, real-time simulation enabled the system to predict machine errors, a benefit in the R&D stage and a way to improve machine operation in service. For instance, machine faults can be monitored to predict when a machine might break down. To prevent such an event, maintenance could be carried out in advance. This preventative maintenance would save time and effort, and most importantly, enable the machine to continue performing productive revenue-generating work for longer. The company would not be exposed to an unforeseen breakdown. This is why companies are moving toward predictive maintenance based on real-time simulation (*cf.,* CIMdata, 2018).

Mattera *et al.* (2018) explained how simulation can be used to reduce energy consumption by predicting faults as well. The simulation in this case would be used to predict the optimal amount of used energy during different environmental conditions so that any deviation from the optimal case would be noted to maintain sustainable and environmentally friendly consumption.

14.5.4 Applying real-time simulators in services

Outsourcing is a growing business trend that began with the outsourcing of elements of the manufacturing process (Hätönen and Eriksson, 2009). It has continued to include other business functions, such as human resource management and R&D. Many multinational enterprises, such as PC manufacturers, outsource all their major technology requirements, implying that technology is not seen as key to their success or a necessary core competency (Buckley, 2011). More value can be created by other activities such as building a brand.

The market research agency Research & Markets (2015) actually forecasted an 8.1% annual growth in R&D outsourcing from 2015 to 2019. Another key reason for this outsourcing development trend is virtual R&D, which offers benefits such as cost efficiency and reduces heavy internal R&D investment risk. However, virtual R&D is also a specialized activity. As a result, there is room for R&D- and innovation-shrewd companies to provide virtual environments and simulator-driven processes to their customers.

An R&D company can collaborate with a machine manufacturer and provide the necessary user data collection and testing. Additionally, it may not be cost efficient for every company to develop expertise in market research or to integrate product development processes, because their new product releases may be infrequent. A company specializing in providing these services could thus benefit from economies of scale and more-established knowledge bases, making this business model a tempting option. Real-time simulation methods could be used for market research as several test users can try virtual models efficiently.

One example of outsourced R&D is the pharmaceutical testing for Food and Drug Administration (FDA) approval in India. Due to lower costs and an abundant educated workforce, many Indian firms have begun to offer services to Western pharmaceutical companies (Manavalan and Sinfield, 2017). Information technology and protocol standardization allow drug testing to be performed in a way that is more cost-optimized. This has given rise to a multitude of companies that specialize in a particular phase of the drug development R&D process.

Similarly, by focusing on real-time simulation technologies, companies can offer outsourcing services in a particular segment, such as heavy vehicles and machinery, that include events in which customers and users participate in the development process. From these events, the manufacturer can receive market data and valuable knowledge regarding potential customers' preferences.

14.5.5 Applying real-time simulators in sales and marketing

Schneider and Hall (2011) reported that the "biggest problem" in a problematic new product launch is "lack of preparation". They suggested that because companies are often so focused on designing and manufacturing new products, they do not put enough early effort into marketing. An immediate and more realistic idea of different value drivers becomes available by introducing community-based, real-time tools that simulate real-world functionality for potential customers. Simulation can substitute for real observation and can provide expansive realistic data. This information on how potential users may cope with different situations can then help marketeers and salespeople optimize products for their intended customer base.

A product with a catalogue of value-creating features serves as a practical example of using simulation to enhance marketing and sales. For example, a car dealer could use a simulator to give potential customers the opportunity to test the effects of a car's various available options (e.g., a more effective engine). The ease with which customers could try out these extras in real-life scenarios may result in more of them being sold, which results in a better bottom line for the dealer. Simulations can also provide information about intangible attributes, such as feel, which are less frequently addressed in customer surveys. This would also lead to cost savings for the car dealer, who would be able to stock fewer cars for test drive purposes.

In general, the advantages for marketeers and salespeople can be found in customer value analysis, user training, and product demonstrations. Real-time simulation lets more people participate in the testing phase, as well as in further phases of the product development lifecycle. This provides information for various marketing activities and market research. Simulation data can also be "topped up" with interviews after the simulation itself, where user behavior can be observed in real time by the marketeer. Furthermore, marketeers may be able to develop their market information capabilities, i.e., the processes by which firms can learn about markets and apply this market knowledge along the way (Vorhies and Morgan, 2005).

14.5.6 The effect of real-time simulation on business models

The aforementioned effects of real-time simulation on the value chain will result in changes to the overall business model. If real-time simulation is used during the development process, for example, it affects effort and time, because the simulation reduces the need for physical prototyping and therefore affects cost and resource demand. The business model presents a way for the business to capture value and deliver it to customers. In this way, the business model is similar to the value chain, which aims at pinpointing the actions that add value to products.

Financial resources are required to begin applying real-time simulation. In addition, to bring on any new technology, a company must add expertise for that technology to its workforce. So, to ensure continued competitiveness by introducing real-time simulation, a company must not only commit financial resources, but it must upgrade its human resource as well.

The business model would also face some changes regarding key company activities. When it starts using real-time simulation, more data can be gathered from operating machines, leading to more possibilities to incorporate activities that benefit from this data. For example, it becomes possible to provide accurate aftersales services by predicting faults using real-time data. Another way simulation can affect business activities is providing training services for employees or customers.

Combining the gains of real-time data, some B2B companies could benefit from certain partnerships with other firms that provide services with these data, so real-time simulation provides opportunities to network and cooperate with other partners, which will improve business processes and subsequently the value proposition for customers.

The value proposition could be the most affected block of the business model canvas, because many real-time simulation benefits transfer to the customer. One of these benefits is providing the customer the opportunity to give feedback and participate in developing products and services so that value can transfer to a wider audience. Predicting faults, training, and maintenance could be enhanced with real-time simulation, thus building more value to pass on as part of aftersales services. Real-time simulation makes it possible to track data throughout the product lifecycle, leading to greater customer benefit.

The ability to share real-time data enabled by real-time simulation can enhance a company's relationship with customers as they become more involved during different processes – from R&D to when the product or service is in their hands and being consumed. Being able to track the data through the product lifecycle may increase customer trust and loyalty to the company and make them feel safer.[2]

As a company introduces real-time simulation, the customer base could be divided into those who favor utilizing such a new innovative technology and those who do not. This technology could also add new segmentation according to the demand for the services and benefits presented by real-time simulation. If the company targets one or more of the previously mentioned segments, the new technology will generate a new type of customer interested in the benefits that real-time simulation has to offer before and after the buying action. For instance, customers may be interested in the data collected from their purchased machines and may want to use the data for different purposes to achieve their goals in predicting faults, reducing costs, or optimizing performance.

Company stakeholders could communicate and share real-time data as well. This will necessitate new and effective communication channels to distribute information between company headquarters and its dealers. As for physical channels, simulation could optimize distribution channels to cover as much area as possible with the right timing and portfolio of products introduced as needed. If real-time storage and vehicle status data is available, the company could further optimize its distribution channels, because accurate input data will help the simulation to model the situation in more detail.

All of these real-time simulation benefits will eventually affect company revenue both directly, by adding more activities and services to the business model or more value to propositions and optimizing offerings (which could increase sales), and indirectly by decreasing costs during R&D, marketing, and other value chain processes.

14.6 Discussion and conclusions

Real-time simulation is a complicated concept for non-specialized managers, and they must properly understand its functions and applications to correctly use it throughout the business process model and reap its full benefits.

This chapter presented some of these applications in different value chain activities such as R&D, product development, and marketing. Notably, advanced simulation technologies make it possible to describe increasingly complex mechanical systems, so the potential benefits and uses of these technologies should be considered. When the R&D and in-house product development functions of manufacturing companies are already making use of real-time simulation techniques, a starting point for many, it may also mean that it is time for them to proactively consider developing future real-time simulation skills to enhance their market research and customer interface management competencies.

Real-time simulation clearly offers advantages. Simulations can lead to higher success rates for new product launches, as well as cost savings. However, an R&D operation and product development model based on real-time simulation requires manufacturers to upgrade their capabilities. For example, they must bring on new skills to manage various stakeholders. Required marketing capabilities may also relate to the product development processes, for instance, by which firms develop and manage product and service offerings and market information management (Vorhies and Morgan, 2005).

Marketing and sales can also benefit from virtual environments. In a survey focusing on the success factors of Israeli high-tech startups; product perceived utility, comprehensive market knowledge, reliable marketing plans, and the marketing and R&D relationship were considered to be important (Chorev and Anderson, 2006). Properly integrating real-time simulation with marketing and sales activities can lead to improvements for all these factors.

As customers are able to test a product in a virtual environment, they are able to experience its different utility benefits. At the same time, marketing and sales personnel are able to learn more about the marketplace, that is, their existing and potential customers. This learning should lead to more reliable marketing plans that match targeting, segmentation, and unique selling propositions.

Training as a value-added service may also become more integral in product offerings, which would increase sales. If this information, stemming both from simulation and face-to-face interactions with users, can be communicated to R&D via functioning market information management systems, the added value from marketing and sales activities can be used to enhance the entire R&D and product development process. Therefore, the marketing and sales tactics required for various customer segments must still be considered independently, because experience and usage needs may differ segment by segment.

Using real-time simulations for various purposes can also be a challenge for companies. For example, the large pool of data stemming from simulation users may be difficult to digest. As a result, the outsourcing of simulation activities might be a viable option for many manufacturing firms, which provides opportunities for other companies to master this part of the product development process in the value chain. For the R&D firms that may get the contracts though, there may be a need to upgrade capabilities in relationship management.

This chapter presented the possible uses of real-time simulation for different aspects of the value chain, starting from product development and continuing through customer receipt. Mevea (2018c) discussed the possibility of analyzing machine usage data with digital twins to gain valuable insights into product behavior. This enables operators and consulting companies to find ways to improve machine use. Training as a part of customer service or internal training could both benefit from simulated scenarios in different environments. Predicting faults, in the R&D phase or during machine operation, is another benefit that real-time simulation can provide that saves time and resources.

Aiming to guide managers and increase awareness of this new technology and how it affects business models, this chapter also mentioned the use of real-time simulation during the R&D, sales, and marketing phases, as well as for after-sales service. Ultimately, real-time simulation was found to impact each of the nine blocks of the business model canvas. Still, changes in business models may differ depending on the industry and the market. This chapter accordingly displayed a general idea that can be adjusted to match a company's situation at hand.

As for future research, it would be beneficial to further explore the benefits of the data gathered by real-time simulation, how it may affect machine learning, and how real-time simulation in the value chain can affect different business model blocks. Artificial intelligence is being used on a larger scale, which is encouraging more research on the subject. According to Gartner (2018), 14.2 billion connected things will be in use in 2019. That total will reach 25 billion by 2021, producing an immense volume of data. Therefore, these data are driving the growth of artificial intelligence, leading to the greater possibility of its use in real-time simulation to teach smart machines that are capable of learning.

Another possibility for further research would be to specify the effect and use of real-time simulation in certain industries to explore how it can increase variety or give stability to the industry employing this technology.

Notes

1 A business ecosystem can be defined as the "organisms of the business world – including stakeholders, organizations, and countries – involved in exchanges, production, business functions, and … … trade through both marketplace competition and cooperation" (see Hult *et al.*, 2020, p. 44).

2 Brettel *et al.* (2014) point out that one key obstacle to the establishment of close collaborations between companies is the absence of trust: This stems from the fact that many managers are not used to share critical information with other companies.

References

Ancona, D.G., and Caldwell, D.F. (1992). Bridging the boundary: external process and performance in organizational teams. Administrative Science Quarterly, 37, 634–665.

Astrom. K.J. and Canudas-De-Wit, C. (2008). Revisiting the LuGre friction model. Control Systems, IEEE, 28(6), 101–114.

Baden-Fuller, C., & Haefliger, S. (2013). Business models and technological innovation. Long Range Planning, 46(6), 419–426.

Bayo. E. and Ledesma, R. (1996). Augmented Lagrangian and mass-orthogonal projection methods for constrained multibody dynamics. Nonlinear Dynamics, 9(1–2), 113–130.

Bélanger, J., Venne, P., & Paquin, J. N. (2010). The what, where and why of real-time simulation. Planet Rt, 1(1), 25–29.

Brettel, M., Friederichsen, N., Keller, M., & Rosenberg, M. (2014). How virtualization, decentralization and network building change the manufacturing landscape: An Industry 4.0 Perspective. International Journal of Mechanical, Industrial Science and Engineering, 8(1), 37–44.

Brown, S.L. and Eisenhardt, K.M (1995). Product development: Past research, present findings, and future directions. Academy of Management Review, 20(2), 343–378.

Buckley, P.J. (2011). International integration and coordination in the global factory. Management International Review, 51(2), 269–283.

Bughin, J. Catlin, T. Hirt, M. Willmott, P. (2018). Why Digital Strategies Fail. McKinsey Quarterly. [online document]. [Accessed 02 January 2019]. Available at: www.mckinsey.com/business-functions/digital-mckinsey/our-insights/why-digital-strategies-fail.

Chesbrough, H. Rosenbloom, R. S. (2000). The role of the business model in capturing value from innovation: evidence from Xerox Corporation's technology spin-off companies. Harvard Business School Working Paper, no. 01-002, 1–40.

Chorev, C. and Anderson, A.R. (2006). Success in Israeli high-tech start-ups; Critical factors and process. Technovation, 26, 162–174.

CIM. (2018). Digital Twins, Changing the Way We Engineer, Validate, Market and Operate our Products. CIMdata eBook.

de Jalon, J.G. and Eduardo, B. (2012). Kinematic and dynamic simulation of multibody systems: the real-time challenge. New York: Springer Science & Business Media.

De Souza, I. D. T. Silva, S. N. Teles, R. M. Fernandes, M. A. C. (2014). Platform for Real-Time Simulation of Dynamic Systems and Hardware-in-the-Loop for Control Algorithms. [online document]. [Accessed 19 July 2018]. Available at: www.mdpi.com/1424-8220/14/10/19176/htm

Djelassi, S. and Decoopman, I: (2013). Customers' participation in product development through crowdsourcing: issues and implications, Industrial Marketing Management, 42(5), 683–692.

Finnair Flight Academy (2018). Simulators for airlines. [online document]. [Accessed 03 January, 2019]. Available at: www.finnairflightacademy.com/en/simulators/simulators-for-airlines

Füller, Johann, Roland Schroll and Eric von Hippel (2013). User generated brands and their contribution to the diffusion of user innovations. Research Policy, 42(6–7), 1197–1209.

Gartner (2018). Gartner Identifies Top 10 Strategic IoT Technologies and Trends, Gartner Symposium/ITxpo 2018, November 4–8 in Barcelona, Spain.

Hamari, J., Koivisto, J., & Sarsa, H. (2014). Does gamification work? – a literature review of empirical studies on gamification., System Sciences (HICSS), 2014 47th Hawaii International Conference on: IEEE, 3025–3034.

Hannibal, M., & Knight, G. (2018). Additive manufacturing and the global factory: disruptive technologies and the location of international business. International Business Review, 27(6), 1116–1127.

Hätönen, J., & Eriksson, T. (2009). 30+ years of research and practice of outsourcing – exploring the past and anticipating the future. Journal of International Management, 15(2), 142–155.

Hopkins, R. (2011). "What is crowdsourcing"? In P. Sloane (Ed.), A guide to open innovation and crowdsourcing United Kingdom. Kogan Pag, pp. 15–21.

Howe, J. (2006a). The rise of crowdsourcing, [online document]. [Accessed 22 March, 2019]. Available at: www.wired.com/2006/06/crowds/

Howe, J. (2006b) Crowdsourcing: a definition [online document]. [Accessed 22 March 2019]. Available at: www.crowdsourcing.com/

I-SCOOP, Digitization, digitalization and digital transformation: the differences [online document]. [Accessed 02 January, 2019]. Available at: www.i-scoop.eu/digitization-digitalization-digital-transformation-disruption/

Hult, G. T. M., Gonzalez-Perez, M. A., & Lagerström, K. (2020). The theoretical evolution and use of the Uppsala Model of internationalization in the international business ecosystem. Journal of International Business Studies, 51(1), 38–49.

Jaiswal, S. Islam, M. I. Hannola, L. Sopanen, J. Mikkola, A. (2018). Gamification Procedure based on Real-time Multibody Simulation. Lappeenranta University of Technology.

Jaiswal, S., Korkealaakso, P., Åman, R., Sopanen, J., & Mikkola, A. (2019). Deformable terrain model for the real-time multibody simulation of a tractor with a hydraulically driven front-loader. IEEE Access, 7, 172694–172708.

Kohli, A.K., and Jaworski, B.J. (1990). Market orientation: the construct, research propositions, and managerial implications. Journal of Marketing, 54(2), 1–18.

Korkealaakso, P., Rouvinen, A., Moisio, S., and Peusaari, J. (2007). Development of a real-time simulation environment. Multibody System Dynamics, 17(2–3), 177–194.

Manavalan, S., and Sinfield, C. (2017). Conducting Clinical Trials In India: Opportunities And Challenges. Clinical Leader, Guest Column, August 8, 2017. [Accessed 30 August 2020]. Available at: www.clinicalleader.com/doc/conducting-clinical-trials-in-india-opportunities-and-challenges-0001.

Mattera, C. G. Jradi, M. Shaker, H. R. (2018). Online Energy Simulator for building fault detection and diagnostics using dynamic energy performance model. International Journal of Low-Carbon Technologies, 13(3), 231–239.

Mevea, (2018a). Accelerating Intelligent Machine Development and Operation: Digital Twin and AI [online document]. [Accessed 28 December 2018]. Available at: https://mevea.com/news-events/blog/digital-twin-and-ai-accelerating-intelligent-machine-development.

Mevea (2018b). Product development, [online document]. [Accessed 28 December 2018]. Available at: https://mevea.com/solutions/digital-twin/product-development/.

Mevea (2018c). Operations, [online document]. [Accessed 03 January 2018]. Available at: https://mevea.com/solutions/digital-twin/operations/.

Mohr, J., Sengupta, S. and Slater, S. (2010). Marketing of high-technology products and innovations, (3 ed.). Upper Saddle River, NJ: Prentice Hall.

Osterwalder, A., and Euchner, J. (2019) Business Model Innovation, Research-Technology Management, 62(4), 12–18,

Osterwalder, A., and Pigneur, Y. (2010). Business Model Generation: a Handbook for Visionaries, Game Changers, and Challengers. Hoboken, NJ: John Wiley.

Pell, A., Meingast, A., and Schauer, O. (2016). Trends in Real-time Traffic Simulation [online document]. [Accessed 8 July 2018]. Available at https://reader.elsevier.com/reader/sd/ACFE706377EF8374E610DD447368D2BB57FE7E232911F8FB91FE36E516D60D4B948F463D136FC6F88A26BC19822D0B9D

Research and Markets (2015) Global R&D Outsourcing Market 2015–2019. Available at www.researchandmarkets.com/research/98m9c4/global_randd [Accessed 10 July 2018].

Rubmann, M. Lorenz, M. Gerbert, P. Waldner, M. Justus, J. Engel, P. Harnisch, M. (2015). Industry 4.0: The Future of Productivity and Growth in Manufacturing Industries. [online document]. [Accessed 10 July 2018]. Available at: www.inovasyon.org/pdf/bcg.perspectives_Industry.4.0_2015.pdf

Schneider, J. and J. Hall, (2011). Why most product launches fail. Harvard Business Review, (April): 21–23.

Strange, R., and, Zucchella, A. (2017). Industry 4.0, global value chains and international business. Multinational Business Review, 25(3), 74–184.

Trcka, M., and Hensen J. L. M. (2010). Overview of HVAC system simulation. Automation in Construction, 19(2), 93–99.

Von Hippel, E. (1982). Get New Products from Customers. Harvard Business Review, 60(2, March–April), 117–22.

Vorhies, D. W., & Morgan, N. A. (2005). Benchmarking marketing capabilities for sustainable competitive advantage. Journal of Marketing, 69(1), 80–94.

Watton, J. (1989). Fluid power system, Englewood Cliff: Prentice Hall.

Zott, C. Amit, R., and Massa, L. (2011). The business model: recent developments and future research. Journal of Management, 37(4), 1019–1042.

Publication V

Suuronen, S., Ukko, J., Eskola, R., Semken, S., and Rantanen, H.
Systematic literature review for digital business ecosystems in the manufacturing industry: prerequisites, challenges, and benefits

Reprinted with permission from
CIRP Journal of Manufacturing Science and Technology
37, 414-426, 2022

CIRP Journal of Manufacturing Science and Technology 37 (2022) 414–426

Contents lists available at ScienceDirect

CIRP Journal of Manufacturing Science and Technology

journal homepage: www.elsevier.com/locate/cirpj

A systematic literature review for digital business ecosystems in the manufacturing industry: Prerequisites, challenges, and benefits

Sami Suuronen[a,b], Juhani Ukko[a,*], Roope Eskola[c,d], R. Scott Semken[c], Hannu Rantanen[a]

[a] LUT University, School of Engineering Science, Department of Industrial Engineering and Management, Mukkulankatu 19, FI-15210 Lahti, Finland
[b] Raute Oyj, Technology, Rautetie 2, FI-15550 Lahti, Finland
[c] LUT University, School of Energy Systems, Department of Mechanical Engineering, Yliopistonkatu 34, FI-53850 Lappeenranta, Finland
[d] Raute Oyj, Research and Development, Rautetie 2, FI-15550 Lahti, Finland

ARTICLE INFO

Available online xxxx

Keywords:
business ecosystem
digital business ecosystem
DBE
systematic literature review
digital platform
digital twin
smart manufacturing
industry 4.0

ABSTRACT

Digitalization has disrupted how organizations collaborate and compete resulting in the development of new collaborative value-creation networks such as the Digital Business Ecosystem (DBE). A literature review shows that DBEs are being studied by various scholars from different perspectives in manufacturing. Digital Business Ecosystem is studied in many contexts in manufacturing, and it is creating both opportunities and challenges for manufacturing. By providing a systematic literature review of the prerequisites, challenges, and benefits of DBEs for manufacturing, this paper helps to alleviate this shortcoming and reveals how digital business ecosystems can dramatically impact the industry. A total of 149 research journal articles were included in this literature review, which uncovered nine prerequisites, eight challenges, and eight benefits for DBEs and led to five trends for future study. Also noted are practical issues that managers who work in manufacturing DBEs should address.

Introduction

Digitalization is disrupting traditional business models and reshaping organizational structures (Tripsas, 2009; Yoo, 2010; Brouthers et al., 2016) [186]. And to better understand digitalization as a phenomenon, scholars have increasingly begun to examine digital ecosystems [121,141,20], digital business ecosystems [142] and digital platforms (Boudreau, 2012; Reuver et al., 2018).

Digitalization phenomena are being studied from a number of different perspectives and discussed using a variety of nomenclatures. Information Systems (IS) scholars are studying what they call *digital platforms* (Tiwana, 2014) [120]. Economics scholars talk about *two-sided* and *multi-sided markets* [18,134] (Evans and Schmalensee, 2013). Management scholars refer to *ecosystems* instead of either platforms or markets. Management literature studies have explained what business ecosystems are [73,106], how innovation occurs in business ecosystems [16,3,4] and how these affect competitive advantage (Sanders 2007) [170].

As Reuver et al. (2018) pointed out, there are various definitions for a Digital Ecosystem (DE) and a Digital Platform (DP). This study views the DE as analogous to a biological ecosystem. Just as a biological ecosystem enables life, the DE is an enabler in the digital world. Inspired by its natural counterpart, a digital ecosystem is defined as a distributed, adaptive, and open socio-technical system with the properties of self-organization, scalability, and sustainability [20].

Digital ecosystems are of no value if not part of a Business Ecosystem (BE). Moore first introduced the concept of a business ecosystem in 1993 [106]. In 1996, he described it more precisely as follows. "*An economic community supported by a foundation of interacting organizations and individuals – the organisms of the business world. This economic community produces goods and services of value to customers, who are themselves members of the ecosystem. The member organism also includes suppliers, lead producers, competitors, and other stakeholders. Over time, they coevolve their capabilities and roles, and tend to align themselves with the direction set by one or more central companies. Those companies holding leadership roles may change over time, but the function of ecosystem leader is valued by the community because it enables members to move toward shared visions to align their investments, and to find mutually supportive roles.*" (Moore, 1996: 26)

* Corresponding author.
E-mail addresses: sami.suuronen@raute.com, sami.suuronen@student.lut.fi (S. Suuronen), juhani.ukko@lut.fi (J. Ukko), roope.eskola@raute.com (R. Eskola), scott.semken@lut.fi (R.S. Semken), hannu.rantanen@lut.fi (H. Rantanen).

https://doi.org/10.1016/j.cirpj.2022.02.016
1755-5817/

Fig. 1. Digital ecosystem, business ecosystem, and digital business ecosystem alignment.

On its own, the business ecosystem is no longer sufficient to ensure success in manufacturing. The approach has nearly run its course, and its survival depends on successful integration with the digital ecosystem. Combining business and digital ecosystems results in new collaborative organizational networks that are referred to as Digital Business Ecosystems (DBEs) (Stanley et al., 2010) [142]. Fig. 1 illustrates.

The DBE is an extension of Moore's [106] business ecosystem in which digital platforms play a dominant role. Digital platforms are technological infrastructures that allow member firms to develop, configure, and deliver advanced services efficiently and on an unprecedented scale [130,186,51]. The companies that have leveraged digital platform business models have grown dramatically over the past decade [49]. For example, Apple, Microsoft, and Amazon are the most valuable companies in the world today [31]. At the same time, many manufacturers are struggling with how they can leverage digital platforms [86].

In the manufacturing literature, Digital Business Ecosystem is studied in many contexts. To upgrade traditional manufacturing, Smart Manufacturing (SM) has been studied [80,91,138] (Wang et al., 2021). The goal of SM is to have fully integrated, collaborative manufacturing systems that meet changing demands and conditions in real time in the factory, in the supply network, and in the marketplace satisfying customer needs [80,111]. Industry 4.0 is usually referred to as Smart Manufacturing.

Additionally, Industry 4.0 fundamental ICT infrastructures enable the application of higher-level technologies such as Artificial Intelligence (AI) [187,6,78,94] (Reinhardt et. al., 2020). Its main purpose is to enhance, extend, and integrate production processes at intra- and inter-enterprise levels [64,184]. To enhance network connectivity between enterprises, Smart Production Networks are being studied [149,163]. In Smart Production Networks, connected SM systems can respond in real time to dynamic changes in local production systems and external supply chains [96].

Studies about Digital Twins (DT) and how they are used in manufacturing have been of high interest [70,95,127,159,175] (Tao et al., 2017A). A DT is a digital representation of a real-world system or entity. The Internet of Things (IoT) is needed to provide the context to a DT (Tao et al., 2017B; [25], [79]. There are also many studies about DT applications in a manufacturing context. Bao et al. [15] proposed an approach for DT modeling and operation for shop-floor manufacturing and scheduling. Park et al. [118] designed and implemented a DT to solve problems of personalized production and distributed manufacturing systems. Tao and Zhang (2017A) studied the concept of a DT shop floor, which defined four components: the physical shop-floor, the virtual shop-floor, the shop-floor service system, and shop-floor digital twin data. Rosen et al. [135] presented how a DT is transforming a cyber-physical production system from to a nonautonomous to an autonomous system. Cheng et al. reported that in Digital Business Ecosystems, the DT can bring about full value-chain collaboration in collaborative product development, collaborative manufacturing, operations, and maintenance [26].

There are also studies about Industrial Internet Platforms (IIPs) [65,173,174]. IIPs manage the interaction between physical and cyber components. They are core to the operation of industrial systems [173]. Wide-ranging IIP work has been carried out by GE Predix, ABB Ability, Siemens MindSphere, PTC ThingWorx, etc. The GE strategy for the Predix platform is for it to be a cloud-based operating system for manufacturers. GE wants its platform to become for machinery what Android is for smartphones [177]. The Predix platform gives manufacturers a better understanding and advanced analytics to continuously improve processes [177]. The ABB Ability platform enables data-driven decision making (Ability, 2021). MindSphere connects about a million devices and systems to provide predictive maintenance services for the devices (Petrik and Herzwurm, 2019). PTC ThingWorx is an industrial innovation platform that focuses on harvesting data and delivering valuable insight to users [96].

Lately Volkswagen, Amazon Web Services (AWS), and Siemens have introduced an Industrial Cloud solution to connect 18 locations [9]. The plan is to allow other companies, such as suppliers, to integrate into the cloud in the future. This Industrial Cloud solution is the basis for achieving more efficient processes and increased productivity. It makes it possible for partners to provide software applications directly to manufacturing plants. With respect to application development, one location can be highly scalable because there are more than 100 locations of the Volkswagen Group. Moreover, the solution can also be offered to the automotive industry at large.

The availability of Smart manufacturing, Industry 4.0, Industrial Internet Platforms, Digital platforms, and Digital Twins in Digital Business Ecosystems makes it possible to exploit Digital Servitization. Digital Servitization can enable radical changes in manufacturing [146,147] enabling companies to shift from a product-centric to a service-centric business model (Kowalkowski et al., 2017A). Digital Business Ecosystem is studied in many contexts in manufacturing, and it is creating both opportunities and challenges for manufacturing. By providing a systematic literature review of the prerequisites, challenges, and benefits of DBEs for the manufacturing industry, this paper aims to alleviate this shortcoming and reveal how digital business ecosystems can impact manufacturing. The research questions that guided the literature review are as follows.

RQ 1. What are the prerequisites for a digital business ecosystem in manufacturing?

RQ 2. What are the main challenges facing a digital business ecosystem in manufacturing?

RQ 3. What are the main benefits coming from a digital business ecosystem in manufacturing?

The following paragraphs describe the detailed steps of the applied research approach. This is followed by a section that presents the findings of the research in regard to each of the above research questions. Section 4 proposes ideas for follow-on research, and the final section discusses how the study contributes to the field and draws conclusions.

Research approach

Scopus was used to find relevant articles about digital business ecosystems for manufacturing. Table 1 lists the initial limits placed on the search results. Only published articles from journals in English were searched. For this initial screening, the search produced 44,3 million hits.

Table 1
First limits in Scopus search.

Limiting type	
Publication stage	Final
Document type	Article
Source type	Journal
Language	English

Table 2
Scopus searches (*PORE* = *platform* OR *ecosystem*).

Search	Keywords (title-abstract-keywords)			Journal title	Hits	Act	Abstract Hits
1.	*PORE*				573388		
2.	*PORE*	AND	Industry OR service		72147		
3.	*PORE*	AND	Industry		30918		
4.	*PORE*	AND	Service		45167		
5.	*PORE*	AND	Industry	Information	144	Proceed	37
6.	*PORE*	AND	Service		464		
7.	*PORE*	AND	Digital AND service		54	Proceed	
8.	*PORE*	AND	Industry	Operation	21	Proceed	45
9.	*PORE*	AND	Service		81	Proceed	
10.	*PORE*	AND	Industry	Strategy	94	Proceed	28
11.	*PORE*	AND	Service		112	Proceed	
12.	*PORE*	AND	Industry	Innovation	96	Proceed	20
13.	*PORE*	AND	Service		154	Proceed	
14.	*PORE*	AND	Industry	Product	268	Proceed	79
15.	*PORE*	AND	Digital AND industry		21		
16.	*PORE*	AND	Service		547	Proceed	
17.	*PORE*	AND	Digital AND service		12		
18.	*PORE*	AND	Industry	Service	161	Proceed	44
19.	*PORE*	AND	Service		1473		
20.	*PORE*	AND	Digital AND service		62	Proceed	
21.	*PORE*	AND	Industry	Business	268		51
22.	*PORE*	AND	Digital AND industry		43	Proceed	
23.	*PORE*	AND	Service		325		
24.	*PORE*	AND	Digital AND service		40	Proceed	
				Final hits			304
				Final hits without duplicates			264

A second layer of limitation was applied by only searching for articles that included forms of *platform* and *ecosystem* in the title, abstract, or list of keywords. The wildcard (*) was added to assure that all forms of each would be found. The entry in the search was *PORE* = **platform** OR **ecosystem**. As Table 2 shows, there were over 570 thousand hits. Almost 300 thousand of these came from searching for **platform** and 271 thousand from searching for *ecosystem*.

Additional keywords (*industry*, *service*, and *digital*) were then added to further narrow search results, again using the (*) wildcard to find all forms of the words. For example, *industry* was entered as *industr**. The 2nd search looked for *PORE* with the keyword *industry* or the keyword *service*, which reduced the number of hits to just over 72 thousand.

Because the keyword *ecosystem* resulted in numerous hits from journals that target non-industrial topics such as nature, the ecology, natural materials, environments, energy, *etc.*; a third layer of limitations was added to the search criteria. Subsequent searches were designed to target more relevant journals. Seven new keyword categories were defined to establish this journal relevancy: *information*, *operation*, *strategy*, *innovation*, *product*, *service*, and *business*. These were used to search journal titles. See searches 5 through 24. The specific keywords used were as follows.

- Information – Information management, information systems, information technology
- Operation – Operations management
- Strategy – Strategic management
- Innovation – Innovation management
- Product – Product and production
- Service – Service and servitization
- Business – Business management

Fig. 2 illustrates the steps of the search process. Searches were divided into two groups, those with 200 hits or less and those with greater than 200 hits. The journal abstracts were read for the first group (≤200) to determine if the articles seemed to be relevant to this study. For the second group, a second search of the titles and abstracts of the > 200 hits was carried out with the additional keyword *digital* added. The results of this second search were also divided into two groups, those with 40 hits or less and those with greater than 40 hits.

For the first group (≤40), the results were ignored. Instead, the abstracts of the 200 most cited articles from the search made before applying the keyword *digital* were read to determine if they were relevant. For the second group (> 40), the abstract of every article found was read to determine those relevant to this study.

Completing all the search process steps left a total of 304 relevant articles. After removing duplicates, the number dropped to 264. Each of these articles was read to reveal if they addressed one of the previously presented research questions. After eliminating those that did not, the total number of useful articles dropped to 115. Divided up by journal title category keyword, there were 28 information, 13 operation, 19 strategy, 9 innovation, 18 product, 13 service, and 15 business articles.

In even a systematic literature search, it is likely that not all important works are found. Nonetheless, these works should not be ignored. Therefore, snowball sampling [13] was also applied to identify and analyze expertize and potential articles in the field of digital business ecosystems in manufacturing. In line with the overall strategy in selecting and analyzing literature, the snowball sampling procedure relied on a thorough reading and understanding of candidate works rather than on a cutoff crieria for inclusion or exclusion. Identifing the experts in the field and becoming familiar with their studies as well as their sources made it possible to recognize and apply many new keywords. Additional searches were conducted on Scopus and Google Scholar using keywords such as Smart Manufacturing, Industry 4.0, Smart Production Networks, Digital Twins, Industrial Internet Platforms, and Digital Servitization. Snowball sampling identified 33 new and relevant articles that were included in the study increasing the total number of articles to 149.

Findings

The candidate articles were read and any findings in the articles were tagged according to the three research questions addressing prerequisites, challenges, and benefits. There were an impressive list of relevant findings. Each item classified under each research

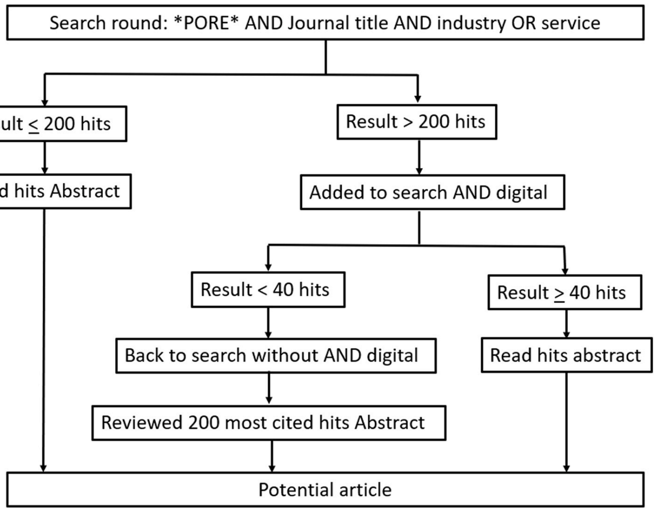

Fig. 2. Searching process steps.

question was read again and many articles were reviewed a second time. Upon completion of the review process, the discovered prerequisites, challenges, and benefits for successful DBE implementation in manufacturing were compiled and are presented in this paper.

Main prerequisites for DBE in manufacturing

Table 3 summarizes the findings classified under the research question "What are the prerequisites for a digital business ecosystem in manufacturing?" The table itemizes the prerequisites and gives a definition for each. Each item is defined more comprehensively in the paragraphs that follow the table.

Prerequisite 1: Business ecosystem

The Digital Business Ecosystem (DBE) is an extension of Moore's [106] business ecosystem. A business ecosystem is a set of interacting entities, organizations, and individuals that build their capabilities and roles and rely on one another for their overall performance and survival [71,106]. Business ecosystems don't emerge just spontaneously [73]. The BE is one of the necessary layers in a DBE [150]. A DBE can only emerge in a business ecosystem in manufacturing.

Prerequisite 2: Digital ecosystem

The digital ecosystem is a second layer needed in a DBE [150]. It plays a crucial role. The DE provides the digital technical capabilities that enable the development of a digital business ecosystem in manufacturing. In other words, without DE it would be impossible to fully utilize the benefits of digital technologies such as Artificial Intelligence (AI), Digital Twins (DT), Industrial Internet Platforms (IIPs), Big Data, Machine Learning, and Digital Servitization.

Prerequisite 3: Digital platform(s)

The presence of a digital ecosystem and business ecosystem in manufacturing alone does not enable member cooperation in a DBE. There must also be a digital platform. A DP is the technological infrastructure that enables the efficient development, configuration, and delivery of advanced services [51,186]. The digital platform also establishes multi-sided markets that bring actors together [46,185]

Table 3
Prerequisites for a digital business ecosystem in manufacturing.

Prerequisites for DBE	Definition	References
1. Business ecosystem	BE is one layer in a DBE.	Moore (1996) [106], Stanley et al. (2010), Jacobides et al. [73]
2. Digital ecosystem	DE is one layer in a DBE.	Briscoe [20]
3. Digital platform(s)	DPs enable DBE members to enhance DBE performance, innovate, collaborate, deliver services and give vision to manufacturing asset through DT	Meyer et al. (2001), Gawer et al. (2008), Franco et al. [51], Yoo et al. [185], Ransbotham et al. (2011), Yoo et al. [186], Evans et al. (2016), Lu et al. [95]
4. Digital platform acceptance from the DBE members	Without acceptance by the members, DPs are useless.	Gawer et al. (2008), Fuller et al. (2020)
5. Members interacting through DPs	Members active role needed in DPs to gain benefits of DBE.	Adner [4], Peltoniemi [123], Teece [160], Senyo et al. (2018), Tao et al. [158]
6. DP requires strong leadership	Strong leadership increases the chance to succeed and adapt to changes.	Iansiti et al. (2004), Williamson et al. (2012), Clarysse et al. [29], Teece [161], Greve et al. (2017)
7. DP must offer value for the members.	Increasing members value in DP will also boost its adoption.	Pfeffer [122], Wernerfelt (1989)
8. Easy access to DP membership	A lower entry-point for members minimizes expansion risks at all levels and layers.	Cusumano et al. (2002)
9. Trust	Trust can be the highest barrier to success of DBE.	Wiedmann et al. [182], Tao et al. [158]

Table 4
Challenges for DBE in manufacturing.

Challenges for DBE	Definition	References
1. Launching DP for a successful DBE	The typical chicken-and-egg problem, SM challenges, information integration, costs, required effort to create DT	Parker et al. (2010), Evans and Basole [48], Parker et al. (2020), Gawer et al. (2013), West et al. [180], Uysal et al. (2021), [173], Fuller et al. (2020), Qi et aal. (2020)
2. DBE is a new environment	DBE is a new and complex landscape with both competition and collaboration.	Iansiti et al. (2004), Gawer et al. (2013), Srinivasan et al. (2018), Aarikka-Stenroos et al. (2012)
3. DP (system) structure	There are multiple ways to structure a DP.	Yoo et al. [185], Greve et al. (2017), Ojala et al. [113], Hakanen et al. (2018), Benkler (2006), Farrel et al. (2003), Cheng et al. [26], Qi et al. [127]
4. Commitment to share profits	Leader should not squeeze profits from their developers.	Farrel et al. (2010), [173]
5. DP Leadership	There should be a balance of control and freedom for DP members.	Suarez (2004), Yoffie et al. (2006) West et al. (2006), Hagiu (2009), Boudreau (2010), Gawer (2010),
6. DBE size comes with its own challenges	A DBE comprises many companies and members (compared to individual company structure).	Jacobides et al. [73], Cooper et al. (2018), Parida et al. (2017), Parida et al. [116], Sjödin et al. [146], Lager et al. (2017), Kohtamäki et al. [81],
7. Winner-take-all situation	The DP owner plays a monopoly role in its industry.	Eisenmann et al. (2009), Zhu et al. (2012)
8. Building trust	Member trust in data, systems, and sharing the benefits with high expectations	Wiedmann et al. [182], Harland et al. (2015), Tao et al. [158], Qi et al. [127], Menon et al. [101], Al-Rubaye et al. [7], Kowalkowski et al. (2017B), Raddats et al. [129]

and provide members the opportunity to enhance DBE performance, innovate, and collaborate [141]. A DBE may involve multiple platforms at different levels [161].

The digital twin can play a role as part of the digital platform. It gives vision to Smart Manufacturing and Smart Production Networks. With better information from manufacturing, DBE members can improve situational awareness and enhance operations [95]. The digital twin can even be considered a must for manufacturing. Without a clear view of the information model for a physical entity, data transmitted can lose meaning and context in cyberspace [95].

Prerequisite 4: Digital platform acceptance from the DBE members

Regarding the role of the DP in a DBE, Gawer and Cusumano (2008) argued that not all digital platforms can become industry wide. A digital platform must gain acceptance from the DBE members in manufacturing. To earn this acceptance, the DP must (1) perform a function that is essential to the broader technological system and (2) solve a business problem for a significant percentage of firms and users in the manufacturing industry (Gawer and Cusumano, 2008). There are multiple reasons for not accepting a digital platform related to challenges presented in Chapter 3.2. For example, since members focus on the benefits of the DP and assume it instantly saves time and money, they can have very high expectations, which may not be realized (Fuller et al., 2020).

Prerequisite 5: Members interacting through DPs

The digital platform in a DBE should be developed to solve current essential technical problems [102]. However, as nothing more than a technological infrastructure, the DP cannot bring DBE benefits without the committed engagement of members in manufacturing. To provide insight into Smart Manufacturing and Smart Production Networks, DP data must be open to DBE members. Otherwise members will continue to work in silos, ruining the benefits of the DBE. Openness of the platform, trust, and security are the main reasons for restricting members to use the platform [158].

Therefore, DBE members play a key role in implementing a successful digital platform. To create value and fully exploit a DBE, members must cooperate. The literature does not clearly define the point when a BE becomes a DBE. The critical point is probably when the digital platform(s) is opened to BE members and the main DBE characteristics become evident.

The main characteristics born along with DBE implementation are symbiosis, co-evolution, and self-organization (Senyo et al. 2018). Symbiosis influences the interdependences of the DBE partners, processes, and technologies (Senyo et al. 2018). It leads to synergy between entities and co-creates value. According to Adner [4], co-creation of value is much more effective than single-organization value creation. Therefore, it is important for organizations to combine their strengths and weaknesses for a greater value proposition in manufacturing.

Co-evolution refers to how a DBE transforms from one stage to another (Moore, 1996; Senyo) [90]. Transformation takes place when one or two key DBE members recognize new opportunities or threats. Other interdependent members also must adapt to the changes in manufacturing. Teece [160] claimed that co-evolution occurs in a business ecosystem when one individual influences others to cooperate to achieve an objective that cannot be achieved by one person alone. This is equally true for the DBE. Overall, the evolution of a DBE is different from the evolution of other organizational networks. In other networks, individual organizations can transform without help from outsiders. Self-organization refers to the DBE's ability to learn from its environment events (*e.g.*, new requirements, opportunities, or threats) and accordingly respond to environmental changes [123] in manufacturing.

Prerequisite 6: DP requires strong leadership

The digital platform of a DBE must have strong leadership in manufacturing. The more powerful firms in a business ecosystem are most likely to succeed in forming and leading digital platforms (Greve et al. 2017). The *keystone* company's role is to ensure that each member of the DBE remains in good health [29].

The Norwegian oil industry built a digital platform to serve their digital business ecosystem across company boundaries. The strong leadership there probably came from the government. The critical success point was to create a stand-alone network and shared digital platform where members can share data and cooperate (Liyanage et al., 2006). Data sharing, communication, and operations improved significantly via the digital platform. Liyanage and Langeland (2008) estimates that this transformation process will give the Norwegian oil industry a savings of 30% in operating costs and increase the efficiency of oil exploitation by 10%.

Prerequisite 7: DP must offer value for the members

If a hosting firm wants to profit from external resources owned and controlled by other businesses, the host must offer something valuable in exchange [122] (Wernerfelt, 1989). Today, this means the digital platform owner must offer value to encourage members to join the digital platform in manufacturing. A DP usually relies on the technological leadership of the one or two firms that provide the platform [162]. DBE members can provide other members constructive input and useful complementary goods and the opportunity to align investments and strategies. Company members that aim to become digital platform leaders in a digital business ecosystem must develop a clear vision of the DP and promote this vision to other potential key DBE members (Gawer and Cusumano 2013).

Prerequisite 8: Easy access to DP membership

To ensure that a DBE does not fail at the onset, it should make it as easy as possible for potential members to participate [30]. Allowing all users to easily join the digital platform lowers the risk of any potential rival digital platforms being started. Access should be easy at all levels and layers.

Prerequisite 9: Trust

Trust is one of the most important prerequisites to building a successful DBE. Even if a system has high-level technological features, lack of trustworthiness may be the highest barrier to its success [182] in manufacturing. Information Technology can promote a feeling of being watched or controlled [182]. If there is no trust in the digital platform or between its members, a digital platform will not lead to a healthy and effective DBE. Some studies have shown that with respect to new technologies, privacy protection is more important than any potential benefit [182]. Block Chain technology can be applied to any size or type of data transaction., and it can break down barriers to trust for the digital platform. Collaboration and mutual trust among DBE members can be strengthened by sharing decentralized database information [158].

Main challenges for DBE in manufacturing

Table 4 summarizes the findings classified under the research question "What are the main challenges facing a digital business ecosystem in manufacturing?" The table itemizes the challenges and gives a definition for each. Each item is defined more comprehensively in the paragraphs that follow the table.

Challenge 1: Launching DP for a successful DBE

Digital platforms play a key role in a digital business ecosystem for manufacturing. Evans and Basole [48] wrote that digital platforms are becoming increasingly complex and research is not keeping pace. Launching a digital platform for the consumer industry faces a typical chicken-and-egg hurdle [119]. If there aren't enough members from each side of the DP, it does not become established in the digital business ecosystem for manufacturing. The digital platform should be readily accessible. Gawer and Cusumano (2013) suggested that the interfaces around the DP must be sufficiently open to enable other concerns to easily *plug in* complements and to allow them to innovate and make money on their investments.

Implementing the Smart Manufacturing (SM) systems and technologies required by a DBE is not easy. It takes time, considerable resources, and effort [180]. It also demands a change in thinking and more open manufacturing. Products and systems should become intelligent, digital, and interconnected. Information integration is one of the most serious issues for SM [169]. A digital platform requires real-time information from various enterprise information systems (EIS) including human resource management (HRM) systems, customer relationship management (CRM) systems, enterprise resource planning (ERP) systems, and manufacturing executive systems (MES). Integration between these EISs is challenging. EISs are developed by different companies at various times, and this can lead to the formation of several information islands [173].

Software companies and IT organizations are not catching up with all the new technological developments and paradigms [169]. The costs of IT-infrastructure are still prohibitively high. For example, an AI needs a high-performance hardware and software infrastructure to effectively execute its algorithms. Even though Amazon, Google, Microsoft and NVIDIA offer cloud-based applications to break the barrier to demand, the costs are still too high for data analytics (Fuller et al., 2020). The same kind of cost issues face the implementation of digital twins. Moreover, digital twin development takes time. They are not constructed rapidly (Qi et al., 2020).

Challenge 2: DBE is a new environment

In manufacturing, leaders and competitors in a DBE have to navigate a complex landscape where both competition and collaboration occur (Gawer and Cusumano 2013). This is a new landscape for traditional manufacturing, and it brings new challenges and threats. DPs can also be seen as a threat by digital entrepreneurs. The changes brought about can obsolete the competencies of some developers [148]. Every member of a DBE must remain healthy. Weakness in a single critical area can harm the entire digital business ecosystem [71]. For example, Aarikka-Stenroos and Jaakkola [1] describe the need for the customer and providers to enact new roles when engaging in value co-creation via digital services. Interaction between the buyer and seller is transformed from being transaction-based to becoming a relationship-based collaboration.

Challenge 3: DP (system) structure

There are multiple ways to structure digital platforms. Building a generalized digital platform can adversely affect industries it has not been adequately configured to serve [60]. From a strategic viewpoint, one of the key innovation imperatives is to learn how to design, build, and sustain a vibrant digital platform in manufacturing. DP success or failure depends in the long run on its capability to implement a feasible layered modular architecture for other members [113].

The leader of the digital platform must decide which layer(s) they will permit other firms to extend [185]. Cheng et al. [26] presented an enterprise collaboration framework under a digital twin enhanced industrial internet, which includes a resource layer, a data/model integration layer, the ontology of an interoperability layer, a business logic layer, and a presentation layer. The layered structure also determines what data are shared. The key to data sharing is not how data are shared, but why data are shared [63]. For example, designers may not have easy access to the data they need from all layers to innovate products [127].

Challenge 4: Commitment to share profits

Members invest innovation in the digital platform. Farrell and Katz [50] recognized that DP leaders must commit to equitably sharing profits with the other DP members. Squeezing from complementary members negatively affects DP growth. As a result, it makes it easier for rival platforms to succeed. Industrial internet platforms have not yet resulted in profitable business for host companies in manufacturing. Because of financial problems, for example, GE is planning to divest itself of Predix [173].

Challenge 5: DP Leadership

DP leaders should encourage external content providers to stimulate growth and contribute to the platform's success (Boudreau, 2010; Gawer, 2010; Hagiu, 2009; Yoffie and Kwak, 2006; Suarez, 2004). However, some level of control is required. Without control, the DP can become too inconsistent and fragmented and, as a result, less useful for developers and customers in manufacturing (West et al. 2006). On the other hand, too much variance makes it difficult to capture value from innovation.

Challenge 6: DBE size comes with its own challenges

A robust DBE comprises many manufacturing companies and members. Unlike standalone corporations, digital business ecosystems are not hierarchically controlled [73]. Therefore, moving a DBE toward a desired destination takes more time and effort than does moving a standalone concern.

Table 5
Benefits of DBE and definitions in manufacturing.

Benefits for DBE	Definition	References
1. New business opportunities	A DBE provides new business opportunities for its members.	Oliva et al. (2003), Eisenmann et al. [38], Menor et al. (2007), Reinartz et al. (2008), Kohtamäki et al. [82], Baines et al. (2014), Prida et al. (2014)
2. Value co-creation	Value is co-created with member cooperation, and processes can improve through data-driven evidence-based practices.	Arthur [10], Moore (1996), Adner [4], Rocket et al. (2006), Adner et al. (2010), Gawer et al. (2012), Chen et al. [24], Storbacka et al. [151], Reuver et al. (2018), Garcia Martin et al. [54], Lu et al. [95], Evans et al. (2015), Lin et al. [89], Da Xu et al. (2014), Cheng et al. [26], Tao et al. [156], Söderberg et al. [144], Lu et al. [96]
3. Innovation increase	A company's innovation capability is strengthened by exposure to other innovation types.	Gupta et al. (1990), Wheelwright et al. (1992), Davenport [35], Baldwin et al. (2006), Jeppesen et al. (2006), Heffner et al. (2008), Law et al. (2008), Hienerth et al. (2011) McAfee et al. [99], Ceccagnoli et al. (2012), Chen et al. [23], Cusumano (2020), Lee et al. [88] Gawer et al. (2013), Gawer et al. (2014), Desouza et al. (2014), Hienerth et al. [69], Sharma et al. [139], [8], Tan et al. (2016, 2017), Eloranta et al. (2016), Myhren et al. [108]
4. Gain competitive advantage	A healthy DBE improves all members and builds a barrier against rivals. It can offer new dimensions to competitive advantage.	Mitchell et al. (1996), Gawer et al. (2002), Iansiti et al. (2004), Adner et al. (2010), Tiwana et al. (2010), Ghazawneh et al. (2010), Eatonet et al. (2015), Lu et al. [95], Tao et al. (2017A), Rosen et al. [135]
5. Resources and knowledge increase	A DBE can fill key resource gaps.	Covillo et al. (1997), Chetty et al. (2003), Iansiti et al. (2004), Oviatt et al. (2005), Ojala et al. [113],
6. New venture potential	The new venture potential arising from a DBE is usually underestimated.	Arthur (2011), Henfridsson et al. (2013)Evans et al. (2016), Parker et al. [120], Watanabe et al. (2017), Boudreau [19], Ojala et al. [113]
7. Cost and risk management	DBE decreases overall costs and risks, when there are members innovating and offering solutions.	Eisenmann et al. [38], Kotha et al. (2011), Lusch et al. (2015), Greve et al. (2017),
8. Provides modularity to fulfill customer needs	Modularity offers a greater opportunity fulfill customer needs.	Baldwin et al. (2000), Baldwin et al. (2009)

The availability of Industrial Internet Platforms has led to an explosive growth in digital services and data for manufacturing. However, this has resulted in a digitalization paradox for many companies [34,116]. Increasing revenues from digital services are failing to deliver greater profits because of increased costs. Digital service planning often overestimates revenue streams and underestimates the high degree of customization required and the operating and maintenance costs of delivered services. Moreover, digital services can also cannibalize existing profitable business models [146]. Many companies continue to struggle with how they can best leverage digital platforms [86] and how to master the platform service innovation transition [81] (Parida et al., 2017).

Challenge 7: Winner-take-all situation

A winner-take-all situation is more likely in a DBE, when networks are positive and strong, multi-homing to other networks is expensive, and there are no differentiation opportunities in manufacturing (Eisenmann et al., 2009). Zhu and Iansiti [188] wrote that a monopoly outcome occurs when users and developers have favorable expectations of a DP, *i.e.*, when members of the digital business ecosystem believe that everyone will eventually join the platform. These findings are based on consumer markets, but this is also a possible threat and outcome in manufacturing. DBE environments are new for manufacturing.

Challenge 8: Building trust

Much of the literature refers to the benefits of external knowledge. For example, Proctor and Gamble (P&G) gets over 50% of its new ideas from external sources (P&G). However, people are reluctant to submit their ideas if they do not believe they will be fairly compensated for them (Harland and Nienaber 2015). The challenge is how to maximize external innovation with the greatest amount of multi-sided benefits and trust. However, the data that drives manufacturing processes and the enterprise are sensitive, which causes a series of data problems such as data fusion, data synchronization, data calculation, data security, etc. [158].

In manufacturing, representing the physical in the cyber world is still a challenge [127]. Users cannot trust the digital platform if the physical and cyber worlds are not tightly integrated and synchronized in real time. This negatively affects digital servitization. The inability to correctly describe physical resources presents challenges to collaboration processes [158].

High expectations and the hype of digitalization is negatively affecting trust in manufacturing. Industrial Internet platform studies concerning the maintenance of intelligent products and studies on the operation of manufacturing systems is limited [101](Al-Rubaye et al., 2017). Often, manufacturing companies will consider the road to digital servitization to be smooth. They assume the manufacturer can just move from one end of the product service continuum to the other [114]. This assumption is increasingly being questioned (Kowalkowski et al., 2017B) [129].

Main benefits of DBE in manufacturing

Table 5 summarizes the findings classified under the research question "What are the main benefits coming from a digital business ecosystem in manufacturing?" The table itemizes the benefits and gives a definition for each. Each item is defined more comprehensively in the paragraphs that follow the table.

Benefit 1: New business opportunities

Manufacturing companies are continuously looking for new business opportunities. According to Baines and Lightfoot (2014), customers want a more and more complete continuum of products and services. In DBEs, a digital platform enables companies to innovatively discover different kinds of new business opportunities, where charging fees can be earned by both sides via transactions or advertising [38]. They also make it easier to recognize changes in market demand. A digital platform enables the detection of customer needs, allows the sharing of product or service information, and integrates internal and external information making it possible to develop new services and maintain extant services [100]. The availability of new services may give a company access to new business opportunities [114], improve efficiency [43], increase revenues and enhance customer satisfaction (Prida et al., 2014), enrich relationships (Reinartz and Ulaga 2008), and increase differentiation of offerings [82].

Benefit 2: Value co-creation

In 1996, Moore found that value chains does not follow a linear downstream path. Value is actually produced by a network of companies with many horizontal relationships (Moore, 1996). The value created by networks is substantially greater than what an individual company can produce on its own [4]. The DP of a manufacturing digital business ecosystem brings the network of member companies closer together. Digital platforms become increasingly valuable as more members adopt them. Moreover, increasing the number of users and complementaries increases a DP's innovation production and value (Gawer and Casumo 2012). Physical machines become more valuable, when applications and services for them are available, which can trigger positive feedback cycles [10]. Digital platform and digital servitization is not only changing the way manufacturers innovate products and services, it is also transforming how members create, deliver, and capture customer value [54].

According to the "two-sided markets" theory (Rochet et al., 2006), a DBE leader should look at service providers as customers. When all DBE members share produced value, they are more committed to co-creating value for both customers and DBE members. Value sharing motivates and encourages all members to participate in total value creation [24]. Each company's value-creation success often depends on the other DBE members (Adner et al., 2010). According to Storbacka et al. [151], actor engagement is a microfoundation for value co-creation. They emphasized that without actor engagement, there is no resource integration, and value cannot be co-created.

Connectivity and data tracking throughout the manufacturing process allow operations to be transformed into data-driven evidence-based practices that make it possible to track the sources of product faults, analyze production efficiency and identify bottlenecks, and predict future resource requirements [95]. Computing and analysis enables capability for equipment failure prediction, energy analysis optimization, predictive maintenance, product quality analysis, and market demand forecasting (Evans and Annunziata, 2015; Da Xu et al., 2014) [89].

With a digital twin, a manufacturer can achieve full value-chain collaboration where downstream and upstream enterprises can successfully achieve product collaborative development, collaborative manufacturing, operation, and maintenance [26]. With a DT, it is possible to simulate, predict, and optimize physical manufacturing systems and processes. A digital twin with intelligent algorithms can achieve data-driven operation monitoring and optimization (Tao et. al., 2018), develop innovative products and services [144], diversify value creation, and encourage innovative new business models [97]. Connecting DTs between manufacturers, gives them the means to build virtually connected Smart Production Networks. A network of DT's provides visibility into operations performance across networks and offers the option to predict future needs [95].

Benefit 3: Innovation increase

Companies who can more rapidly and efficiently launch new product are often more profitable and better positioned when competition increases [62,181]. Empirical evidence shows that companies have successfully used internal platforms to help control the high costs of production and inventory and reduce time to market. Inside-only platforms, however, can lead to limited and constrained innovation (Gawer and Cusumano 2013). Generally, innovation is the result of recombining existing resources [11], and when more people are involved in this recombination, there are more innovative approaches. Innovation-management literature refers to the advantages of external knowledge. For example, P&G acquires over half of its ideas from external sources.

Combining more data and more DBE-platform members results in a greater potential for boosting innovation, competition, and productivity over a wide range of fields [8,23]. The data availability also improves decision-making processes [95,139], new product development (Tan et al. 2016; Tan et al. 2017), and customer relationships [23,35,99]. As manufacturing becomes more digital and openness allows stakeholders to better manage and capture data, more innovative ideas will come from outside the company [41,56] providing incremental and radical service innovation opportunities [76,108].

Lee et al. [88] argued that companies need to share ideas with customers and other members on collaborative efforts. They divided innovation into four phases: closed innovation (depends on inner capabilities), collaborative innovation (focuses on the exchange of ideas with other parties), open innovation (encompasses a wide range of collective wisdom), and co-innovation. As an example of co-innovation, when Apple opened their digital platform to app developers, the value of iPhone skyrocketed [110]. The digital platform plays a key role in sharing knowledge and executing open co-innovation in manufacturing. Knowledge sharing results in more new ideas towards developing new business opportunities [67], and it improves business processes, products, and services [87].

Moreover, innovation is increasingly shifting away from producer companies and towards product users and technologies [69] (Hippel 2005), which increases the need for DBEs to share information and knowledge at low cost for participating members. Prior research shows that innovative users share their thoughts with their peer community, and that these users enjoy significant support from the community in the new product development process (Baldwin et al., 2006; Franke and von Hippel, 2003) [53,68,75]. Information technology hardware and software owners; such as Microsoft, IBM, and SAP; often have partnership programs for members to encourage complementary innovation within digital platforms (Ceccagnoli et al. 2012).

Yoo et al. [185] underline the importance of layered modular architectures in digital platforms. The flexibility and rapid adaptability to changes in technology and consumer preference must remain in layered architectures [40,154]. Architectures must achieve sufficient scale and stability to allow companies to extract revenue from a large customer base over an extended period of time [3] (Boudreau 2010, West 2003).

Product innovation is more in tune with customer need when customers are involved in the product development process. Troisi et al. [168] described how the Muliano Bianco company launched a digital platform so its customers could give feedback, vote, and offer new ideas. After only nine months, they received 1800 ideas, 19,000 votes, and 15,000 comments about their products. The expectation is that companies will leverage their platforms for innovation and transaction purposes and to make technological advances. For example, Big Data (BD) and Artificial Intelligent (AI) will boost innovation to wider range of product-service applications [31]

Benefit 4: Gain competitive advantage

Mitchell and Singh (1996) found that firms pursuing alliance relationships were more likely to survive in the industry than firms engaged in arm's length relationships where buyers and sellers act independently without one party influencing the other. In software development, the alliance relationship is between app developers and platform providers [59,167] (Eatonet et al., 2015).

Digital platform members tend to share a common belief in the aims of the platform, and member performance is tied to overall performance of the business ecosystem [71]. Moreover, a business ecosystem leader can develop a digital platform that can later become a manufacturing DBE. The leader can invest in configuring the DP while ensuring that participating members are taking an appropriate supporting role, thereby increasing the performance of the entire digital business ecosystem [3]. A healthy DBE can be a barrier

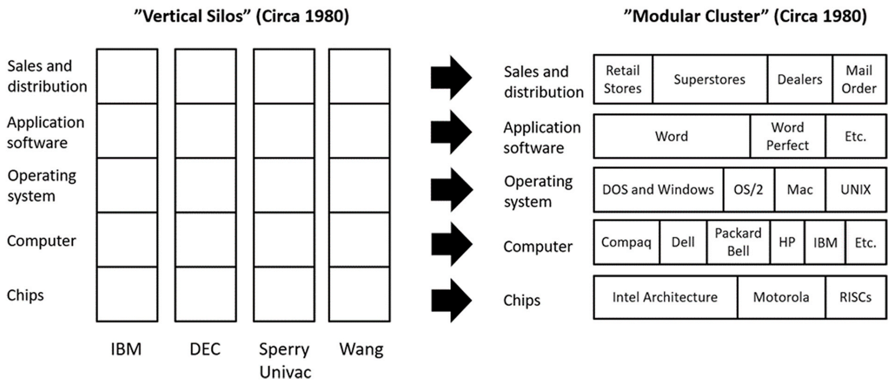

Fig. 3. Vertical silos versus modular cluster (adapted from Groove, 1996, p.44).

to entry for rival technologies [55], and it can entice new members to join.

DBEs can deliver new dimensions to competitive advantage. For example, when including personal data in smart manufacturing such as weight, health data, activity data, and emotional status, it helps to establish models to understand personal well-being and factory working conditions. This can help to design human-centered human-machine collaboration strategies to improve the physical and psychological health of workers and to achieve the best possible production performance [95].

A digital twin can simulate different manufacturing plans in the virtual space and discover potential risks and conflicts in advance, *i.e.*, before it actually happens in a manufacturing process (Tao and Zhang, 2017A). DT can also plan and optimize whole manufacturing process [135].

Benefit 5: Resources and knowledge increase

Continuous progress results in a need for new technologies and innovations, which consequently results in the need for new kinds of resources [113] in manufacturing. A single company does not possess all the resources and knowledge needed to explore and continuously exploit changing markets. Companies like Microsoft and Intel generally depend on the voluntary participation of other firms to bring about a vibrant ecosystem of complementary and competing offerings [71]. Networks are seen as a foundation from which businesses can benefit from resources held by other firms [77,152] (O'Gorman & Evers, 2011). By exploiting network relationships, a new venture can fulfill key resource gaps (Coviello et al. 1997). Studies have also found that companies with a shortage of resources can leverage their existing relationships to further develop their resource pool (Chetty et al. 2003; Oviatt *et al.* 2005) [32,105]. Knowledge sharing in networks makes it possible to respond to customer requirements more quickly and at lower cost (Sher and lee 2004).

Benefit 6: New venture potential

International New Ventures (INVs) are entrepreneurial concerns that internationalize earlier and expand quickly into foreign markets. INVs are disrupting existing ecosystems, radically changing existing business models, and reshaping industry structures (Evans et al. 2016; Watanabe et al. 2017) [120]. Ojala et al. [113] wrote that little attention is given in the literature to the resources that new ventures can develop in international networks, especially, those small firms operating in digital markets where technologies are rapidly evolving (Arthur 2011, Henfridsson and Bygstad 2013). Digital platform environments are an opportunity for new ventures, but a threat to established DBE members. New entrepreneurial businesses are *born open* in multi-sided platforms [19].

Benefit 7: Cost and risk management

In DBEs, digital platforms minimize the costs of searching for both seeking services and service providers [60]. They provide an opportunity to profit from multiple sides of the platform [38]. Lusch and Nambisan [98] found that service exchange in service ecosystems is not very efficient without a digital platform. The DP helps to both free-up and enhance resources through efficient and effective service exchange. However, expanding their portfolio of additional services may lead some manufacturing firms to lose business focus, experience difficulty dealing with more complex interactions, and face a more uncertain future [22]. To avoid these issues, a manufacturer could offer additional services to both members and new ventures while remaining focused on its own business.

Major challenges in servitization are leading many firms to increase revenues as profits are dropping. This is known as the service paradox [58]. Reim et al. [131] mentioned that fulfilling specialized services for customers also comes with higher development and delivery costs. These findings support the logic of a DBE. Leading companies should not shoulder the burden alone. A leader company can open up the business using a digital platform and allocate risks and knowhow to other members to the benefit of all in manufacturing.

Generally, digital platforms have the potential to restructure industries [83], which results in efficient ecosystems and lower overall manufacturing cost. Innovative companies will adapt to the changes and *heavy* companies that cannot adapt will not survive.

Benefit 8: Provides modularity to fulfill customer needs

Baldwin and Clark (2000) found that the computer industry became more horizontal after IBM deployed a modular architecture and encouraged suppliers to provide both hardware and software for personal computers (PCs). Later, Baldwin and Woodard [16] explained how the PC industry changed. See Fig. 3. In the near future, other industries might face the same phenomenon. Companies are increasingly shifting from being *vertical silos* towards becoming *modular clusters*. Why? Modularity provides more opportunity to offer customers a product with specific options. In addition to giving the customer a product that better meets his or her needs, in the long run, the modularity lowers cost overall by restructuring for the entire manufacturing industry.

For the PC industry, vertical silos meant that each PC manufacture had its own component and software manufacturers. This meant that components were not universal across PCs. With the encouragement of IBM, the PC industry standardized both hardware and software, which ultimately led to substantially lower PC costs and prices. For Intel, vertical silo life was a significant challenge. Consumers don't buy microprocessors, they buy PC's. Once the industry adopted the modular cluster model, Intel quickly learned that boosting innovation would lead to increased PC sales, which would in turn support their microprocessor business. As an added benefit, by coordinating PC industry innovation, Intel protected its business from rivals (Gawer et al. 2002).

Future DBE trends in manufacturing

This section presents future trends for DBEs in manufacturing based on synthesis of the findings for prerequisites, challenges, and benefits. The description of an individual future trend is presented first followed by presentation of the actual future trend *(FT1.-FT5.).*

According to Moore (1996), a business ecosystem is a set of members that includes suppliers, lead producers, competitors, and other stakeholders. A business ecosystem offers value to customers by providing goods and services. Over time, capabilities and roles co-evolve, and they tend to align with the direction of one or more central companies. These central manufacturing companies play leadership roles in the BE. The leader role is valued by the community because it enables members to follow the shared vision and play mutually supportive roles. In manufacturing, there are many central companies of different size. Production factories can be seen as central to the BE. Around production factories, there are many other key member types. In many cases, the production machines used by production factories are provided by various BE members seen as technology leaders. Technology leaders play two roles: as a key member of the production factory and as a central company in its own BE. Production machinery is intellectual property, and all technology leaders want to protect their completive advantage. This makes the sharing of all data among all DP members problematic. And, blocking information from DP members encourages the formation of silos, which can keep the DBE from fully realizing potential benefits.

However, it is increasing clear that traditional business ecosystems can no longer support an optimally healthy manufacturing business. Today, a digital business ecosystem has become a must for production factories, technology leaders, and other companies working in manufacturing. The essential element to building a DBE is having a robust digital platform where members can cooperate, co-create value, and innovate. Thus, we propose the following trend for the future.

FT1. DBE environments are increasingly being pushed by technology leaders in the manufacturing industry

If a single company, not in central role, tries to introduce a new digital platform to the industry at large, it might not be accepted by other industry companies. Gaining acceptance is more difficult when a single company attempts to force a change in the business ecosystem. Acceptance of a new digital platform will become more likely if a central company brings it forward in cooperation with other key members of the industry community. As a result, technology leaders in manufacturing must convert their business ecosystems to digital business ecosystems to deliver next level services to production factories. The business of a technology leader must transform from one that delivers traditional machines and maintenance services to one that delivers smart machines with a digital twin. This gives them the means to utilize unlimited digital technologies and solutions. The digital twin can play the role of a digital platform and enable production factories to connect the digital twins for smart machines together to achieve Smart Manufacturing in a DBE environment.

Many production factories use machinery provided by several technology leaders. This could lead to a number of technology leaders each bringing forward its own digital twin. As a result, it is likely that in the near future, production factories will be presented with multiple digital twins representing their complete production system. Thus, we propose the following trend for the future.

FT2. Because there are several technology leaders in manufacturing reluctant to work with competitors, production factories will soon be presented with multiple digital twins

Uysal and Mergen [169] mention that information integration is one of the most serious issues currently facing Smart Manufacturing. The increasing number of digital twins provided by different technology leaders will not decrease this challenge. International standards will be needed so that all technology leaders can deliver compatible digital twins to production factories.

A digital platform gives production factories the opportunity to select from among a variety of products and digital services. Each factory can purchase a unique combination that they believe gives maximum value. Giving production factories the opportunity to choose their desired products and digital services will increase modularity, which may, in turn, lead to a service paradox (increasing revenues and dropping profits) [58] and/or digitalization paradox [34,116] for the technology leaders. To avoid this, technology leaders should encourage participating members to offer digital services in a digital platform. Production factories will not receive the service they want, and innovation will not reach its full potential if the technology leader is unwilling to open its business to other ecosystem members. Thus, we propose the following trend for the future.

FT3. To maximize the full potential of DBE and to avoid the service and digitalization paradox, the technology leader should open its business to other ecosystem members

As reported by Mitchell and Singh (1996), businesses in an alliance relationship are more likely to survive than firms engaging in arm's length relationships, and technology is evolving rapidly in digital markets (Arthur 2011, Henfridsson and Bygstad 2013). Continuous progress results in a continual need for new technologies and innovations that demand new kinds of resources [113]. A single company does not and cannot maintain all the resources required to keep up with the everchanging forward movement of technological advancement. On its own, the ability to innovate is limited (Gawer and Cusumano, 2013). Without reaching out to the other ecosystem players, the technology leader will certainly suffer from insufficient knowledge. To ensure adequate resources and to promote innovation, the technology leader must open its business to other members of the ecosystem and encourage new ventures.

New ventures in a mature industry often attract little attention. Nonetheless, new ventures often disrupt existing ecosystems, radically changing existing business models and shaping industry structures (Evans et al. 2016; Watanabe et al. 2017) [120]. New ventures positively impacted the phone industry when technology leaders opened up the development of phone applications to outside players. A similar result is likely for manufacturing when technology leaders have a digital platform and business opened for members and new venture. Thus, we propose the following trend for the future.

FT4. New ventures will positively impact the DBE in manufacturing.

A digital platform can establish two- and multi-sided markets, which has many positive effects in manufacturing. The digital platform brings its players closer together [46,185]. Innovation has increasingly shifted from producer companies to product users and technologies [69] (Hippel, 2005). The shift increases the need for a digital platform, so information can be shared more efficiently. User information is also very valuable. Better understanding the user makes it more likely that a company can apply its development resources correctly and better meet user needs. When companies exist on both sides of the market, they can more easily identify and adopt more effective business models [38]. Two- and multisided markets will fuel the next round of innovations and value co-creation in manufacturing DBEs. Thus, we propose the following trend for the future.

FT5. A digital platform can establish two- and multisided markets and fuel the next round of innovations and value co-creation in manufacturing.

Contribution of the study and conclusions

New collaborative value creation networks referred to as digital business ecosystems have been the subject of study in recent years. A DBE is considered as an extension of a business ecosystem in which a digital platforms plays a dominant role. Digital Business Ecosystem is studied in many contexts in manufacturing, and it is creating both opportunities and challenges for manufacturing. By providing a systematic literature review of the prerequisites, challenges, and benefits of DBEs for the manufacturing industry, this paper helps to alleviate this shortcoming and reveals how digital business ecosystems can dramatically impact manufacturing.

The Scopus database was searched for relevant literature. The main journals covering information, management, strategy, innovation, product, production, service, and business areas were searched. 149 research journal articles were included in this literature review, which uncovered nine prerequisites, eight challenges, and eight benefits for DBEs and led to five trends for future studies. The study shows that researchers have been more interested in benefits than prerequisites and challenges.

Five future trends for DBEs in manufacturing are candidates for further research. As one major contribution, this study suggests that future research can focus on these five future trends.

Firstly, technology leaders are more likely pushing DBE environments in manufacturing. If a single company without a central company role is trying to introduce a new digital platform to the industry at large, it might not be accepted by other industry companies. A single company cannot force change in the business ecosystem.

Secondly, multiple digital twins will be introduced by technology leaders in production factories. Competition makes technology leaders reluctant to collaborate. Before collaboration can occur, technology leaders must convert their business ecosystems to digital business ecosystems to deliver next level services to their production factories. In other words, technology leaders must transform from being concerns that deal with traditional machines and maintenance services to ones that deliver smart machines with digital twins.

Thirdly, to achieve the full potential of DBE and avoid a service and digital paradox, technology leaders should open their businesses to other ecosystem members. Continuing to operate independently and keeping ecosystem members in information silos will ultimately be a risk to their own businesses. Innovation will not be able to reach its full potential, and production factories will not be receiving the service they want and need.

Fourthly, new ventures will positively impact DBEs in manufacturing. On their own, companies have limited ability to innovate. When a central company opens its business to other members, it encourages new ventures as well. For example, new ventures positively impacted the phone industry when a technology leader opened up the development of phone applications to outside players.

And finally, digital platforms can establish two- and multisided markets in manufacturing, which will fuel the next round of innovation and value co-creation. When companies share information, there is co-created innovation and value. When companies can exist on both sides of the market, they can adopt more effective and innovative business models.

This work contributes and provides new insights to the under-researched topic of digital business ecosystems in manufacturing by revealing prerequisites, challenges, and benefits and proposing research topics for further studies. The study should be of benefit to directors and managers working in the manufacturing industry. Manufacturers can start considering how the impending digitalization of their industry might affect their businesses and their business models. Hopefully, they can get a better sense of where they are now and how to proceed. The study should enhance understanding of the digital business ecosystem and how it will affect the entire manufacturing industry.

As a limitation, the study did not focus on the impacts of DBEs on sustainability. However, the effects of DBEs on sustainability, encompassing economic, environmental, and social aspects of sustainability (cf. [136] should be studied. An important research topic could be, for example, how to find a balance, in terms of power and economy, between the world's largest technology companies and other ecosystem players. However, sustainability as a topic is so broad that it requires a number of separate studies and therefore was excluded from this study.

Declaration of Competing Interest

The authors declare that they have no known competing financial interests or personal relationships that could have appeared to influence the work reported in this paper.

References

[1] Aarikka-Stenroos, L., Jaakkola, E., 2012, Value Co-creation in Knowledge Intensive Business Services: A Dyadic Perspective on the Joint Problem Solving Process. Industrial Marketing Management, 41/1: 15–26.
[3] Adner, R., Kapoor, R., 2010, Value Creation in Innovation Ecosystems: How the Structure of Technological Interdependence Affects Firm Performance in New Technology Generations. Strategic Management Journal, 31/3: 306–333.
[4] Adner, R., 2006, Match Your Innovation Strategy to Your Innovation Ecosystem. Harvard Business Review, 84/4: 98–107.
[6] Aceto, G., Persico, V., Pescapé, A., 2020, Industry 4.0 and Health: Internet of Things, Big Data, and Cloud Computing for Healthcare 4.0. Journal of Industrial Information Integration, 18:100129.
[7] Al-Rubaye, S., Kadhum, E., Ni, Q., Anpalagan, A., 2017, Industrial Internet of Things Driven by SDN Platform for Smart Grid Resiliency. IEEE Internet of Things Journal, 6/1: 267–277.
[8] Akter, S., Wamba, S.F., 2016, Big Data Analytics in E-commerce: A Systematic Review and Agenda for Future Research. Electronic Markets, 26/2: 173–194.
[9] Atanasovski, P. (2020, accessed in 1.5.2021). Volkswagen opens the Industrial Cloud community. The Internet of Things on AWS – Official Blog. ⟨https://aws.amazon.com/blogs/iot/volkswagen-opens-the-industrial-cloud-community/⟩.
[10] Arthur, W.B., 1989, Competing Technologies, Increasing Returns, and Lock-in by Historical Events. The Economic Journal, 99/394: 116–131.
[11] Arthur, W.B., 2009, The Nature of Technology: What it is and How it Evolves. Simon and Schuster.
[13] Bakker, R.M., 2010, Taking Stock of Temporary Organizational Forms: A Systematic Review and Research Agenda. International Journal of Management Reviews, 12/4: 466–486.
[15] Bao, J., Guo, D., Li, J., Zhang, J., 2019, The Modelling and Operations for the Digital Twin in the Context of Manufacturing. Enterprise Information Systems, 13/4: 534–556.
[16] Baldwin, C.Y., Woodard, C.J., 2009, The Architecture of Platforms: A Unified View. Platforms, Markets and Innovation, 32.
[18] Boudreau, K.J., Hagiu, A., 2009, Platform Rules: Multi-sided Platforms as Regulators. Platforms, Markets and Innovation, 1:163–191.
[19] Boudreau, K.J. (2017). Platform Boundary Choices & Governance: Opening-Up While Still Coordinating and Orchestrating. Entrepreneurship, Innovation and Platforms. AGJ Furman, BS Silverman, S. Stern. Emerald Publishing Limited, 37, 227-297.
[20] Briscoe, G (2009). "Digital Ecosystems". PhD thesis. Imperial College London.

[22] Cenamor, J., Sjödin, D.R., Parida, V., 2017, Adopting a Platform Approach in Servitization: Leveraging the Value of Digitalization. International Journal of Production Economics, 192:54–65.
[23] Chen, H., Chiang, R.H., Storey, V.C., 2012, Business Intelligence and Analytics: From Big Data to Big Impact. MIS Quarterly, 1165–1188.
[24] Chen, Z., Dahlgaard-Park, S.M., Yu, L., 2014, Service Quality Management and Ecosystem Theory. Total Quality Management & Business Excellence, 25/9–10: 1190–1205.
[25] Cheng, J., Chen, W., Tao, F., Lin, C.L., 2018, Industrial IoT in 5G Environment Towards Smart Manufacturing. Journal of Industrial Information Integration, 10:10–19.
[26] Cheng, J., Zhang, H., Tao, F., Juang, C.F., 2020, DT-II: Digital Twin Enhanced Industrial Internet Reference Framework Towards Smart Manufacturing. Robotics and Computer-Integrated Manufacturing, 62:101881.
[29] Clarysse, B., Wright, M., Bruneel, J., Mahajan, A., 2014, Creating Value in Ecosystems: Crossing the Chasm Between Knowledge and Business Ecosystems. Research Policy, 43/7: 1164–1176.
[30] Cusumano, M.A., Gawer, A., 2002, The Elements of Platform Leadership. MIT Sloan Management Review, 43/3: 51.
[31] Cusumano, M.A., Yoffie, D.B., Gawer, A., 2020, The Future of Platforms. MIT Sloan Management Review, 61/3: 46–54.
[32] Coviello, N.E., 2006, The Network Dynamics of International New Ventures. Journal of International Business Studies, 37/5: 713–731.
[34] Cooper, R.G., Sommer, A.F., 2018, Agile–Stage-Gate for Manufacturers: Changing the Way New Products Are Developed Integrating Agile Project Management Methods into a Stage-Gate System Offers Both Opportunities and Challenges. Research-Technology Management, 61/2: 17–26.
[35] Davenport, T.H., 2006, Competing on Analytics. Harvard Business Review, 84/1: 98.
[38] Eisenmann, T., Parker, G., Van Alstyne, M.W., 2006, Strategies for Two-sided Markets. Harvard Business Review, 84/10: 92.
[40] El Sawy, O.A., Malhotra, A., Park, Y., Pavlou, P.A., 2010, Seeking the Configurations of Digital Ecodynamics: It Takes Three to Tango. Research Commentary. Information Systems Research, 21/4: 835–848.
[41] Eloranta, V., Turunen, T., 2016, Platforms in Service-driven Manufacturing: Leveraging Complexity by Connecting, Sharing, and Integrating. Industrial Marketing Management, 55:178–186.
[43] Eggert, A., Hogreve, J., Ulaga, W., Muenkhoff, E., 2014, Revenue and Profit Implications of Industrial Service Strategies. Journal of Service Research, 17/1: 23–39.
[46] Evans, D.S., Schmalensee, R., 2016, Matchmakers: The New Economics of Multisided Platforms. Harvard Business Review Press.
[48] Evans, P.C., Basole, R.C., 2016, Revealing the API Ecosystem and Enterprise Strategy via Visual Analytics. Communications of the ACM, 59/2: 26–28.
[49] Evans, P. C., Gawer, A. (2016). The rise of the platform enterprise: A global survey.
[50] Farrell, J., Katz, M.L., 2000, Innovation, Rent Extraction, and Integration in Systems Markets. The Journal of Industrial Economics, 48/4: 413–432.
[51] Franco, R.D., Bas, Á.O., Esteban, F.L., 2009, Modeling Extended Manufacturing Processes with Service-oriented Entities. Service Business, 3/1: 31–50.
[53] Franke, N., Shah, S., 2003, How Communities Support Innovative Activities: An Exploration of Assistance and Sharing Among End-users. Research policy, 32/1: 157–178.
[54] Martin, P.C.G., Schroeder, A., Bigdeli, A.Z., 2019, The Value Architecture of Servitization: Expanding the Research Scope. Journal of Business Research, 104:438–449.
[55] Gawer, A., Cusumano, M.A., 2002, Platform Leadership: How Intel, Microsoft, and Cisco Drive Industry Innovation, Vol. 5. Harvard Business School Press, Boston, MA: 29–30.
[56] Gawer, A., Cusumano, M.A., 2014, Industry Platforms and Ecosystem Innovation. Journal of Product Innovation Management, 31/3: 417–433.
[58] Gebauer, H., Fleisch, E., Friedli, T., 2005, Overcoming the Service Paradox in Manufacturing Companies. European Management Journal, 23/1: 14–26.
[59] Ghazawneh, A., Henfridsson, O., 2013, Balancing Platform Control and External Contribution in Third-party Development: The Boundary Resources Model. Information Systems Journal, 23/2: 173–192.
[60] Greve, H.R., Song, S.Y., 2017, Amazon Warrior: How a Platform Can Restructure Industry Power and Ecology'. Entrepreneurship, Innovation, and Platforms. Emerald Publishing Limited.
[62] Gupta, A.K., Wilemon, D.L., 1990, Accelerating the Development of Technology-based New Products. California Management Review, 32/2: 24–44.
[63] Hakanen, E., Rajala, R. (2018). Material Intelligence as a Driver for Value Creation in IoT-enabled Business Ecosystems. Journal of Business & Industrial Marketing.
[64] Haleem, A., Javaid, M., 2019, Additive Manufacturing Applications in Industry 4.0: A Review. Journal of Industrial Integration and Management, 4/04:1930001.
[67] Heffner, M., Sharif, N., 2008, Knowledge Fusion for Technological Innovation in Organizations. Journal of Knowledge Management.
[68] Hienerth, C., Lettl, C., 2011, Exploring How Peer Communities Enable Lead User Innovations to Become Standard Equipment in the Industry: Community Pull Effects. Journal of Product Innovation Management, 28/s1: 175–195.
[69] Hienerth, C., Lettl, C., Keinz, P., 2014, Synergies Among Producer Firms, Lead Users, and User Communities: The Case of the LEGO Producer–user Ecosystem. Journal of Product Innovation Management, 31/4: 848–866.
[70] Hu, L., Nguyen, N.T., Tao, W., Leu, M.C., Liu, X.F., Shahriar, M.R., Al Sunny, S.N., 2018, Modeling of Cloud-based Digital Twins for Smart Manufacturing with MT Connect. Procedia Manufacturing, 26:1193–1203.
[71] Iansiti, M., Levien, R., 2004, The Keystone Advantage: What the New Dynamics of Business Ecosystems Mean for Strategy, Innovation, and Sustainability. Harvard Business Press.
[73] Jacobides, M.G., Cennamo, C., Gawer, A., 2018, Towards a Theory of Ecosystems. Strategic Management Journal, 39/8: 2255–2276.
[75] Jeppesen, L.B., Frederiksen, L., 2006, Why Do Users Contribute to Firm-hosted User Communities? The Case of Computer-controlled Music Instruments. Organization Science, 17/1: 45–63.
[76] Johansson, A.E., Raddats, C., Witell, L., 2019, The Role of Customer Knowledge Development for Incremental and Radical Service Innovation in Servitized Manufacturers. Journal of Business Research, 98:328–338.
[77] Johanson, J., Vahlne, J.E., 2009, The Uppsala Internationalization Process Model Revisited: From Liability of Foreignness to Liability of Outsidership. Journal of international business studies, 40/9: 1411–1431.
[78] Kim, J.H., 2017, A Teview of Cyber-physical System Research Relevant to the Emerging IT Trends: Industry 4.0, IoT, Big Data, and Cloud Computing. Journal of Industrial Integration and Management, 2/03:1750011.
[79] Kumar, A., 2018, Methods and Materials for Smart Manufacturing: Additive Manufacturing, Internet of Things, Flexible Sensors and Soft Robotics. Manufacturing Letters, 15:122–125.
[80] Kusiak, A., 2018, Smart Manufacturing. International Journal of Production Research, 56/1–2: 508–517.
[81] Kohtamäki, M., Parida, V., Patel, P.C., Gebauer, H., 2020, The Relationship Between Digitalization and Servitization: The Role of Servitization in Capturing the Financial Potential of Digitalization. Technological Forecasting and Social Change, 151:119804.
[82] Kohtamäki, M., Partanen, J., Parida, V., Wincent, J., 2013, Non-linear Relationship Between Industrial Service Offering and Sales Growth: The Moderating Role of Network Capabilities. Industrial Marketing Management, 42/8: 1374–1385.
[83] Kotha, S., Basu, S., 2011, Amazon and eBay: Online Retailers as Market Makers. The Market Makers: How Retailers are Reshaping the Global Economy. Oxford university press: 155–180.
[86] Lager, T., 2017, A Conceptual Framework for Platform-based Design of Non-assembled Products. Technovation, 68:20–34.
[87] Law, C.C., Ngai, E.W., 2008, An Empirical Study of the Effects of Knowledge Sharing and Learning Behaviors on Firm Performance. Expert systems with applications, 34/4: 2342–2349.
[88] Lee, S.M., Olson, D.L., Trimi, S., 2012, Co-innovation: Convergenomics, Collaboration, and Co-creation for Organizational Values. Management Decision.
[89] Lin, S. W., Miller, B., Durand, J., Joshi, R., Didier, P., Chigani, A.,. & Witten, B. (2015). Industrial internet reference architecture. Industrial Internet Consortium (IIC), Tech. Rep.
[90] Liu, K., Nakata, K., Li, W., & Baranauskas, C. (2018). Digitalisation, Innovation and Transformation. In 18th IFIP WG (Vol. 8, pp. 16-18).
[91] Liu, Q., Leng, J., Yan, D., Zhang, D., Wei, L., Yu, A., Chen, X., 2021, Digital Twin-based Designing of the Configuration, Motion, Control, and Optimization Model of a Flow-type Smart Manufacturing System. Journal of Manufacturing Systems, 58:52–64.
[94] Lu, Y., 2017, Cyber Physical System (CPS)-Based Industry 4.0: A survey. Journal of Industrial Integration and Management, 2/03:1750014.
[95] Lu, Y., Liu, C., Kevin, I., Wang, K., Huang, H., Xu, X., 2020, Digital Twin-driven Smart Manufacturing: Connotation, Reference Model, Applications and Research Issues. Robotics and Computer-Integrated Manufacturing, 61:101837.
[96] Lu, Y., Peng, T., Xu, X., 2019, Energy-efficient Cyber-physical Production Network: Architecture and Technologies. Computers & Industrial Engineering, 129:56–66.
[97] Lu, Y., Xu, X., 2019, Cloud-based Manufacturing Equipment and Big Data Analytics to Enable On-demand Manufacturing Services. Robotics and Computer-Integrated Manufacturing, 57:92–102.
[98] Lusch, R.F., Nambisan, S., 2015, Service Innovation: A Service-dominant Logic Perspective. MIS Quarterly, 39/1: 155–176.
[99] McAfee, A., Brynjolfsson, E., Davenport, T.H., Patil, D.J., Barton, D., 2012, Big Data: The Management Revolution. Harvard Business Review, 90/10: 60–68.
[100] Menor, L.J., Roth, A.V., 2007, New Service Development Competence in Retail Banking: Construct Development and Measurement Validation. Journal of Operations Management, 25/4: 825–846.
[101] Menon, K., Kärkkäinen, H., Gupta, J.P., 2016, Role of industrial internet platforms in the management of product lifecycle related information and knowledge. IFIP International Conference on Product Lifecycle Management. Springer, Cham: 549–558.
[102] Meyer, M.H., Mugge, P.C., 2001, Make Platform Innovation Drive Enterprise Growth. Research-Technology Management, 44/1: 25–39.
[105] Murmann, J.P., Ozdemir, S.Z., Sardana, D., 2015, The Role of Home Country Demand in the Internationalization of New Ventures. Research Policy, 44/6: 1207–1225.
[106] Moore, J.F., 1993, Predators and Prey: A New Ecology of Competition. Harvard Business Review, 71/3: 75–86.
[108] Myhren, P., Witell, L., Gustafsson, A., Gebauer, H., 2018, Incremental and Radical Open Service Innovation. Journal of Services Marketing.
[110] NIA, 2011, Platform Strategy to Lead a Quantum Jump in the Powerful Korea. IT Future Strategy, 1–16.
[111] NIST, Smart Manufacturing Operations Planning and Control Program, ⟨https://www.nist.gov/programs-projects/smart-manufacturing-operations-planning-and-control-program⟩ (Accessed 8 May 2021).

[113] Ojala, A., Evers, N., Rialp, A., 2018, Extending the International New Venture Phenomenon to Digital Platform Providers: A Longitudinal Case Study. Journal of World Business, 53:725–739.
[114] Oliva, R., & Kallenberg, R. (2003). Managing the Transition From Products to Services. International Journal of Service Industry Management.
[116] Parida, V., Sjödin, D., Reim, W., 2019, Leveraging Digitalization for Advanced Service Business Models: Reflections from a Systematic Literature Review and Special Issue Contributions. Sustainability, 11/2: 391.
[118] Park, K.T., Nam, Y.W., Lee, H.S., Im, S.J., Noh, S.D., Son, J.Y., Kim, H., 2019, Design and Implementation of a Digital Twin Application for a Connected Micro Smart Factory. International Journal of Computer Integrated Manufacturing, 32/6: 596–614.
[119] Parker, G.G., Van Alstyne, M.W., 2005, Two-sided Network Effects: A Theory of Information Product Design. Management Science, 51/10: 1494–1504.
[120] Parker, G. G., Van Alstyne, M. W., & Choudary, S. P. (2016). Platform revolution: How networked markets are transforming the economy and how to make them work for you. WW Norton & Company.
[121] Peláez, J.I., Cabrera, F.E., Vargas, L.G., 2018, Estimating the Importance of Consumer Purchasing Criteria in Digital Ecosystems. Knowledge-Based Systems, 162:252–264.
[122] Pfeffer, J., 1987, A Resource Dependence Perspective on Intercorporate Relations. Intercorporate Relations: The Structural Analysis of Business, 1/1: 25–55.
[123] Peltoniemi, M., 2006, Preliminary Theoretical Framework for the Study of Business Ecosystems. Emergence: Complexity & Organization, 8/1.
[127] Qi, Q., Tao, F., Zuo, Y., Zhao, D., 2018, Digital Twin Service Towards Smart Manufacturing. Procedia Cirp, 72:237–242.
[129] Raddats, C., Kowalkowski, C., Benedettini, O., Burton, J., Gebauer, H., 2019, Servitization: A Contemporary Thematic Review of Four Major Research Streams. Industrial Marketing Management, 83:207–223.
[130] Ransbotham, S., Kane, G.C., 2011, Membership Turnover and Collaboration Success in Online Communities: Explaining Rises and Falls From Grace in Wikipedia. Mis Quarterly, 613–627.
[131] Reim, W., Parida, V., Örtqvist, D., 2015, Product–Service Systems (PSS) Business Models and Tactics–a Systematic Literature Review. Journal of Cleaner Production, 97:61–75.
[134] Rochet, J.C., Tirole, J., 2003, Platform Competition in Two-sided Markets. Journal of the European Economic Association, 1/4: 990–1029.
[135] Rosen, R., Von Wichert, G., Lo, G., Bettenhausen, K.D., 2015, About the Importance of Autonomy and Digital Twins for the Future of Manufacturing. IFAC-PapersOnLine, 48/3: 567–572.
[136] Saunila, M., Nasiri, M., Ukko, J., Rantala, T., 2019, Smart Technologies and Corporate Sustainability: The Mediation Effect of Corporate Sustainability Strategy. Computers in Industry, 108:178–185.
[138] Shahbazi, Z., Byun, Y.C., 2021, Integration of Blockchain, IoT and Machine Learning for Multistage Quality Control and Enhancing Security in Smart Manufacturing. Sensors, 21/4: 1467.
[139] Sharma, R., Mithas, S., Kankanhalli, A., 2014, Transforming Decision-making Processes: A Research Agenda for Understanding the Impact of Business Analytics on Organisations. European Journal of Information Systems, 23/4: 433–441.
[141] Selander, L., Henfridsson, O., Svahn, F., 2013, Capability Search and Redeem Across Digital Ecosystems. Journal of information technology, 28/3: 183–197.
[142] Senyo, P.K., Liu, K., Effah, J., 2019, Digital Business Ecosystem: Literature Review and a Framework for Future Research. International Journal of Information Management, 47:52–64.
[144] Söderberg, R., Wärmefjord, K., Carlson, J.S., Lindkvist, L., 2017, Toward a Digital Twin for Real-time Geometry Assurance in Individualized Production. CIRP Annals, 66/1: 137–140.
[146] Sjödin, D., Parida, V., Kohtamäki, M., Wincent, J., 2020, An Agile Co-creation Process For Digital Servitization. Journal of Business Research.
[147] Sklyar, A., Kowalkowski, C., Tronvoll, B., Sörhammar, D., 2019, Organizing for Digital Servitization: A Service Ecosystem Perspective. Journal of Business Research, 104:450–460.
[148] Srinivasan, A., Venkatraman, N., 2018, Entrepreneurship in Digital Platforms: A Network-centric View. Strategic Entrepreneurship Journal, 12/1: 54–71.
[149] Stamer, F., Bizenberger, P., Häfner, B., Lanza, G., 2021, Deriving Collaboration Cases in Production Networks Considering Smart Services. Procedia CIRP, 96:33–38.
[150] Stanley, J., Briscoe, G., 2010, The ABC of Digital Business Ecosystems. Communications Law. Journal of Computer, Media and Telecommunications Law, 15/1.
[151] Storbacka, K., Brodie, R.J., Böhmann, T., Maglio, P.P., Nenonen, S., 2016, Actor Engagement as a Microfoundation for Value Co-creation. Journal of Business Research, 69/8: 3008–3017.
[152] Sullivan Mort, G., Weerawardena, J., Liesch, P., 2012, Advancing Entrepreneurial Marketing: Evidence from Born Global Firms. European Journal of Marketing, 46/3–4: 542–561.
[154] Tanriverdi, H., Rai, A., Venkatraman, N., 2010, Research Commentary—reframing the Dominant Quests of Information Systems Strategy Research For Complex Adaptive Business Systems. Information Systems Research, 21/4: 822–834.
[156] Tao, F., Cheng, J., Qi, Q., Zhang, M., Zhang, H., Sui, F., 2018, Digital Twin-driven Product Design, Manufacturing and Service with Big Data. The International Journal of Advanced Manufacturing Technology, 94/9: 3563–3576.
[158] Tao, F., Zhang, Y., Cheng, Y., Ren, J., Wang, D., Qi, Q., Li, P., 2020, Digital Twin and Blockchain Enhanced Smart Manufacturing Service Collaboration and Management. Journal of Manufacturing Systems.
[159] Tao, F., Qi, Q., Wang, L., Nee, A.Y.C., 2019, Digital Twins and Cyber–physical Systems Toward Smart Manufacturing and Industry 4.0: Correlation and Comparison. Engineering, 5/4: 653–661.
[160] Teece, D.J., 2007, Explicating Dynamic Capabilities: The Nature and Microfoundations of (Sustainable) Enterprise Performance. Strategic Management Journal, 28/13: 1319–1350.
[161] Teece, D.J. (2014). Business ecosystems. Entry in. Palgrave Encyclopedia of Management, 10(9781137294678.0190).
[162] Teece, D.J., 2017, Dynamic capabilities and (digital) platform lifecycles. Entrepreneurship, Innovation, and Platforms. Emerald Publishing Limited.
[163] Thomas, A., Morris, W., Haven-Tang, C., Francis, M., Byard, P., 2021, Smart Systems and Collaborative Innovation Networks for Productivity Improvement in SMEs. Journal of Open Innovation: Technology, Market, and Complexity, 7/1: 3.
[167] Tiwana, A., Konsynski, B., 2010, Complementarities between Organizational IT Architecture and Governance Structure. Information Systems Research, 21/2: 288–304.
[168] Troisi, O., D'Arco, M., Loia, F., Maione, G., 2018, Big Data Management: The Case of Mulino Bianco's Engagement Platform for Value Co-creation. International Journal of Engineering Business Management, 10. 1847979018767776.
[169] Uysal, M.P., Mergen, A.E., 2021, Smart Manufacturing in Intelligent Digital Mesh: Integration of Enterprise Architecture and Software Product Line Engineering. Journal of Industrial Information Integration, 22:100202.
[170] Vargo, S.L., Maglio, P.P., Akaka, M.A., 2008, On Value and Value Co-creation: A Service Systems and Service Logic Perspective. European Management Journal, 26/3: 145–152.
[173] Wang, D., Ren, J., Cheng, Y., Tao, F., 2020, An aggregated-tasks oriented manufacturing services scheduling toward industrial Internet platforms. 2020 IEEE 16th International Conference on Automation Science and Engineering (CASE). IEEE: 716–721.
[174] Wang, J., Xu, C., Zhang, J., Bao, J., Zhong, R., 2020, A Collaborative Architecture of the Industrial Internet Platform for Manufacturing Systems. Robotics and Computer-Integrated Manufacturing, 61:101854.
[175] Wang, J., Ye, L., Gao, R.X., Li, C., Zhang, L., 2019, Digital Twin for Rotating Machinery Fault Diagnosis in Smart Manufacturing. International Journal of Production Research, 57/12: 3920–3934.
[177] Weber, A., 2017, GE 'Predix'the Future of Manufacturing. Assembly, 60/3: GE70–76.
[180] West, M., Wilson, N., James, K., 2017, Hype Cycle for Application Development. :G00314060. Gartner Technical Report.
[181] Wheelwright, S.C., Clark, K.B., 1992, Revolutionizing Product Development: Quantum Leaps in Speed, Efficiency, and Quality. Simon and Schuster.
[182] Wiedmann, K.P., Hennigs, N., Varelmann, D., Reeh, M.O., 2010, Determinants of Consumers' Perceived Trust in IT-ecosystems. Journal of Theoretical and Applied Electronic Commerce Research, 5/2: 137–154.
[184] Yli-Ojanperä, M., Sierla, S., Papakonstantinou, N., Vyatkin, V., 2019, Adapting an Agile Manufacturing Concept to the Reference Architecture Model Industry 4.0: A Survey and Case Study. Journal of Industrial Information Integration, 15:147–160.
[185] Yoo, Y., Henfridsson, O., Lyytinen, K., 2010, Research commentary—The New Organizing Logic of Digital Innovation: An Agenda For Information Systems Research. Information systems research, 21/4: 724–735.
[186] Yoo, Y., Boland Jr., R.J., Lyytinen, K., Majchrzak, A., 2012, Organizing for Innovation in the Digitized World. Organization Science, 23/5: 1398–1408.
[187] Zhang, C., Chen, Y., 2020, A Review of Research Relevant to the Emerging Industry Trends: Industry 4.0, IoT, Blockchain, and Business Analytics. Journal of Industrial Integration and Management, 5/01: 165–180.
[188] Zhu, F., Iansiti, M., 2012, Entry into Platform-based Markets. Strategic Management Journal, 33/1: 88–106.

ACTA UNIVERSITATIS LAPPEENRANTAENSIS

1023. CHOUDHURY, TUHIN. Simulation-based methods for fault estimation and parameter identification of rotating machines. 2022. Diss.

1024. DUKEOV, IGOR. On antecedents of organizational innovation: How the organizational learning, age and size of a firm impact its organizational innovation. 2022. Diss.

1025. BREIER, MATTHIAS. Business model innovation as crisis response strategy. 2022. Diss.

1026. FADEEV, EGOR. Magnetotransport properties of nanocomposites close to the percolation threshold. 2022. Diss.

1027. KEPSU, DARIA. Technology analysis of magnetically supported rotors applied to a centrifugal compressor of a high-temperature heat pump. 2022. Diss.

1028. CHAUHAN, VARDAAN. Optimizing design and process parameters for recycled thermoplastic natural fiber composites in automotive applications. 2022. Diss.

1029. RAM, MANISH. Socioeconomic impacts of cost optimised and climate compliant energy transitions across the world. 2022. Diss.

1030. AMADI, MIRACLE. Hybrid modelling methods for epidemiological studies. 2022. Diss.

1031. RAMÍREZ ANGEL, YENDERY. Water-energy nexus for waste minimisation in the mining industry. 2022. Diss.

1032. ZOLOTAREV, FEDOR. Computer vision for virtual sawing and timber tracing. 2022. Diss.

1033. NEPOVINNYKH, EKATERINA. Automatic image-based re-identification of ringed seals. 2022. Diss.

1034. ARAYA GÓMEZ, Natalia Andrea. Sustainable management of water and tailings in the mining industry. 2022. Diss.

1035. YAHYA, MANAL. Augmented reality based on human needs. 2022. Diss.

1036. KARUPPANNAN GOPALRAJ, SANKAR. Impacts of recycling carbon fibre and glass fibre as sustainable raw materials for thermosetting composites. 2022. Diss.

1037. UDOKWU, CHIBUZOR JOSEPH. A modelling approach for building blockchain applications that enables trustable inter-organizational collaborations. 2022. Diss.

1038. INGMAN, JONNY. Evaluation of failure mechanisms in electronics using X-ray imaging. 2022. Diss.

1039. LIPIÄINEN, SATU. The role of the forest industry in mitigating global change: towards energy efficient and low-carbon operation. 2022. Diss.

1040. AFKHAMI, SHAHRIAR. Laser powder-bed fusion of steels: case studies on microstructures, mechanical properties, and notch-load interactions. 2022. Diss.

1041. SHEVELEVA, NADEZHDA. NMR studies of functionalized peptide dendrimers. 2022. Diss.

1042. SOUSA DE SENA, ARTHUR. Intelligent reflecting surfaces and advanced multiple access techniques for multi-antenna wireless communication systems. 2022. Diss.

1043. MOLINARI, ANDREA. Integration between eLearning platforms and information systems: a new generation of tools for virtual communities. 2022. Diss.

1044. AGHAJANIAN MIANKOUH, SOHEIL. Reactive crystallisation studies of CaCO3 processing via a CO2 capture process: real-time crystallisation monitoring, fault detection, and hydrodynamic modelling. 2022. Diss.

1045. RYYNÄNEN, MARKO. A forecasting model of packaging costs: case plain packaging. 2022. Diss.

1046. MAILAGAHA KUMBURE, MAHINDA. Novel fuzzy k-nearest neighbor methods for effective classification and regression. 2022. Diss.

1047. RUMKY, JANNATUL. Valorization of sludge materials after chemical and electrochemical treatment. 2022. Diss.

1048. KARJUNEN, HANNU. Analysis and design of carbon dioxide utilization systems and infrastructures. 2022. Diss.

1049. VEHMAANPERÄ, PAULA. Dissolution of magnetite and hematite in acid mixtures. 2022. Diss.

1050. GOLOVLEVA, MARIA. Numerical simulations of defect modeling in semiconductor radiation detectors. 2022. Diss.

1051. TREVES, LUKE. A connected future: The influence of the Internet of Things on business models and their innovation. 2022. Diss.

1052. TSERING, TENZIN. Research advancements and future needs of microplastic analytics: microplastics in the shore sediment of the freshwater sources of the Indian Himalaya. 2022. Diss.

1053. HOSEINPUR, FARHOOD. Towards security and resource efficiency in fog computing networks. 2022. Diss.

1054. MAKSIMOV, PAVEL. Methanol synthesis via CO2 hydrogenation in a periodically operated multifunctional reactor. 2022. Diss.

1055. LIPIÄINEN, KALLE. Fatigue performance and the effect of manufacturing quality on uncoated and hot-dip galvanized ultra-high-strength steel laser cut edges. 2022. Diss.

1056. MONTONEN, JAN-HENRI. Modeling and system analysis of electrically driven mechatronic systems. 2022. Diss.

1057. HAVUKAINEN, MINNA. Global climate as a commons — from decision making to climate actions in least developed countries. 2022. Diss.

1058. KHAN, MUSHAROF. Environmental impacts of the utilisation of challenging plastic-containing waste. 2022. Diss.

1059. RINTALA, VILLE. Coupling Monte Carlo neutronics with thermal hydraulics and fuel thermo-mechanics. 2022. Diss.

1060. LÄHDEAHO, OSKARI. Competitiveness through sustainability: Drivers for logistics industry transformation. 2022. Diss.

ISBN 978-952-335-902-4
ISBN 978-952-335-903-1 (PDF)
ISSN 1456-4491 (Print)
ISSN 2814-5518 (Online)
Lappeenranta 2022